Pontifícia Universidade Católica
do Rio de Janeiro

Alex Rubén Huamán De La Cruz

Air quality monitoring and assessment: a multidisciplinary study

Tese de Doutorado

Thesis presented to the Programa de Pós-Graduação em Química of PUC-Rio in partial fulfillment of the requirements for the degree of Doutor em Química.

Advisor: Prof. Adriana Gioda

Rio de Janeiro,

August 2018

Pontifícia Universidade Católica
do Rio de Janeiro

Alex Rubén Huamán De La Cruz

Air quality monitoring and assessment: a multidisciplinary study

Thesis presented to the Programa de Pós-Graduação em Química of PUC-Rio in partial fulfillment of the requirements for the degree of Doutor em Química.

Prof. Adriana Gioda
Advisor
Departamento de Química – PUC

Prof. Tatiana Dillenburg Saint'Pierre
Pontifícia Universidade Católica do Rio de Janeiro – PUC-Rio

Prof. Sergio Machado Corrêa
Universidade do Estado do Rio de Janeiro – UERJ

Prof. Christiane Beatrice Duyck
Universidade Federal Fluminense – UFF

Prof. Marcelo Corrêa Bernardes
Universidade Federal Fluminense – UFF

Dra Luciana Maria Baptista Ventura
Instituto Estadual do Ambiente – INEA

Prof. Jiang Kai
Departamento de Química – PUC-Rio

Prof. Marcio da Silveira Carvalho
Vice Dean of Graduate Studies
Centro Técnico Científico – PUC-Rio

Rio de Janeiro, August 20th, 2018

Alex Ruben Huaman De La Cruz

Holds a degreee in chemical Engineering (Universidad Nacional del Centro del Peru), and a MSc degree in Metrology (Pontifícia Universidade Católica do Rio de Janeiro, 2013).

Bibliographic data

Huamán De La Cruz, Alex Rubén

Air Quality monitoring and assessment: a multidisciplinary study / Alex Rubén Huamán De La Cruz; orientador: Adriana Gioda - 2018

v., 228f:il. Color. ; 30cm

Tese (Doutorado) – Pontifícia Universidade Católica do Rio de Janeiro, Departamento de Química.

Inclui bibliografia

1. Química – Teses – Teses. 2. Qualidade do ar;. 3. Biomonitoramento;. 4. Elementos traço 5. R. I. Gioda, Adriana. II. Pontifícia Universidade Católica do Rio de Janeiro. Departamento de Química. III. Título.

I would like to express my deepest gratitude to my parents Ruben and Isabel and my loved brothers Rony, Romina and Kevin who supported me on this journey. Thank you.

Acknowledgments

It has been a long journey finishing this thesis and it would have been much harder without the aid of many excellent people.

First and foremost, I would like to thank my supervisor, Prof. Adriana Gioda, for the energy, encouragement, and enthusiasm that she brought to our meetings, and for his selfless dedication, a wealth of knowledge, advice/feedback, patience, flexibility and general support during my Ph.D. studies.

I would like to thank CAPES (Coordenação de Aperfeiçoamento de Pessoal de Nível Superior) for funding this Ph.D. studentship.

I would like to thank Prof. Tatiana Dillenburg Saint'Pierre (LABSPECTRO) for the collaboration in the ICP-MS analysis, and for sharing their entire lab infrastructure.

My gratitude also goes to the members of the jury who accepted to examine and evaluate my work.

I would like to thank the Department of Chemistry at PUC-Rio (especially our secretary Fatima Almeida) for the opportunity and acceptation in the Pos-doctorate program.

Last but no least, I would to thank all my friends and colleagues especially the ones from the research front (LQA, LABSPECTRO) for keeping me sane and nurtured with healthy relationships and support.

Thank you all.

Abstract

Huamán De La Cruz, Alex Rubén; Gioda, Adriana (Advisor). **Air quality monitoring and assessment: a multidisciplinary study.** Rio de Janeiro, 2018. 228p. Tese de Doutorado - Departamento de Química, Pontifícia Universidade Católica do Rio de Janeiro.

Air pollution is one of the serious problems that the world currently facing. Their understanding it is very complex due to the close relationship of the pollutants, meteorological variables, and land uses influence their composition. Actually, there are two traditional approaches for collecting samples relevant to air and atmospheric deposition which are related to monitoring studies. The first approach involves the direct collection of airborne particulate matter (PM) which aimed quantitative studies at local, short/medium range or global transport of pollutants, including health-related studies related to size fractionate airborne particulate matter ($PM_{2.5}$ and PM_{10}). Their application on large-scale implied expensive investments due to both high costs of maintenance and logistic problem to install the instrumental equipment at all needed locations. The second approach uses an air pollution monitor which is considered as a non-expensive, yet reliable, and relatively simple. Therefore, monitoring air quality by using living organisms as biomonitors has received increasing attention in recent years because certain types of biological organisms provide a measure of integrated exposure over certain amount of time and enrich the substance to be determined so that the analytical accessibility is improved and the measurements uncertainty reduced. In this work, the most of studies were approached in the use of biomonitors as tool suitable to assess the air quality of different locations. This thesis had six principal objectives: 1) passive biomonitoring with lichens; 2) biomonitoring of air quality near industrial area; 3) active biomonitoring with Tillandsia species; 4) a comparison of biomonitoring using three different species of Tillandsia; 5) air quality in 2016 Olympic Games; 6) correction of spectral overlap. Biomonitors were collected from control site, transplanted and exposed into the study area of interest for a time period determined to accumulate trace elements. Trace elements were measured by inductively coupled plasma mass spectrometry (ICP-MS) and the concentrations results were treated with chemometric tools.

Results show the ability of lichens and Tillandsia species to accumulate

trace elements and chemometric tools helped to identify possible emission sources. In the first objective were identified three possible sources of emission: vehicular sources, soil resuspension (natural origin) and agricultural practices. In the second objective was proved that black particles were emitted mainly from leather industry. The third objective shows the vehicular emissions as the main source of pollution in the urban areas, use of agrochemicals in the peri-urban areas and soil resuspension represented by rural areas. The fourth objective shows that all Tillandsia species proved to be good biomonitors. The fifth objective demonstrated that strategies control and traffic regulation implanted by the government of Rio de Janeiro influenced in the reduction of pollutants during the Olympic period. In the sixth objective, Lasso shows better results when predict values of rare earth elements were analyzed.

Keywords

Biomonitoring; trace elements; multivariate analysis; air pollution; multivariate calibration methods

Resumo

Huamán De La Cruz, Alex Rubén; Gioda, Adriana (Orientador). **Monitoramento e avaliação da qualidade do ar: um estudo multidisciplinar.** Rio de Janeiro, 2018. 228p. Tese de Doutorado - Departamento de Química, Pontifícia Universidade Católica do Rio de Janeiro.

A poluição do ar é um dos sérios problemas que o mundo enfrenta atualmente. Sua compreensão é muito complexa devido à estreita relação dos poluentes com as variáveis meteorológicas e o uso da terra os quais influenciam sua composição. Atualmente, existem duas abordagens tradicionais para a coleta de amostras relevantes para a deposição atmosférica e estudos atmosféricos relacionados aos estudos de monitoramento. A primeira abordagem envolve a coleta direta de material particulado (PM) transportado pelo ar que objetivou estudos quantitativos em forma local, de curto/médio alcance ou de transporte global de poluentes, incluindo estudos relacionados à saúde relacionados ao tamanho de material particulado: $PM_{2.5}$ e PM_{10}. Sua aplicação em grande escala implica em investimentos caros devido a altos custos de manutenção e problemas logísticos para instalar o equipamento instrumental em todos os locais necessários de amostragem. A segunda abordagem usa um biomonitor para avaliar a poluição do ar que é considerado como não custoso, mas confiável e relativamente simples. Portanto, monitorar a qualidade do ar usando organismos vivos como biomonitores recebeu atenção crescente nos últimos anos, porque certos tipos de organismos biológicos fornecem uma medida de exposição integrada em determinado período de tempo e enriquecem a substância a ser determinada para que a acessibilidade analítica seja melhorada e a incerteza das medições reduzida. Neste trabalho, a maioria dos estudos foi abordada no uso de biomonitores como ferramenta adequada para avaliar a qualidade do ar de diferentes locais. Esta tese teve seis objetivos principais: 1) biomonitoramento passivo com líquens; 2) biomonitoramento da qualidade do ar próximo a área industrial; 3) biomonitoramento ativo com espécies de Tillandsia; 4) uma comparação do biomonitoramento usando três espécies diferentes de Tillandsia; 5) qualidade do ar nos Jogos Olímpicos de 2016; 6) correção de sobreposição espectral. Os biomonitores foram coletados do local de controle, transplantados e expostos na área de estudo de interesse por um período de tempo determinado para acumular

oligoelementos. Os oligoelementos foram medidos por espectrometria de massa com plasma indutivamente acoplado (ICP-MS) e os resultados das concentrações foram tratados com ferramentas quimiométricos.

Os resultados mostraram a capacidade dos líquenes e das espécies de *Tillandsia* de acumular elementos traço e ferramentas quimiométricos ajudaram para identificar possíveis fontes de emissão. No primeiro objetivo foram identificadas três possíveis fontes de emissão: fontes veiculares, re-suspensão do solo (origem natural) e práticas agrícolas. No segundo objetivo foi provado que partículas negras foram emitidas principalmente da indústria do couro. O terceiro objetivo mostra as emissões veiculares como principal fonte de poluição nas áreas urbanas, uso de agroquímicos nas áreas peri-urbanas e ressuspensão do solo representada pelas áreas rurais. O quarto objetivo mostra que todas as espécies de *Tillandsia* provaram ser bons biomonitores. O quinto objetivo demonstrou que o controle de estratégias e a regulação do tráfego implantado pelo governo do Rio de Janeiro influenciaram na redução de poluentes durante o período olímpico. No sexto objetivo, Lasso mostrou os melhores resultados quando os valores preditivos de elementos de terras raras foram analisados.

Palavras-chave

Biomonitoramento; elementos-traço; analises multivariado; poluição do ar; métodos de calibração multivariada.

Table of Contents

List of Figures

List of Tables

List of Abbreviations

ANOVA – Analysis of variance

CO – Carbon monoxide

CRM – Certified reference material

EDXRF – Energy-dispersive X-ray fluorescence

EF – Enrichment factor

EN – Elastic net

FAAS – Flame atomic absorption spectrometry

GIS – Geographic information system

HCA – Hierarchical cluster analysis

Hi-Vol – High volume air sampler

ICP-MS – Inductively coupled plasma mass spectrometry

INAA – Instrumental neutron activation analysis

Lasso – Least absolute shrinkage and selection operator

LD – Limit of detection

LQ – Limit of quantification

MRRJ – Metropolitan region of Rio de Janeiro

NIST – National Institute of Standards and Technology

NOx – Nitrogen oxides

O_3 - Ozone

PAHs - Polycyclic aromatic hydrocarbons

PCA – Principal components analysis

PCR – Principal component regression

PLS – Partial least squares

PM – Particulate matter

PM_{10} – Fine particles with aerodynamic diameters less than 10 μm

$PM_{2.5}$ – Fine particles with aerodynamic diameter less than 2.5 μm

RE – Relative Error

REE – Rare earth elements

RH – Relative humidity

RJ – Rio de Janeiro

REP – Relative Error of Prediction

RMRJ – Metropolitan Region of Rio of Janeiro

RMSE – Root Mean Square Error

RMSEC – Root Mean Square Error of Calibration

RMSECV – Root Mean Square Error of Cross Validation

RMSEP – Root Mean Square Error of Prediction

RR – Ridge regression

SPMR – São Paulo Metropolitan Region

SO_2 – Sulphur dioxide

SR – Solar Radiation

SRM – Standard Reference Materials

T - Temperature

TE – Trace elements

VOCs – Volatile organic compound

WD – Wind Direction

WS – Wind Speed

WHO – World Health Organization

1
Introduction

1.1.
Pollution and air pollution

Pollution (environmental pollution) can be defined as the presence, addition and/or discharge of any substance/compounds/chemicals (pollutants) in form (solid, liquid, or gas) or any form of energy (e.g. heat, sound, and radioactivity) at the environment [1]. The kinds of pollution are classified like air pollution, water pollution and land pollution.

Air pollution is defined as the presence of pollutants in the air and is recognized as a very complex issue and serious threat of the modern society due to the presence of one or more pollutants, at levels that pose high risk and harmful to the environment and the health human [2]. Usually the pollutants are emitted into the atmosphere in form gaseous or particulate matter (PM) or combination of both resulting from man's activities or natural sources. Particulate matter either with an aerodynamic size of 10 μm or less (PM_{10}) or with an aerodynamic diameter size of 2.5 μm or less ($PM_{2.5}$), usually contains different toxic elements inside their composition causing air pollution through the atmospheric deposition [3].

Air pollution has been recognized as the world top problem in many strategic environmental policies. However, it is still inadequately corroborated by regulatory monitoring due to the balance between costs and practical constraints. The variability in air pollution patterns additionally emphasizes a need for feasible approaches to an extensive screening of pollutants. To achieve highly temporally and spatially resolved measurements, biomonitoring (e.g. the use of living organisms to determine changes in the environment has been utilized in the investigating of a complementary method to regulatory measurements).

As consequence of air pollution he World Health Organization (WHO) estimates that around 7 million people die every year from exposure to fine and coarse particles in polluted air that penetrate deep into the cardiovascular system and lungs, causing diseases and 91% of the world's population lives in place where air quality exceeds WHO guidelines limits [4].

1.2. Biomonitoring

Biomonitoring may be described as the use of cosmopolite bio-organisms and biomaterials to obtain qualitative or quantitative information on certain characteristic of the biosphere [5,6]. The use of these bio-organisms is considered as non-expensive tools, yet reliable and suitable to evaluate the air quality status in a country or region. The sampling is relatively simple, the monitoring can be carried out in short-long time periods, many sites simultaneously, and remote areas [7].

Biomonitoring is intimately related to use of two terms; bioindicators and/or biomonitors, which refer to use of organisms, communities or part of it, that depicts the occurrence of pollutants on the basis of specific symptoms, reactions, morphological changes and/or concentrations. A bioindicators can be defined as the use of organisms with the aim of obtains information on the quality of the environment. A biomonitor, on the other hand, is used to obtain information on the quantitative aspects of the quality of the environment, being classified as sensitive or accumulative. Therefore, the bioaccumulation is the process where the result is the equilibrium between intake/discharge of pollutants from and into the surrounding environment [6].

Sensitive biomonitors can be used as integrators of stress caused by pollutants, to estimate the biological effects of pollutants based on either optical effects as morphological changes related to the environment and/or changes in physical/chemical aspects as photosynthetic or respiratory activities, or alteration in the activity of different enzymes systems. Accumulative bioindicators or bioaccumulators have the ability to store a range of pollutants in their tissues without being harmed and can be used for the integrated measurement of the concentration of contaminants in the environment [6,8].

Bioaccumulation methods of air pollution can be carried out in two ways: active and passive monitoring (Figure 1.1). Passive monitoring refers to sampling of native species inside the areas of interest, and measurement of the accumulated contaminants in the thallus by chemical analysis, while in active monitoring, the bio-organisms (mosses, lichens, tillandsia, etc.) are collected from an area with clean air (non-polluted area), transplanted to polluted areas and exposed during a period of time well defined. After the exposure time, the transplanted samples are collected and then analyzed for pollutants (trace elements, gases (e.g SO_2, NOx, CO, O_3), VOCs, PHAs, etc.) accumulated [9].

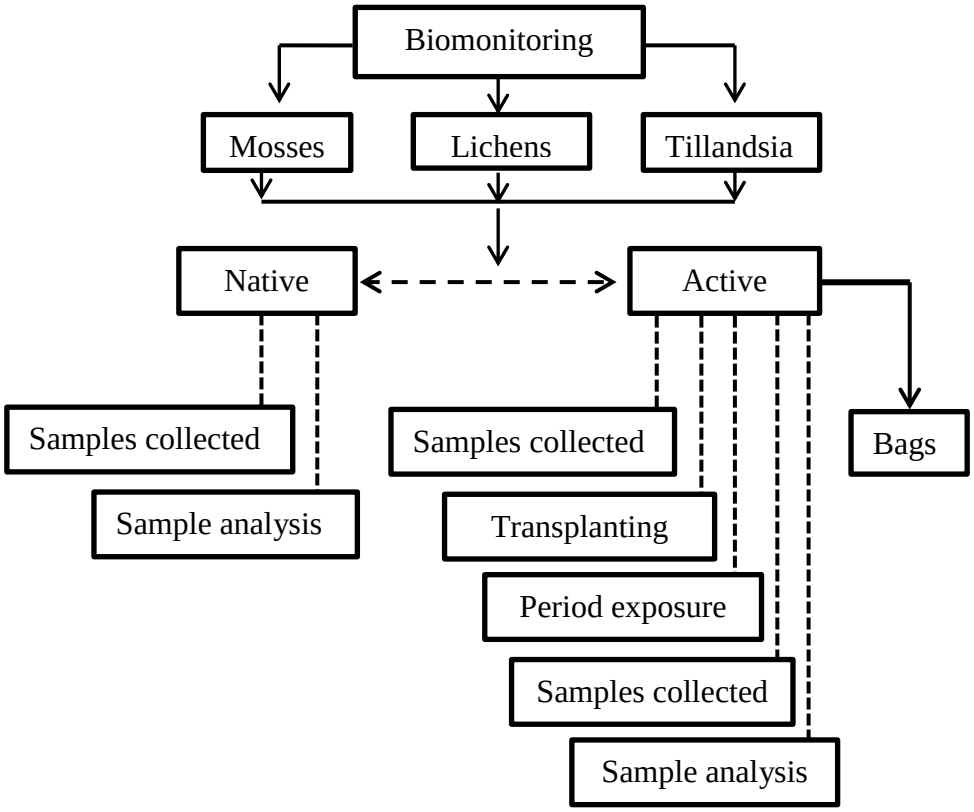

Figure 1.1 General scheme of biomonitoring methods using three different biomonitors

Biomonitoring assumes that the concentration of trace elements in aerosols and deposition, determined using a proper biomonitors reflects proportionally the conditions or health of ecosystem [5,6]. This implies that the biomonitor should be concentrate the element of interest and quantitatively reflect its ambient

conditions. In general, a good biomonitor should be present the following charfacteristics:

- Accumulate pollutants without being killed;
- Be perennial;
- Pollutants should be easily measured and the information should provide information about the level of pollutant deposition;
- Be resistant, sedentary, of scarce mobility;
- Be easy to collect and identify; and
- Be representative of area of study.

1.2.1. Lichens as biomonitor

Lichens are considered one of the most studied biomonitors, and were defined as “permanent control systems” for air pollution assessment because of their high sensitivity towards specific pollutants and ability to store pollutants in their biological tissues [6,9,10].

Lichens consist of a symbiotic association of two organisms composed of a fungus partner (the mycobiont) and a green or blue-green alga partner (the photobiont) in which the algal provides essential nutrients (it contains chlorophyll) through photosynthesis for the fungal, while fungal is responsible for taking up water and mineral and supplies mechanical support to the alga [7,9,10].

Figure 1.2 Flavoparmelia caperata lichen

Lichens occur in many environmental conditions and can grow on almost any surface as bark trees, mosses, on other lichens, rocks, walls, gravestones,

roofs, exposed to soil surfaces. Lichens are perennial, grow slowly and do not have cuticles or stoma, making them perfect biomonitors due to that all the contaminants are absorbed over the entire surface of the lichen (thallus).

1.2.2. Tillandsia species

Tillandsia or commonly known as air plants are epiphytes plants (grows upon another plant) accounting for approximately 550 of the over 2500 species of the bromeliad family. They are natives in warmer climates and can be found from jungle to arid desserts environments, thus as also from high mountains regions to sea level in different size, shape, texture, bloom, and color [11]. Most *Tillandsia species* use their root as anchors to attach themselves to trees, electric wires, rocks, etc., and to absorb water and nutrients of air through their leaves called trichrome. These plants are hardy, adaptable and tolerant to extreme environmental conditions, that require minimal care and minimal conditions as bright light and good air circulation and water [11].

Figure 1.3 *Tillandsia* species a) *Tillandsia tricholepis;* b) *Tillandsia usneoides*; c) *Tillandsia meridionalis*; and d) *Tillandsia capillaris*

1.3. Trace elements

Trace elements (TE) are chemical elements and natural constituents of the earth's crust with a density greater than 5 g/cm^3 and an atomic number greater than twenty, except alkali metals, alkaline earth, lanthanides and actinides [12]. The elements are considered as TE when the presence of the elements are found to concentrations below mg kg^{-1}. Most of the trace elements may be important in the nutrition of plants, animals or humans (e.g. Cu, Cr, Mn, Ni, V, and Zn). In contrast others elements may do not have positive nutritionl effects (e.g. Cd, Hg, and Pb). However, all elements may cause toxic effects, even some of them at a very content level. Their toxicity depend basically on their chemical form, residence time, and their concentration [6,12–14]. Because of these elements do not decay with time, their emission, accumulation and dispersion into environment is a serious problem due to the increasing combustion of fossil fuels, urbanization, and expansion of industrial activities [6,12]. The sources of TE can come of both, natural or anthropogenic origin.

1.3.1. Natural

The main source of elements released in the environment comes from crustal material through of both weathering on (dissolved) and erosion from (particulate) the Earth's crust (surface) or injected into the atmosphere by volcanic activity. Both sources account for 80% of all the natural sources, while the forest fires and biogenic sources, account for 10% each [15].

1.3.2. Anthropogenic

The anthropogenic emissions de trace elements mainly enter into environment via three routes: (i) deposition of atmospheric particulates (e.g. smelting, mining, fossil fuel combustion, municipal waste incineration, phosphate mining and cement production); (ii) disposal of metal enriched sewage sludge and sewage effluents, use of fertilizers and pesticides as agrochemicals, and animal

waste released on terrestrial and aquatic environment; and (iii) by-product of mining processes.

1.4. Rare earth elements (REE)

Rare earth elements (REE) is a group of seventeen chemical elements of the periodic table, specifically fifteen lanthanides plus scandium (Sc, 21) and yttrium (Y, 39). The lanthanides conform the followings elements: lanthanum (La, 57), cerium (Ce, 58), praseodymium (Pr, 59), neodymium (Nd, 60), promethium (Pm, 61), samarium (Sm, 62), europium (Eu, 63), gadolinium (Gd, 64), terbium (Tb, 65), dysprosium (Dy, 66), holmium (Ho, 67), erbium (Er, 68), thulium (Tm, 69), ytterbium (Yb, 70), and lutetium (Lu, 71) [16]. These elements have a variety of isotopes and some have nuclear origins.

REE are moderately abundant in the earth's crust, some even more abundant than copper, lead, gold, and platinum, but are not concentrated enough to make them easily exploitable economically, although there are minerals where lighter (LREE, La-Eu) and heavier (HREE, Gd-Lu) are concentrated. The importance of the REE is reflected by their similar chemical properties that arise as a result of their trivalent charge and the similar ionic radii. Furthermore, the importance come from the stability of their distribution after their fractionation processes in the mantle, so they attest for their original mineral phase even after being mobilized into the hydrosphere. However, this feature makes to the REE relatively difficult to separate from one another. Actually the REE are found in a numerous consumer product such as laptop computers, disk drives, cell phones, televisions, and are used in automotive catalytic converters, petroleum refining, lasers, security applications, fuel cells, magnetic resonance imaging, agricultural, hybrid electric vehicles, solar energy, light-emitting diodes, windmills, permanent magnets, battery alloys, ceramics, wind turbines, compact fluorescent light bulbs and powerful tools for tracing geochemical processes [17–22].

1.5. Layout of this manuscript

This Ph.D. thesis is an article-based one, which means that section "Results and discussion" is an adaptation of journal papers already published,

submitted or yet to submit. For the sake of simplicity, the material and methods are introduced in the traditional way and the reader is just to referred backward, when one reaches this section in the papers (Section 4 to Section 7).

The thesis chapters are organized as follows:

Chapter 1 introduces the introduction and Chapter 2 the objectives of the study.

Chapter 3 presents all the methodology, statistical tools and materials that were adopted for the elaboration of the results discussed in Chapters (4 to 7).
Chapters 4 to 7 are scientific articles resulting from the researches that were published (Chapter 4 and 5) and submitted (Chapters 6, 8 and 9) to international journals (Chapter 7 in process):

Chapter 4 approached the method of passive biomonitoring (*in situ*) which the lichen species *Flavoparmelia caperata* were collected in different context (urban, peri-urban and rural areas) with the aim of quantified the concentration of sixteen elements (Al, As, Ba, Ca, Cd, Cr, Cu, Fe, K, Mn, Ni, Pb, Rb, Sb, V, and Zn), and determine their possible sources of pollution. To this end, chemometric tools, such as Hierarchical Cluster Analysis (HCA) and Principal Component Analysis (PCA) were used.

Chapter 5 presents a study of atmospheric deposition of toxic elements (As, Ba, Cr, Cu, Fe, Ni, Pb, Sb, V, and Zn) near to a tannery industry by collecting black material deposited on leaf surfaces of cinnamon trees. The aim was to verify if black material collected for three periods (May 2016, September 2018, and October 2017) on the surface of the plants are from natural origin or related to tanning activities.

Chapter 6 approached the method of active biomonitoring using the specie *Tillandsia capillaris* as biomonitor in Huancayo city, Junín, Peru. The objective of this study was to investigate the air quality of urban, peri-urban areas, and one rural area, thus as their map distribution of each trace element.

Chapter 7 presents a study in which three species of *Tillandsia* (*T. meridionalis, T. tricholepis,* and *T. usneoides*) were used as biomonitors with the aim to evaluate and to compare the air quality in different areas (industrial and urban) inside the city of Rio de Janeiro, Brazil.

Chapter 8 depicts a study related to the evaluation of the impact of the Rio 2016 Olympic Games on air quality in the metropolitan region of Rio de Janeiro. In this study, three periods were considered: A (before the Olympic Games – July 1 – August 4, n=35 days); B (during the Olympic and Paralympic Games - August 5 - September 18, n = 44 days), and C (after the Olympic Games - September 19 - October 31, n = 43 days). The objective was to evaluate the influence and behavior (reduction or increase) of the pollutants (PM_{10}, SO_2, CO, O_3 and NOx) in six different areas (Bangu, Iraja, São Cristóvão, Tijuca, Copacabana and Centro) from Rio de Janeiro city.

Chapter 9 presents a work which, four calibration multivariate methods were proposed: two regularization methods (Ridge Regression (RR) and Least Absolute Shrinkage and Selection Operator (Lasso)) and two reduction methods (Principal Components Regression (PCR) and Partial Least Squares (PLS)) with the aim to correct spectral interferences and spectral overlap from light rare earth elements (REEs) and barium polyatomic ions (MO^+ and MOH^+) over the heavy rare earth elements, during the analysis by inductively coupled plasma mass spectrometry (ICP-MS).

Chapter 4 - De La Cruz, A. R. H., De La Cruz, J. K. H., Tolentino, D. A., & Gioda, A. (2018). Trace element biomonitoring in the Peruvian andes metropolitan region using Flavoparmelia caperata lichen. *Chemosphere*, *210*, 849–858. https://doi.org/10.1016/j.chemosphere.2018.07.013.

Chapter 5 - Cruz, A. R. H. D. La, & Ferreira, L. D. S. C. (2018). Biomonitoring of Toxic Elements in Plants Collected Near Leather Tanning Industry. *Journal of the Brazilian Chemical Society*, *0*(0), 1–9. https://doi.org/http://dx.doi.org/10.21577/0103-5053.20180174 J.

Chapter 6 - De La Cruz, A. R. H., Ayuque, O. R. F., De La Cruz, R. W. H., Gioda, A. (2018). Air quality biomonitoring of trace elements in the metropolitan area de Huancayo using transplanted *Tillandsia capillaris* as biomonitors. Submitted to the Journal: Annals of the Brazilian Academy of Sciences.

Chapter 7- De La Cruz, A. R. H., Andrade, V. P., Antaki, C. Z., Dos Santos, E. J. M., De Souza, J. R., Saint'Pierre, T. D., Gioda, A. (2018). Use of three *Tillandsia*

species as biomonitors for evaluating urban-industrial pollution in Brazil. Aimed Journal: Ecological Indicator.

Chapter 8 - De La Cruz, A. R. H., Calderon, E. R. D., França, B. B., Réquia, W. J., Gioda, (A). (2018). Evaluation of the impact of the Rio 2016 Olympic Games on air quality in the city of Rio de Janeiro, Brazil. Submitted to the Journal: Atmospheric Environment.

Chapter 9 - De La Cruz, A. R. H., Saint'Pierre, T. D., Gioda, A. (2018). Application of univariate and multivariate calibration methods for interferences correction in the determination of Rare earth Elements by Inductively Coupled Plasma Mass Spectrometry. Submitted to the Journal: International Journal of Environment Analytical Chemistry.

2
Objectives

2.1.
Geral objective

To evaluate the air quality in different locations using a variety of tools: Biomonitoring passive and active, chemical analysis, method development, application of statistical tests, and multivariate methods.

2.2.
Specific objectives

- To use the *Flavoparmelia caperata* lichen as biomonitor to evaluate the air pollution levels of 16 trace elements (Al, As, Ba, Ca, Cd, Cr, Cu, Fe, K, Mn, Ni, Pb, Rb, Sb, V, and Zn) at different locations (urban, peri-urban and rural site).
- To verify if black particles deposited in the soil and on the surface of the leaves from cinnamon trees near leather industry are from natural origin or related to tanning activities.
- To use the specie *Tillandsia capillaris* as biomonitors to investigate the air quality of trace elements and their distribution in urban, peri-urban and rural areas around the Huancayo city.
- To evaluate comparatively the biomonitoring capacity of three *Tillandsia* species (*T. meridionalis, T. tricholepis,* and *T. usneoides*) and assess the atmospheric levels of trace elements determined in different urban and industrial areas
- To evaluate the ambient air pollution before, during, and after the 2016 Rio Olympic Games using multiple comparisons of means to assess the temporal variation and compare our results to those from similar studies.
- To construct multivariate models with the aim to interference correction in the rare earth element analysis.

3
Materials and Methods

Since this thesis is based on an article layout for the presentation of the section "Results and discussion", the statistical tools (item 3.1) and methods (item 3.2 to 3.7) will be presented here and omitted in the respective articles.

3.1.
Statistical tools

3.1.1.
Least Significant Difference (LSD)

LSDs are basically and extend Student's *t* test which uses a more comprehensive estimate of the "noise" or error in the data. Least Significant difference is the value at a particular level of statistical probability (e.g. $p < 0.05$ – means with 95% accuracy). The difference between two means is declared significant at any desired level of significance if it exceeds the value derived from the general formula:

$$LSD = \frac{t(\sqrt{2MSE})}{\sqrt{n}} \quad (1)$$

where *t* is the critical, tabled value of the t-distribution with the degrees of freedom (df) associated with mean squared error (MSE), the denominator of the F statistic and n is the number of scores used to calculate the means of interest. LSD is a simple calculation that allows the means of two or more pre-determined varieties to be compared.

3.1.2.
Tukey's Honestly-significant-difference (HSD) test

Tukey's test is a single-step multiple comparison procedure and statistical test. It allows comparing the means of the *t* levels of a factor after having rejected the null hypothesis of equality of means using the ANOVA technique. Tukey's

test was designed for a situation with equal sample sizes per group, but can be adapted to unequal sample sizes as well. The formula for Tukey's test is presents in equation 2:

$$HSD = q\frac{\sqrt{MSE}}{\sqrt{n}} \quad (2)$$

where *q* is the relevant critical value of the studentized range statistics and *n* is the number of scores used in calculating the group means of interest.

3.1.3. Ward's method (Minimum variance method)

Ward's method, in statistics is a criterion applied in hierarchical cluster analysis (HCA). Ward's method is an alternative to single-link clustering. This method starts with *n* cluster, each containing a single object. These *n* cluster are combined to make one cluster containing all objects. Therefore, the Ward's method says the distance between two clusters, A and B, is how much the sum of squares will increase when we merge them:

$$\Delta(A,B) = \sum_{i\in AUB}\|\vec{x}_i - \vec{m}_{AUB}\|^2 - \sum_{i\in A}\|\vec{x}_i - \vec{m}_A\|^2 - \sum_{i\in B}\|\vec{x}_i - \vec{m}_B\|^2 \quad (3)$$

$$= \frac{n_A n_B}{n_A + n_B}\|\vec{m}_A - \vec{m}_B\|^2 \quad (4)$$

3.1.4. Pearson's correlation

The Pearson correlation coefficient is a measure of the strength of the linear relationship between two variables *X* and *Y*. The Pearson's correlation can range from -1 to 1. If the value is 1, indicates a total positive linear correlation, 0 represent nonlinear correlation, and -1 value indicate the total negative linear correlation.

3.1.5. Shapiro-Wilk Test

The Shapiro-Wilk test is a test to tell if a random sample comes from a normal distribution. The test rejects the hypothesis of normality when the p-value ≤ 0.05.

3.2.
Passive monitoring with *Flavoparmelia caperata* lichen

The following description of material and methods refer to chapter 4, page 67.

3.2.1.
Study area and sampling sites

Huancayo is the capital of the Junín region of Peru. Located at about 3,500 meters above sea level, it is the main commercial center of the Peruvian Central Andes and features an estimated population of 507,075 as of 2016 [23]. Huancayo encompasses an area of 319.4 km^2 and is nestled in the Mantaro Valley, surrounded by mountains that act as natural barriers to air circulation (see Figure E.1) and agricultural cities that produce a significant amount of vegetables, grains, potatoes, and other crops [24]. The climate is temperate with an annual mean temperature of 12 °C and precipitation of 517 mm [25]. Western and southwestern winds prevail in the region (Figure E.2).

Vehicular traffic is likely the main source of pollution in the area. There is an automotive park with 64,576 vehicles [23] that use unleaded gasoline, diesel oil, or compressed natural gas as fuel. Pollutants are also released from point sources, such as car repair businesses, domestic heating systems, construction/demolition activities and long-distance pollutant transport from mining and metallurgical companies located approximately 100 km from the city [26].

The MAH has peculiar peri-urban characteristics due to the strong interaction between its urban and rural areas[27,28]. According to land use, anthropogenic activities, and proximity to pollutant emission sources, the ten sampling sites were divided into two urban sites: Huancayo (U1) and Chilca (U2), seven peri-urban areas: Huancan (PU1), Sicaya (PU2), San Agustin de Cajas (PU3), Concepcion (PU4), Orcotuna (PU5), Chupaca (PU6), and Huayucachi (PU7); and one rural area, Ahuac (R). A non-contaminated area was categorized as a control site (CS). More details about the sampling sites are presented in Table 3.1 and Figure 3.1.

Table 3.1 Short description of the sampling sites

Sites	Latitude Longitude	Population (A)	Description
Huancayo (U1)	12°4′ 20″ S 75°12′ 29″ W	117,559	Residential and commercial area with an intense car, trucks, bus, railway, and motorbike traffic.
Chilca (U2)	12°4′ 44″ S 75°12′ 7.7″ W	86,496	Urban-residential-commercial area with little industries and heavy traffic road
Huancan (PU1)	12°6′ 29″ S 75°12′ 14″ W	21,212	A neighbor from U2 is an urban area with high-density traffic and agricultural activities.
Sicaya (PU2)	12°0′ 59.96″ S 75°16′41.95″ W	8,048	Located to 11.2 km far from U1, at hand-right of central road. It is considered the largest area of farmland with light traffic
San Agustín de Cajas (PU3)	11°59′ 45.52″ S 75°14′ 43.42″W	11,378	Located to 9.9 km far from U1, at left-right of central road, has medium traffic flow and agricultural activities.
Concepción (PU4)	11°55′ 06″ S 75°18′ 46.4″ W	14,829	Located at 21.6 km far from U1 with heavy traffic, agriculture, commerce, handicraft, dairy plant and touristic activities
Orcotuna (PU5)	11° 58′ 07″ S 75° 18′ 28″ W	4,137	Located at 17.2 km of U1, which developed activities as agriculture, livestock and artisanal manufacturing.
Chupaca (PU6)	12° 03′ 36″ S 75° 17′ 24″ W	22,099	It is crossed by the Cunas River with heavy traffic, commerce, agriculture, and livestock.
Huayucachi (PU7)	12°8’15.91’’ S 75°13’23.85’’W	8,581	Has medium traffic flow and dedicated exclusively to agriculture and livestock
Ahuac (R)	12° 4′ 52.94″ S 75° 19′ 7.79″ W	5,929	A rural area far from the main roads and downtown
Control site (CS)	12° 8′ 10.32″ S 75° 8′ 26.37″ W		Place covered by thousands of trees and far city, considered as a place with the minimum impact of pollutants

[A] Estimated population 2016 [23].

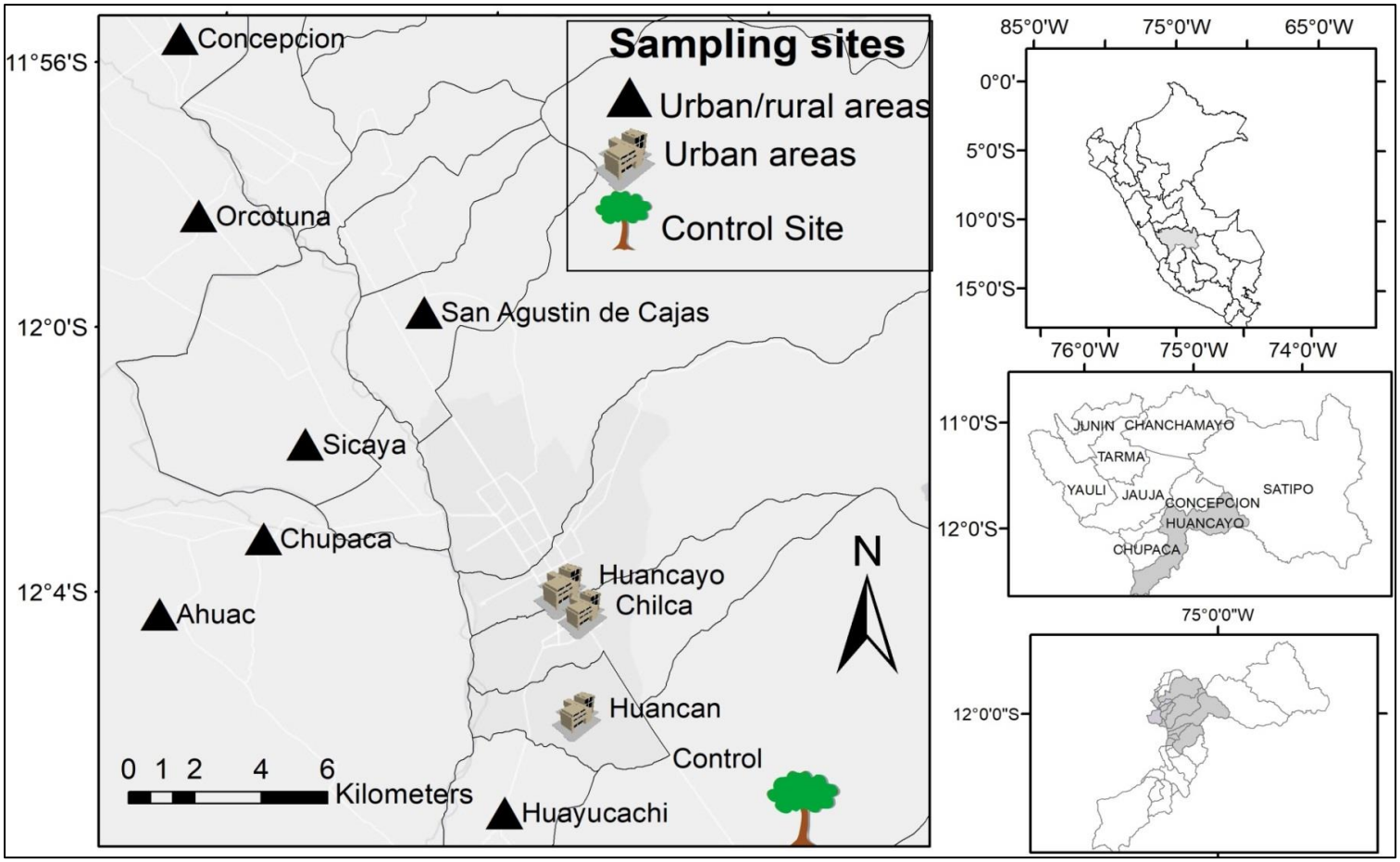

Figure 3.1 Location of the sampling sites. Map prepared with Arc GIS 10.0 software

3.2.2. Sampling and analysis procedures

The foliose lichen *F. caperata* was selected for use in this study because it is very common in South America, easy to recognize and sample, and is present in the study area. Samples were collected from eucalyptus tree trunks located at each sampling site (Figure 3.1) from January to February 2017 after a week of sunny weather. At each sampling site, a determined number of individual samples (N) were collected from an area with a diameter of 500 m, with a minimum distance of 100 m between each sample, to avoid pseudoreplication. In total, 63 (U1=7, U2=5, PU1=6, PU2=6, PU3=6, PU4=8, PU5=6, PU6=7, PU7=6, and R=6) lichen samples with approximately the same diameter were collected to avoid age-related differences. Lichen samples (CS=5) were also collected from a non-contaminated area to serve as controls. Latex gloves were used to detach the thallus of the lichen from the substrate at a height of 1.5 - 2.0 m to avoid contamination by soil particles. Paper bags were used to store samples, which were brought to the laboratory for analysis [29].

In the laboratory, lichen samples were manually cleaned not washed, so that the elements trapped on the surface could be measured. Cleaning was performed with plastic materials and latex gloves and was intended to remove extraneous materials, such as dead lichen tissue, bark substrate, other lichen or mosses species, and insects. After cleaning, the samples were dried at 65 °C, milled, homogenized, sieved (about 50 mesh), and stored in Falcon tubes. About 200 ± 3 mg of each lichen sample was weighted in triplicate and submitted for chemical decomposition and subsequent analysis. Chemical decomposition was carried out using 65 % HNO_3 (3.0 mL), H_2O_2 (0.5 mL), and HF (0.1 mL) at 200 °C in a Savillex Teflon bottle for four hours on a hot plate [30,31]. After decomposition, the samples were suitably diluted to reach 2 % HNO_3 and then were analyzed with quadrupole Elan DRC II inductively coupled plasma mass spectrometer (ICP-MS) (PerkinElmer SCIEX, Norwalk, CT, USA). The instrumental conditions in which lichen samples were analyzed are presented in Table E.1 (Supplementary Material). To correct and/or compensate for non-spectral interferences and matrix effects, ^{103}Rh was used as the internal standard (IS). Trace elements were quantified by six-point external calibration. All the

reagents ($HNO_3/HF/H_2O_2$) were of high purity, and the solutions were prepared with ultrapure water (18.2 MΩ cm) obtained from a Milli-Q water (Milli-Q water purification system, Millipore Corp., USA).

To check the accuracy of decomposition and analytical procedures, three certified reference materials for plants were used: SRM 1515 'Apple leaves', and SRM 1573 'Tomato leaves' which were published by National Institute of Standards and Technology (NIST, Gaithersburg, USA) and BRC-670 'Aquatic plant', which was published by the Institute for Reference Materials and Measurements (European Commission, Belgium). All the obtained results were within the certified and/or suggested values. Estimated using the relative standard deviation of three replicates, the precision of analysis was found to be below 7% and recovery was found to be 70% - 120% (Table E.2 - Table E.4, Supplementary Material).

3.2.3. Enrichment factor

The enrichment factor (EF) was computed as a percentage for each element and monitoring point using the following equation:

$$EF_E\,(\%) = \frac{CE_A - CE_C}{CE_C} x\ 100 \qquad (5)$$

where EF_E is the enrichment factor of the Element E, CE_A is the concentration of element E in the lichen sample, and CE_C is the concentration of Element E in the control sample. For the interpretation criteria, EF values greater than 100 % were considered to indicate significant enrichment (i.e., a concentration at least twice that of the control site). EF values of 50 – 100 % were to indicate moderate enrichment, while EF values of less than 50 % were considered to indicate normal conditions [32].

3.2.4. Multivariate analysis

Differences between the concentrations of trace elements at the control site and monitoring sites were analyzed by a one-way analysis variance (ANOVA),

and subsequent post-hoc comparisons were performed using the least significant difference (LSD) Tukey test. A value of $p < 0.05$ was considered significant.

Principal component analysis (PCA) with Varimax rotation was used to identify potential sources of elements in the study area. PCA was performed on a standardized (zero mean and unit variance) lichen data set. Only significant factors (Fas) with Eigenvalues greater than 1 were considered to be meaningful in the analysis and interpretation [33]. Loading correlation coefficients with values of 0.7 or higher for Fas and the original variables were considered to be influential sources of each Fa.

Furthermore, hierarchical cluster analysis (HCA) with Ward's method of linkage and squared Euclidean distance to identify similarities was used to segregate and characterize associations within the group of elements based on concentration levels as well as to identify probable pollution sources. All statistical analyses were performed using CRAN R free software, version 3.3.2 [34] using the following R packages: factoextra [35], ggplot2 [36], cluster [37,38], and psych [39].

3.3. Biomonitoring near leather industry

The following description of material and methods refer to chapter 5, page 83.

3.3.1. Study area

This study was conducted in the city of Nova Esperança do Sul (S1, 29° 24′ 24″ S, 54° 49′ 50″ W), state of Rio Grande do Sul (RS), Brazil (Figure 3.2). The city S1 is located in the southernmost part of the country with 5,087 inhabitants [40], and cover an area of about 190,85 km^2 of which 0.72 % is related to the urban area, 27,15 % is used to agricultural activities and 72 % is field. The climate is subtropical and the temperature varies between a maximum of 38 °C and a minimum of 3 °C, with 17,8 °C as medium temperature [41]. The average annual of precipitation is of 1795 mm and the relative humidity varies from 30 to 95%. The predominant wind direction is from the southwest (called "minuano") and north [41]. In this region, two sites were chosen: S1A (center), located about 300 m far from the tannery and S1B (plateau), located about 5 km from the

tannery.

As the presence of sooty mold, a fungus spread by insects may cause deposits of black particles on leaves of various plants, an erroneous affirmation may be stated if only the study area was evaluated. In order to identify if black particles deposited on leaf surface in S1 are from the natural or anthropogenic origin, an area located about 100 km from Rio de Janeiro (RJ) without pollution of industries or traffic influence, but with tree leaves containing black particles on the leaf surfaces was considered. Lumiar (S2, 22° 22′ 0.12″ S, 42° 12′ 0″ W), district of Nova Friburgo, Brazil (Figure 3.2) is a mountainous region in the Atlantic Forest covering an area of 7 km^2 and 5,000 inhabitants [40]. Climate is warm and temperate with average annual precipitation and temperature of 1437 mm and 19.5 °C, respectively.

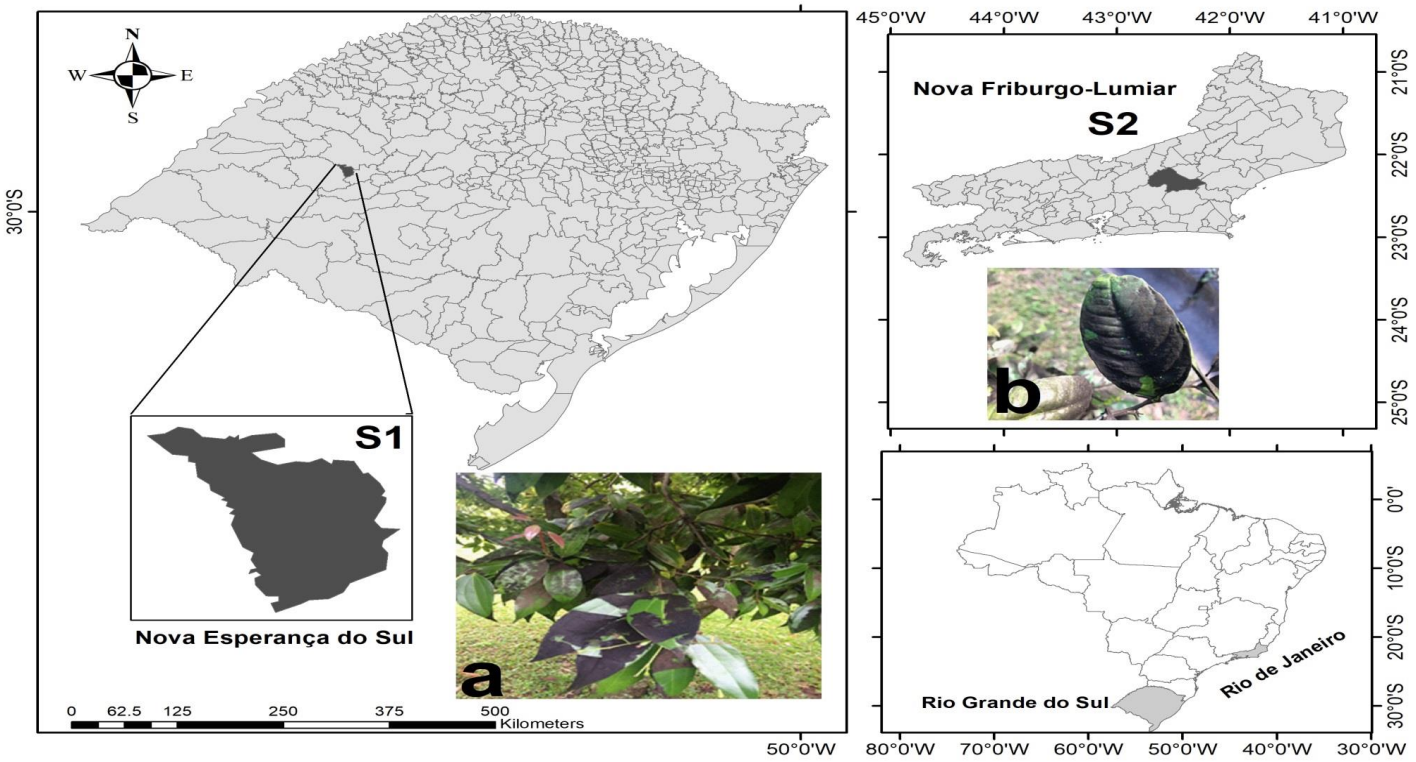

Figure 3.2 Location of the study area and samples collected in (S1) Nova Esperança do Sul, RS and (S2) Nova Friburgo-Lumiar, RJ. (a) Leaves of cinnamon tree covered by black particles at S1 and (b) leaves of citrus lemo tree covered by black particles at S2. The map was prepared with ArcGIS 10.0 software.

3.3.2. Sampling

Sampling of cinnamon tree (*Cinnamon zeylanicum*) leaves was carried out in three periods; May 2016 (P1), September 2016 (P2) and October 2017 (P3) at Nova Esperança do Sul (S1). Cinnamon trees grow in tropical areas, have left of medium size and are elongated, slender, and oval to lanceolate in shape. About 300 g of both leaves without black particles on its surface (termed clean leaves (CL)) at S1A (CLS1A) and S1B (CLS1B) and leaves with particles at S1A were collected in the three periods (Figure 3.2). Leaves containing black particles were not found at site S1B. Additional dry leaves (DL) were also collected at S1A (termed DLS1A). Soil samples (about 500 g) were also collected at the surface and at 10 cm depth in places adjacent to the trees from which leaf samples were collected (SS1A and SS1B).

For comparison purpose, clean leaves (CLS2) and leaves of the lemon tree (citrus lemon) covered by black particles (PS2) (Figure 3.2) were collected at Lumiar (S2) on February 2017. Sampling collection was at a height of 1.5-2 meters above the ground, using gloves latex, stored in self-sealing plastic bags and subsequently transported to the laboratory.

3.3.3. Sample preparation and chemical analysis

In the laboratory, the material (black particles) deposited on leaf surface was carefully removed using a plastic knife and stored in Falcon tubes (50 mL). From each site and period, approximately 5 g of black particles were removed from leaves surfaces to guarantee the homogeneity during analysis. The black particles, clean leaves, and soil samples were dried in an oven at 50 °C until completely dried. Dried samples were grounded in agate ceramic mortar, homogenized, sieved (passed through a 100 mesh nylon sieve) and stored in Falcon tubes. The elements were extracted from 250 ± 3 mg samples using mixed-acid digestion HNO_3 (3.0 mL) + H_2O_2 (0.5 mL) and HF (0.1 mL) method into a Teflon bottle (Savillex, Minnesota, USA) on a hotplate for 4 h at 250 °C [42]. After digestion, the samples were cooled, opened and evaporated at 175 °C to begin the drying. In order to remove remnant HF, 3.0 mL of HNO_3 was added and

evaporated of two to three times [43] and then transferred into a Falcon tube (15 mL) and diluted with deionized water. The concentration of As, Ba, Cr, Cu, Fe, Ni, Pb, Sb, V, and Zn in the final solutions were measured by Inductively Coupled Plasma Mass Spectrometry (ICP-MS), using an Elan DRC II mass spectrometer (PerkinElmer, USA). Prior analysis of ICP-MS, the instrumental parameters were adjusted to provide minimal oxide formation rates of Ce (< 3 %) and double charged species ratio of Ba (< 2 %), respectively. Operating conditions for sample analysis by ICP-MS are presented in Table 3.2.

Table 3.2 Instrumental conditions for the ICP-MS measurements.

ICP-MS conditions	Values
RF power / W	1150
Frequency /MHz	27.2
Plasma gas flow rate / (L min^{-1})	1.5
Auxiliary gas flow rate / (L min^{-1})	0.55
Nebulizer gas flow rate / (L min^{-1})	0.97
Sample uptake rate / (mL min^{-1})	0.6
Measurement mode	Dual (PC/analog)
Acquisition time /s	1
Dwell time /ms	200
Replicates	6

The oxide ratio of CeO^+/Ce^+ and double charged species ratio of BaO^+/Ba^+ were maintained below 0.03 and 0.02, respectively. ICP-MS: inductively coupled plasma mass spectrometry; RF: radio frequency.

^{103}Rh was used as internal standard (IS) to correct and/or compensate non-spectral interferences and matrix effects. The elements were quantified through a six-point external calibration. Blank and triplicate samples were analyzed to provide quality control. The sample digestion and analysis procedure were checked using three certified reference material (CRM): SRM 1648a “Urban Particulate Matter”, SRM 1515 “Apple Leaves”, and SRM 8704 “Buffalo River Sediment” which were published by National Institute of Standards and Technology (NIST, Gaithersburg, USA).

The limits of detection (LOD) and limits of quantification (LOQ) were calculated as three times and ten times the standard deviation of 10 blank measurements divided by the slope of the analytical curve. Table 3.3 shows the LOD, LOQ, and the extraction efficiencies of the CRMs used. As it is seen, extraction efficiencies higher than 80 % were obtained for most elements in both CRMs.

3.3.4. Statistical analysis

Differences between concentrations of toxic elements among clean leaves (CL), black particles collected at each period (P1, P2, and P3), and soil samples were analyzed by a one-way analysis variance (ANOVA), and subsequent *post-hoc* comparison was made using significant difference (LSD) Tukey's test (value of $p < 0.05$ was considered to be significant).

The enrichment factor (EF) using the concentration of each toxic element was calculated by Equation 1 with the aim to evaluate the source contribution:

$$\mathrm{EF_X} = \frac{(\mathrm{C_X}/\mathrm{C_n})_{\mathrm{sample}}}{(\mathrm{C_X}/\mathrm{C_n})_{\mathrm{background}}} \quad (6)$$

where Cx and Cn are the concentration of the element X and *n* in the sample and in the background. "Sample" refers to the concentrations of the elements present in the black particles removed from the leaves at Nova Esperança do Sul (S1) and Lumiar (S2), while "background" for S1 consists in the average soil composition value of both soils (superficial and deep) collected in the surrounding [14,44], while the crustal composition given by Taylor and MacLennan [45] was considered for S2. Fe was used as a reference. If EF < 1, the element is depleted in the environment and natural sources are predominant. If EF > 1 means that the element is relatively enriched in the environment; while EF > 5 suggests that a large fraction of the element may be ascribed to anthropogenic sources [46,47].

Hierarchical cluster analysis (CA) was used to identify and characterize the association of the group of elements as well as to have an idea of the probable source. Statistical analyses were performed using CRAN R [34] free software through the following packages: ggplot2 [36], dplyr [48], and ClusterofVar [37].

Table 3.3 Limits of detection (LOD) and limits of quantification (LOQ) by ICP-MS and concentration of Certified Reference Materials of leaves (NIST SRM 151 – apple leaves), PM (NIST SRM 1648 – urban particulate matter) and sediment (NIST 8704 – Buffalo river sediment) used to evaluate the extraction efficiencies.

Element.	LOQ / (µg g-1)	LOD / (µg g^{-1})	SRM – Apple leaves			SRM – Urban Particulate matter			SRM- Buffalo river sediment		
			Certified value / (µg g^{-1})	Found value / (µg g^{-1})	% Extracted	Certified value / (µg g^{-1})	Found value / (µg g^{-1})	% Extracted	Certified value / (µg g^{-1})	Found value / (µg g^{-1})	% Extracted
As	0.004	0.013	0.038±0.007	0.041±0.011	108	115.5±3.9	94.1±4.2	81.5	17	16±2	94
Ba	0.11	0.36	49±2	45.13±1.22	77.9	-	-	-	413±13	409±21	99
Cr	0.02	0.07	0.30	0.34±0.03	113	402±13	347±10	86.3	121.9±3.8	122.4±3.0	100
Cu	0.01	0.04	5.64±0.24	4.94±0.51	87.6	610±70	616±21	101	5.64±0.24	5.04±0.34	89
Fe	4.16	13.73	83±5	76±7	91.0	3.92±0.21	3.53±0.03	90.0	3.97±0.10	3.86±0.20	97
Ni	0.02	0.06	0.91±0.12	1.02±0.05	112	81.1±6.8	80.3±5.2	99.0	42.9±3.7	41.5±2.12	96
Pb	0.09	0.30	0.47±0.02	0.44±0.03	93.3	6550±33	6573±21	94.2	150±17	138±12	92
Sb	0.002	0.006	0.013	0.012±0.004	90.9	45.4±1.4	29.4±3.1	65	3.07±0.32	2.85±0.42	93
V	0.02	0.08	0.26±0.03	0.30±0.04	115	127±11	138±8	109	94.6±4.0	91.2±3.2	96
Zn	0.15	0.49	12.50±0.30	13.40±1.30	107	4800±270	4286±167	89.2	408±15	419±7	103

- Not reported

3.4.
Active biomonitoring in Huancayo city

The following description of material and methods refer to chapter 6, page 94.

3.4.1.
Study area

The present study was undertaken in the metropolitan area of Huancayo, region Junín (Peru). It is inhabited by 507,075 people [23] and located up 3200 meters above sea level. Huancayo Metropolitan, a Peruvian mountain city, represents a zone peri-urban in development, nestled in the valleys of the Mantaro River and bordered by mountains that act as natural barriers for air circulation, avoiding the pollutant dispersion. Huancayo city has an important agricultural development in their peripheral areas and it is considered central Peru's economical and social center. The climate is temperate with an annual mean temperature of 12 °C and precipitation of 517 mm [25]. Western and southwestern winds prevail in this area (Figure F.1 – Supplementary material). Five sites were chosen for *Tillandsia capillaris* transplanting (Figure 3.3): (a) Huancayo (H, urban area at 3,259 m.a.s.l): The downtown Huancayo, densely populated, where the main source of pollutants is vehicular traffic, (b) Tambo (T, urban area at 3,260 m.a.s.l): neighbourhood of Huancayo city with similar characteristics of downtown, (c) Chupaca (Ch, agricultural-urban area at 3,263 m.a.s.l): is a peri-urban area (it has rural and urban characteristics) situated to 9.7 km southwest of Huancayo. Traffic is medium compared to H and T but has large extensions of agricultural land, (d) San Agustin de Cajas (SC, agricultural-urban at 3280 m.a.s.l): located 9.9 km north of Huancayo city, also is a peri-urban area with land used to agricultural practices, and (e) the rural area, located to 20 km of main urban areas. Traffic is much less than downtown and is mainly composed of public transport and interprovincial buses.

3.4.2.
Transplant experiments

Tillandsia capillaris specimens were collected from the Eucalyptus tree trunk at Paucara (12° 42' 0" S, 74° 41' 0" W), Acobamba Province, Huancavelica

(Peru). This area is located to the south of Huancayo city at approximately 138 km of distance and is characterized by having a minimum contact with pollutants emission sources (considered unpolluted site). Net bags containing ~50 g (6-8 plants) were prepared according to Wannaz and Pignata, (2006) and transplanted simultaneously (active biomonitoring) to the study area In each area, seven bags were hung 2.5 m over the ground at different distances. The process of transplantation was held on the 10th September until 22th of December 2017 and corresponds to the spring season with the minor possibility of rains. After the exposure period, plants were collected, stored in paper bags and transported to the laboratory. Baseline element concentrations were obtained analyzing original samples before transplantation. More detail about transplanting sites can be found in Table F.1.

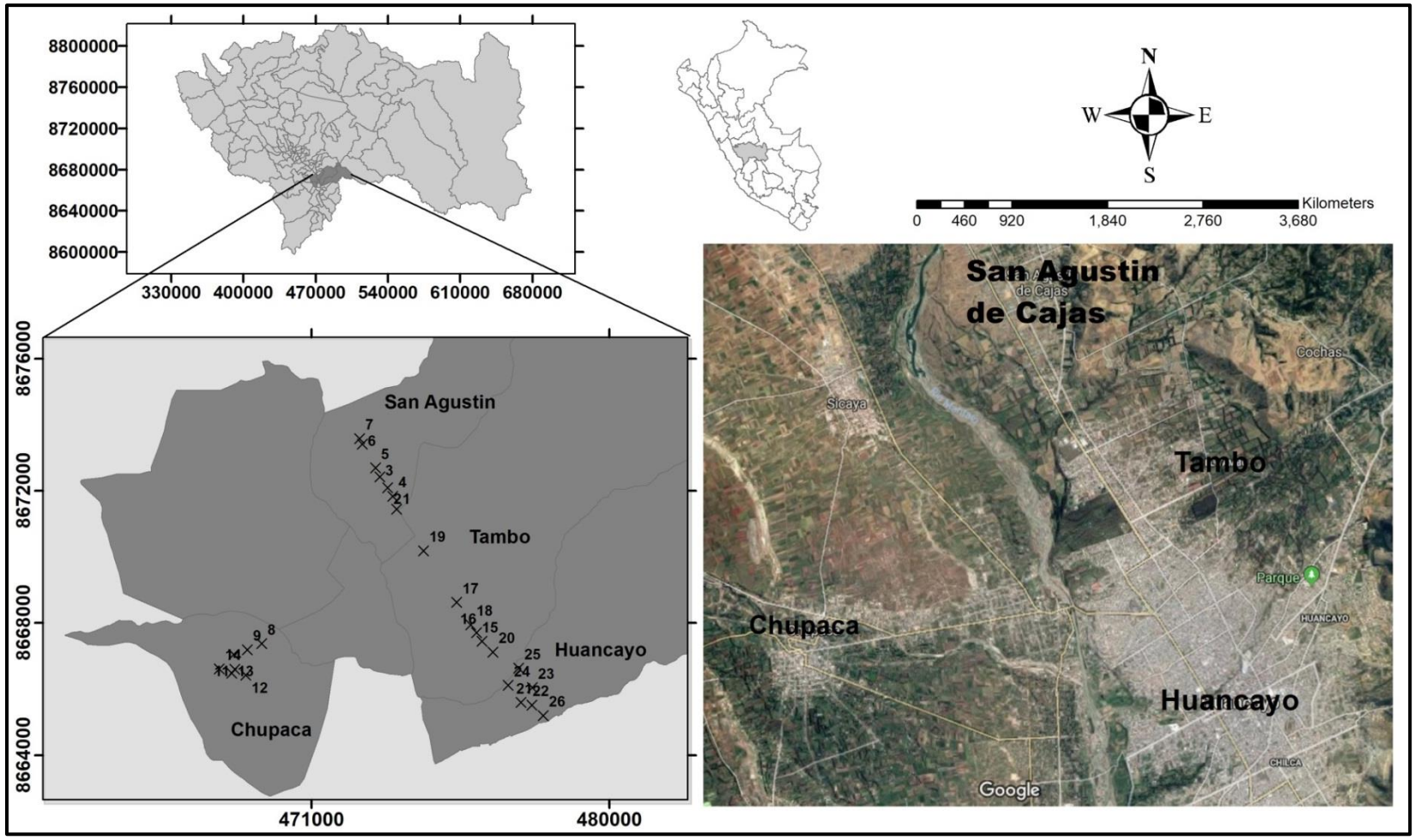

Figure 3.3 Biomonitoring exposure sites in the Metropolitan area of Huancayo, Peru. The Map was prepared with Arc GIS 10.0 software

3.4.3.
Major and trace elements determination

First, all samples were dried until constant weight in an oven at 60 ± 2 °C and then ground in an agate mortar. About 200 ± 3 mg of each sample in triplicate into a Savillex (Teflon bottle) were weighted. Samples were digested using a suprapure mixture of 3.0 mL bi-distilled HNO_3 (Duo-PUR, Milestone, USA), 0.5 mL H_2O_2, and 0.1 mL HF in at hot plate at 250 °C for four hours [30]. After digestion achieved, the samples were cooled, opened and evaporated at 200 °C to beginning dryness. In order to remove remnant HF, 3.0 mL of bi-distilled HNO_3 was added and evaporated to beginning dryness tree times, and then finally the samples solutions were diluted suitably containing 5% HNO_3 into a Falcon tube (15 mL).

Major elements (Al, Ca, Fe, K, and Na) and trace elements (As, Ba, Cd, Ce, Co, Cr, Cu, La, Mn, Ni, Pb, Sb, Sc, Sr, U, V, and Zn) concentrations were analyzed by Inductively Coupled Plasma Mass Spectroscopy (ICP-MS, NexION 300 PerkinElmer, USA). Rh was used as an internal standard to correct data for instrumental drifts and plasma fluctuations. All the solutions were prepared with high purity water (18.2 MΩ cm) obtained from a Milli-Q water system (Milli-Q water purification system, Millipore Corp., USA). Analytical curves with six points for each element were used and fitted using linear regression.

3.4.4.
Analytical quality control

The accuracy of the analysis were checked using the certified reference material (CRM) of plant SRM 1515 “apple leaves” which was published by National Institute of Standards and Technology (NIST, Gaithersburg, USA). Blank samples were measured in parallel with the decomposition and the analysis of the samples. The recoveries were expressed as the ratio of the concentration measured to certified concentrations of SRM 1515. Major and trace elements concentration were expressed in dry weight (μg g^{-1} DW). All certified elements presented satisfying recoveries in the 86.4-112% range (Table 3.4).

Table 3.4 Values obtained for the Certified Reference Material NIST SRM 1515 (n=3).

Elements	Certified	Measured	% extracted
Al	286 ± 9	277 ± 37	96.9
As	0.038 ± 0.007	0.034 ± 0.003	90.4
Ba	49 ± 2	45 ± 3	90.9
Ca	15260 ± 1500	13859 ± 700	90.8
Ce	3.00	2.91 ± 0.22	96.9
Cd	0.013 ± 0.002	0.012 ± 0.002	90.2
Co	0.09	0.10 ± 0.02	112.0
Cr	0.30	0.32 ± 0.10	105.9
Cu	5.64 ± 0.24	5.05 ± 0.28	89.5
Fe	83 ± 5	90 ± 22	107.8
K	16100	15186 ± 814	94.3
La	20	18 ± 2	91.5
Mn	54 ± 3	51 ± 4	94.4
Na	24.4 ± 1.2	24.7 ± 1.1	101.0
Ni	0.91 ± 0.12	0.95 ± 0.07	104.3
Pb	0.47	0.42 ± 0.04	89.4
Sb	0.01	0.014 ± 0.003	106.7
Sc	0.030	0.030 ± 0.001	108.9
Sr	25 ± 2	22 ± 3	86.4
V	0.26 ± 0.03	0.24 ± 0.02	90.7
Zn	12.5 ± 0.3	11.3 ± 0.8	90.6

3.4.5. Statistical treatments

Exposed-to-baseline (EB) ratio has been used to evaluate emission sources of the elements measured. The values obtained from this ratio were assessed according to the scale adopted by Frati et al. 2005 [50], where EB ratio values between 0.75 and 1.25 indicate normal conditions in the environment; while 1.25 < EB < 1.75 indicate accumulation, and EB ratio > 1.75 indicates severe

accumulation of pollutants, which may be related to anthropogenic emission sources.

In order to identify possible groups of elements as tracers of natural or anthropogenic sources of the elements measured in the *T. capillaris* samples, hierarchical cluster analysis (HCA) with Ward's method was used. All statistical analysis in this study was performed by the CRAN R [34] free software.

3.5. Active monitoring with three species of *Tillandsia* genus

The following description of material and methods refer to chapter 7, page 108.

3.5.1. Studied areas and description

The metropolitan region of Rio de Janeiro city (MRRJ, 22° 54′ 10.08″ S, 43° 12′ 28.08″ W), located in Rio de Janeiro state (RJ), Brazil is a large area considered the second largest in Brazil and third largest in South America consisting of 21 municipalities (Belford Roxo, Duque de Caxias, Rio Bonito, Maricá, Niterói, Seropédica, Japeri, Nilópolis etc.) and the capital RJ state. The metropolitan area has a surface total of 6 744.634 km2 and about 12.6 million inhabitants, while the Rio de Janeiro state has 6.498.837 inhabitants estimated in 2016 [40]. This region is the second largest industrial center with industries such as: oil refineries, naval, metallurgical, petrochemical, gas, steel, textile, graphic, publishing, construction, pharmaceutical, cement, furniture, among others. Moreover, the transport medium is integrated by several lines of buses, trains, ferry boats, minor vehicles (taxi, motorbike), which serve to connect inner or externally cities through of roads, freeways, and expressways.

3.5.2. Transplant experiments

A determined number of samples (n=50) of each specie *T. Meridionalis*, *T. usneoides* and *T. tricholepis* individuals for transplanting of similar ages and sizes were collected in April 2017 at Tijuca Forest (un-polluted site). Of a total of

samples, three samples of each specie were randomly selected. These samples were considered as the reference sample (blank) for each specie.

Bags separating each *Tillandsia* specie (three species of each of *T. meridional, T. tricholepis* and similar mass of *T. usneoides*) containing approximately 250 ± 2 g to compensate the mass was prepared according to Bermudez et al. (2009) [51] and transplanted simultaneously to eight areas (Figure 3.4) with different atmospheric pollution sources during May 01-June 31 of 2017.

In each area 6 bags (2 bags by specie) were placed hung or tied on trunk or branches of the trees (specifically under leafs to avoid a direct contact with the rain) at 2 m about ground level for 1 and 2 months (i.e., from 01 may 2017 to 31 may, from 01 may to 31 June respectively, days with rain was not considered). After the determined exposure time, the samples were carefully collected, placed in paper bags and transported to the laboratory. In the laboratory, the samples were cleaned manually of any extraneous material (spider web, insects) using latex gloves, then cleaned samples were dried in an oven at 60 °C, grounded in a ceramic agate mortar and pass through a sieved (about 100 mesh) to homogenize the sample. In Table 3.5 and Figure 3.4 are described and presented the transplanting sites.

Table 3.5 Sites description

Sites	GPS latitude Longitude	Short description
Bus station Novo Rio (NR)	22° 53′ 56.96″ S 43° 14′ 40.00″ W	Located in the downtown with high traffic of bus connecting several cities and regions of Brazil.
Bus station Alvorada (TA)	23° 00′ 4.79″ S 43° 21′ 57.79″ W	Located in Barra da Tijuca, with a very high traffic of bus.
Bus station Central (TC)	22° 54′ 12.61″ S 43° 11′ 29.94″ W	Located in the strict city center, high-intensity traffic, parking lot, railway, subway.
Roadside of Copacabana (C)	22° 58′ 4.85″ S 43° 11′ 16.49″ W	Road with intense traffic bus, cars and a lot of shopping mall
Boat and bus station in Niteroi (N)	22° 53′ 27.63″ S 43° 7.0′ 32.58″ W	Near Guanabara bay with high traffic of boats and bus, and near to parking lot.
Rocinha's Favela (RF)	22° 59′ 9.65″ S 43° 14′ 39.85″ W	Located south zone of Rio de Janeiro with high-intensity traffic (motorbike, cars, truck, bus)
Sao Conrado (HSC) Highway	22° 59′ 34.22″ S 43° 15′ 6.66″ W	Highway with very high intense traffic, two supermarkets and one shopping mall.
Santa Cruz (SC) in the street Joao XXIII	22° 54′ 4.79″ S 43° 43′ 10.86″ W	Located in the direct vicinity of steel industry "Companhia siderurgica do Atlantico (CSA).
Tijuc Forest	22° 56′ 59.61″ S 43° 16′ 17.29″ W	Tropical rainforest considered to be the world's largest urban forest representing the baseline material.

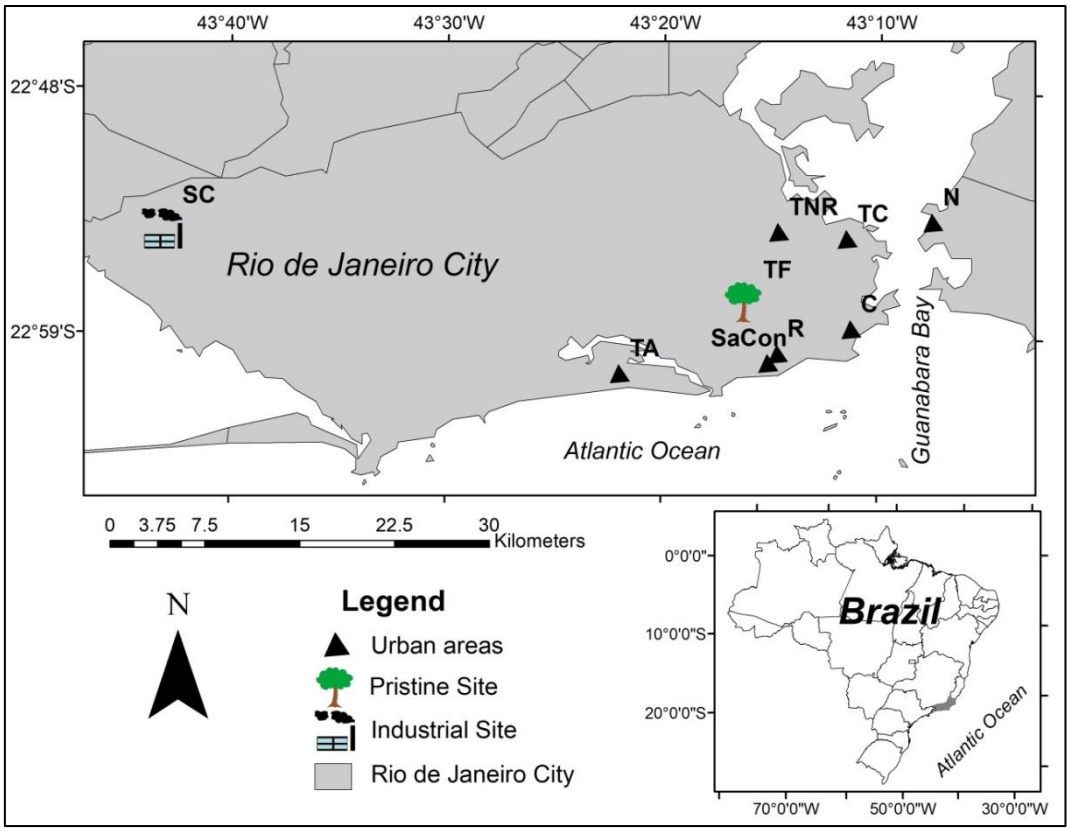

Figure 3.4 Rio de Janeiro area with the location of the pristine and transplanting sites. SC: Santa Cruz, TA: Terminal Alvorada, TF: Tijuca Forest, TNR: Terminal Novo Rio, TC: Terminal Central, C: Copacabana road, N: Niteroi, R: Rocinha, and SaCon: São Conrado highway.

3.5.3. Chemical analysis

Tillandsia samples were digested using triplicate masses about 200 ± 3 mg of each sample using analytical balance into a savillex (Teflon bottle) and adding 3 mL (HNO_3, 65%), 0.5 mL (H_2O_2,), and 0.1 mL (HF,) suprapure mixture acid in at hot plate during four hours and 250 °C [30] at the Laboratório de Espectrometria Atômica (LABSPECTRO, Rio de Janeiro, Brazil) and Laboratório de Quimica Atmosferica (LQA, Rio de Janeiro, Brazil). Finally, the samples were diluted suitably containing 5% HNO_3 and analyzed with Inductively Coupled Plasma Mass Spectroscopy (ICP-MS ELAN DRC II, PerkinElmer, USA) using Rh as internal standard to correct data for instrumental drifts and plasma fluctuations. All the solutions were prepared with high purity water (18.2 MΩ cm) with a Milli-Q-system (Millipore). Standard solution SPEX from the United States was used as the standard.

3.5.4.
Quality control

ICP-MS results were checked by multiple analyses (triplicate) of the samples and certified reference material of plants (SRM 1515 and SRM 1573) from the National Institute of Standards and Technology (NIST, Gaithersburg, USA) and (BRC-670) from Institute for Reference Materials and Measurements (IRMM, European Commission, Belgium). In addition, the blank was measured in parallel with the decomposition and the analysis of the samples. According to the measurements of the repeated samples and reference materials, the precisions, relative standard deviation (RSD), were below 3%. The recovery was 92-108% for ICP-MS. Values for all blank samples were near or to less than detection limits of ICP-MS, and the results were between 79%-105% of the certified values, with coefficients of variation (CV) ≤ 16%.

3.5.5.
Statistical analysis

Normality of the data were assessed using the Shapiro-Wilk test, and non-normal distributed variables were log10 transformed before carrying out parametric statistics. Summary statistics were used to obtain the means and standard deviation and one way ANOVA (Fisher Test, $p < 0.05$) was used to identify the significant difference between pairs of means among the elements and sampling sites with subsequent Least Significant Difference (LSD) post-hoc Tukey test. In order to calculate the accumulation rates of each element after exposed samples of *Tillandsia* species collected in a control site (samples with basal concentration) was used the exposed-to-control ratio (EC ratio) described by Frati et al. (2005) [50], who evaluated the EC ration in five scales: i) 0-0.25: severe loss (SL); (ii) 0.25-0.75: loss (L); (iii) 0.75-1.25: Normal (N); (iv) 1.25-1.75: accumulation (A); (v) >1.75: severe accumulation (SA). Furthermore, hierarchical cluster analysis was performed to identify and characterize group association of elements and thus discuss possible source contamination.

All statistical analysis in this study was performed by the CRAN R [34] free software.

3.6.
Air Quality in the 2016 Olympic Games

The following description of material and methods refer to chapter 8, page 122.

3.6.1.
Study area

This study was conducted in the Rio de Janeiro city that makes up the metropolitan region of Rio de Janeiro state (MRRJ), Brazil. The MRRJ is considered the second largest region in Brazil and the third largest area in South America. The MRRJ has 12.6 million inhabitants and an area of 6,744,634 km^2 divided into 21 municipalities [40]. Vehicular emissions are the main source of air pollution in the MRRJ [52]. According to the last inventory of mobile sources for the city of Rio de Janeiro for 2018 [53], the total fleet (passenger cars, buses, trucks etc.) includes about 3 million vehicles, which are mainly fueled by diesel, natural gas (GNV), ethanol, and gasoline. Stationary sources of air pollution in the MRRJ include oil refineries, naval, metallurgical petrochemical construction, and power plants. Average temperature ranges from 21.1 °C (winter) to 27.3 °C (summer). The climate is dry and cool during the winter and wet and rainy in the summer.

3.6.2.
Study period

The 2016 Olympic Games and Paralympic Games were carried out in Rio de Janeiro from August 5th to August 21st, and from September 7th to September 18th. We defined Olympic Games season into 3 periods: A (before Olympic Games, July 1st -August 4th, n=35 days), B (during Olympics and Paralympic Games, August 5th -September 18th, n=44 days), and C (after Olympic, September 19th - October 31st, n=43 days). The definition of the time period in our analysis corresponds to similar periods considered in previous studies [54–56].

3.6.3.
Sampling and measurement

Figure 3.5 shows the spatial distribution of the sampling sites. Daily concentration (μg m^{-3}) of PM_{10}, O_3, SO_2, and NOx (NO and NO_2) and CO (ppm) were provided by the Municipal Secretary of Conservation and Environment (SCMA) of Rio de Janeiro. These data are estimated by six air pollution monitoring stations (Table 3.6 and Figure 3.5): Bangu (B), Iraja (I), São Cristóvão (SC), Tijuca (T), Copacabana (Cop), and Centro (C). Note that Table 3.6 shows a description of the games that occurred near each station. Meteorological data were measured with an automated weather system installed in each sampling site. This data includes values of wind speed (m s^{-1}), wind direction (degrees), temperature (°C), total solar radiation (W m^{-2}), relative humidity (%), and precipitation (mm). The configuration of the air pollution monitoring network is presented in Table G.1, and the equipment and method used are described in Table G.2 (Supplementary material).

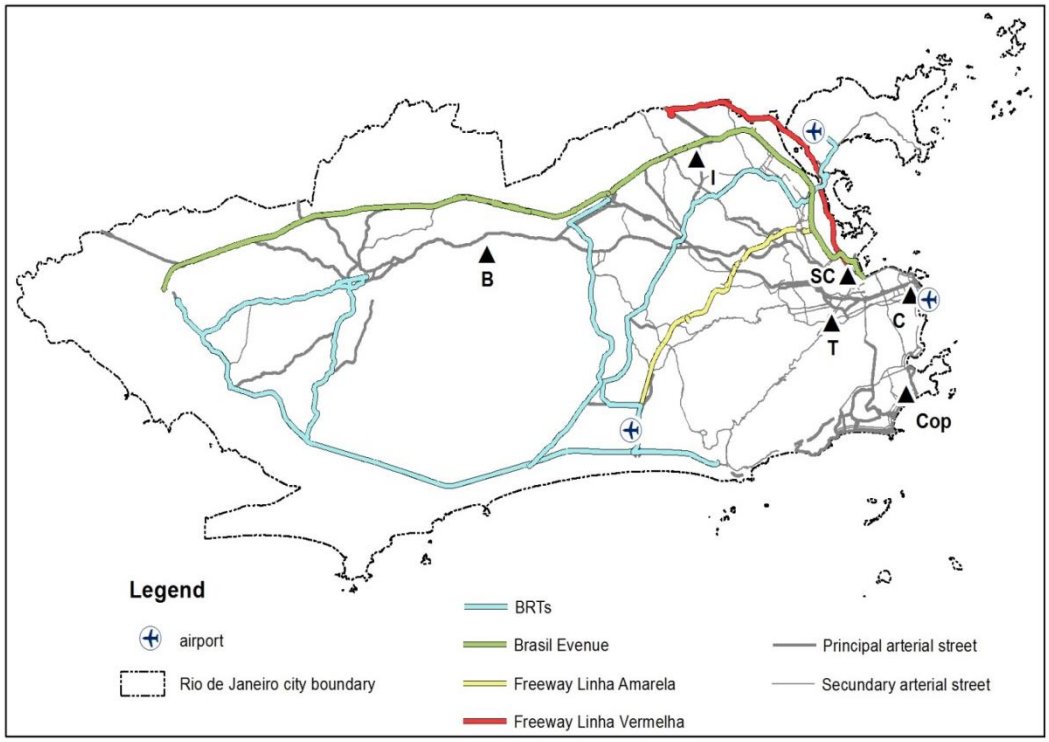

Figure 3.5 Spatial distribution of the monitoring stations in Rio de Janeiro, B=Bangu, I=Iraja, SC= São Cristóvão, T=Tijuca, Cop=Copacabana, and C=Centro.

Table 3.6 Description of the air pollution monitoring stations

Sites	Coordinates	Population	Games	Location /source type
Bangu (B)	22°53’14.28”S 43°28’14.75”W	243,000	Canoe slalom, mountain bike, BMX, shooting, equestrian, hockey, rugby and modern pentathlon	Urban/traffic
Iraja (I)	22°49’53.89” S 43°19’38.89” W	100,000	Located in the Northern Zone of Rio de Janeiro city. It is a Residential area and it is cut by Brazil Avenue, one main highway linking several cities.	Urban/traffic
São Cristovão (SC)	22°53'52.07" S 43°13'18.28" W	26,510	Football finals, volleyball, archery and marathon, thus as open and closing ceremonies of Olympic Games	Urban/traffic, road dust
Tijuca (T)	22°55'30.03" S 43°13'57.27" W	181,810	Located in the Northern Zone of Rio de Janeiro city. It is a Residential area with several bus lines and by subway Line that contain four stattions.	Urban/traffic
Copacabana (Cop)	22° 57’53.88” S 43°10’49.69” W	150,000	Beach volleyball, triathlons, sailing, rowing, and also the canoe sprint in the Lagoon Rodrigo de Freitas (7min, 3 km from Cop).	Urban/traffic, marine spray
Centro (C)	22°54’25.49”S 43°10’54.89”W	41,142	During the Olympic Games was presented music in life and set up a giant screen to observe the competitions.	Urban/traffic, road dust

3.6.4.
Data analysis

We used multiple comparisons of means – Tukey test (Fisher test, $p < 0.05$) to identify the significant difference among the pollutants measured at each sampling site in the three Olympic Games periods. Hourly averages of pollutants were plotted for each period and monitoring stations to explore diurnal variations. NO/NO_2, NO_2/NO, and $O_3/[NO_2/NO]$ ratios were plotted with the aim to estimate mixture of pollutants.

Finally, we used Pearson's correlation analysis to evaluate the inter-relations among the hourly average bases of pollutants concentrations and meteorological parameters.

3.7.
Multivariate calibration for the correction of interferences

The following description of material and methods refer to chapter 9, page 143.

3.7.1.
Reagents and Materials

Deionized water ($\rho \geq 18$ MΩ cm) was obtained from a Milli-Q system (Millipore, Milford, USA) and used to prepare solutions and samples. Nitric acid (65 %, Merck, Darmstadt, Germany) was submitted twice to sub-boiling distillation in a quartz apparatus (Berghof Laborprodukte, Germany). Hydrofluoric acid (40 % Merck, Germany) and boric acid (CAQ-Casa da Química, São Paulo, Brazil) were of pure grade. Single element standard solution of each REEs (1000 mg L^{-1}), Ba (1000 mg L^{-1}), Rh (1000 mg L^{-1}) and multielement standard solution of REEs (1000 mg L^{-1}) were purchased from Merck. For ICP-MS analysis, all samples and solutions were prepared to contain 5 % HNO_3, as well as the blanks.

Certified Reference Materials (CRM) employed in this study comprised BRC-670 Aquatic plant from European Commission (Belgium), apple leaves (SRM-1515a) and tomato leaves (SRM-1573a), both from National Institute of Standards & Technology (NIST, USA). These CRMs were employed to verify the

accuracy of the univariate calibration by Ordinary Linear Regression (OLS) and the proposed multivariate calibration methods. The certified concentrations of each REE in the three certified reference material of plants are depicted in Table H.1 (Supplementary material).

All measurements were performed in quadrupole ELAN DRC II ICP-MS equipment (PerkinElmer, USA), with a Meinhard nebulizer, a cyclonic spray chamber (Glass Expansion, Australia), a plasma torch with an alumina injector, platinum cones and a four-channel peristaltic pump (Mini plus 3 model, PerkinElmer, USA). Typical instrument operating conditions for the analysis of REEs are listed in Table H.2 (Supplementary material). To correct and/or compensate non-spectral interferences and matrix effect, ^{103}Rh was used as internal standard (IS) [57–60]**,** which was introduced online, by means of a T-piece.

3.7.1.1. Procedures

An experimental design of 5-level and 15-factor calibration design was performed using five concentration levels for each one of the fifteen analytes to be analyzed. The design aims to span the mixture space fairly well; where there are between 5 to 8 mixtures for each analyte at each concentration level (Table H.1). According to the literature [61,62], a whole of forty mixtures (named analytical solutions) represent well a 15^5 design (15 factors, each with 5 levels, 155 = 759375 total runs). For this purpose, single element standards of each REEs and barium were used. The concentration for each level for each analyte (REEs and Ba) is based on the concentration in three plant certified reference samples. The forty analytical solutions of this design were used as calibration set and fifteen analytical samples prepared of the same manner were used as a validation set to test the predictive ability of the developed multivariate models. Table 3.7 represents the concentration design matrix of the 55 analytical solutions analyzed. In both, calibration and validation sets, the dependent variable is represented by X-matrix (signal intensity of the REEs and Ba isotopes measured by ICP-MS in the different analytical solutions) and the independent variable by Y-vector (concentration) [63].

Table 3.7 Analytical solution concentrations (μg L^{-1}) for calibration set and validation set.

ID	La	Ce	Pr	Nd	Sm	Eu	Gd	Tb	Dy	Ho	Er	Tm	Yb	Lu	Ba
A1	30	30	5	5	10	20	10	5	10	5	20	5	0.8	0.5	800
A2	5	20	0	30	10	1	20	0.5	0	2	0.8	5	5	2	500
A3	5	30	10	20	5	10	5	10	10	0.8	5	2	10	0	1800
A4	30	20	5	5	5	10	5	10	5	1	0.8	0.5	20	0.5	1800
A5	10	10	20	40	0	10	10	1	20	5	5	2	0.8	0.5	800
A6	5	40	1	20	5	5	1	5	2	1	0.8	0.8	0.5	0.8	500
A7	30	20	20	10	5	10	1	2	1	0.5	0.5	5	2	5	2000
A8	10	30	5	5	1	10	0.5	2	0.5	0	10	0	10	5	1500
A9	30	40	10	30	20	5	10	0	5	1	2	0.8	1	10	1000
A10	5	30	5	5	0.5	1	10	0.5	0.8	0	20	0.5	0.5	4	500
A11	20	10	0.5	10	1	1	5	0.8	0.5	5	0.5	0.8	5	2	1000
A12	10	40	10	30	0.5	10	20	5	10	10	10	1	2	0.5	1800
A13	30	20	0.5	5	10	0.5	1	10	2	10	1	5	0	4	1500
A14	20	30	20	10	20	0.5	0	2	1	0.8	2	2	0.8	4	1000
A15	20	0	5	10	5	1	20	2	1	2	20	1	0.5	8	2000
A16	20	40	20	5	0	5	10	2	0.5	0.5	5	0.5	0.8	10	500
A17	40	40	0.5	10	5	20	0	5	10	1	2	2	2	4	2000
A18	30	30	20	20	10	0	5	1	20	5	1	5	10	2	1500
A19	20	10	0.5	20	5	5	0.5	0	1	10	10	1	2	1	1200
A20	20	10	1	20	1	10	10	10	5	2	0.5	2	20	0.5	1800
A41	10	20	10	20	1	10	5	1	1	2	1	2	0.5	1	500
A42	30	10	1	30	5	20	10	0	10	5	20	10	1	1	800
A43	40	40	10	30	0.5	0.5	0.5	1	2	0	10	1	2	4	2000
A44	5	20	1	10	5	0	10	10	1	0.5	0.5	2	8	5	1500
A45	5	20	1	5	0	5	20	1	0.5	0.5	2	0.5	0	4	2000
A46	40	10	5	10	1	1	0.5	0.8	0	10	1	10	0	0.8	1200
A47	5	0	0.5	30	10	10	5	0.5	0.8	0.8	0	1	0.8	10	1000
A48	10	20	10	10	5	0.5	1	5	2	2	10	0	5	0	800
A49	30	0	1	20	1	10	0	5	10	1	0.8	0.8	0.5	0.8	800
A50	10	0	10	10	5	20	1	5	0.5	5	5	2	0.8	1	1800
A51	20	30	5	40	20	10	10	5	10	1	0.8	2	8	10	1800
A52	5	20	5	10	0	5	5	1	0.8	0.5	2	10	1	0.8	800

Continuation of Table 3.7

ID	La	Ce	Pr	Nd	Sm	Eu	Gd	Tb	Dy	Ho	Er	Tm	Yb	Lu	Ba
A53	20	20	1	30	15	1	20	5	2	0	1	0.8	20	8	1500
A54	30	30	0	20	20	0.5	5	0.8	20	5	2	1	1	0.5	1800
A55	40	40	0.5	20	5	5	1	0.5	0	1	5	0.5	1	1	1200

A = analytical solutions

The whole dimension of the resulting X-matrix is of 2530 data points concerning to signal intensities of 46 isotopes of all REEs and barium (46 variables/column) measured in 55 analytical solutions (55 samples/rows). Combining the spectral data represented by signal intensities (X-matrix) and the prepared concentrations of each analyte (Y-vector), respectively, multivariate calibration models were constructed using the packages pls [64] and glmnet [65] from CRAN R [34] free software.

Prior to the construction of the multivariate calibration models, the signal data was standardized adjusting the predictors of each variable in X-matrix and Y-vector to have mean equal to zero (centering) and variance equal to the unity (scaling). This option is recommended and useful when dataset presents variables with different chemical properties and/or different scales of magnitude, otherwise, the system will be controlled by variables with higher variance values [66].

Optimization of each model was carried out selecting an optimal tuning parameter: number of principal components or latent variables (LVs) for PCR and PLS, and λ value for RR and Lasso through *K*-fold cross-validation (CV) [66,67]. Finally, with the tuning parameter selected, each multivariate model and analyte is re-fit and used to predict unknown new samples.

For the univariate regression, an analytical curve of six points (0.2, 0.5, 5, 10, 20 and 40 μg L^{-1}) was built with the REEs multielement standard solution.

In order to identify potential statistical differences in prediction accuracy among the multivariate methods, Wilcoxon signed-rank test was applied.

4
Trace metals biomonitoring in the Peruvian Andes metropolitan region using *Flavoparmelia caperata* lichen

Alex Rubén Huamán De La Cruz[a, b], Jusber Kevin Huamán De La Cruz[c], Daniel Alvarez Tolentino[d], Adriana Gioda[a,*]

[a]Pontifical Catholic University of Rio de Janeiro (PUC-Rio), Department of Chemistry, Rio de Janeiro, Brazil

[b]National University of Centre of Peru (UNCP), Faculty of Chemical Engineering, Av. Mariscal Ramon Castilla Km. 5. No 3809, El Tambo, Huancayo, Peru

[c]National University of Centre of Peru (UNCP), Faculty of Nursing, Av. Mariscal Ramon Castilla Km. 5. No 3809, El Tambo, Huancayo, Peru

[d]Alas Peruanas University (UAP), Faculty of Environmental Engineering, Av. Coronel Parra s/n Paradero 5, Pilcomayo, Huancayo, Peru

*Corresponding author: Adriana Gioda - Email: agioda@puc-rio.br

Published: *Chemosphere 210 (2018) 849-858*

Abstract

In the present study, *in situ* lichens (*Flavoparmelia caperata*) were used to assess the deposition of atmospheric trace elements in the metropolitan area of Huancayo (Junín, Peru). In total, ten sampling sites were chosen and categorized as urban, peri-urban (rural-urban) and rural areas according to land use. In

addition, samples were also collected from a non-contaminated area categorized as a control site. The concentrations of 16 trace elements were measured using an inductively coupled plasma mass spectrometer (ICP-MS) and examined by enrichment factor (EF), hierarchical cluster analysis (HCA), and principal component analysis (PCA). Twelve of the 16 trace elements in urban and peri-urban sites present concentration higher than those at the rural and control sites ($p < 0.05$). The EF results revealed significant enrichment (at least twice that of the control site) of Ba, Cr, Cd, Pb, Sb, V, and Zn at most sites. PCA and HCA showed that more elements were derived from vehicular sources and fewer from agricultural and natural sources.

Keywords: Lichen biomonitoring; Central Andes; Trace elements; Air pollution; peri-Urban growth.

4.1. Introduction

Atmospheric emission of toxic trace elements in the form of particulate matter has been a major concern due to their adverse effects on human health and the environment [68,69]. Air monitoring studies are the process of collecting samples of air with the aim to quantify the concentration of pollutants in the air of an area of interest. However, these studies are restricted to large cities or private industries, which have high budgets and can buy and to maintain the expensive equipment needed for classical standard techniques [70].

Lichen species are widely used in biomonitoring studies of air pollution as either a bioindicator to assess environmental quality after any change in the composition of lichen communities or a bioaccumulator (biomonitor) of pollutants that offers quantitative information concerning certain characteristics of the biosphere [42,71]. Biomonitoring studies can be performed by collecting and analyzing indigenous organisms (i.e., passive biomonitoring) or by exposing organisms collected from an unpolluted site to polluted sites for a certain period of time [5].

Lichens are composed of two different organisms that are symbiotically associated: an alga (i.e., cyanobacterium) and a fungus (i.e., mycobiont). They can

grow in a range of environments, including the surfaces of rocks, trees, and man-made structures. These organisms are perennial, resilient, and long-lived, and they can survive in even the most extreme environments, such as the deserts or Antarctica [72]. Lichens are considered to be efficient biomonitors due to their large-scale dependence upon the environment for nutrition, slow growth rate, longevity, ability to tolerate large quantities of pollutants, and ability to reflect the deposition and concentration of trace elements from the atmosphere. In addition, lichen species can be easily sampled, are low-cost, and allow a wide area or several areas, to be monitored simultaneously [73,74].

Since lichens have no waxy cuticle or stomata, they uptake nutrients, gases, and water directly from the atmosphere across the whole thallus surface. Trace elements are typically deposited on the surface of lichens as either dry particulates or dissolved materials. Then, they are absorbed (accumulated) by a variety of mechanisms, such as particulate trapping, ion exchange, hydrolysis, extracellular electrolyte sorption, and passive and active intracellular uptake [75].

Biomonitoring studies have used several lichen species as biomonitors of airborne trace elements and have been published worldwide. For instance, Loppi et al. (2004) [74] and Koz et al. (2010) [76] used *F. caperata* lichen as a passive biomonitor, and demonstrated that Pb was related to vehicular traffic, the main source of atmospheric pollution in Italy and Turkey. Likewise, in Brazil, using *Canoparmelia texana* lichen, Fuga et al. (2008) [77] revealed high concentrations of Co concentration related to metallurgical processing plants and Br and Zn related to industrial and vehicular emissions. In Thailand, research involving active biomonitoring using the foliose lichen *P. tinctorum* associated high concentrations of As, Cd, Co, Cr, Hg, Hg, Ni, Sb, Ti, and V with industrial origins, while high concentrations Cd, Cu, Pb, and Zn were related to vehicle emissions and agriculture [78].

In Peru, studies measuring the multielemental composition of the environment using biomonitors are scarce. The only such study was carried out by Bedregal et al. (2009) [79] in Lima, the capital of Peru, and employed active biomonitoring using *Tillandsia capillaris* and *Usnea sp*, lichen. The results obtained showed significant pollution in some areas of the city related to industrial activities and vehicular emissions.

Over the last decades, the metropolitan area of Huancayo (MAH) suffered from significant deterioration of air quality due to increases in the number of vehicles, rapid urbanization, migration, and land use [28,80]. However, until now, studies monitoring air quality were not carried out in this area due to a lack of government interest, suitable environmental policies, and economic support. It is important to use biomonitors to assess the air quality in this area because they can help overcome some of the aforementioned issues.

The aims of this work were to use *Flavoparmelia caperata* lichen as a biomonitor to evaluate the pollution levels of different sites located in the MAH, provide quantitative information concerning the concentration of some toxic trace elements, and determine its possible sources of pollution.

4.2. Materials and methods

The reader is referred to the description in section 3.2, page 38.

4.3. Results

4.3.1. Trace element content and enrichment factor

Table 4.1 shows the mean concentration ± standard deviation (S.D) and the ANOVA results for Al, As, Ba, Ca, Cd, Cr, Cu, Fe, K, Mn, Ni, Pb, Rb, Sb, V, and Zn from each monitoring site (including the control site), which were measured using *F. caperata* lichen samples collected *in situ*. The highest concentrations of most elements were observed in the two urban areas (U1 and U2); high concentrations of Ba, Cu, Fe, and Zn were observed at U1; while Al, Ca, V, and Ni were elevated at U2. Regarding the peri-urban sites, As and Pb were higher at PU4; while Cd, Cr, K, Mn, and Sb were elevated at PU6. PU4 and PU6 were located 20 and 9 km away from the main urban area, respectively.

The concentrations of every element at most urban and peri-urban sites were higher than those at the control site (CS). However, this was not true for As at U2, Ca at PU2, PU3, PU5, and PU7; Cu at PU5; and K and Rb at PU1, PU2, PU3, PU5, and PU7. In total, the concentrations of 12 of the 16 elements were

higher at the urban and peri-urban sites than at the control site ($p < 0.05$): Ba at U1, U2 and PU4; Ca at U1, PU1, PU4, and PU6; Cu at PU3; Cu and Ni at U1, U2, PU1, PU4, PU6 and PU7; Fe, V, and Zn at U1, U2, and PU6; Mn at PU6; Sb at U1, U2, PU1, PU4, PU5, and PU6; and Cd, Cr, and Pb at all sites. Similar concentrations were observed for some trace elements in peri-urban, rural, and control site.

Table 4.1 Comparison of mean values (± standard deviation) with µg g^{-1} dry weight (DW) and results of the analysis of variance (ANOVA) of the trace elements measured in F. caperata lichen at monitoring sites and control site from the metropolitan area of Huancayo, Junín, Peru.

Element	CS N=5	U1 N=7	U2 N=5	PU3 N=6	R N=6	PU6 N=7	PU1 N=6	PU2 N=6	PU5 N=6	PU4 N=8	PU7 N=6	ANOVA p-value [a]
Al (%)	0.44±0.02 f	0.61±0.02 b	0.66±0.02 a	0.59±0.02 c	0.52±0.02 e	0.61±0.02 b	0.61±0.02 b	0.58±0.02 c	0.52±0.02 e	0.54±0.02 d	0.58±0.02 c	***
As	3.7±0.4 d	4.0±0.5 d	3.8±0.6 d	4.7±0.5 c	4.2±0.6 d	5.2±0.5 b	4.7±0.6 c	4.2±0.5 d	4.2±0.4 d	6.2±0.7 a	5.2±0.4 b	***
Ba	26±3 g	79±2 a	71±3 b	46±2 e	38±2 f	78±2 a	62±3 c	47±2 e	39±3 f	52±3 d	51±3 d	***
Ca (%)	1.07±0.05 d	1.41±0.04 e	1.48±0.06 e	1.11±0.06 f	1.00±0.06 c	1.31±0.05 a	1.34±0.07 b	0.98±0.04 c	0.95±0.03 c	1.29±0.05 a	1.04±0.03 d	***
Cd	0.13±0.04 e	0.34±0.04 d	0.31±0.04 d	0.43±0.05 c	0.34±0.05 d	0.56±0.06 a	0.46±0.05 b	0.43±0.03 c	0.49±0.04 b	0.58±0.04 a	0.45±0.05 c	***
Cr	3.8±0.4 g	9.6±0.4 b	9.4±1.0 b	7.2±0.3 d	5.8±0.3 f	10±0.5 a	7.9±0.5 c	6.7±0.4 e	6.5±1.0 e	7.1±0.4 d	7.1±0.5 d	***
Cu	5.0±0.4 f	9.6±0.5 a	9.0±0.6 b	7.4±0.5 d	4.9±0.7 f	9.3±0.5 a	8.3±0.8 c	5.7±0.3 e	4.9±0.4 f	8.9±0.7 b	7.9±1.0 c	***
Fe (%)	0.20±0.02 f	0.36±0.02 a	0.33±0.01 b	0.29±0.02 c	0.23±0.02 e	0.35±0.02 a	0.31±0.02 c	0.24±0.02 e	0.26±0.02 d	0.30±0.02 c	0.28±0.02 d	***
K (%)	0.47±0.03 b	0.56±0.02 d	0.54±0.02 d	0.43±0.02 e	0.60±0.02 a	0.60±0.03 a	0.49±0.04 b	0.47±0.01 b	0.51±0.03 c	0.52±0.02 c	0.45±0.01 e	***
Mn	60±3 e	85±3 d	81±4 d	90±2 b	81±3 d	103±4 a	88±6 b	98±3c	86±4 d	86±2 d	83±3 d	***
Ni	2.4±0.3 d	3.7±0.4 a	3.7±0.3 a	3.5±0.3 a	2.8±0.2 b	3.7±0.3 a	3.7±0.2 a	3.2±0.3 c	2.9±0.2 b	3.2±0.2 c	3.3±0.2 c	***
Pb	8.7±1.2 e	26±3 b	26±3 b	22±3 c	8.7±2 e	19±4 d	25±3 b	22±3 c	17±3 d	32±4 a	22±3 c	***
Rb	9±2 c	13±2 a	12±2 a	9±1 c	13±3 a	14±3 a	10±2 c	9±2 c	9±2 c	13±3 b	10±2 c	***
Sb	0.91 ± 0.06 e	1.81±0.16 a	1.67±0.17 a	1.30±0.15 b	0.82±0.09 d	2.05±0.18 a	1.81±0.40d	1.10±0.12 b	1.02±0.13 d	1.91±0.17 a	1.50±0.13 c	***
V	3.7±0.5 f	8.1±0.6 b	9.6±0.4 a	5.5±0.3 d	3.5±0.2 f	8.5±0.3 b	7.0±0.7 c	5.2±0.2 d	4.8±0.4 e	5.9±0.3 d	5.5±0.5 d	***
Zn	50±4 g	141±5 a	136±6 a	78±5 d	61±4 f	140±8 a	115±4 b	69±4 e	66±5 e	110±6 b	96±4 c	***

[a] Values on each horizontal line followed by the same letter do not differ significantly (p=0.05), N=number of individual lichen samples collected in each site. * Significant at 0.05 probability level. ** Significant at 0.01 probability level. *** Significant at 0.001 probability level.

The EF of the 16 elements measured at each sampling site were calculated as described in section 3.2.3 and are shown in Figure 4.1 and Figure 4.2. The elements that were enriched significantly (i.e., concentrations at least twice those at the control site) included Ba and Cr at U1, U2, PU1, and PU6; Cd at all sites; Pb at all sites except R and PU5; Sb at PU4 and PU6; V at U2, PU1, and PU6; and Zn at U1, U2, PU1, PU4, and PU6. Moderate enrichment was observed for As at PU4; Cr at PU5; Ba and Cr at PU2, PU3, PU4, and PU7; Cu at U1, U2, PU1, PU4, PU6, and PU7; Mn at PU2 and PU6; Ni at U1, U2, PU1, PU6, and PU7; Pb at PU5; Rb at R and PU6; Sb at U1, U2, PU1, and PU7; V at U1 and PU4; and Zn at PU3. Normal conditions were found for Al, Ca and K all sites; As at all sites except PU4; Ba at R and PU5; Cu at R, PU2, PU3, and PU5; Fe, Ni, and V at R, PU2, PU3, PU5, and PU7; Mn at all sites except PU2 and PU6; Pb at R; Rb at all sites except PU6; Sb and Zn at R, PU2, and PU5.

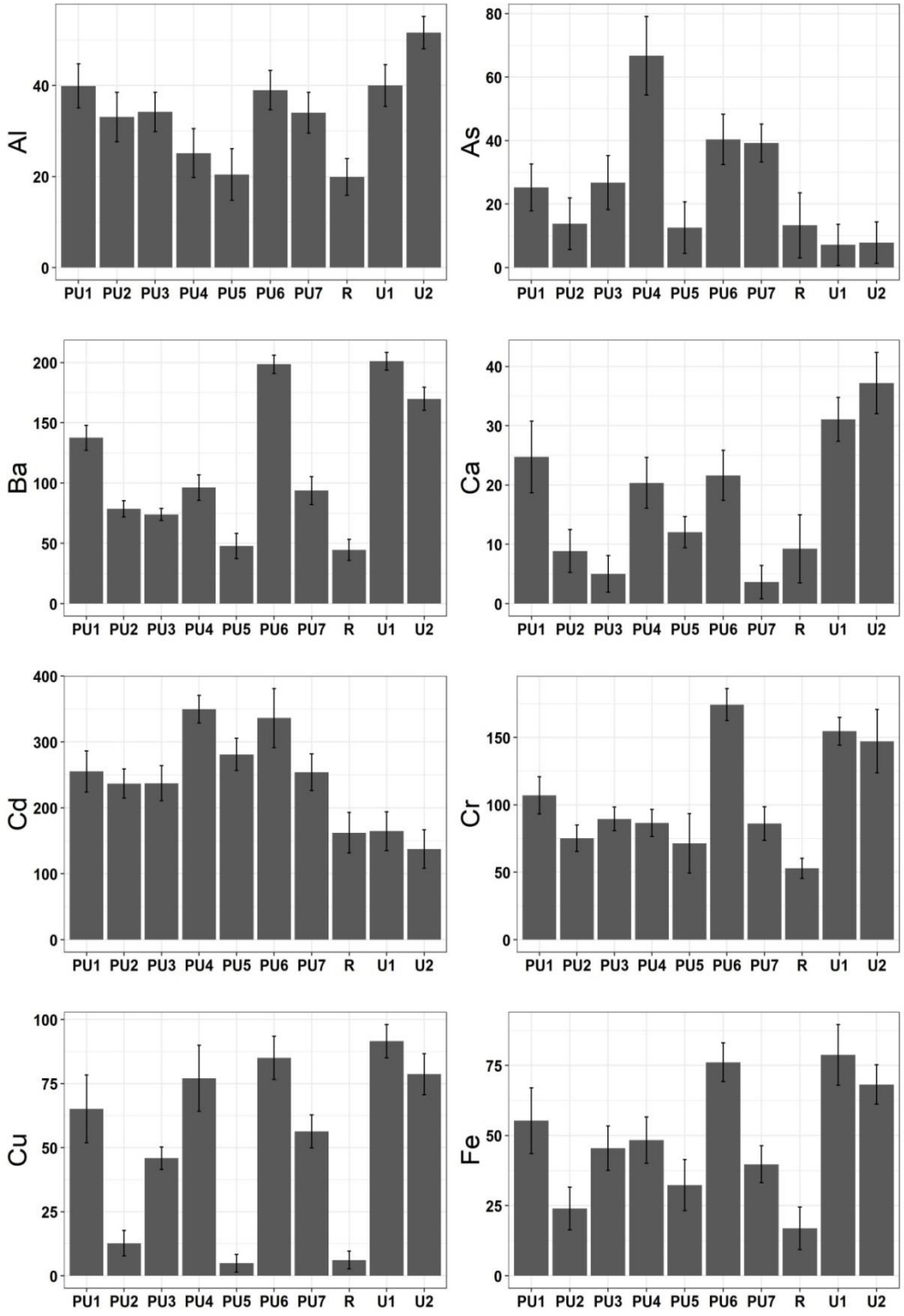

Figure 4.1 Enrichment factor (EF) ± standard deviation for the elements Al, As, Ba, Ca, Cd, Cr, Cu, and Fe at the 10 sites at which in F.caperata lichen was sampled during the present study.

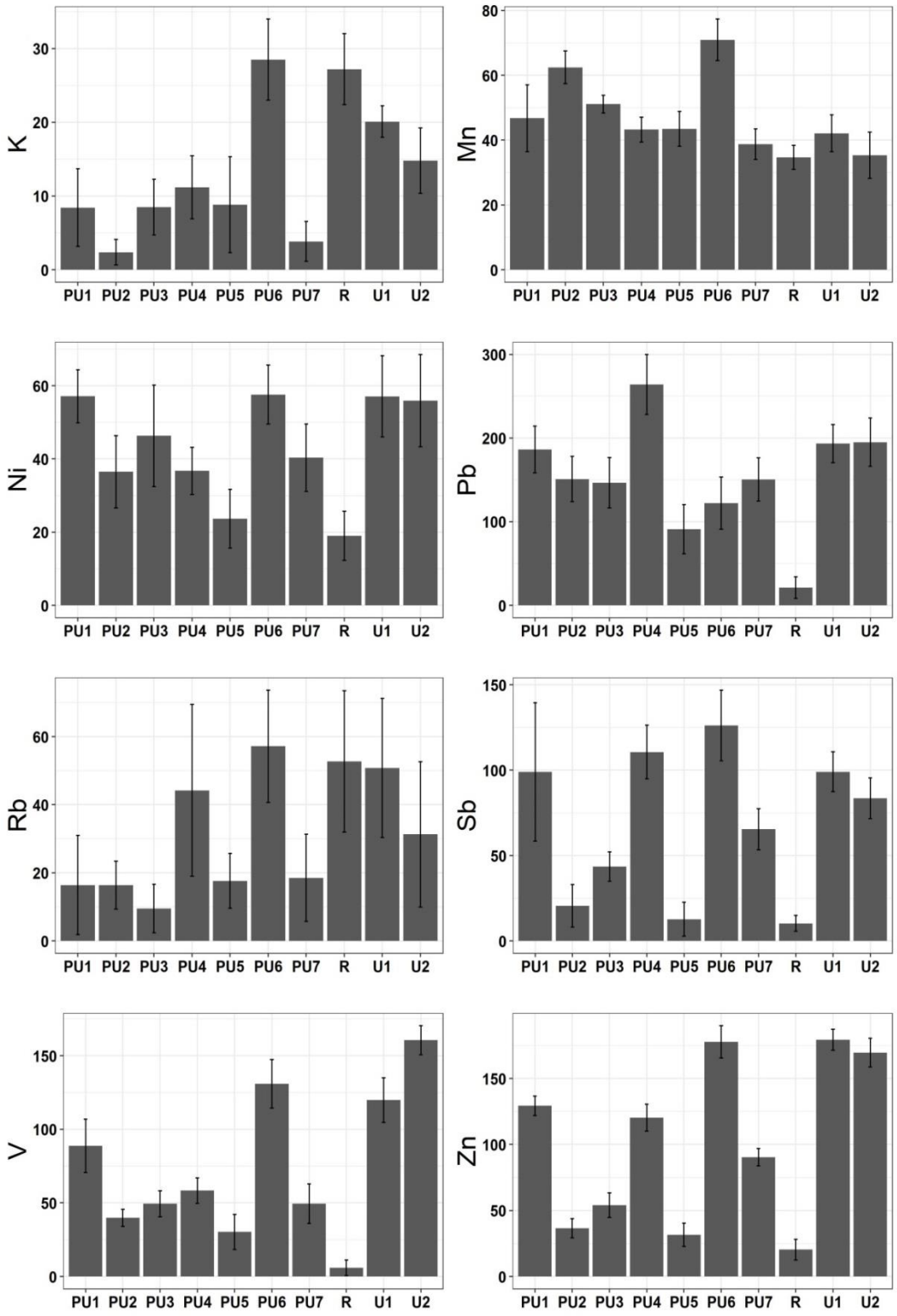

Figure 4.2 Enrichment factor (EF) ± standard deviation for the elements K, Mn, Ni, Pb, Rb, Sb, V, and Zn at the 10 sites at which in F.caperata lichen was sampled during the present study.

4.3.2.
Exploratory analysis data obtained by ANOVA and HCA

As shown in Table 4.1, significant differences ($p < 0.05$) among the mean concentrations at all sampling sites were found. However, no significant differences ($p > 0.05$) were observed among some sites, including U1 and U2 for Zn, Pb, Sb, Cr, and Ni, and U1, U2, R, and PU6 for Rb.

HCA was performed on the lichen data set. First, the sampling sites (including the CS) were classified according to their mean concentrations, revealing three distinct groups. Group I consisted of the rural area (R) and control site (CS). Group II was comprised of two urban sites (U1 and U2), which were closely linked, and one peri-urban site (PU6). Group III included the other peri-urban areas: PU1, PU2, PU3, PU4, PU5, and PU7. A dendrogram depicting the clusters (groups) of sampling sites is shown in Figure E.3. The HCA results indicate that sampling sites belonging to the same group share similar characteristics based on the element content of lichen and may be considered have similar air quality. The dendrogram (Figure 4.3) enabled division of the elements into three groups. Mn, As, and Cd constituted Group I; K and Rb formed Group II; and Cr, Fe, V, Ba, Zn, Ca, Cu, Sb, Pb, Al, and Ni were included in Group III.

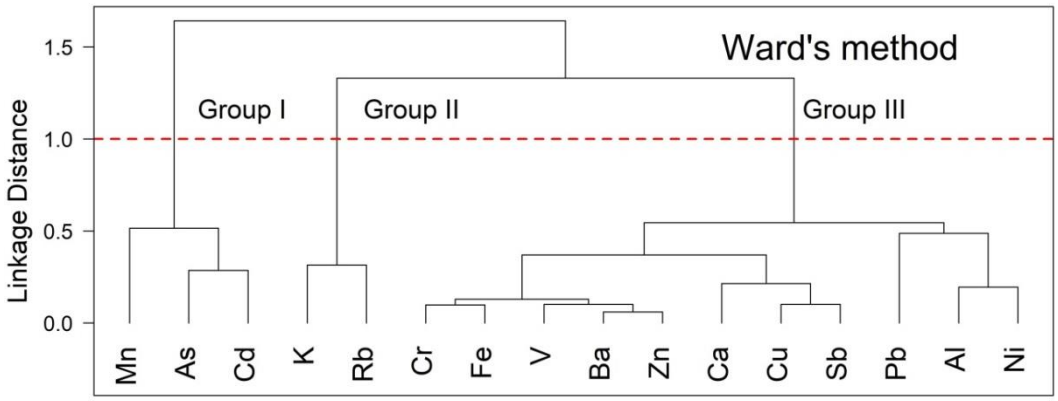

Figure 4.3 Results of the hierarchical cluster analysis (dendrogram) of the trace element concentrations measured in F. caperata.

4.3.3.
Principal component analysis

PCA is a technique for reducing the dimensionality of large datasets, improving the interpretability and minimizing information loss. PCA finds directions in the space that capture maximal variance of a data set through the orthogonal transformation of a set of correlated variables into a reduced set of uncorrelated variables called factor or principal components (PCs) [81].

The lichen data set containing the enrichment factor of 16 trace elements from 10 monitoring sites (16 variables x 63 samples) were submitted to principal components analysis. Log transformations were applied *prior* PCA when necessary to comply with the assumptions of the variance of homogeneity and residual normality. Loadings are the coefficients of correlation between individual factors and the elements. Loading values close to unity indicates that the element is characteristic of that particular source. As presented in Table 4.2, the results of PCA after Varimax rotation show three factors featured Eigenvalues greater than 1 and explaining 74% of the total variation in the dataset. Biplots among factors are presented in Figure S4 (Supplementary Material). Factor 1 accounts for 47% of the total variance and shows high positive loading for Al, Ba, Cr, Cu, Fe, Ni, Pb, Sb, V, and Zn (Table 4.2). Ca, K, and Rb show high loading in factor 2, which accounts for 14 % of the total variance. Factor 3 explains 13 % of the total variance and was observed high positive loadings for As, Cd, and Mn. The commonalities of Al, As, Ba, Cd, Cr, Cu, Fe, K, Ni, Pb, Sb, V, and Zn in the dataset were in the range 0.66-0.90 indicating that each element was satisfactorily apportioned to the identified factors. However, Ca, Mn, and Rb showed communalities values lower than 60 %, suggesting that a substantial fraction of their concentrations of these elements could not be apportioned to factors whose Eigenvalues were > 1.

Table 4.2 Factor (Fa) loadings of the three extracted factors (principal component analysis, varimax standardized rotation) for F. caperata lichen samples (enrichment factor) and the respective communalities (comm). Loadings greater than 0.70 (shown in bold) are considered to be significant.

Element	**Factors**			
	Fa1	Fa2	Fa3	Comm
EF lichens				
Al	0.80	-0.11	-0.23	0.71
As	0.02	-0.15	0.80	0.66
Ba	0.90	0.28	-0.04	0.90
Ca	0.34	0.61	-0.15	*0.51*
Cd	0.01	-0.11	0.90	0.83
Cr	0.84	0.36	0.01	0.84
Cu	0.85	0.12	0.14	0.76
Fe	0.87	0.24	0.11	0.83
K	0.06	0.87	-0.10	0.78
Mn	0.22	0.11	0.60	*0.41*
Ni	0.87	-0.04	0.08	0.76
Pb	0.76	-0.29	0.25	0.73
Rb	-0.02	0.77	0.06	*0.59*
Sb	0.86	0.16	0.24	0.81
V	0.87	0.01	0.10	0.77
Zn	0.92	0.20	0.10	0.91
Eigenvalue	7.79	2.36	1.62	
% of total variance	0.47	0.14	0.13	
% of cumulative variance	0.47	0.61	0.74	

Principal component analysis (PCA) with Varimax rotation. kaiser-Meyer-Olkin (KMO) measure of sampling adequacy.

4.4. Discussion

The mean concentrations of macronutrients, micronutrients and trace elements measured in lichen samples decreased in the following order: Ca > Al > K > Fe > Mg > Zn > Ti > Mn > Ba > Sr > Pb > Rb > Cr > Cu > V > As > Ni > Sb

> Co > Cd. Most element concentrations were higher at the peri-urban and urban sites than at the rural and control sites. The highest concentrations of Zn were observed at U1, U2, and PU4, which may reflect the intense heavy traffic suffered by these areas in recent years. Elevated Pb concentrations were found at most of the sampling sites, despite the fact that leaded gasoline has been prohibited in Peru since 2009 [82]. The high levels of Pb may be due to the fact that Pb cannot be destroyed, is persistent, is strongly adsorbed to soil and old cars may still be in circulation at the automotive park. Similar results (i.e., higher Pb content) were reported for the urban areas of Seville, Spain [46], Asunción, Paraguay [83] and Busher, Iran [84]. The most elevated Sb concentrations were found at sites with a heavy circulation of vehicles (U1, U2, PU1, PU4, and PU6). PU1 is near main urban areas, while PU4 and PU6 both feature highways linking these sites to other cities. Similarly, Agnan et al. 2013 [30] reported that Sb, Sn, Pb, and Cu were found in an urban area of France due to local factories and car traffic.

Moderate enrichment of Cu was found by Naderiza et al. (2016) [84] in urban and industrial areas of Bushehr, Iran. Fujiwara et al. (2011) [85] identified Pb, Zn, and Ba as traffic markers, while Janta and Chantara (2017) [68] concluded that Cr, Pb, Cu, and Zn derive mainly from vehicular sources. Querol et al. (2008) [86] suggested that Sb, Cu, Zn, Ba, and Fe are markers of wear of brakes or other vehicular parts and may be considered indicators of re-suspension caused by traffic. Ba, V, Ni, Zn, Cu, and Sb have been related to traffic emissions [46,87,88], and V and Ni have been mostly associated with the oil combustion process employed by diesel engines [71,89].

In this study, PCA produced three factors. The first factor shows that 10 elements Al, Ba, Cr, Cu, Fe, Ni, Pb, Sb, V, and Zn were positively correlated with factor loadings higher than 0.70 (Table 4.2). On the one hand, some of these elements (Ba, Cr, Pb, Sb, V, and Zn) had EFs greater than 100 % for most sampling sites in or around urban areas, and on the other hand, Al, Cu, Fe, and Ni, had EFs less than 100 % (Figure 4.1 and Figure 4.2), which may indicate the presence of geogenic and anthropogenic sources. Factor 1 shows that the highest concentrations of Ba, Cr, Pb, Sb, V, and Zn are present at sites close to heavy traffic (urban and some peri-urban areas), suggesting that vehicles are the major source.

The second factor was correlated with three elements: Ca, K, and Rb and showed high loadings accounting for 14 % of the total variance in the dataset (Table 4.2). K and Ca have EFs of less than 50 % at all sites, while Rb has an EF of about 50 at (R and PU6. Possible geogenic sources of these elements may include weathering of minerals, especially silicates, carbonates, and oxides. In addition, Rb can be emitted during coal combustion [90]. Ca and K are important nutrient of organisms, thus their association in Fa2 might derive from the lichen [91].

The third factor 3 comprises three elements As, Cd, and Mn with high positive loadings. Cd is a rare element and non-nutritive element (0.2 mg/kg in the earth crust) that is not likely to be released by soil. However, this element can be added to the soil through natural events (e.g., weathering of rocks containing Cd, sea spray, volcanic activity) and anthropogenic activities (e.g., fossil fuel combustion, manufacture of Cd-Ni batteries, use of rock-phosphate-based fertilizer, and waste incineration) [92–94]. As is a metalloid that can be derived not only from natural sources through weathering and erosion of rocks but also from anthropogenic sources, including industrial emissions, application of fertilizers and pesticides, sewage irrigation, and atmospheric irrigation [95]. Both As and Cd are related to cancer and neurological diseases in humans [96,97]. Mn is an element widely distributed in the earth's crust and is mainly used in metallurgical processes, dry-cell batteries, chemical manufacturing, in the leather and textile industries, and fertilizers [98]. Figueira et al. (2002) [99] related high Cd concentration in an area south of Lisbon, Portugal to the use of fertilizers in rice agriculture. Similarly, Belon et al. (2012) [100] concluded that mineral fertilizers and pesticides used in agricultural activities were the predominant sources of Cd and As in different regions of France. Further, Zhou et al. (2018) [95] related As increase to long-term application of phosphate fertilizers in agricultural activities in China, and Luo et al. (2009) [101] identified different fertilizers to contribute significantly to As and Cd concentrations in soil.

In the Central Highlands of Peru, cases of toxicity in farmers due to intense use of pesticides in Concepcion (PU4) and Chupaca (PU6) increased between 2001 and 2004 [102]. As there is no industrial activity in the study area, the As, Cd, and Mn concentrations found in this study might be related to soil

particles and use of agrochemicals and/or the fertilizers used in agricultural practices.

Hierarchical cluster analysis was used to categorize the sites into three groups. Based on the impact of the potential sources of elements, the groups can be ranked in the following sequence: Group I < Group III < Group II. The R and CS sites both have relatively clean air and thus from Group I. This similarity is not surprising because the rural area is a small community located 20 km away from the main urban area. Group III sites are moderately affected by potential element sources. Group II sites suffer the greatest impact from potential element sources because most of these sites are located near urban areas with high traffic and highways. The results of the HCA show that the concentration of elements in the collected *F. caperata* lichens may be used to classify sampling sites in the study area.

The elements were also categorized into groups using a dendrogram. Based on previous reports, the main source of the elements in Group I - Mn, As, and Cd are used in agrochemicals by farmers. The elements in Group II, K, and Rb appear to have natural sources. The elements in Group III appear to be released by anthropogenic sources, such as vehicles (e.g., exhaust, re-suspension, and abrasion).

The PCA and HCA multivariate statistical techniques indicate that there are three main sources of trace elements in the lichen collected from the study area. Ba, Cr, Fe, Ni, Pb, Sb, and Zn appear to mainly derive from anthropogenic sources, such as traffic. PCA and hierarchical cluster analysis revealed that Mn, Cd, and As were strongly correlated, suggesting that these elements may be released by agricultural practices. According to HCA and PCA, Rb and K were strongly correlated, suggesting that these elements mainly originate from natural sources.

The results of this study confirm that vehicles, soil particles re-suspension and perhaps agricultural activities, are the main sources of emission of trace elements into the air. Moreover, lichen proved to be a cost-effective biomonitoring tool for assessing the levels of airborne trace element pollution in the different areas under study. However, researchers must perform further studies using a larger number of samples and other techniques or methods to obtain a

better understanding of the accumulation of these trace elements, their risk to humans, and air quality in the MAH.

4.5. Conclusions

To our knowledge, the present study is the first report about the level of pollution of airborne trace elements in different areas of the MAH in Peru using *F. caperata* lichen species collected by passive biomonitoring as a biomonitor. The results with the lichen offer a preliminary assessment and general idea of the air quality within the study area. The lichen from the urban sites and some peri-urban sites show higher concentrations of trace elements than those from the rural and control sites. Seven elements (i.e., Ba, Cr, Cd, Pb, Sb, V, and Zn) show significant enrichment at the urban sites and some peri-urban sites, while three elements (i.e., Al, Rb, and K) were found in normal conditions. Although a relatively small number of samples (n=68) was considered in this study, the results of HCA and PCA showed consistent segregation of the trace elements. Most of the elements (i.e., Ba, Cr, Cu, Fe, Ni, Pb, Sb, V, and Zn) were related to vehicle emissions, two (i.e., As and Cd) perhaps may be derived from agricultural activities, and two (i.e., K and Rb) were of natural origin.

The present work confirms that *F. caperata* lichen can be used to efficiently assess air quality based on measurement of accumulated airborne trace elements.

Acknowledgements

The authors are grateful to Coordenação de Aperfeiçoamento de Pessoal de Nível Superior (CAPES), and Fundação de Amparo e Pesquisa do Estado do Rio de Janeiro (FAPERJ) for financial support. T. D. S. thanks to Conselho Nacional de Desenvolvimento Científico e Tecnológico (CNPq) for the scholarship.

5
Biomonitoring of Toxic Elements in Plants Collected Near Leather Tanning Industry

Alex R. H. De La Cruz, [a] *Lorreine D. S. C. Ferreira,* [a] *Vinicius P. Andrade,* [a]

*Adriana Gioda**,a* [*]

[a]Pontifical Catholic University of Rio de Janeiro (PUC-Rio), Department of Chemistry, Rio de Janeiro, Brazil

*Corresponding author: Adriana Gioda - Email: agioda@puc-rio.br

Paper published: *Journal of the Brazilian Chemical Society*

Abstract

The present work aimed the study of atmospheric deposition of toxic elements near to a tannery industry by collecting black material deposited collected on leaf surfaces of cinnamon trees (*Cinnamomum zeylanicum*). Elements such as As, Ba, Cr, Cu, Fe, Ni, Pb, Sb, V, and Zn were analyzed by inductively coupled plasma mass spectrometry (ICP-MS). For comparison purpose, black particles deposited on the leaf surface of lemon trees (*citrus lemon*) collected away from the tannery industry were also analyzed. Results showed that the amount of toxic elements found in the black particles collected near tannery area was significantly higher than the amount of those measured in the comparison site. Enrichment factors (EF) of As and Cr were markedly impacted by anthropogenic emissions, whereas the other elements were moderately/slightly enriched. HCA identified the leather industry as the anthropogenic source, while As possibly comes from the wide use of pesticides and herbicides in agricultural practices. The results indicated that emissions from the leather industry and agricultural activities are the main source of pollution in this area.

Keywords: Leather industry; ICP-MS; Toxic elements; Atmospheric Particles.

5.1. Introduction

Leather industry, an age-old activity, covers the manufacture of diverse consumer products (e.g., footwear, clothes, and leather goods), industrial processes, and has significant economic influence. However, this industry is considered of great concern because to turn the skin into leather (leather tanning) requires several stages and involves the use of large amounts of fresh water and several chemicals such as lime, sodium carbonate, sodium bicarbonate, common salt, sodium sulfate, chrome sulfate, oils, resins, biocides, among other reagents [103,104]. Increased levels of chromium in the environment resulting from the improper discharge of solids, wastewater, and gaseous emission from anthropogenic activities such as leather tanning, steel alloys and stainless steel manufacture, chrome plating, fabrication of paint pigments, wood preserving, textile, ceramic glazes, electroplating, and other activities [105,106].

Atmospheric deposition of toxic elements in form of particulate matter (PM) can reach soils and plants by either dry or wet deposition. Plants are essential organisms (biomonitors) of the ecosystem because they may improve the air quality by filtering, absorbing and accumulating significant quantities of toxic elements [107]. Biomonitoring studies using trees leaves as passive sampler are particularly useful because they have the advantage of high spatial and temporal distribution, low-cost, high distribution density and trapping of atmospheric particles, mostly on the entire leaf surface [108]. The accumulation and distributions of contaminants in plants depend on the plant species, bioavailability, and level of contaminants in the soil and air, and environmental conditions, such as rainfall, wind speed and direction and other factors [109].

In the last years, several plant species have been used as bioindicators of elemental deposition from the atmosphere [110–112]. For instance, *pine* tree leaves have been used as biological indicators for assessing trace element pollution by Cd, Pb, As, and Hg in an industrial ecosystem in Turkey [113]. Leaves of five plants: *Padus serotina, Acer campestre, A. negundo,Quercus robur and Celtis occidentalis* were used to bioindicators to assess the amount and concentration of contaminants in deposited dust in and around the urban city of

Debrecen, Hungary [112], while in Beijing, China, fourteen plant species have been used as bioindicators to evaluate the air pollution in this urban area [114].

The determination of Cr in environmental samples is of great importance due to its toxicity. Chromium is a hard steel-grey toxic element and may occur naturally as chromite ($FeCr_2O_4$) in the environment. This element is usually found in two oxidation states trivalent chromium, Cr (III), and hexavalent chromium, Cr (VI). Other valence states (minus stable or short-lived) in biological materials can also occur. The trivalent form is more abundant and much less toxic and less mobile than Cr (VI). It acts as an essential dietary nutrient to the maintenance of normal glucose tolerance for human and animals in low doses, while Cr (VI) compounds are considered 1,000 times more toxic than Cr (III) [115]. Its toxicity is related to its high redox potential, mobility, and ability to penetrate biological membranes. Chromium (VI) is also known as carcinogenic and mutagenic agent and can cause several diseases [116].

Nova Esperança do Sul, a small city in the south of Brazil, is named capital of the boot and has a big tannery, whose main articles are semi-finished and finished full-grain leather and their use is divided between furniture and automotive industries [117,118]. These goods are mainly sold to the foreign market. In general, leather industries eliminate leftover materials and leather shaving wastes through burning. As the industry is located in the center of the city, there are complaints from the population due to the constant atmospheric emissions [119]. The particles generated during the burning spread throughout the city, leaving the houses dirty, causing bad smell and health problems, although there is no official record. For this reason, the objective of this study was to verify if the black particles deposited in the soil and on the surfaces of plants are from natural origin or are related to tanning activities. The specific goals of this study were (1) to investigate the levels of toxic elements (As, Cr, Cu, Fe, Ni, Pb, Sb, V, and Zn) present in the deposited material on the surface of the leaves of *Cinnamomum zeylanicum*, (2) to assess contamination levels, and (3) to identify the possible sources of toxic elements in a heavily industrialized region (Nova Esperança do Sul, Brazil).

5.2.
Materials and methods

The reader is referred to the description in section 3.3, page 43.

5.3.
Results

5.3.1.
Descriptive statistics

Mean concentration ± standard deviation (S.D) and ANOVA results for As, Ba, Cr, Cu, Fe, Ni, Pb, Sb, V, and Zn from each collection site measured in clean leaves cinnamon at Nova Esperanca do Sul (S1) and of lemon at Lumiar at (S2) collected *in situ* are shown in Table 5.1. Results show that there is a statistically significant difference among sampling sites ($p < 0.05$) for most of the elements measured, except for Sb (all sites) and Ba (S1A and S1B). Dried leaves (DLS1A) collected show higher content of Cr, Cu, Ni, and V than samples collected at the same site (CLS1A). However, it is very immature to attribute the death of the leaves to these elements. Differences ($p < 0.05$) found among elements measured from S2 and S1 may be ascribed to that the leaves were collected in different areas and from different tree species (cinnamon at S1 and lemon at S2). Plants, even being of the same specie accumulates different levels of pollutants if they grow in different environments [120]. Similar to our results, Simon et al. (2016) [121] found significant differences in concentrations of Al, Ba, Cr, Fe, Mn, Si, Sr, and Zn among leaf tissues of three different trees and studied areas.

Table 5.1 Mean values (± standard deviation, S.D.) and results of ANOVA of the elements measured in clean and dry leaves (without material deposited on surface) collected at Nova Esperança do Sul (S1A and S1B) and Lumiar (S2).

Element	S1			S2	
	CLS1A 300 m	DLS1A 300 m	CLS1B 5 km	CLS2	ANOVA p-value[s]
	Mean ± S.D. /(µg g^{-1})	Mean ± S.D. /(µg g^{-1})	Mean ± S.D. /(µg g^{-1})	Mean ± S.D. /(µg g^{-1})	
As	0.37 ± 0.06 B	0.44 ± 0.05 A	0.49± 0.04 A	0.15 ± 0.04 C	a
Ba	65 ± 5 A	63 ± 3 A	69 ± 3 A	27 ± 3 B	a
Cr	0.28 ± 0.04 C	3.82 ± 0.88 A	0.78 ± 0.08 C	2.58 ± 0.20 B	a
Cu	3.96 ± 0.30 C	6.57 ± 0.39 B	8.40 ± 0.68A	2.59 ± 0.29 D	a
Fe	113 ± 8 C	135 ± 19 C	180 ± 35 B	573 ± 18 A	a
Ni	1.27 ± 0.11C	2.40 ± 0.53 B	5.65 ± 0.58A	1.51 ± 0.27 C	a
Pb	0.12 ± 0.03 B	0.15 ± 0.02 B	0.26 ± 0.03A	0.29 ± 0.04 A	a
Sb	0.05 ± 0.01	0.03 ± 0.02	0.02 ± 0.01	0.03 ± 0.01	n.d
V	0.12 ± 0.03 B	0.51 ± 0.14 A	0.42 ± 0.07A	0.42 ± 0.04 A	b
Zn	23 ± 2 A	21 ± 3 A	18 ± 2 b	24 ± 2 A	b

Values on each horizontal line followed by the same capitalized letter do not differ significantly (p = 0.05). [a]Significant at 0.001 probability level. [b]Significant at 0.01 probability level. n.d = no difference.

Table 5.2 shows the elemental concentrations of As, Ba, Cr, Cu, Fe, Ni, Pb, Sb, V, and Zn analyzed and ANOVA results from black particles removed from the leaves collected at S1 (three periods, P1, P2, and P3) and S2 (PS2). All elements present higher concentration values at S1 than S2. Statistically significant differences were observed between the three periods at S1 and PS2 for most of the elements, suggesting that black particles do not have the same origin. A similar tendency was observed for all elements over the three periods.

The analyses of soil samples collected at 300 m and 5 km far from the tannery area (S1) are shown in Table 5.3. Results show minimal variation (not significant difference, p > 0.05) between soils collected at 300 for most elements,

except Sb. In contrast, higher concentration values for all elements collected were observed at 300 m than at 5 km. These results may indicate the influence of anthropogenic sources.

Table 5.2 Mean values (± standard deviation, S.D.) and results of the analysis of variance (ANOVA) of the elements measured in black particles collected at Nova Esperança do Sul (S1) during the three periods (P1, P2, and P3) and Lumiar (PS2).

	S1			S2	
	P1	P2	P3	PS2	
Element	Mean ± S.D. /(μg g^{-1})	Mean ± S.D. /(μg g^{-1})	Mean ± S.D. /(μg g^{-1})	Mean ± S.D. /(μg g^{-1})	ANOVA p-value[x]
As	3.75 ± 0.20 AB	4.12 ± 0.38 A	3.13 ± 0.62 B	0.34 ± 0.05 C	a
Ba	87 ± 3 AB	91 ± 3 A	83 ± 6 B	61 ± 2 C	a
Cr	69 ± 3 A	44 ± 2 B	52 ± 12 B	11 ± 2 C	a
Cu	18 ± 2 B	25 ± 3 A	26 ± 2 A	4.14 ± 0.46 C	a
Fe	7484 ± 189 A	7083 ± 259 A	7107 ± 825 A	4745 ± 123 B	a
Ni	4.01 ± 0.19 A	5.21 ± 0.19 B	5.31 ± 1.11 B	3.05 ± 0.32 B	a
Pb	5.10 ± 0.41 AB	7.40 ± 0.40 A	7.17 ± 2.43 A	2.97 ± 0.30 B	b
Sb	0.37 ± 0.04 A	0.54 ± 0.05 B	0.29 ± 0.02 C	0.05 ± 0.02 D	a
V	24 ± 3 B	32 ± 3 A	25 ± 2 B	6.2 ± 0.3 C	a
Zn	76 ± 2 B	84 ± 5 A	80 ± 2 AB	30 ± 4 C	a

Values on each horizontal line followed by the same capitalized letter do not differ significantly (p = 0.05). [a]Significant at 0.001 probability level; [b]Significant at 0.01 probability level.

Table 5.3 Mean values (±standard deviation, S.D.) and results of the analysis of variance (ANOVA) of the trace elements measured in soil samples collected at 300 m and 5.0 km of distance from the tannery area. All samples collected in October 2017.

Elements	Deep soil 300 m Mean ± S.D. /(µg g^{-1})	Superficial Soil 300 m Mean ± S.D. /(µg g^{-1})	Deep Soil 5.0 km Mean ± S.D. /(µg g^{-1})	ANOVA p-value[x]
As	5.79 ± 1.20 A	5.92 ± 1.19 A	1.54 ± 0.34 B	b
Ba	421 ± 22 A	358 ± 86 A	47.6 ± 1.4 B	a
Cr	47.78 ± 2.24 B	60.93 ± 3.82 A	5.43 ± 0.14 C	a
Cu	83.01 ± 2.15 A	70.81 ± 6.13 B	5.35 ± 0.18 C	a
Fe	54496 ± 1427 A	54940 ± 1486 A	4582 ± 249 B	a
Ni	13.68 ± 1.50 A	9.93 ± 0.83 B	2.10 ± 0.03 C	a
Pb	35.87 ± 2.77 A	34.03 ± 1.48 A	4.93 ± 0.67 B	a
Sb	1.24 ± 0.79 A	0.45 ± 0.07 AB	0.09 ± 0.02 B	n.d
V	167 ± 27 A	183 ± 29 A	18.97 ± 1.11 B	a
Zn	197 ± 5 A	209 ± 9 B	14.73 ± 2.14 C	a

Values on each horizontal line followed by the same letter do not differ significantly (p = 0.05). [a]Significant at 0.001 probability level. [b]Significant at 0.01 probability level. n.d = no difference.

5.3.2. Enrichment factor (EF)

The enrichment factor (EF) of each element was calculated according to equation 1 only for black particles collected at site S1A (three periods independently, P1, P2, and P3) and S2 and are shown in Figure 5.1. EF > 5 suggests anthropogenic influence, as it is seen here for Cr (all periods) and As (P1 and P2) in site SA1, while Ni, Pb, Ba, Zn, Sb, V, and Cu present 1 < EF < 4, indicating a slight enrichment of these elements in the environment. In contrast, EF ≤ 1 were observed for As, Pb, Ba, Zn, Sb, V, and Cu at site S2 suggesting

depletion of these elements in this area (except Cr and Ni). this is not surprising because S2 is a rural area. In general, EF values were in the order Cr > As > Zn > Ni > Cu > Sb > Ba > V > Pb, with Cr exhibiting always the highest levels during the three periods at S1A.

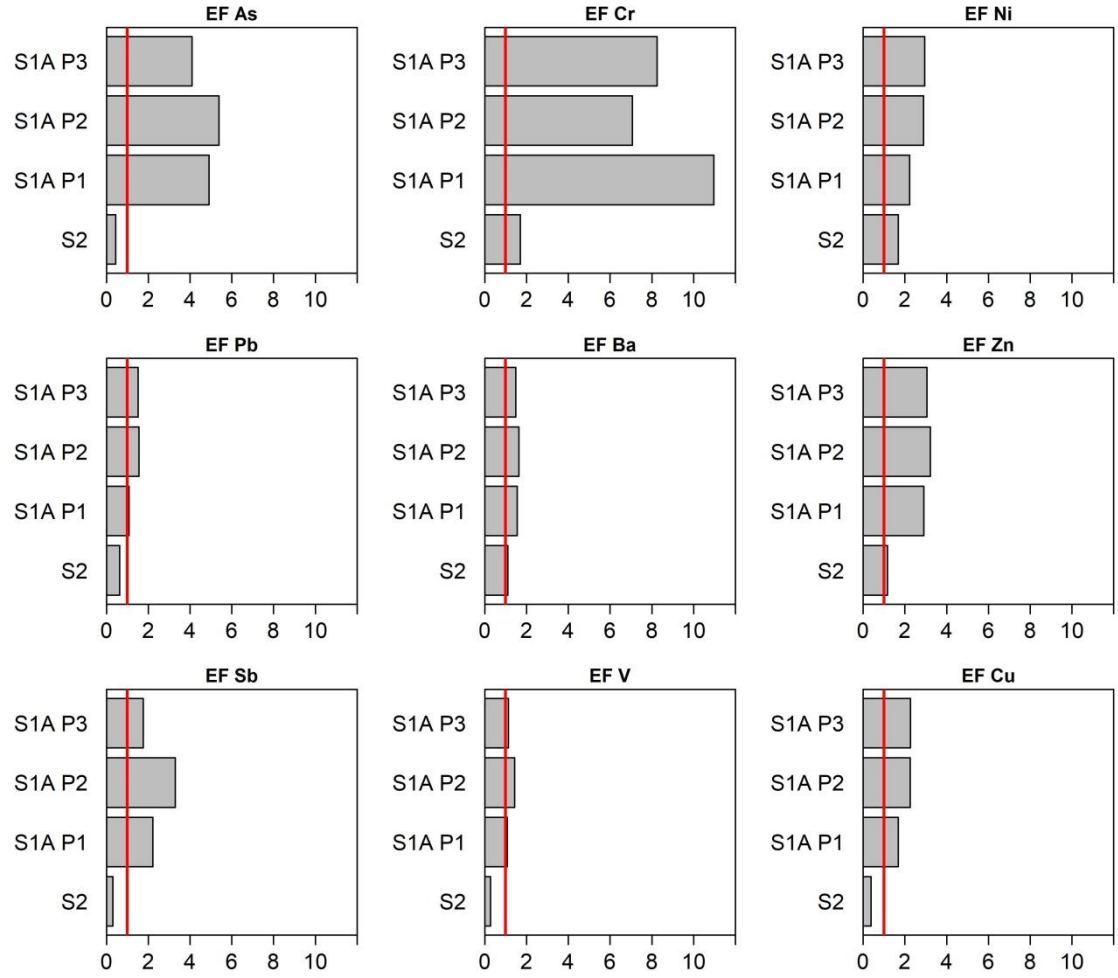

Figure 5.1 Comparison among EFs of the elements measured in black particles removed from leaves in Nova Esperança do Sul, RS (S1) (three periods P1, P2, and P3) and Lumiar, RJ (S2). Fe is used as reference element (red vertical line).

5.3.3. Hierarchical cluster analysis (HCA)

Hierarchical cluster analysis (HCA) was applied to the concentration data of soils (superficial and deep) and black particles removed from leaves (three periods) collected at site S1A (black particles collected at S2 were not

considered). The resulting dendrogram (Figure 5.2) revealed two main Groups: Cr constitutes the Group 1, while Ni, V, Zn, Fe, Ba, Cu, and Pb (subgroup 2A) and As and Sb (subgroup 2B) constitute the Group 2. These results suggest that Group 1 has an anthropogenic origin, while Group 2 may have both a mixture of natural and anthropogenic sources.

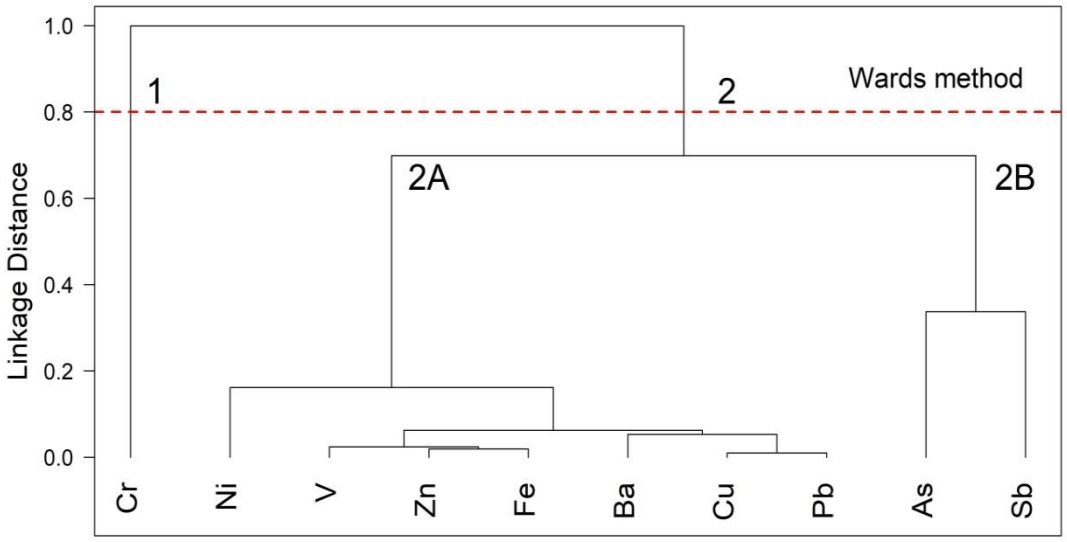

Figure 5.2 Dendrogram representing the grouping of elements based on analysis of black particles removed from leaves of the three sampling periods and soil samples collected at Nova Esperança do Sul, RS (S1A).

5.4. Discussion

Concentration levels of Cr obtained near tannery area (300 m) for both soils and black particles were always higher than samples collected at 5 km and in Lumiar site (S2). In terms of enrichment factor (EF), Cr (EF > 5) and As (EF > 5, two first periods) were clearly enriched in the sampling periods in the center of Nova Esperança do Sul (S1A) and are likely associated with anthropogenic sources. In the literature [104,122–124], several researchers related high concentrations levels of Cr and other toxic elements found in groundwater, effluents, and soils due to poor waste management of leather industries. In the study area, chromium-tanned leather has been used for many decades in the manufacture of a large variety of leather-based products by several companies

installed here; therefore the enrichment of this element may be attributed to the tannery industry. Although arsenic based pesticides are no longer widely used as in the past, chemical elements are persistent and remain in the soil, being accumulated in some plants.

Arsenic is a metalloid that belongs to Group 15 of the periodic table and occurs naturally in the environment [125]. However, this element is related to cancer risk [96,126]. Arsenic is used in the manufacture of several products such as glass, ceramics, electronics, cosmetics, in the pesticides and herbicides formulations [95] and biocides that usually are used to wastewater treatment [127]. The land in the study area is used to produce a variety of products, such as corn, soy, tobacco; cassava, sugar cane and rice, and agrochemical are usually employed by farmers. As there are no other industries in this area, we may affirm that most of As found is related to agricultural activities. In the literature, for instance, Zhou et al. (2018) [95] determined As concentrations in arable soils and found an increasing accumulation trend over past decades, which is related to the long-term application of phosphate fertilizers in agricultural practice, while Botan et al. (2017) [128] related this element to the production of rice grain and complementary medicines.

In relation to the other elements Ni, Pb, Ba, Zn, Sb, V, and Cu, low enrichment of these elements was observed in this area. These elements usually are related to vehicular sources [129–132], and its low enrichment may be explained because this region is a rural area with reduced vehicular fleet.

The Group 1 of HCA shows clearly Cr (Figure 5.1) as a separate variable, which is consistent with the fact that chromium is a key element in the tanning process to obtain leather. From subgroup 2B, it can be noted the presence of Sb, which is a metalloid occurring naturally in the environment as trace elements [125]. However, in the last decades, Sb was associated with traffic because several parts of vehicle contain Sb alloys and other Sb compounds [133–135]. As it is seen in the subgroup 2B from CA, arsenic (As) is a little separated of the other elements, which may indicate that is released from anthropogenic sources but not necessarily from the same source as Ni, Cu, and Zn. Arsenic also occurs naturally and it is noted for their relation with Sb. Both elements were related to

anthropogenic activities that can produce adverse effects on humans and the environment [136].

5.5. Conclusions

This study evaluated the content of toxic elements in a region surrounding a large tannery area, located at Nova Esperança do Sul, Rio Grande do Sul, Brazil. The results of the analysis of black particles collected near the leather industry show higher concentration of all elements analyzed, especially Cr in the three sampling periods compared to an area rural (Lumiar). This result confirmed that the presence of black particles mostly is related to the leather industry than the presence of sooty mold spread by insects. In the same way, soil samples (both deep soil and surface soil) collected around tannery area shown higher concentration for all elements than deep soil collected to 5 km of distance. Enrichment factor higher than 5 were obtained for Cr (three periods) and As (two periods) suggesting anthropogenic influence of both elements. HCA isolated Cr in the first Group demonstrating clearly the influence of this element in the study area, whereas As was related to the use of agrochemicals (pesticides or herbicides) by farmers. On the other hand, EF > 4 for Ni, Pb, Ba, Zn, Sb, and Cu were found, which is in agreement because the study area has rural characteristics.

Acknowledgements

The authors are grateful to Coordenação de Aperfeiçoamento de Pessoal de Nível Superior (CAPES), and Fundação de Amparo e Pesquisa do Estado do Rio de Janeiro (FAPERJ) for financial support T. D. S. thanks to Conselho Nacional de Desenvolvimento Científico e Tecnológico (CNPq) for the scholarship.

6
Air quality biomonitoring of trace elements in the metropolitan area de Huancayo using transplanted *Tillandsia capillaris* as biomonitor

Alex Rubén Huaman De La Cruz,[a, b] Rodolfo Franklin Oscanoa Ayuque,[b]

Rony William Huaman De La Cruz,[b] Adriana Gioda[*]

[a]Pontifical Catholic University of Rio de Janeiro (PUC-Rio), Department of Chemistry, Rio de Janeiro, Brazil

[b]National University of Centre of Peru (UNCP), Faculty of Chemical Engineering, Av. Mariscal Ramon Castilla Km. 5. No 3809, El Tambo, Huancayo, Peru

*Corresponding author: Adriana Gioda - Email: agioda@puc-rio.br

Paper under review: *Annals of the Brazilian Academy of Sciences*

Abstract

The air quality and distribution of trace elements in a metropolitan area of the Peruvian Andes was evaluated using transplanted epiphytic Tillandsia capillaris as biomonitors. Biomonitors were collected from the non-contaminated area and exposed to five sites with different types of contamination for three months in 2017. After exposure, the content of twenty-one elements were determined by ICP-MS analysis. Datasets were evaluated by one-way ANOVA, exposed-to-baseline (EB) ratios, hierarchical cluster analysis (HCA) and map

distribution. Results showed significant differences among sampling sites for several elements.

According to EF ratios for Ba, Cr, Cu, Pb, Sb, and Zn EB ratios value greater than 1.75 were found around urban areas, indicating anthropogenic influence, which can be attributed to vehicular sources. As and Cd, showed the highest values near to agricultural practices, therefore their presence could be related to the employment of agrochemicals (pesticides, herbicides, and phosphate fertilizers). HCA shows that most elements come from vehicular sources and lower from agricultural and natural sources.

Keywords: Active biomonitoring; bioaccumulation; airborne trace elements

6.1. Introduction

Atmospheric deposition of toxic elements continues being a major concern in worldwide because of their negative impact on the environment and human health. In the last decades a significant deterioration of air quality due to urban growing, migration, increasing of vehicles, construction/demolition of roads and buildings, and agricultural practices have been observed in Huancayo city [24,28,80,137]. However, due to the unfortunate lack of suitable environmental policies, government disinterest, and economical support, no measurements of air pollution are carried out in this area. Thus, the use of biomonitors widely used in recent years to evaluate the air quality becomes an important contribution to Huancayo city compared to expensive standard techniques (use of semi and automatic High Volume Sampler (Hi-Vol)). Besides, the use of biomonitors allow us the possibility of monitoring many sites simultaneously by short or long periods of time [138]. Biomonitors can be part or communities of living organisms used to obtain prime information (qualitative and/or quantitative) on aspects of the environment that surround it [139]. Biomonitoring can be applied through of two methods: active and/or passive biomonitoring. Passive biomonitoring refers to collect organisms occurring naturally in the ecosystem or within the area of interest and analyze them. In the method of active

biomonitoring, the biomonitors can be bred in laboratories or collected of pristine sites for posteriorly be exposed in a standardized form (bag technique) within the area(s) of interest for a defined time period.

Lichens and mosses are two biomonitors widely used and recognized in worldwide. However, in recent years several species of the Bromeliaceae family *Tillandsia* species ("air plants") have proved also be appropriate biomonitors because they absorb moisture, nutrients, and minerals directly from the atmosphere due to lack root system that avoid the direct contact with the soil [32,51,140].

A large number of these epiphytic *Tillandsia* species are widely distributed in South America. Regarding the bioaccumulation capacity of atmospheric pollutants by epiphytic *Tillandsia* genus, *Tillandsia capillaris* has proved to be an excellent bioaccumulator of trace elements (TE) in the areas surrounding complex polymetallic mining/smelting in Oruro, Bolivia [141,142]. In Argentina, this species has been widely used to determine polycyclic aromatic hydrocarbons (PAHs) [140], physiological parameters and accumulation of trace elements in different contexts (urban, agricultural, industrial, and mining) [51,138,143–146]. Also, *T. capillaris* was used to assess the accumulation of PAHs and trace elements in urban, suburban and rural areas in Germany [147].

In Peru, studies using biomonitors for the measurement of pollutants in the environment is very scarce. The only study was carried out in Lima using one lichen specie and one specie of *Tillandsia* genus [79].

In the Peruvian Andes, *Tillandsia capillaris* is perennial and endemic specie usually found grows on trees, walls, rocks, cables, and electric poles. Hence, the purpose of this study was to investigate the air quality of vicinities urban, peri-urban, and rural areas and trace element distribution using transplanted specimens of *Tillandsia capillaris* as biomonitors.

6.2. Materials and methods

The reader is referred to the description in section 3.4, page 50.

6.3.
Results

6.3.1.
Trace and major elements concentration in *Tillandsia capillaris*

The arithmetic means, standard deviations, ranges of concentrations and ANOVA results of the elements measured in *T. capillaris* transplanted at the four sites and baseline site are shown in Table 6.1. Overall element concentrations decreased in the following order: Al > Ca > K > Fe > Na > Mn > Ba > Zn > Sr > Cu > Pb > As > Ce > Cr > La > Ni > Co > V > Sb ≈ Sc > Cd. In general, in most transplanted sites the biomonitors showed highest concentration values of the elements measured than baseline samples, confirming the pollutants accumulation capacity of this bromeliad specie. Statistically significant difference ($p < 0.05$) among exposure sites for Ba, Ca, Cd, Cu, Fe, Pb, Sb, and Zn were observed, while significant difference ($p < 0.01$) were found for Al, As, Cr, and Na. No significant differences were observed for K, La, Mn, Ni, Sc, Sr, and V. Highest concentration values of Ba, Cr, Cu, Fe, Pb, Sb, V, and Zn were observed in the urban areas (H and T) than peri-urban areas (Ch and SC). By contrast, the highest values of As and Cd contents were found in Ch and SC sites. These areas have peri-urban characteristics, where residential areas and agricultural areas coexist. Moreover, higher Ca content was found in H, and Ch sites. Calcium is an element considered as a biomarker of cement production [148,149].

Table 6.1 Mean concentrations ± standard deviation S.D. (ug g^{-1} dry weight (D.W)) and ANOVA results of the 21 elements measured in T. capillaris samples exposed during 3 months in the study area and control samples; N = number of samples.

Elements	Baseline (N=5)	Rural (R) (N=5)	Huancayo (H) (N=7)	Tambo (T) N=7	Chupaca (Ch) N=8	Cajas (SC) N=8	ANOVA
	Mean ± SD	Mean ± SD	Mean ± SD	Mean ± SD	Mean ± SD	Mean ± SD	p-value [a]
l	6686 ± 340 b	6852 ± 138 b	9860 ± 169 a	8798 ± 994 a	7348 ± 888 b	6293 ± 1837 b	*p<0.01*
s	2.74 ± 0.22 d	3.47 ± 0.30 d	4.62 ± 0.23 b	4.63 ± 0.57 b	7.93 ± 1.02 a	5.92 ± 0.77 c	*p<0.001*
a	53.01 ± 3.14 d	62.53 ± 3.32 d	106 ± 3 a	107 ± 10 a	84 ± 10 b	71 ± 7 c	*p<0.001*
a	5300 ± 145 c	6017 ± 721 c	10243 ± 773 a	9984 ± 422 a	9330 ± 990 b	6017 ± 721 c	*p<0.001*
e	4.41 ± 0.29 c	5.28 ± 0.32 c	6.70 ± 0.54 a	8.15 ± 1.41 b	5.34 ± 1.02 c	4.66 ± 0.72 c	*p<0.001*
d	0.09 ± 0.04 d	0.22 ± 0.02 c	0.24 ± 0.03 c	0.24 ± 0.05 c	0.33 ± 0.04 b	0.42 ± 0.05 a	*p<0.001*
o	1.39 ± 0.13 b	1.60 ± 0.21 b	1.55 ± 0.11 a	1.54 ± 0.24 a	1.30 ± 0.19 c	1.15 ± 0.23 c	*p<0.05*
Cr	2.79 ± 0.14 e	2.75 ± 0.43 e	6.63 ± 0.20 a	5.33 ± 0.31 b	4.21 ± 0.56 c	3.75 ± 0.49 d	*p<0.001*
Cu	3.77 ± 0.31 e	4.98 ± 0.65 e	18.22 ± 0.66 a	17.14 ± 0.95 b	10.02 ± 1.16 c	8.04 ± 0.76 d	*p<0.001*
Fe	1297 ± 92 e	1609 ± 108 d	2522 ± 132 a	2223 ± 208 b	1757 ± 90 c	1582 ± 185 d	*p<0.001*
K	5772 ± 56 b	5346 ± 364 d	6565 ± 183 a	5219 ± 356 d	5165 ± 550 d	5278 ± 502 c	*p<0.05*
La	2.47 ± 0.38 b	2.58 ± 0.24 b	3.28 ± 0.47 a	3.24 ± 0.37 a	2.82 ± 0.43 b	2.65 ± 0.33 b	*p<0.05*
Mn	197 ± 10 c	181 ± 24 c	179 ± 4 c	231 ± 37 a	213 ± 36 a	211 ± 35 b	*p<0.01*
Na	678 ± 28 b	708 ± 16 b	732 ± 10 b	913 ± 71 a	661 ± 69 b	665 ± 146 b	*p<0.01*
Ni	1.99 ± 0.14 c	3.14 ± 0.36 b	3.19 ± 0.29 a	3.79 ± 0.59 a	3.10 ± 0.77 b	2.89 ± 0.89 b	*p<0.001*
Pb	3.47 ± 0.10 d	5.36 ± 0.84 d	18 ± 2 a	18.0 ± 2.0 a	12.0 ± 1.05 b	8.0 ± 1.2 c	*p<0.001*
Sb	0.32 ± 0.04 e	1.13 ± 0.26 c	2.47 ± 0.28 a	2.26 ± 0.21 a	1.41 ± 0.31 b	0.72 ± 0.14 d	*p<0.001*
Sc	0.87 ± 0.14 b	0.78 ± 0.08 c	0.94 ± 0.04 b	1.17 ± 0.11 a	1.00 ± 0.17 b	0.84 ± 0.21 c	*p<0.001*
Sr	28.24 ± 1.32 b	34.10 ± 2.96 a	34.67 ± 1.06 a	33.68 ± 2.02 a	29.74 ± 2.21 b	29.13 ± 4.39 b	*p<0.001*
V	2.03 ± 0.13 d	2.25 ± 0.38 d	3.97 ± 0.68 a	3.95 ± 0.57 a	3.14 ± 0.45 b	2.52 ± 0.66 c	*p<0.001*
Zn	18.42 ± 1.16 f	29.60 ± 3.48 e	117 ± 5 a	99 ± 5 b	78 ± 8 c	50 ± 5 d	*p<0.001*

[a] Values on each horizontal line followed by the same letter do not differ significantly (ns: not significant). * Significant at 0.05 probability level. ** Significant at 0.01 probability level. *** Significant at 0.001 probability level.

6.3.2.
EB ratios

The EB ratios calculated as described in Section 3.4, are shown in Table 6.2. According to the scale of Frati et al. (2005) [50], values greater than 1.75 are indicative of anthropogenic influence. In this case, As, Ba, Ca, Cd, Cr, Cu, Pb, Sb, V, and Zn showed EB ratios > 1.75 for most exposure sites. While the whole study area present six elements (As, Cd, Cu, Pb, Sb, and Zn) with EB ratios > 2.00, suggesting a strong influence of these elements in the environment of Huancayo city.

Table 6.2 EB ratios calculated for 21 elements measured in the samples of transplanted T. capillaris transplanted in each site, after three months of the exposure period

Elements	Rural	Huancayo	Tambo	Chupaca	Cajas	Average Whole area
Al	*1.35*	*1.35*	*1.47*	1.12	0.89	1.21
As	*1.71*	*1.71*	**1.76**	**2.66**	**2.18**	**2.07**
Ba	**2.00**	**2.00**	**1.96**	*1.68*	*1.35*	**1.75**
Ca	**1.95**	**1.95**	**1.76**	**1.95**	1.20	*1.71*
Ce	1.54	1.54	**1.99**	*1.53*	1.09	*1.54*
Cd	**2.79**	**2.79**	**2.73**	**3.89**	**4.80**	**3.55**
Co	1.10	1.10	1.11	0.97	0.83	1.00
Cr	**2.39**	**2.39**	**1.99**	**1.84**	*1.37*	**1.90**
Cu	**4.86**	**4.86**	**4.34**	**3.08**	**2.13**	**3.60**
Fe	*1.65*	*1.65*	*1.54*	*1.30*	1.07	*1.39*
K	1.14	1.14	1.11	1.13	0.92	1.07
La	*1.37*	*1.37*	*1.40*	*1.29*	1.07	*1.27*
Mn	0.97	0.97	1.16	0.93	0.96	1.01
Na	1.08	1.08	*1.40*	1.00	0.96	1.11
Ni	*1.64*	*1.64*	**1.89**	*1.72*	*1.46*	*1.68*
Pb	**5.77**	**5.77**	**5.17**	**4.13**	**2.44**	**4.38**
Sb	**7.93**	**7.93**	**6.17**	**4.75**	**2.41**	**5.31**
Sc	1.09	1.09	*1.45*	1.20	1.02	1.19
Sr	1.11	1.11	1.16	*1.26*	0.92	1.11
V	**1.93**	**1.93**	**2.13**	*1.74*	1.21	*1.74*
Zn	**7.28**	**7.28**	**5.99**	**4.57**	**3.23**	**5.27**

Normal conditions (0.75-1.25) is with a normal letter, accumulation (1.25 – 1.75) is highlighted in italic, and severe accumulation in bold (> 1.75).

6.3.3.
Hierarchical cluster analysis (HCA)

The dataset of the elements submitted to HCA yielded two distinct groups (Figure 6.1). K, Sr, Na, Mn, Ni, La, Sc, Al, Ce, V, and Co are grouped in Group 1, while Group 2 includes Zn, Cu, Fe, Pb, Ba, Sb, Cr, Ca, Cd and As (closely associated among themselves). The dendrogram indicates that elements belonging to the same group may have the same origin. As it is seen, the Group 1 contains elements related to natural sources; while in Group 2 can be observed elements of anthropogenic origin.

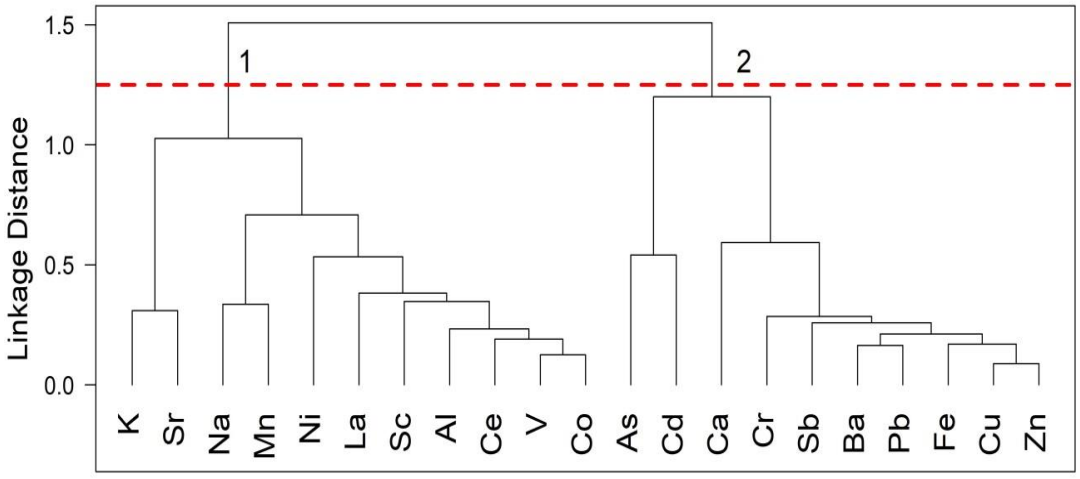

Figure 6.1 Results of the hierarchical cluster analysis (dendrogram) of the elements measured in T. capillaris.

6.4.
Discussion

The EB ratio values obtained for As (T, Ch, and SC sites), Ba (H and T), Ca (H, T, and Ch), Cd (all sites), Cr (H, T, and Ch), Cu (all sites), Pb (all sites), Sb (all sites), V (H and T), and Zn (all sites) were all greater than 1.75, suggesting severe influence of anthropogenic sources in the metropolitan area of Huancayo. Considering the whole study area the average accumulation ($1.25 < EB\ ratio < 1.75$) of Ca, Ce, Fe, La, Ni, and V were observed. On basis of EB ratios, these latter elements are considered enriched, suggesting that despite soil particles are providing part of these elements, their origin could be anthropogenic. Significantly higher EB ratios were found for Cd, Cu, Pb, Sb, and Zn confirming

their anthropogenic origin of these elements, while Al, Co, K, Mn, Na, Sc, and Sr in the whole study area were found to normal conditions in the environment, which could indicate natural origin (Table 6.2).

In the literature, Cd, Cu, Pb, Sb, and Zn are considered toxic elements [15,136,150] being the last four related to vehicular sources in urban areas [145,151]. Effectively, these elements presented higher concentration values around urban areas (T and H sites) from Huancayo city (Table 6.1), where car congestion happens every day and during all day.

The distribution map of As (Figure 6.2) shows high levels of this element to the southwestern and relatively elevated to the north. In this places are located the sites Ch and SC, where the land is used to agricultural practices in the production of different type of crops such as vegetables, corn, potatoes, onions among others.

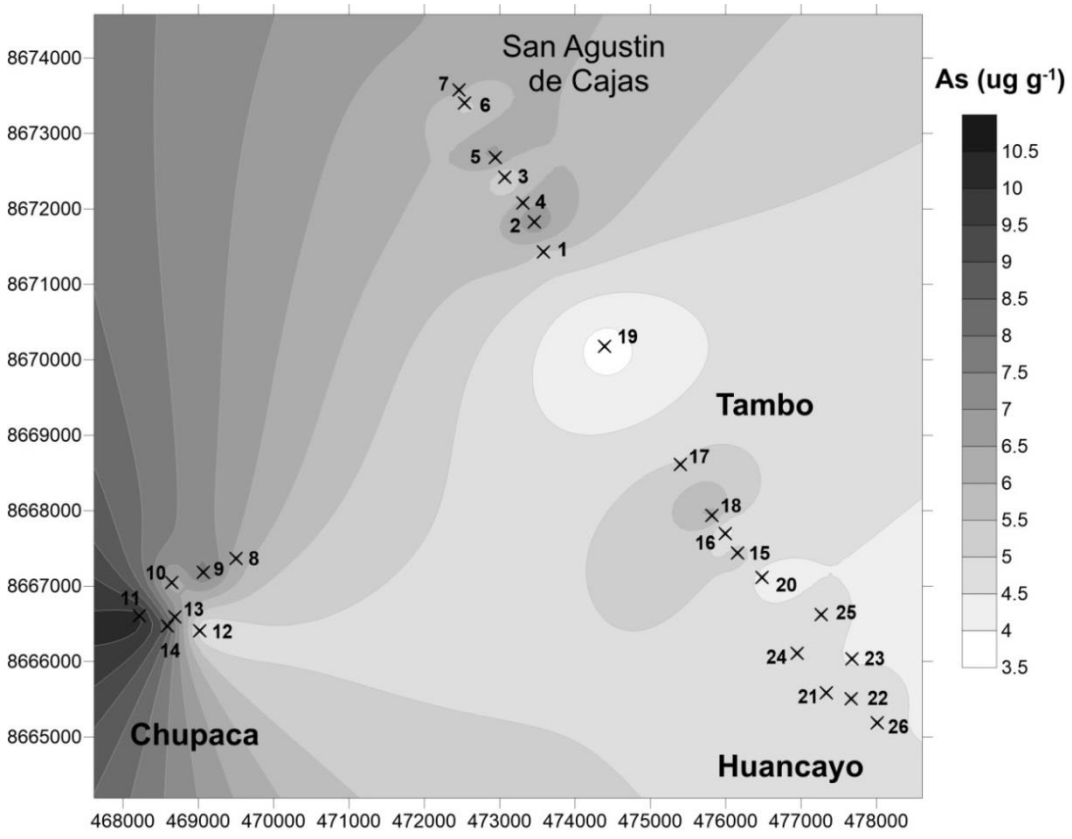

Figure 6.2 Distribution map of As concentrations

The results of Ca concentrations in *T. capillaris* are illustrated in Figure 6.3. Calcium element is considered as a biomarker for cement production [148,149]. As it is seen, calcium element is widely distributed in almost all study

area with the higher content of this element being observed in Ch, T, and H sites. In recent years, both T and H sites suffer a transformation with the demolition of roads and the historic “Plaza Constitucion” located in downtown and the construction of three new supermarkets, while Ch site is facing the built of residential buildings and bridges [24,28]. Despite, the contact with this element may cause cancer [152,153], dust pollution [154] and environmental impact [155,156], construction activities on this area are poorly controlled.

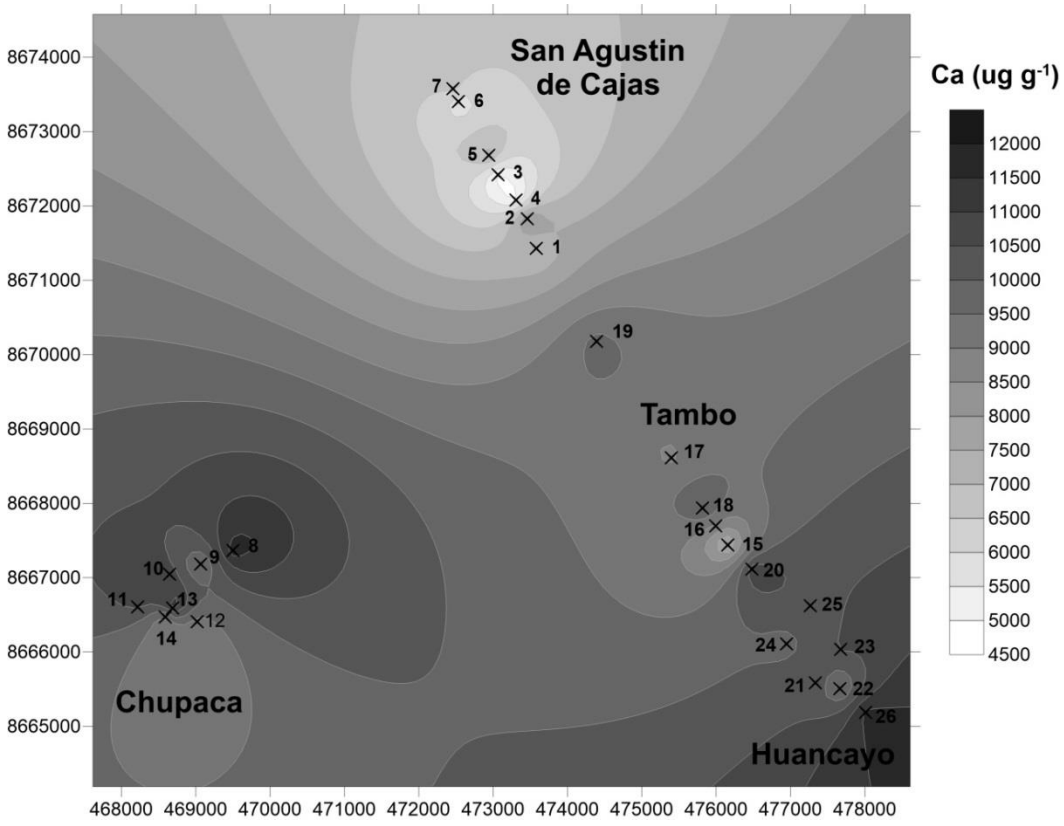

Figure 6.3 Distribution map of Ca concentrations

The highest contents of Cd were detected in the north and southwestern zone from downtown (Figure 6.4), specifically in the two peri-urban areas (Ch and SC) where agricultural activities are developed by farmers. Cadmium occurs naturally in the environment usually linked to zinc [157]. Cadmium usually is emitted by smelting refining of nonferrous elements, fossil fuel combustion, metalliferous mining, incineration waste, phosphate fertilizer production, and by industries using cadmium in rechargeable batteries, pigments, electroplating, solar cells, and as plastic stabilizers. Cadmium in agricultural soils can enter via phosphate fertilizers (0,1-170 mg/kg) [158,159]. Like the land use in areas around

from Metropolitan area of Huancayo is considered suitable for the production annual and biennial of crops [24], a big quantity of Cd may be related to the use of agrochemicals (pesticides, fertilizers, and herbicides).

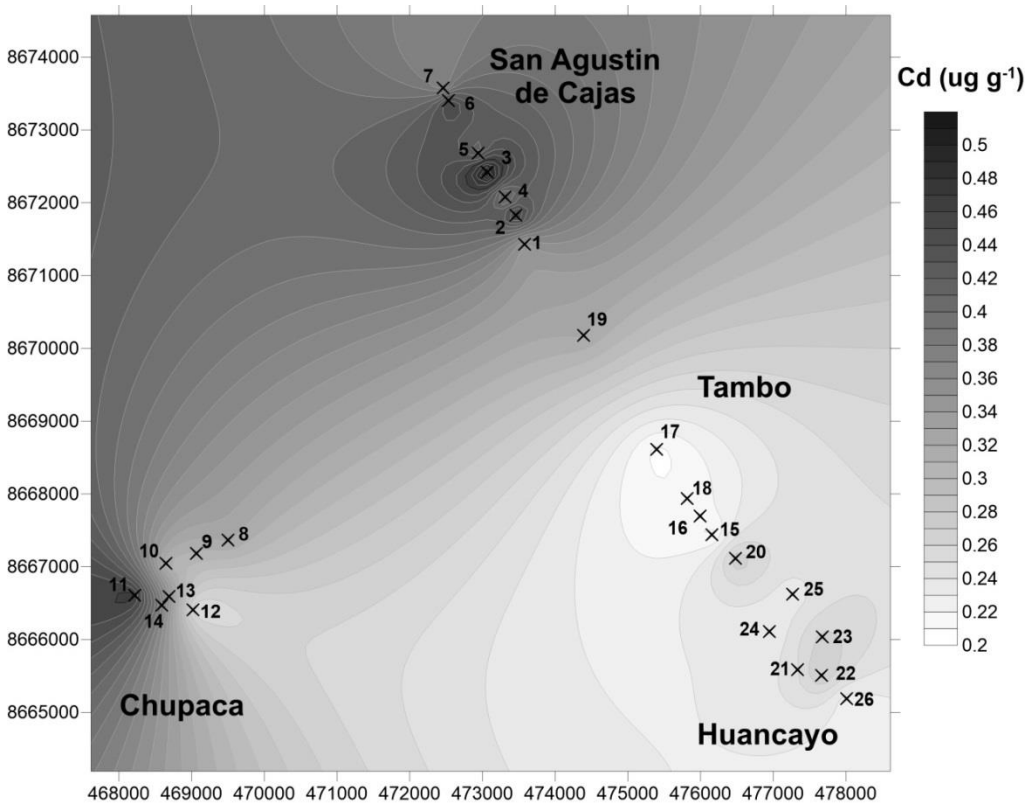

Figure 6.4 Distribution map of Cd concentrations

Lead is a toxic element even at low concentration and is related to vehicular emissions and dust re-suspension [160]. In Peru, leaded gasoline was banned in 2009 [82], however, the distribution map of Pb (Figure 6.5) shows that Pb contamination is still present in this area. A similar result has been reported by De la Cruz et al. (2009) [161] who studied the lead concentrations and its isotope ratios in samples of particulate matter (PM_{10}) before and after non-leaded fuel normative in Zaragoza (Spain) and concluded non statistically significant decrease in average concentration of lead. The higher Pb levels were found in Ch, H and T (the place where exist a gas station approximately twenty years ago). No information about this element was found in the literature for comparison purpose or to affirm decreasing of this element compared to previous years.

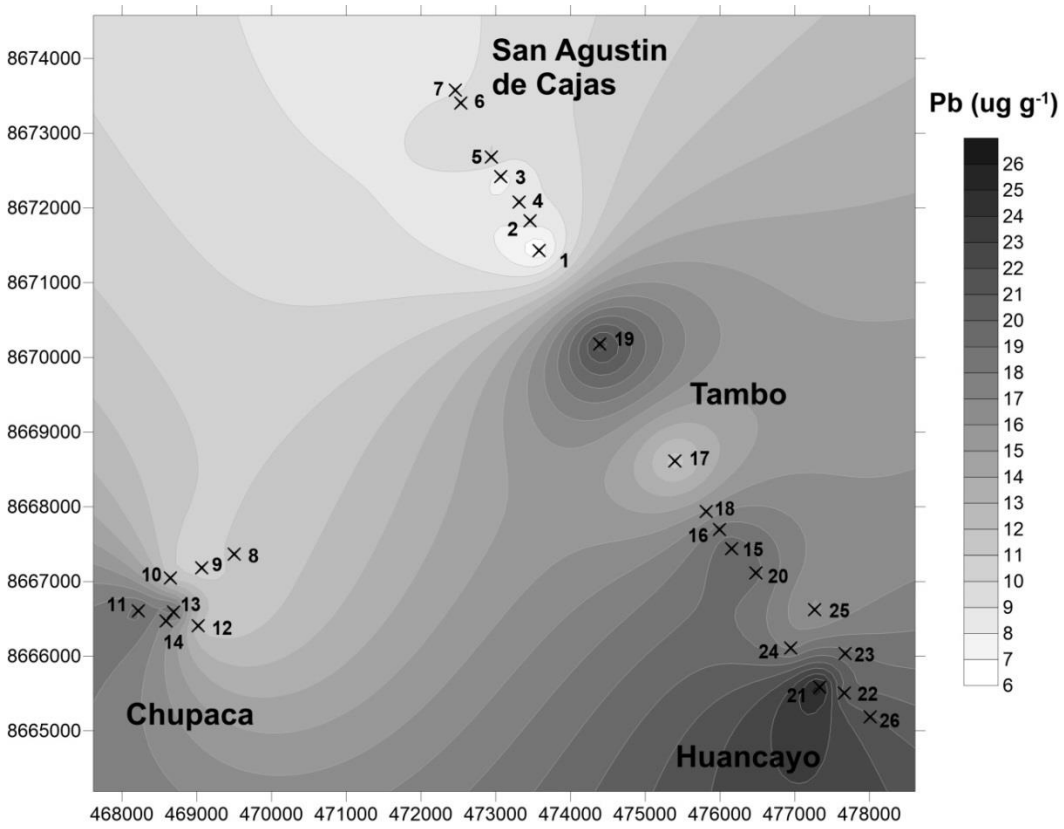

Figure 6.5 Distribution map of Pb concentrations

The distribution map of Sb (Figure 6.6) shows three sites: two urban areas (T and H) and a rural/urban area (Ch) with higher Sb content. Antimony is a metalloid and occurs naturally as trace elements in the environment (soils) [125,134], however in the last decades this element was associated with traffic due to that several parts of vehicle contain Sb alloys and other Sb compounds [133–135]. According to EB ratios and the location, we can conclude that Sb comes from vehicular sources.

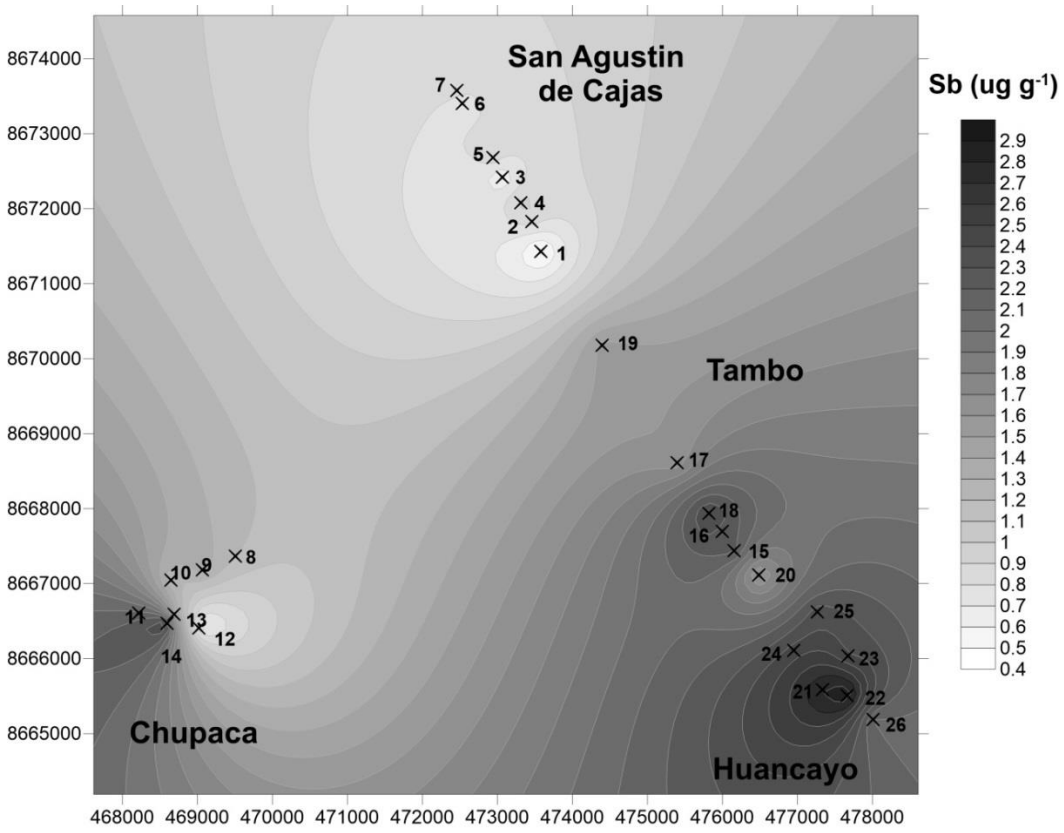

Figure 6.6 Distribution map of Sb concentrations

The distribution map of Zn (Figure 6.7) revealed elevated content of this element in the southeastern, around urban areas, which indicates anthropogenic origin. The highest levels were observed in downtown (H) and its neighbor Tambo city. Both areas have a big circulation of vehicles during all day causing heavy traffic.

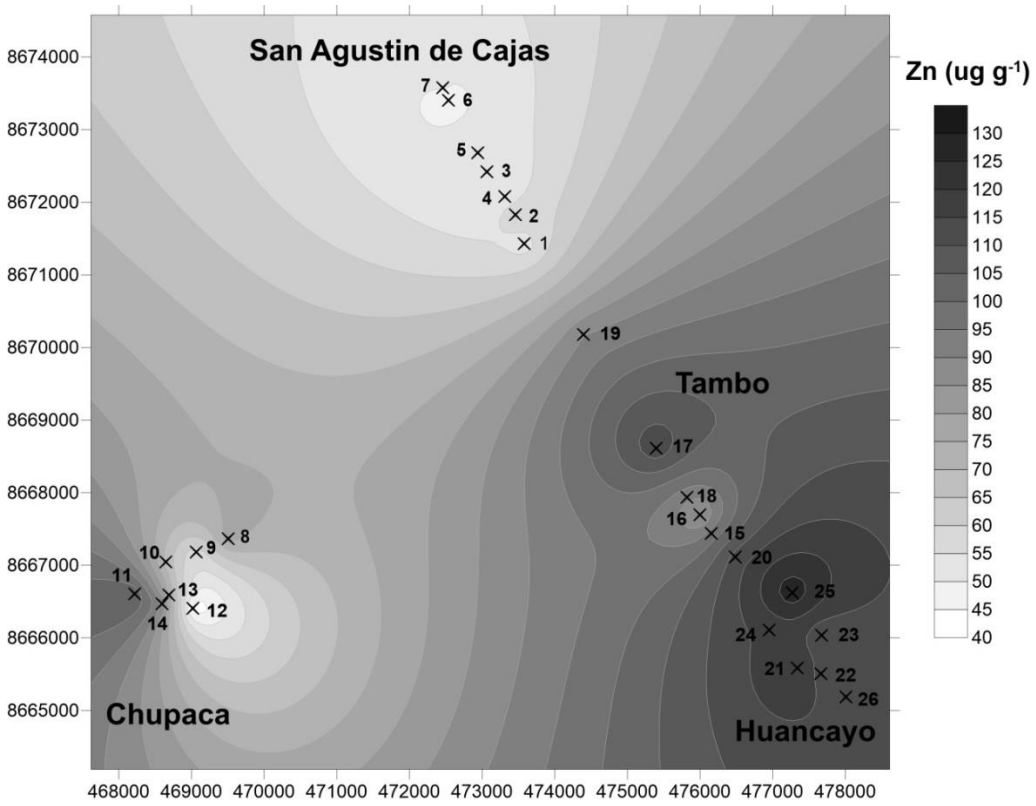

Figure 6.7 Distribution map of Zn concentrations

The hierarchical cluster analysis (Figure 6.1) helps us to elucidate our analysis. The dendrogram shows two groups: the first formed mainly by elements from natural origin (e.g., Co, Sr, Mn, Al), while the second group presented all elements from anthropogenic sources. As it is observed with As and Cd closely related, calcium little separates of the other elements and Sb, Ba, Pb, Zn, Zn, and Cu intimately related each other.

6.5. Conclusions

The Tillandsia capillaris behaved as an effective biomonitor for assessment of air quality in the Metropolitan area of Huancayo. The results of the study show the impact of anthropogenic sources in the study area. Concerning the association between the trace elements and the different anthropogenic activities, highest levels of Cu, Pb, Sb, Zn were found to be related to vehicular emissions, while As and Cd content were found higher in peri-urban areas, relating these elements to

the employment of agrochemicals, while high content of Calcium was observed near construction/demolition areas.

Acknowledgements

The authors are grateful to Coordenação de Aperfeiçoamento de Pessoal de Nível Superior (CAPES), and Fundação de Amparo e Pesquisa do Estado do Rio de Janeiro (FAPERJ) for financial support T. D. S. thanks to Conselho Nacional de Desenvolvimento Científico e Tecnológico (CNPq) for the scholarship.

7
Use of three *Tillandsia* species as biomonitors for evaluating urban-industrial pollution in Brazil

Alex Rubén Huamán De La Cruz, Vinicius de Paiva Andrade, Carlos Zaki Antaki, Ellen Jessica de Souza Macário dos Santos, Jefferson Rodrígues de Souza, Tatiana Dillenburg Saint'Pierre, Adriana Gioda*

Pontifical Catholic University of Rio de Janeiro (PUC-Rio), Department of Chemistry, Rio de Janeiro, Brazil

*Corresponding author: Adriana Gioda - Email: agioda@puc-rio.br

Working paper (In process): *Ecological Indicator* (Aimed journal)

Abstract

Tillandsia species (*T. Meridionalis*, *T. Usneoides*, and *T. Trichopelis*) considered as biomonitors were collected from a non-contaminated site (control site) and transplanted back at ten sites urban (around bus station and highway) and/or industrial in the Metropolitan region of Rio de Janeiro (MRRJ), Brazil. These samples were exposed for two periods of time during May-Jun 2017 to evaluate the accumulation of airborne Al, As, Ba, Ca, Cd, Co, Cr, Cu, Fe, K, Mg, Mn, Ni, Pb, Rb, Sb, Sr, Ti, V, and Zn through ICP-MS analysis. The comparison among study sites indicates that highest values of trace elements concentrations were found at industrial sites than urban sites.

Comparing the three species, results suggested that *Tillandsia tricholepis* accumulated major contents of the most elements measured. Concentrations of Al, Ba, Bi, Cd, Co, Cu, Pb, Sb, and Zn were the highest in urban/traffic and/or suburban/traffic areas. Some of these elements e.g. Ba, Cu, Sb, and Zn are commonly considered as traffic-related elements. In the industrial site, the main element found were Mg, Sr, and Zn. Fe, Mn, Na and V concentrations were much higher in rural/remote areas.

Keywords: Biomonitoring, Tillandsia species, airborne elements, urban/industrial environment, transplants.

7.1. Introduction

Air pollution is not a recent problem of the modern society and may be described by the presence of foreign toxic substances in air at concentrations, residence times, size, distance dispersed, and frequencies could affect adversely the welfare and health human, as well as the environment [1,162,163].

The Environmental Protection Agency (EPA) stated six main air pollutants: Ozone (O_3), Particulate Matter (PM), Carbon Monoxide (CO), Lead (Pb), Sulphur Dioxide (SO_2), and Nitrogen Dioxide (NO_2). Among them, the PM is regarding as the most dangerous due to the presence of toxic elements in their structure, which are introduced into the atmosphere by different sources as urban (e.g., combustion of fossil-based fuels, vehicle component wearing, bare ground sites, construction and demolition sites) [151,164,165] or industrial (e.g., mining ores, steel plant, cement plants) [149,166,167].

Usually, the PM is quantified using automatic high-volume sampler (Hi-Vol) used as atmospheric pollution monitor and filters where are deposited (collected) the PM. Using these filters is possible to reveal the content and presence of elements in air PM prior acid decomposition. However, these sophisticated instruments are expensive, need qualified staff, and usually demand substantial maintenance cost [46,161,168].

Biomonitoring air quality study has rapidly increased over recent decades as an inexpensive and efficient alternative where are used different bio-organisms such as lichen, mosses, tree bark, and Spanish mosses (bromeliad genus) methods, which have been widely used to estimate air pollution, especially of airborne elements during determined period time, low cost, and in several geographical areas simultaneously.

Tillandsia genus or air plants are epiphytic plants of the *Bromeliaceae* family, which are widely distributed on their native habitat in the southern United States, Central, and South America, with a large number of species. These species grows slowly, has an extraordinary ability to obtain water and nutrients from the atmosphere through their leaves called trichomes and are resistant to hydric stress [169].

Among all the species, *Tillandsia usneoides* and/or *Tillandsia capillaris* have been more employed as biomonitors of toxic trace elements in Argentina, Bolivia, Brazil, Italy, Mexico, USA, and Thailand [71,141,142,144,151,170–172], and in Chile, Mexico and Paraguay were used *Tillandsia recurvata* [83,173,174]. For instance, in Brazil, the biomonitoring with *T. usneoides* showed higher element concentrations of Cd, Cr, Cu, Pb, and Zn in the two metropolitan areas: Salvador and Rio de Janeiro than the control sites [175]. Increasing concentrations of As, Ba, Co, Cr, Fe, Rb, V, and Zn were found in *T. usneoides* exposed in urban/industrial areas of the metropolitan region of São Paulo, when compared to control site, being related to vehicular sources, industrial zones, anthropogenic, and soil particles [32]. Plants of *T. usneoides* were exposed in three areas: industrial, urban and agricultural in Campinas, Sao Paulo State, during dry and wet seasons, where the concentration measurements showed higher concentrations of N, Ca, S, Fe, Zn, Cu, B, Co, and Ni. According to seasonal study, Mg and Zn showed higher level concentrations in the wet period and N, Fe, P, Mn, and Fe in dry season [71].

The main purposes of this study were: (i) to quantify element accumulation of twenty-one elements in three *Tillandsia* species in Rio de Janeiro (Brazil) as a biomonitor of environmental status of urban environments; (ii) to provide reference values for these elements in these epiphytic species; and (iii) to asses three sympatric *Tillandsia* as bioindicators of urban element pollution in Rio de Janeiro city.

The main aim of this study is to evaluate comparatively the biomonitoring capacity of *T. usneoides*, *T. tricholepis*, and *T. meridionalis* to assess atmospheric levels of anthropogenic toxic elements, when exposed in polluted sites under tropical seasonal climate and to determine which of them would be recommended for qualitative biomonitoring and discriminate the atmospheric levels associated with distinct emission sources of these elements.

7.2. Materials and methods

The reader is referred to the description in section 3.5, page 55.

7.3. Results and discussion

7.3.1. Descriptive statistics

Table 7.1 shows average concentration values ± standard deviation in μg g^{-1} dry weight (DW) measured in the eight sites (n=32) for the three *Tillandsia* genus; *T. tricholepis*, *T. meridionalis*, and *T. usneoides* after two months exposure compared to concentration values measured (average concentration value of all sites in each study) in *Tillandsia* species reported in the literature using transplanting method (active biomonitoring) in Brazil and another country. After transplanting plants were noted that the three *T.* species remained green during the exposure time, even some showing growth, demonstrating the great facility of these plants to adapt physiologically and metabolically to any environment. Mean concentration of the elements measured in each *T. species* presented in Table 7.1 decreased in the following order: K > Ca > Mg > Al > Fe > Mn > Zn > Ba > Sr > Ti > Rb > Cr > Pb > Co > V > Sb > Cd > As, with little variations among the elements. Higher basal average concentration values (control site) of many trace elements and nutrients (Al, Ba, Cd, Cu, Fe, K, Mg, Mn, Ni, Rb, Ti, and V) measured were observed in plants of *T. tricholepis* in comparison than to other two species. Likewise, in *T. usneoides* was noted higher basal concentration of Cr, Sb, Pb, and Zn. Already, *T. meridionalis* only presented Na, Ca, and Co (Table 7.1). After two months of exposure time, higher levels concentration (except As,

Cr, and Na) were measured in *T. tricholepis* than other two bromeliads analyzed. Comparing the remain species, *T. usneoides* had higher levels of Ca, Cd, Cr, Cu, Fe, Mg, Na, Ni, Pb, Sb, Sr, Ti, V and Zn than *T. meridionalis* (Table 7.1).

To compare the values obtained with the literature was difficult due to: i) were not used still in previous studies *T. meridionalis* and *T. tricholepis* as biomonitor, ii) different exposure period time and geographical area, iii) a limited number of elements reported in previous studies, and iv) different morphology among the species. We compared the values obtained in our study to one previous report that used a similar active transplanting biomonitoring using only *T. usneoides* reporting only five elements (Cd, Cr, Cu, Pb, and Zn) [175]. Cd, Cr, and Cu average concentration values (eight sites) in the present study (urban and industrial context) were higher than urban context (average five-sites) [175], but with lower values of Pb and Zn. The major values may be ascribed to industrial and urbanization growing. However, comparing the same site (Terminal Central), Cr, Cu, and Zn results were in accordance to those obtained in the previous study (Table 7.1). In relation to other studies developed in other cites from Brazil using *T. usneoides,* Salvador city showed lower concentration values of Cd, Cr, Cu, and Zn measured in an urban context [175] than our work, already values reported by Figuereido et al. [32] in specimens transplanted in urban context and low industrial context in São Paulo were in accordance for most elements measured with the present study, except Na (higher concentration values) probably influenced by the sea (Table 7.1). Higher concentration values for most measured elements than our study was reported by Giampoli et al. [71] at the industrial context (chemical and agrochemical industries) in São Paulo, Campinas. In Province Cordova, Argentina [51] measured three elements (Fe, Mn, Zn), with lower values of Mn and Zn than our values obtained, but in accordance to Fe values.

Table 7.1 Average elemental concentration in μg g^{-1} ± standard deviation (SD) in dry weight (DW) of all sampling sites after two months exposure period of three Tillandsia species: T. meridionalis, T. tricholepis and T. usneoides comparing to the literature.

	Meridionalis	*Tricholepis*	*Usneoides*	*Usneoides*	*Usneoides*	*Capillaris*	*Usneoides*	*Capillaris*	*Recurvata*	*Usneoides*	*Usneoides*	*usneoides*
	Brazil, RJ Mean±SD	Brazil, RJ Mean±SD	Brazil, RJ Mean±SD	Brazil, RJ Urban[A]	Brazil, S Urban[A]	Argentina Complex[B]	Brazil, SP Complex[C]	Bolivia, O Mining[D]	Chile Urban[E]	Italy Urban[F]	Brazil, SP Urban[G]	Argentina Urban[H]
Al	709±185	1668±792	715±108					7384±2587	1020±927	145±37		
As	0.43±0.12	0.34±0.12	0.36±0.08			1.63±0.47	0.34±0.04	31±45	1.16±0.64	0.2±0.04		
Ba	49.6±10	58.12±10	46.6±12			73±32	37±8	77±29	17±7	12.5±1.1		
Ca	3319±896	4063±1047	4623±1754			20739±5160	3312±596	5586±1411	8073±4793	4920±390	8200	
Cd	0.70±0.21	1.30±0.36	0.84±0.23	0.30±0.16	0.28±0.03	0.72±0.37		1.04±0.98	0.16±0.07	0.08±0.05		
Co	2.45±0.45	2.48±0.56	1.89±0.35			0.81±0.11	1.63±0.38	2.8±0.9	0.34±0.20	0.15±0.07	9.6	
Cr	3.24±0.9	4.53±1.15	4.57±0.93	2.71±1.16	2.87±1.25	26.7±6.82	2.07±1411	6.8±2.3	2.46±1.43	2±0.1	5.8	
Cu	11.56±1.36	16.31±3.2	17.9±2.9	9.1±2.3	7.2±2.1	8.84±5.07		20±19	11.49±3.75	9.7±1.7	20	
Fe	521±99	917±174	751±127			2685±718	1144±104	5274±1639	686±518	174±38	1305	865.7±104
K	9904±3269	12944±2500	6491±1143				5890±1082	8314±2193	5928±1416	2321±404	4900	
Mg	1651±343	2211±176	1792±275					1776±526	2001±1248	1334±147	900	
Mn	62±8	70±15	43±8			106±11		154±46	73±26	16.7±2.3	44	28.63±2.71
Na	2684±561	943±148	2991±1119			2683±945	116±26	3312±1525	5955±2824	828±130		
Ni	2.10±0.44	2.22±0.66	2.32±0.74			6.87±1.57				2.4±0.8	2.9	
Pb	3.45±0.7	4.60±1.02	5.32±1.3	6.5±1.5	7.02±1.5	5.54±1.19		53±74	5.2±3.1	5.1±1.3	45.6	
Rb	16±5	28±7	14.7±2.5			19.79±6.87	30.1±6.36	11.3±4.1	3.55±0.95			
Sb	0.56±0.17	1.16±0.24	0.95±0.21			0.26±0.09	0.49±0.19	17±19	0.19±0.09	0.34±0.07		
Sr	26.92±4.55	30.02±7.69	28±8.70					45±12	29.9±17.8	65±6	81.1	
Ti	21.7±3.9	31.3±8	20±3					510±178				
V	2.01±0.48	2.4±0.6	2.55±0.45					11.3±3.8	2.35±2.22	0.46±0.13	7.6	
Zn	95±12	125±40	114±21	181±131	34.4±10.4	22.63±5.9	90±29	186±508	70±28	195±47	117	31.40±5.5

A [175], B [144], C [32], D [141], E [173], F [151], G [71], H [51].

7.3.2.
EC ratios

Calculated mean EC ratios for each trace elements and for each *Tillandsia* specie in all sites and exposure periods (one and two months) are presented in form of boxplot diagram in Figure 7.1. These boxplot revealed significant variations in the accumulation levels of the most of the elements measured between the two exposure periods for each bromeliad genus. Considering a reasonable exposure time of two months, some elements were more enriched than other in each *T.* specie showing two scales according Frati et al. (2005) [50]: *T. tricholepis* showed accumulation of Mg and K and presented severe accumulation of Ca, Mn, Co, Zn, Rb, Sb, Cd, and Pb. Already *T. usneoides* accumulated Ti and Ni and showed severe accumulation of V, Fe, Ni, and Cu. Likewise, accumulation of Na and severe accumulation of Ba, Al, Cr, and As was observed *T. meridionalis*. This accumulation pattern with higher EC ratios for As, Cd, Pb, Sb, Zn, Cu, and Ba was consistent with a previous atmospheric study [71,141] confirming these elements as main pollutants of urban/industrial and terrestrial/dust sources. Maximum published EC ratios in *T. tricholepis* were about 1.81, 1.47, and 1.55 respectively for Fe, Mn and Zn after a 3-month exposure in an industrial context by Bermudez et al. (2009) [51] who indicated this specie as the best accumulator of these elements. A similar result of EC ratio for Fe (1.79) but with higher values of Mn (2.51) and Zn (2.44) was found in this work after two months of exposure (Figure 7.2). While *T. usneoides* showed similar EC ratios of Mg, K, Fe, Mn and Co in an industrial/urban/agricultural context [71] according to our obtained values. The EB ratios for *T. meridionalis* varied in the following order: Cu > Pb > Cd > Zn > Sb > As > Ni > Cr > Mg > Cr > Fe > V > Ti > Mn > K. Studies reporting EC ratios of elements using *T. meridionalis* still do not exist in the literature. Among the elements was observed that K in the three *T.* species, exhibited a very weak accumulation (EC ratios between 0.86 to 1.52) during the exposure period, showing depletion after transplantation in the most of sites studied (Table 7.1). This phenomenon already was noted by several authors [32,71,141,164,176] employing different biomonitors (i.e., *Tillandsia*, mosses, lichen, tree bark). EC ratios for two months exposure period from each site and *T.* specie with ANOVA analysis using transplanting sites as mean comparison

criterion for trace element accumulation (elements with EC ratios higher) are presented in Figure 7.1 to Figure 7.3. The results of the ANOVA analysis showed similarities and differences between sites and element accumulation. These similarities probably due to that the most of the transplanting sites chosen were around or near a bus terminal in the urban areas, and the dissimilarities can be attributed to the number and type cars (train, VLT, bus, truck, motorcycle). Moreno et al. (2015) [177] made a comparison of the urban air quality among sites with the presence of bus, subway and pedestrian commutes in Barcelona, Spain. Their results showed higher CO_2 levels related the passenger number, and notable differences and distribution of inhalable particle that can range from alumino-siliceous to ferruginous as Mn, Co, Zn, Sr and Ba in the subway environment and higher levels of Sb and Cu around bus terminal [177].

7.3.2.1. Tillandsia meridionalis

Considering EC ratios (Figure 7.1), it can be seen that Zn, Pb, V, and Ba were highly enriched in the vicinities of urban site NR (bus terminal that linked another countries and states from Brazil). On the other hand, higher accumulation of Fe and Cr was observed in an industrial site SC (steel industry). Likewise higher accumulation of Ni, Cu, and Sb was related to freeway site (HSC). The remains elements showed similar accumulation among the sites.

7.3.2.2. Tillandsia tricholepis

In this *T.* specie (Figure 7.1) Zn, Pb, Ni, Cd, and V showed higher accumulation in bus terminal called NR. Higher EC ratios values were observed for Fe and Cd in the industrial site. Besides higher accumulation of Cu and As was noted in the freeway site.

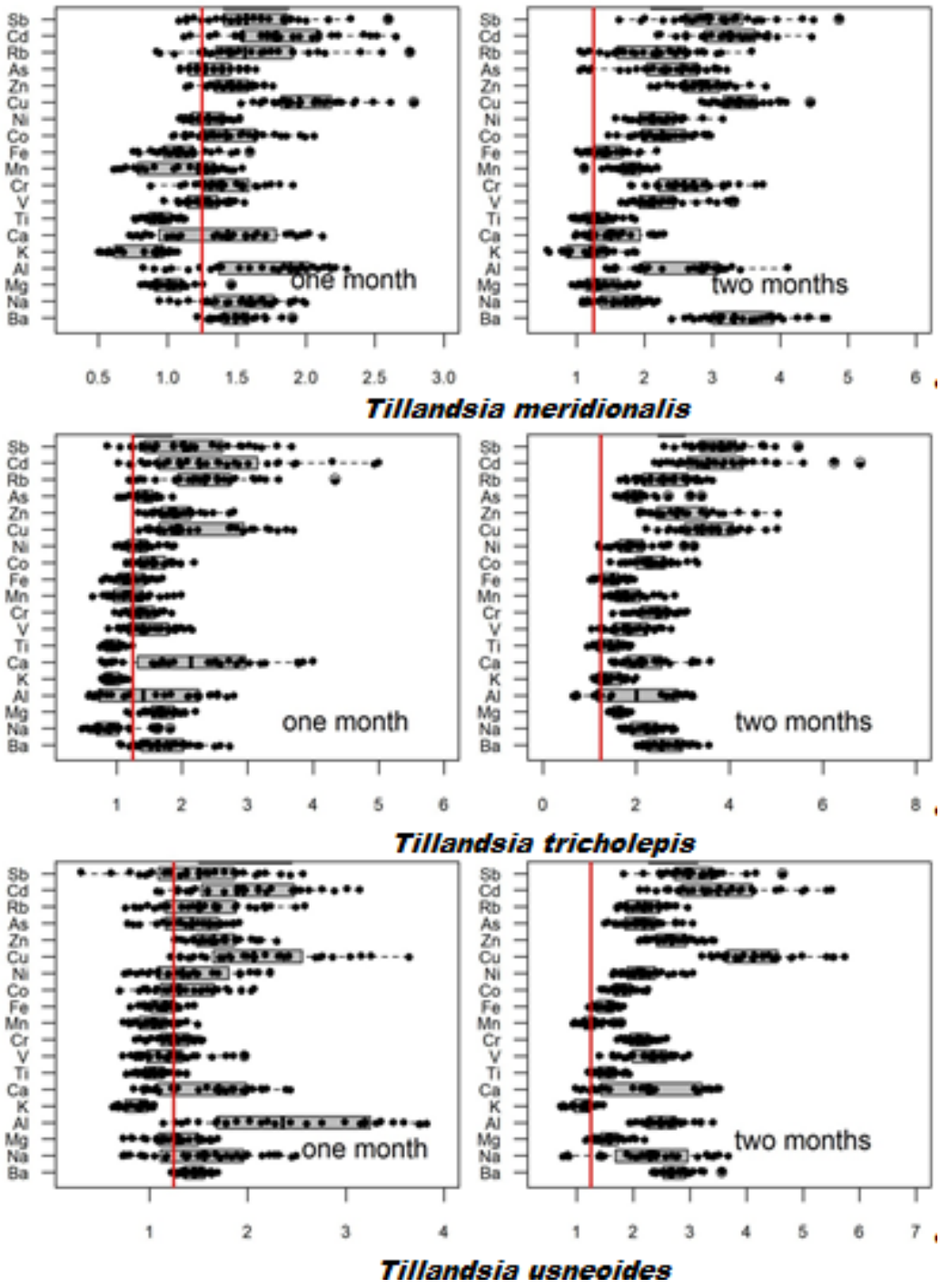

Figure 7.1 Box plot representation of EC ratio of the element evaluated in plants of T. meridionalis, tricholepis, and usneoides in all sites, during one and two months exposure periods. The lines that divided the rectangles indicates the median. Values above 1.25 (highlighted by the red line) represent the accumulation of the element relative to the control site.

7.3.2.3.
Tillandsia Usneoides

In Fig. 5 the most of the elements had similar accumulation (Zn, Pb, Cd, V, Co, Cr, As, and Sb) in the vicinities of bus terminals. In the industrial site only Fe was enriched. Already, only three elements presented higher EC ratios for Cu, Ni, and Ba, all observed in freeway site (HSC).

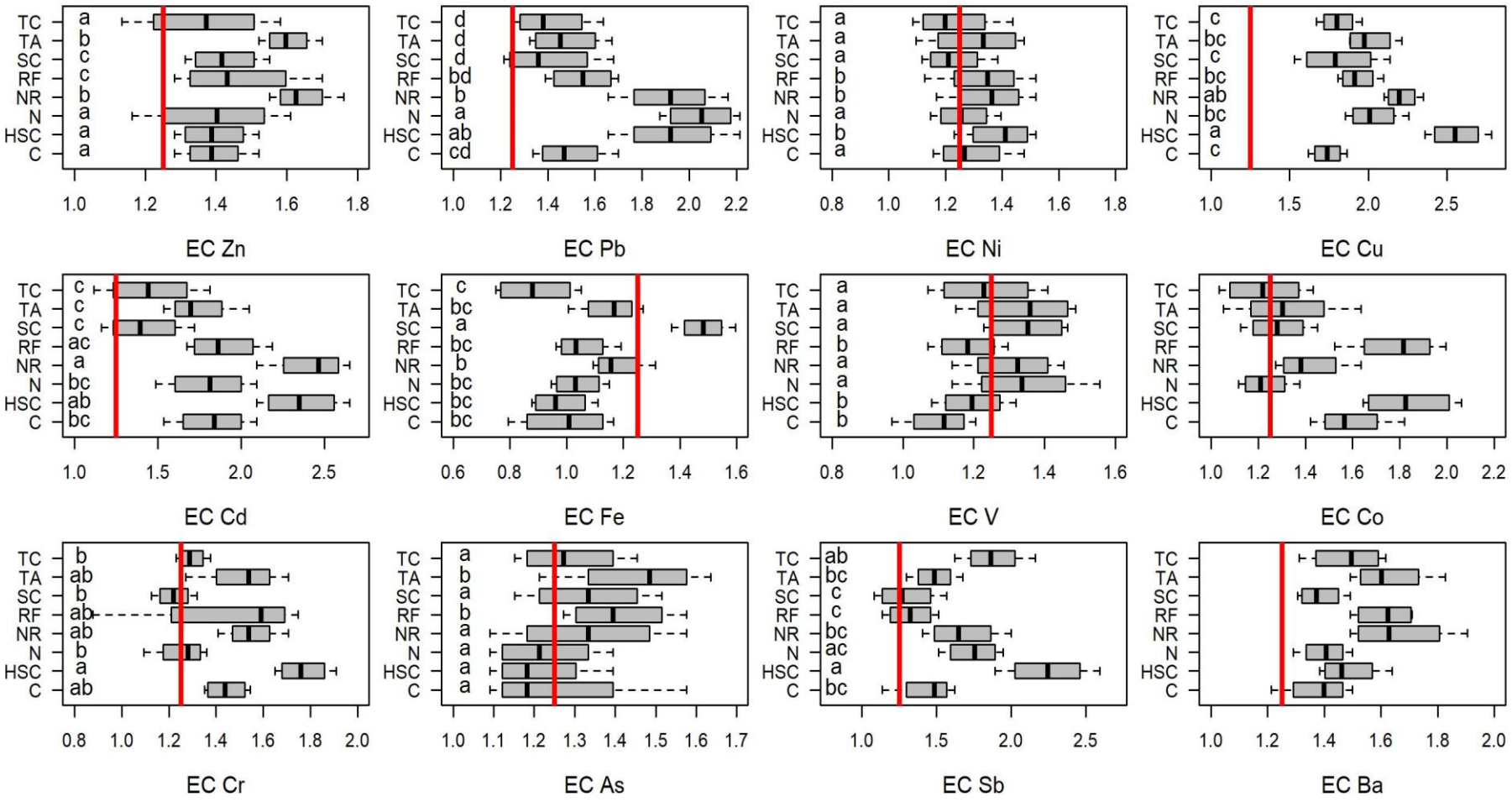

Figure 7.2 Box plot representation of EC ratios of samples of T. meridionalis in each site, during one month exposure period. Values above 1.25 (highlighted by red line) represent the accumulation of the element relative to the control site. Distinct letters indicates significant

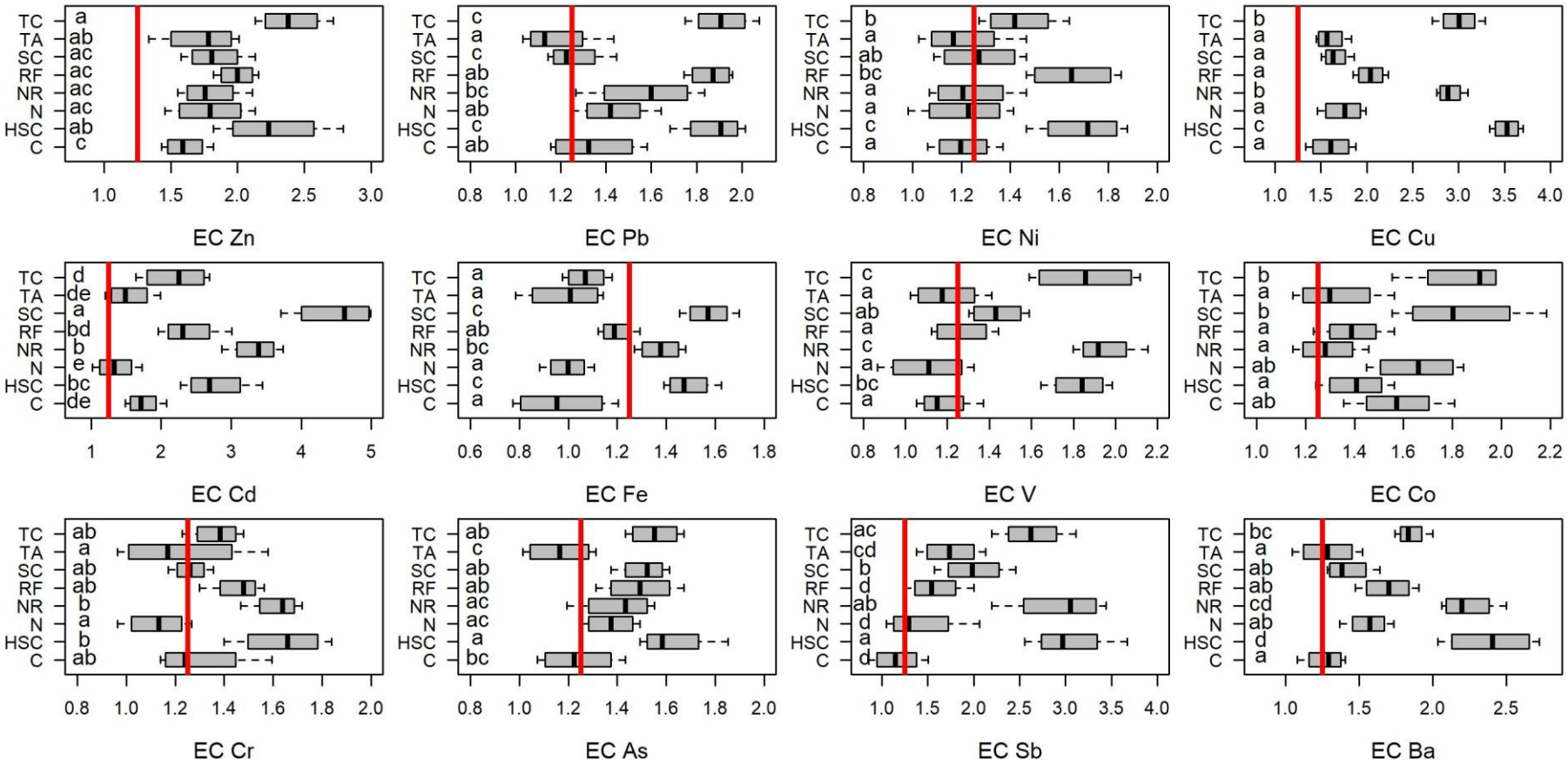

Figure 7.3 Box plot representation of EC ratios of samples of T. tricholepis in each site, during two month exposure period. Values above 1.25 (highlighted by red line) represent the accumulation of the element relative to the control site. Distinct letters indicates significant differences among exposure sites.

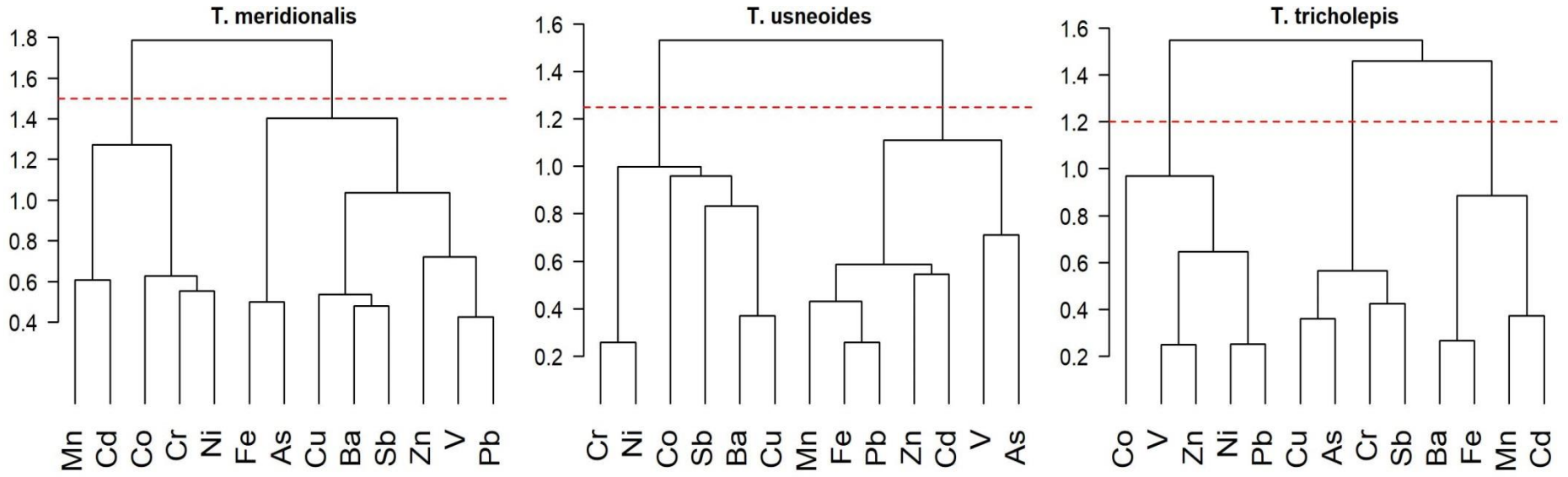

Figure 7.4 Hierarchical cluster analysis of the chemical elements with EF > 2 or more enriched values in plants of T. meridionalis, T. tricholepis, and T. usneoides.

7.4. Conclusions

The three *Tillandsia* species behaved as an effective and reliable biomonitors to evaluate the air quality around industrial and urban context. Higher concentration of most of the elements analysed (Al, As, Ba, Ca, Cd, Co, Cr, Cu, Fe, K, Mg, Mn, Na, Ni, Pb, Rb, Sb, Sr, Ti, V, and Zn) were measured in samples of *T. tricholepis* than *T. usneoides* and *T. meridionalis*. Besides, their use allowed us to characterize different emission sources at a local scale.

Taking account the number of elements accumulated in each *T.* species we propose an order of efficiency for these three bromeliad species, i.e., *T. tricholepis* > *T. usneoides* > *T. meridionalis*.

Acknowledgements

The authors are grateful to Coordenação de Aperfeiçoamento de Pessoal de Nível Superior (CAPES), and Fundação de Amparo e Pesquisa do Estado do Rio de Janeiro (FAPERJ) for financial support T. D. S. thanks to Conselho Nacional de Desenvolvimento Científico e Tecnológico (CNPq) for the scholarship.

8
Evaluation of the impact of the Rio 2016 Olympic Games on air quality in the city of Rio de Janeiro, Brazil

Alex Ruben Huaman De La Cruz[a, d], Enrique Roy Dionisio Calderon[a],

Bruno Bôscaro França[b], Weeberb J. Réquia[c], Adriana Gioda[a, *]

[a] Pontifical Catholic University of Rio de Janeiro, Department of Chemistry, Rio de Janeiro, Brazil

[b] Prefeitura do Rio de Janeiro

[c] School of Public Health, , Department of Environmental Health, Harvard University, Boston, United States

[d] National University of Centre of Peru (UNCP), Faculty of Chemical Engineering, Av. Mariscal Ramon Castilla Km. 5. No 3809, El Tambo, Huancayo, Peru

*Corresponding author: Adriana Gioda - Email: agioda@puc-rio.br

Paper under review: *Atmospheric Environment*

Abstract

Increase in air pollution levels is a frequent problem in Sports Mega-events worldwide, including Word Cup and Olympic Games. Information on air quality before and during these Mega-events can guide the implementation of air pollution control. Rio de Janeiro became the first South American city ever to host the Summer Olympic Games. The city has triggered several infrastructure projects to build and renovate sports centers and to improve transportation. We argue that

further investigation of the air pollution implications of the Rio Olympic Games is required. Such work could offer a meaningful contribution to our knowledge of the environmental impacts associated with the major sporting event. We assess the air quality in Rio de Janeiro city measuring the pollutants PM_{10}, SO_2, CO, O_3, and NOx (NO and NO_2) during three study periods in 2016: (A) before the 2016 Olympic Games, July 1st -August 4th, n=35 days, (B) during the games, August 5th -September 18th, n=44 days, and (C) after the games, September 19th - October 31st, n=43 days. Then, we compare our results to those from similar studies. Our results showed that during the Olympic period, PM_{10}, SO_2, CO, and NOx (NO + NO_2) were reduced by 17, 26, 13, 49, and 12%, respectively. After the games (comparing the period B and C), these pollutants were reduced by 19, 17, 31, 36, and 25%. In contrast, O_3 concentrations increased 26% and 7% during (comparing period A and B) and after (comparing period B and C) the games, respectively. The concentration of most of the pollutants (except O_3, in unique site) did not exceed the limits of the Brazilian guidelines in the three periods. Our findings show a reduction of concentration for some pollutants during and after the games. This reduction may be related to the control and regulation implanted by the environmental and transportation agencies in Rio de Janeiro, which included the restriction of circulation of cargo vehicles, prohibition of the use of private vehicles near the games sites, and transit supply strategy adopted by the local government. This work can inform the development of more targeted and locally tailored air pollution management policies.

Keywords: Air quality; 2016 Olympic Games; Rio de Janeiro; Temporal analysis

8.1. Introduction

Mega-events such as the Olympic Games and the FIFA World Cup may provide potential benefits for the host city, including an increase in recognition and tourism [178–180], economic growth [181,182], and modernization of the infrastructure [183,184]. However, hosting a major sporting event can also lead to negative impacts related to socio-economic and environmental aspects. Previous investigations have shown that mega-events may increase crime rate, living cost,

traffic congestion, air pollution, noise, and construction waste [185–188]. For example, in Sydney, the 2000 Olympics Games stimulated future tourism, cultural identity, investment, jobs, and provided new urban infrastructure, however, the living cost was increased by 21% [187]. The 2002 FIFA World Cup in South Korea provided benefits related to cultural development, nevertheless traffic congestion, ambient air pollution, construction costs, and social problems became much higher [189]. The Chinese government adopted some air pollution control strategies during the 2008 Beijing Olympic Games. Studies have shown reductions in PM_{10}, $PM_{2.5}$, SO_2, CO, NO, and NO_2 when compared to the 2008 Beijing Olympic period to the non-Olympic period [54,56,190]. Considering the public health impacts associated to this improvement in air quality during the 2008 Beijing Olympic Games, Li et al. (2010) [191] show that hospital visits per asthma and mortality were reduced by 60% and 8%, respectively.

Numerous studies argue that the public health impacts of Mega-events-related air pollution are the main economic externalities for the hosting city [192–200]. While there is a wealth of previous research that has investigated the association between air pollution and Mega-events, little work has assessed this association from the 2016 Olympic Games in Rio. To our knowledge, Godoy et al. 2017 [201] and Siqueira et al. 2017 [202] were the only researchers that estimated air pollution impacts prior 2016 Rio Olympics Games in the proximity of the sport venues, and their efforts were focused on the estimations of Particulate Matter (PM) and Volatile Organic Compounds (VOCs).

Considering that (i) increase in air pollution levels is a frequent problem in many Mega-events worldwide; (ii) information on air quality before and during these Mega-events can guide the implementation of air pollution control; (iii) Brazil in the last years have been facing rapid developed and economic growth that has triggered an increase in the fleet vehicle mainly in urban centers, capitals, and metropolitan regions; and (iv) since Rio de Janeiro became the first South American city ever to host the Summer Olympic Games, the city has triggered several infrastructure projects to build and renovate sport centers, and to improve transport, including the implementation of a network fully integrated among rail system, boats and bus-based of bus rapid transit corridors; we argue that further

investigation of the air pollution implications of the Rio Olympic Games is required.

Such work could offer a meaningful contribution to our knowledge of the environmental impacts associated with the major sporting event, showing how air pollution concentration can differ by hosting city. Therefore, we evaluate ambient air pollution before, during, and after the 2016 Rio Olympic Games. Specifically, we utilize multiple comparisons of means to assess the temporal variation. Finally, we compare our results to those from similar studies.

8.2. Materials and methods

The reader is referred to the description in section 3.6, page 60.

8.3. Results and discussion

8.3.1. Descriptive results

Table 8.1 shows the average pollutant concentrations and meteorological values over the study area (mean of all monitoring sites) for the three periods - before (A), during (B) and after (C) the 2016 Olympic Games. For comparison, we also present in Table 8.1 pollutant concentrations reported in previous Olympic Games (studies found in our literature review). Our literature review on the impact of Mega-events on air quality shows that our results are in agreement with those from similar studies (Table 8.1). For instance, Su et al. 2015 [54] evaluated the air quality in Beijing before, during, and after the 2008 Olympic period. Comparing with the period before, Su et al. (2015) [54] shows that concentrations of PM_{10} and NO_2 decreased 54.1% and 34.5% respectively during the Olympic period. Wang et al. (2013) [56] reported results for the same game, comparing the same periods, but accounted for other pollutants. The authors show that levels of O_3, SO_2, CO, NO, and NO_2 decreased, 22%, 41%, 22%, 39%, and 37%, respectively. Besides, Schleicher et al. (2012) [90] concluded that after applied aerosol source control measures, such as reducing traffic and shutting

down industries, a huge impact on reduction of particulate matter (PM_{10} and $PM_{2.5}$) in Beijing was observed. According Ardini et al. (2010) [203], suitable traffic management strategies may help to mitigate effects on emissions, ambient concentrations, human exposure, and health effects of traffic-related air pollution in urban areas. In 2010 Asian Games, during the games, after transportation restriction and industrial emission control, levels of PM_{10}, NO_2, and SO_2 decreased in 9.22 %, 3.27 %, and 4.22 %, respectively [198]. In the 2012 London Games, it was reported a reduction of 0.22% and 0.13% for PM_{10} and NOx, respectively, after traffic management arrangements during the Olympic period [200].

Table 8.1 Average pollutant concentrations and meteorological values during the three periods in the 2016 Rio Olympic Games and in other games (studies found in our literature review).

	Period	PM_{10} ($\mu g/m^3$)	O_3 ($\mu g/m^3$)	SO_2 ($\mu g/m^3$)	CO (ppm)	NO ($\mu g/m^3$)	NO_2 ($\mu g/m^3$)	T (°C)	RH (%)
This study, Brazil	Before (A)	54±27	25±18	6.0 ±3.9	0.4±0.3	21±31	50±29	20.8±4.5	59.7±15.4
	During (B)	45±17	32±22	4.4±6.0	0.4±0.2	11±17	44±23	22.4±5.1	59.3±18.3
	After (C)	36±15	34±20	3.7±3.0	0.2±0.2	7±12	33±17	22.6±5.4	64.5±17.2
Beijing [54]	Before	151±106					43±13	24.6±2.8	62.6±12.2
	During	70±35					28±7	24.8±2.4	69.3±9.6
	After	108±66					66±25	10.5±3.1	50.6±17.9
Beijing [197]	Baseline		129					22.8	68.5
	Before		146.5					27.1	72.7
	During		119.8					23.8	72.2
Beijing [56]	Before		106.7	18.58	0.74	0.61	24.8	27.3	54.8
	During		84.22	10.99	0.58	0.37	15.6	25.1	64.4
Beijing [55]	During	83±43		11±3.5			28±6.6		
Beijing [190]	Before		153.13	16.24	0.47				
	During		113.87	6.29	0.35				
Asian Games [198]	Before	89±43		34.6±27.3			66.4±31.8	19±4	19±3
	During	81±24		33.2±16.5			64.3±19.9	64±15	62±12

Note: before the games (A), during the games (B), after the games (C). T: temperature, RH: relative humidity.

We present in Table 8.2 the variation of air pollutants and meteorological variables among Olympic periods (A, B, and C) for each station. Table 8.2 shows that during the Olympic period (B), PM_{10}, SO_2, CO, NO, and NO_2 levels were reduced by 16.9, 26.4, 12.9, 49.0, and 12.5%, respectively, when compared to period A. We also observed that these pollutants levels decreased by 18.9%, 16.9%, 30.9%, 35.5%, and 25.3%, respectively, compared to C period. O_3 was the only pollutant that increased during period B and C. Our results showed an increase of 26.5% (period B compared to period A) and 7.1% (period C compared to period B) for O_3. The increase of O_3 may be attributed to increasing in temperature and reduction of NO levels between both periods (B compared to A and C compared to B (Table 8.2). Similar results were found during the 2008 Beijing Olympic Games [204].

The reduction in concentration levels of pollutants may be attributed to the policies adopted by the govern of Rio de Janeiro during the Olympic Games, such as strong communication among population, interaction with class entities, school holidays, collective vacations, the restriction of circulation of cargo vehicles and prohibition of the use of private vehicles to avoid blocking of streets in the surroundings of games sites. During the Games period (B), the speed and flow of traffic were monitored in the main roads and near sports facilities. With this monitoring, it was observed an increase of 7% in the average speed and reduction of 11% in the average vehicular flow. Specifically, about cargo vehicles, the average speed increased by 18% in the morning peak [205].

The reduction after Olympic period (C) may be attributed to the transit supply strategy adopted in the city and the construction/implantation of new BRT

corridors during the Olympic period and that up now are used. This mega innovation implanted by local govern allowed the implementation of a suitable urban planning and an integrated high-capacity transit network fully integrated with buses, boats, suburban rail, and light rail transit (LRT), which result in an increased from 18% to 63% of the daily trips made by mass transit, benefiting almost 1.5 million passengers per day [183].

Compared to Reference value was observed increased of PM_{10} of 48% and 23% in relation to A and B period, respectively. In contrast insignificant reduction of 0.3% was found after the Olympic period.

Table 8.2 Variation (%, air pollutants and meteorological variables) among Olympic periods (A, B, and C) for each pollutant and air pollution monitoring station

Pollutant	Period comparison														Reference, RJ		
	Tijuca		Centro		Copacabana		São Cristovão		Bangu		Iraja		Study area				
	A-B (%)	B-C (%)	A-B (%)	B-C (%)	A-B (%)	B-C (%)	A-B (%)	B-C (%)	A-B (%)	B-C (%)	A-B (%)	B-C (%)	A-B (%)	B-C (%)	A-R (%)	B-R (%)	C-R (%)
PM_{10}	-9.4	-13.4			8.3	-5.9	-25.5	-31.7	-30.0	-23.0	-29.4	-29.9	-16.9	-18.9	48.0	23.0	-0.3
O_3	48.5	-0.3	24.9	0.2	19.2	10.4	5.2	28	23.0	6.0	35.9	5.9	26.5	7.1			
SO_2	8.9	-37.2			-29.0	-25.0	-29.0	-32	-70.0	80.0	6.5	-1.7	-26.4	-16.9			
CO	-10.4	-13.9	-8.5	-	-27.0	-38.0	-20.0	-68	-14.0	-31.0	-8.5	-25.6	-12.9	-30.9			
NO	-39.8	-14.9		23.3					-42.0	-48.0	-57.0	-52	-49	-35.5			
NO_2	-10.6	-20.1							7.1	-41.0	-27.0	-21.0	-12.5	-25.3			
Meteor.																	
T	7.7	0.9			5.6	1.5	6.3	-0.1			6.1	-0.2	6.4	0.53			
RH	-0.8	8.8			1.4	3.7	-2.7	11.3	-1.5	29.9	-0.9	8.5	-0.9	12.2			

Note: A-B: Difference % (before-during), B-C: Difference % (during-after), white space: not measured, R: reference value (average of eight years) reported by Pacheco et al. (2017) [267], which the authors evaluated only PM_{10} in Rio de Janeiro. T: temperature, RH: relative humidity.

8.3.2.
Temporal analysis of ambient concentration

Figure 8.1 to Figure 8.3 show the comparison of the mean concentrations at each site and study period (A, B, and C) estimated with the *Tukey* test (Fisher test, $p < 0.05$). The same information on pollutants concentrations and meteorological variables for all sites, each period (including the whole study period, Jul 01-Oct 31, n=122 days), and each monitoring station are presented in Table S3.

For CO (Figure 8.1), we found significant difference ($p < 0.05$) in most of the sites (except Iraja) between the period A (before Olympic Games) and during Olympic Games (B). We observed decreases in CO concentrations in period B for all sites. We estimate significant difference ($p < 0.05$) between the period B and the period after Olympic Games (C) in all sites. Since vehicular exhaust is the main source of CO [206], our results suggest that reduction in CO level may be attributed to traffic flow arrangement adopted during Olympic Games.

NO concentrations (Figure 8.1) showed significant difference ($p < 0.05$) in all sites for both comparison periods (A and B, and B and C), with concentration reduction in the periods B and C. Studies, have shown that NOx (NO and NO_2) is produced during combustion of fuel at high temperatures, and in areas with high motor vehicles traffic [207]. Therefore, the reduction of number of cars implanted by the local government during the Olympic Games may be related to the decreases of NOx levels.

Analysis of SO_2 (Figure 8.1) showed a significant difference ($p < 0.05$) in most of the sites (except Iraja) between the periods A and B. We observed SO_2 reduction in three sites (Copacabana, Sao Cristovão, and Bangu) and increases in two sites (Tijuca and Iraja). Comparing the periods B and C, our results showed a significant difference in four sites (except Iraja) with SO_2 concentrations reductions in most of the sites (except Bangu). No significant differences ($p > 0.05$) among the Olympic periods in Iraja station may be explained because the Avenue Brasil, one of the main highways which condense a high number of vehicles pass near monitoring of Iraja.

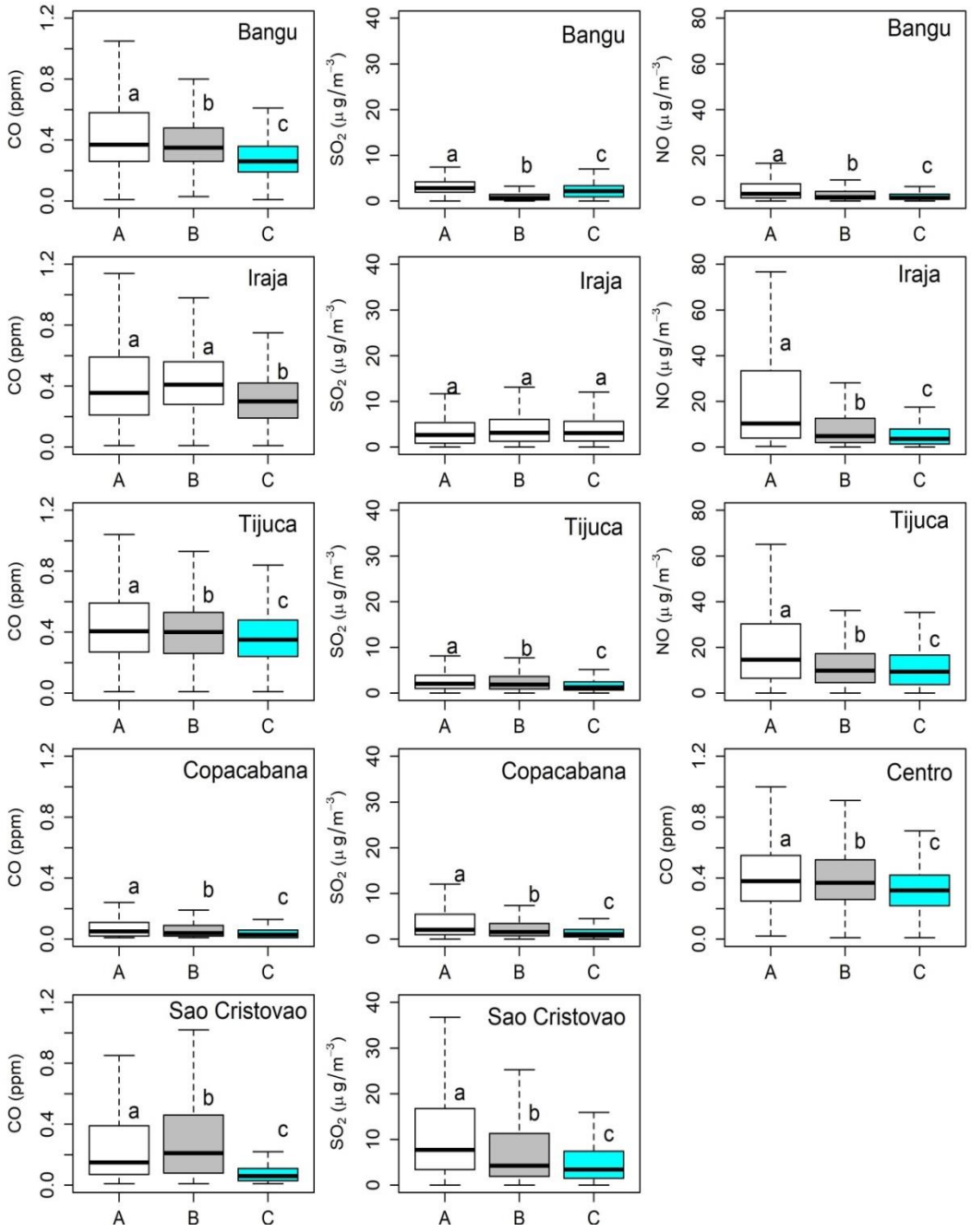

Figure 8.1 Box plots summarizing the comparison of CO, SO_2, NO, in all sampling sites and the three Olympic periods (A, B, and C). The heavy horizontal line crossing the box is the median, the bottom, and the top are the lower and upper quartiles, and the whiskers are the minimum and the maximum values. Means with the same letter and color (a, b, and c) code are not significantly different (Tukey multiple comparisons of means, $p < 0.05$).

We found significant differences ($p < 0.05$) between the periods A and B in five sites (except Sao Cristóvão) for O_3 concentrations (Figure 8.2). An increased in O_3 concentrations is observed in all sites during period B. Similar

results were observed when we compared the periods C and B. Here we found significant difference ($p < 0.05$) in three sites (Copacabana, Sao Cristovão, and Iraja). Ozone as a secondary pollutant is formed by a complex photochemical process involving VOCs and NOx [208]. Higher O_3 concentrations were observed in Bangu. This region presents temperature significantly warmer than its surrounding areas due to topographical urban (heat islands) conditions which may increase O_3 concentrations. Geraldino et al. [209] investigated the potential factors that contribute to frequent high levels of O_3 in Bangu and concluded that high O_3 concentrations were related to pollutant transport mainly from industrial areas, which it is triggered by photochemical activity associated to adverse meteorological and topographical conditions. The average level of O_3 increased in the Olympic Period (B) for all sites, suggesting that O_3 was not successfully controlled. However, we highlight that it is complex to control O_3 concentrations in Rio de Janeiro because the formation of ozone is favored due to their topographical and meteorological conditions of this city [209].

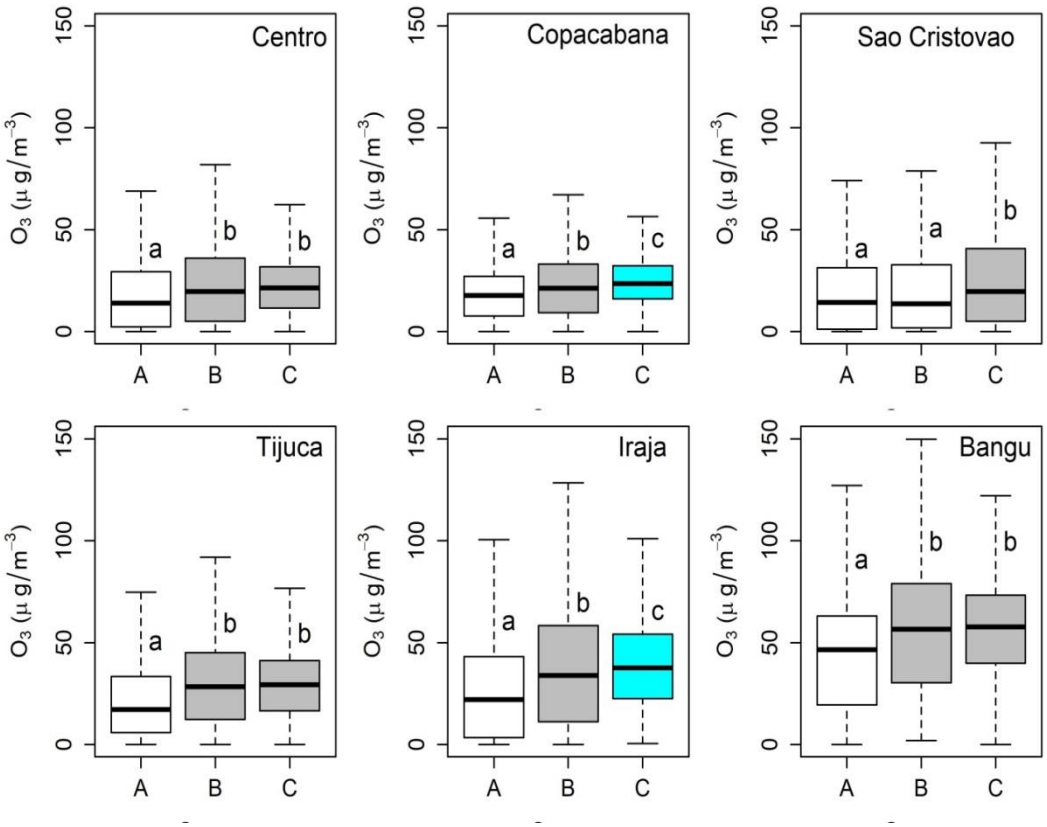

Figure 8.2 Box plots summarizing the comparison of O_3 in all sampling sites and the three periods (A, B, and C). The heavy horizontal line crossing the box is the

median, the bottom, and the top are the lower and upper quartiles, and the whiskers are the minimum and the maximum values. Means with the same letter and color (a, b, and c) code are not significantly different (Tukey multiple comparisons of means, $p < 0.05$).

Figure 8.3 shows substantial difference ($p < 0.05$) in PM_{10} concentrations in all sites between the periods A and B with reduction of PM_{10} concentration in four sites (except Copacabana) during the period B. Comparing the period C and B, it was found significant difference and PM_{10} reduction in all sites. Higher PM_{10} concentrations were measured in Copacabana. The monitoring station from Copacabana is surrounding by buildings and is aside from a subway terminal, bus stop which may influence its higher PM_{10} concentrations found in this area.

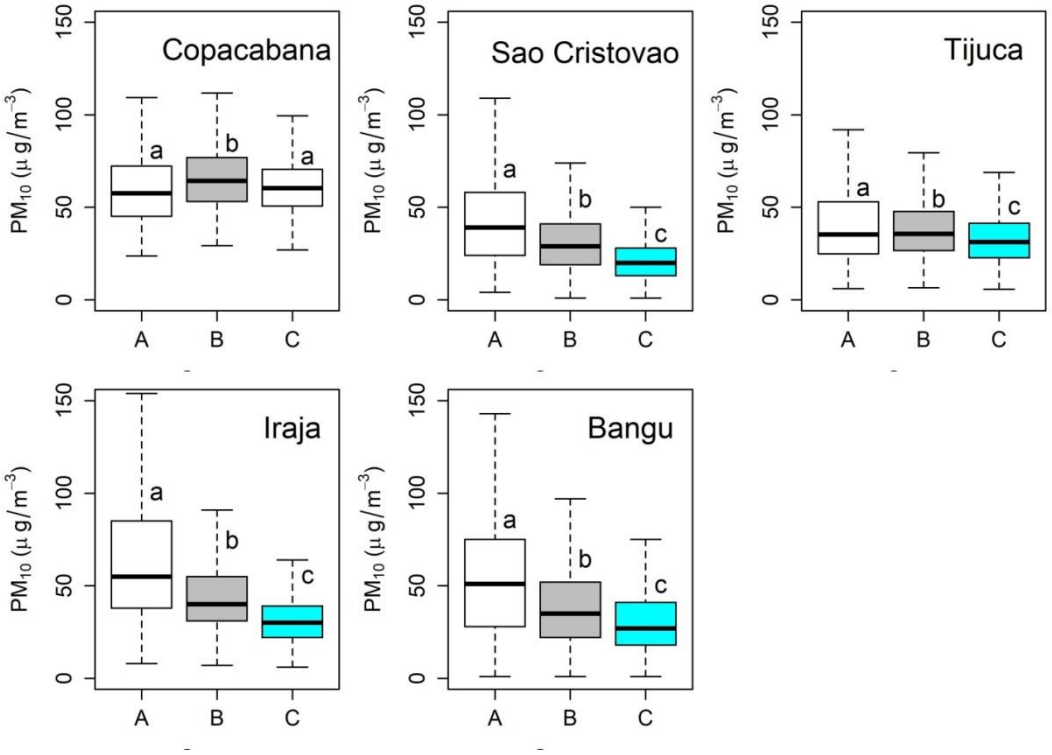

Figure 8.3 Box plots summarizing the comparison of PM_{10} in all sampling sites and the three periods (A, B, and C). The heavy horizontal line crossing the box is the median, the bottom, and the top are the lower and upper quartiles, and the whiskers are the minimum and the maximum values. Means with the same letter and color (a, b, and c) code are not significantly different (Tukey multiple comparisons of means, $p < 0.05$).

In Figure 8.4, we illustrate the diurnal distribution (hourly average) of the pollutants (O_3, NOx (NO + NO_2), SO_2, PM_{10}, and CO) in each Olympic Games period. Concentrations of CO and NOx showed double peaks with higher concentrations between 6:00 - 9:00 and 20:00 - 22:00 (Figure 8.4). The results suggest that CO and NOx come from combustion-related primarily to fossil fuel combustion of motor vehicles. Lower concentrations of CO observed during Olympic Games can be attributed to relative low number of vehicles. According to Martins et al. (2015) [210], 98% of CO in the metropolitan region of Rio de Janeiro comes from vehicular sources.

PM_{10} had one peak between 09:00-13:00, with a maximum value at 11:00 (Figure 8.4). We suggest that traffic exhaust is not the unique source of PM_{10}. Its concentration level may be attributed to other sources, including secondary aerosol, road dust, and long-range transports [211,212].

O_3 reaches the maximum concentration between 13:00 and 14:00 (Figure 8.4). This is due to the photochemical property of the pollutant and with the presence of NOx and CO, as discussed above. The O_3 concentration began to decrease when sunlight decreases, reaching lower concentration levels at night. The lowest O_3 concentrations are observed during the early morning. In the city of Rio de Janeiro, exceedances of O_3 were reported in Bangu, Iraja and Campo Grande during 2012 and 2013 [210]. The exceedance was observed exclusively on weekends, while decreased in concentration of primary pollutants was observed over the weekends, which may be attributed to the reduction of emission of vehicles.

The concentration of SO_2 showed to be more stable with slightly increased levels along daytime (08:00-17:00) – (Figure 8.4). This may be attributed to the short lifetime of the pollutant. SO_2 concentrations were lowest registered among the pollutants studied, indicating few industrial influences. Higher SO_2 levels were observed in São Cristovão (13:00-14:00) in the two first periods, which may reflect the combustion of fossil fuels since coal and petroleum contain sulfur compounds [206]. The station in Sao Cristovao is located next two main express lanes (Linha Vermelha and Avenida Brasil) and bus terminal Novo Rio that connect several areas of Rio de Janeiro. A general decreasing SO_2 concentrations level at night was observed in all stations and the three periods. Some similarities found between sites may suggest a homogeneous source pollutant for all sites

(vehicular exhaust, industrial processes), whenever monitoring stations are located close busy avenues, intense vehicular movement.

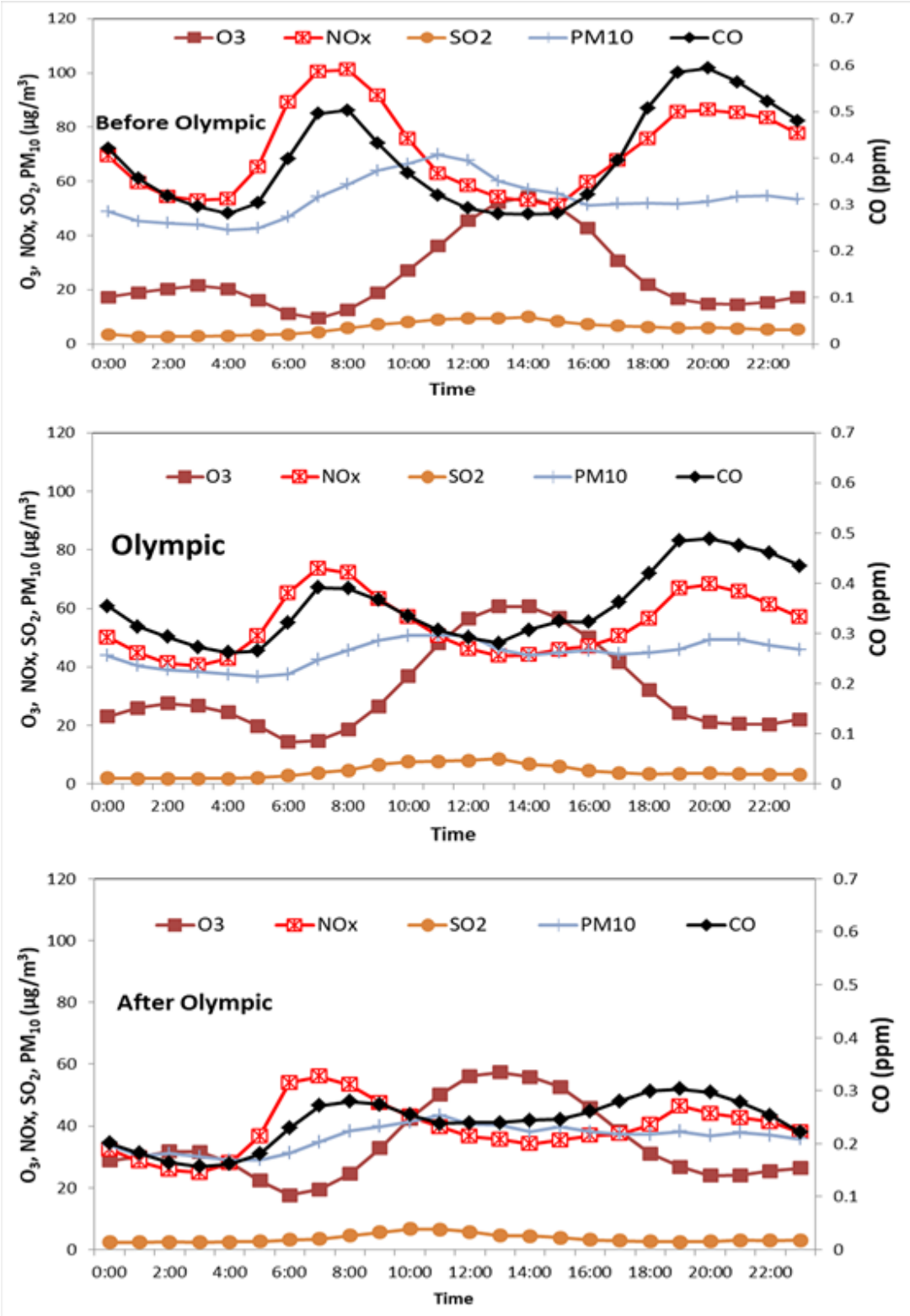

Figure 8.4 Diurnal variation of O3, NOx, SO2, PM10 and CO for the three 2016 Olympic Games period: before (up), during (middle), and after (bottom).

The hourly variation of the ratios of $[O_3]/([NO_2/NO])$, NO_2/NO, and NO/NO_2 are plotted in Figure 8.5. The ratio of $[O_3]/([NO_2/NO])$ remains at a level below 5 (except in the period A) at night when exists more fresh NO in the atmosphere. After sunrise, the peak of NO_2/NO grows slowly during the daytime. The ratio of NO/NO_2 rises rapidly when sunrise appears, suggesting that most of the NO was oxidized into NO_2. Higher O_3 concentrations observed in Bangu station may be attributed to the lowest NO concentration levels (Table G.3 – Supplementary material) that favors to O_3 accumulation in the atmosphere. O_3 levels in Bangu exceeded the limits of CONAMA (160 μg m^{-3}) as observed in Figure 8.2. The results for O_3 are similar to those found in 2015 by Martins et al. 2015 [210] in the same station.

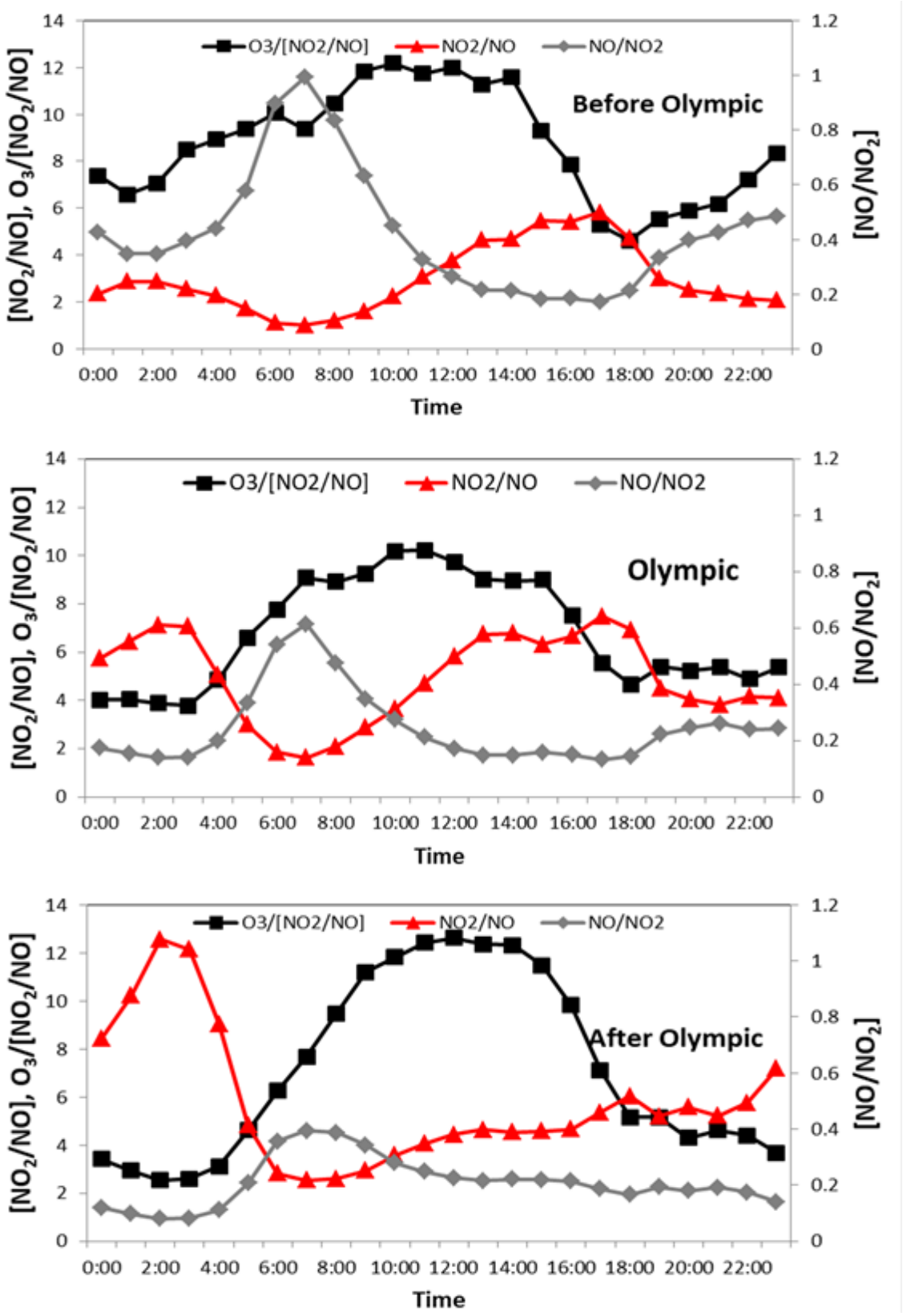

Figure 8.5 Ratio of [NO/NO_2], [NO_2/NO], and $O_3/[NO_2/NO]$ for the three different 2016 Olympic periods.

Figure 8.6 shows the Pearson correlation matrix among hourly mean of each pollutant and meteorological parameters for the two periods (A and B). The results indicate that CO is positively correlated with NO_2, but negatively with O_3, in both periods A and B. Our findings suggest that both pollutants (CO and NO_2) are related to the same source, likely vehicular emission during vehicular congestion [211]. O_3 has stronger positive correlations with SO_2, solar radiation, temperature, and wind speed, but it is negatively correlated with NO, NOx, relative humidity, and wind direction. Positive correlation with solar radiation and temperature are attributed to that these parameters are key to produce photochemical reactions [192].

As expected, the negative correlation with NO described the formation of NO_2 and O_2 from the reaction between O_3 and NO [213]. While NOx is consumed for photochemical reactions in the daytime, producing lots of O_3 [196]. Relative humidity is negatively correlated with O_3, due to cloudy and precipitation days prevent the entry of sunlight, which disfavors photochemical production of ozone.

PM_{10} has strong positive correlation with SO_2, solar radiation, and temperature, but it is negatively correlated with relative humidity and wind direction. Positive correlation between the PM_{10} and temperature in this study suggests that ambient temperature affects the concentration of PM_{10}. Temperature increases the chemical reaction in the atmosphere resulting in the formation of finer particles that naturally contributes to the concentration of $PM_{10.}$ SO_2 suggest that this gas contributes to the formation of secondary aerosol (fine sulfate particles) that form part of the PM_{10} concentration in the atmosphere. The negative correlation with relative humidity may be attributed to the precipitation level which through wash-out processes can reduce the concentration of the

pollutants in the atmosphere. Strong winds contribute to the dispersion of pollutants, thus decreasing its concentration in the air [214]. SO_2 has stronger positive correlations with solar radiation, temperature, and wind speed, and it is negatively correlated with relative humidity and wind direction. Results on positive and negative correlations observed between the concentration of pollutants and the meteorological variables indicate the influence of the meteorological variables on the level of the pollutants.

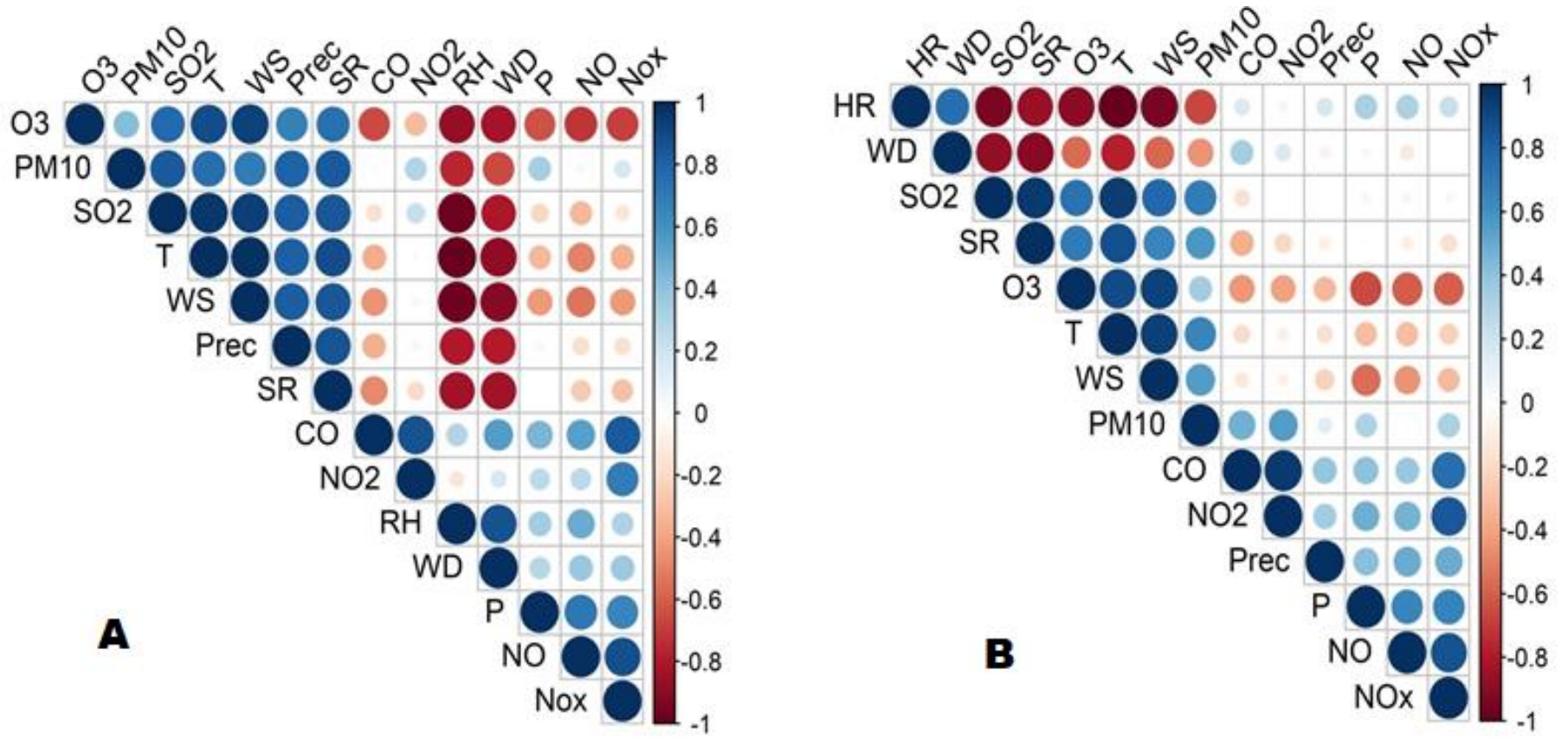

Figure 8.6 Pearson correlation matrix among hourly mean for PM_{10}, NO, NO_2, NOx, SO_2 and O_3, and meteorological parameters from period A (Before Olympic Games) and B (During Olympic Games).

8.4. Conclusions

We observed differences in the concentration levels for all pollutants at different monitoring stations during the three periods. In general, there were reduced levels of the pollutants in the Olympic period studied (B) due to traffic management and urban planning implanted by the local government. We suggest that the decreasing in pollutants concentrations found in this work can be attributed to that during critical days (ceremonies and closing) the main roads and neighborhoods around the facilities were blocked each day. The pollutants did not exceed the Brazilian air quality standard. This suggests that the air quality in the Rio de Janeiro city was under the limits and the pollution would not cause health impacts to the local population and the visitors.

The hourly distribution of pollutants indicates a profile characteristic for each pollutant. Higher peaks of CO and NOx were displayed during heavy traffic flow, demonstrating fuel emission as the main source. Significant correlations between pollutants and meteorological conditions proved that the concentration of pollutants is intimately associated with the meteorological variables.

This work provides a meaningful contribution to our knowledge of the air pollution impacts associated with the major sporting event, showing how air quality differed by hosting city. This can inform development of more targeted and locally tailored air pollution management policies.

Acknowledgements

The authors are grateful to Coordenação de Aperfeiçoamento de Pessoal de Nível Superior (CAPES), and Fundação de Amparo e Pesquisa do Estado do Rio de Janeiro (FAPERJ) for financial support T. D. S. thanks to Conselho Nacional de Desenvolvimento Científico e Tecnológico (CNPq) for the scholarship.

9
Application of univariate and multivariate calibration methods for interferences correction in the determination of Rare earth Elements by Inductively Coupled Plasma Mass Spectrometry

Alex Rubén Huaman De La Cruz, Tatiana D. Saint'Pierre, Adriana Gioda*

Pontifical Catholic University of Rio de Janeiro (PUC-Rio), Department of Chemistry, Rio de Janeiro, Brazil

*Corresponding author: Adriana Gioda - Email: agioda@puc-rio.br

Paper under review: *International Journal of Environmental Analytical Chemistry*

Abstract

In this work, two regularization methods (Ridge Regression (RR) and Least Absolute Shrinkage and Selection Operator (Lasso)) and two reduction methods (Principal Components Regression (PCR) and Partial Least Squares (PLS)) are proposed to correct spectral interferences from light rare earth elements (REEs) and barium polyatomic ions over the heavy rare earth elements, in inductively coupled plasma mass spectrometry (ICP-MS) analysis. Response dataset of solutions containing REEs and Ba in combination with the proposed calibration methods were used to build multivariate models to predict REEs concentrations in samples. Ten-fold cross-validation (CV) was used to optimize the models. Prediction performance was evaluated through the analysis of Certified Reference Materials (CRM). Results show superiority of multivariate calibration regression over univariate regression. The predicted concentrations using the multivariate models were in good agreement with the certified values and shown relative error lower than 10 %. Among all models, Lasso shows lowest root mean square of prediction (RMSEP) values and more interpretable results than RR, PLS, and PCR.

Keywords: Lasso; Ridge Regression; Rare earth elements; Inductively coupled plasma mass spectrometry; Prediction performance

9.1. Introduction

The rare earth elements (REEs) are a group composed of seventeen elements, 15 lanthanides (ranging from La (Z = 57) to Lu (Z = 71) and 2*d* elements - Sc (Z = 21) and Y (Z = 39)), whose physical and chemical properties are quite similar. The importance of REEs increased in last years, making them extensively employed in various fields, such as geology [17], industrial processes [18], agriculture [215], and modern technologies as national defense, healthcare, computer, and networks [216,217]. An indiscriminate demand for the above-mentioned applications and inadequate disposal can result in environmental accumulation of waste, which can be harmful to human health and other organisms as reported in the literature [218–221].

Among other analytical techniques, the determination of REEs is preferably carried out by means of inductively coupled plasma mass spectrometry (ICP-MS), due to its multielemental determination ability at low limits of detection, high sensitivity, and selectivity [222–225]. However, the ICP-MS is impaired by spectral overlaps either/both from polyatomic ions (MO^+ and MOH^+) of light REEs over heavy REEs, and matrix-induced polyatomic ions of BaO^+ and $BaOH^+$ over REEs from *m/z* 146 to *m/z* 155, e.g., $^{135}BaO^+$ on $^{151}Eu^+$, $^{144}NdO^+$ and $^{144}SmO^+$ on $^{160}Gd^+$ and $^{143}NdO^+$ on $^{159}Tb^+$ [43,226].

A large number of correction approaches has been applied to overcome these difficulties, such as optimization of instrument settings [227], desolvation techniques [228], algebraic correction schemes [229], dynamic reaction cell [43], high-resolution ICP-MS instruments [230,231], chromatographic separation [232], and other separation processes [233,234]. Nevertheless, most of these approaches show specific disadvantages, such as high cost, time-consuming processing, low detection sensitivity and limitations of analyses related to a small number of elements.

Standard linear method is the most applied and simplest approach for modeling the relationships between a chemical, biological or physical property of a sample and its composition. Usually, Ordinary Least Squares (OLS) estimator works well when the relation between response and the predictor is linear and for a single component present in the samples, it means no interference, which is often not the case in ICP-MS analysis [235]. In this case, the OLS fails to construct the prediction model, because the input data are high dimensional and multi-collinear, resulting in two problems: i) *prediction accuracy*, when $n \approx p$ (n = number of samples; p = number of variables), OLS fit increases dramatically the variance and may result in overfitting and poor estimates on unknown samples, and ii) *interpretability*, with a large number of predictors ($p > n$), the variability of the OLS fit increases dramatically and the variance of these estimates increases to infinite. To avoid overfitting, a bias-variance trade-off must be achieved [236]. Prediction and interpretation can sometimes be improved by shrinking some coefficients to 0. By making this, the bias is sacrificed a little to reduce the variance, providing a better prediction of the components in a mixture [237–239].

In the last decades, a variety of multivariate statistical methods have been successfully applied to solve spectral overlapping in spectroscopy and spectrophotometry quantitative analysis [240–242]. The principle of multivariate calibration is to construct a mathematical model that relates the multivariate response (independent variables), $x_1, x_2, \ldots x_n$, to one or more dependent variables of interest, y, and such a model can be used to efficiently predict the concentration of unknown samples. Principal component regression (PCR) and partial least squares regression (PLS) are two well-known multivariate calibration methods most widely used for this purpose [243–245]. Both known as reduction methods are results from the principal component analysis (PCA) and perform latent variable decomposition relating two blocks of variables, matrices X and Y, which may contain spectral and concentration data, respectively. The matrix decomposition can be expressed in terms of scores and loadings based on the sum of f latent variables, as follows:

$$X = TP^T + R = \sum t_f p'_f + R \quad (7)$$

$$Y = UQ^T + F = \sum u_f q'_f + F \quad (8)$$

where *T* and *P* are the scores and loading matrices of *X*, respectively; *U* and *Q* are the score and loading matrices of *Y*, respectively; and *R* and *F* are the model error in *X* and *Y*, matrices, respectively. Each latent variable is obtained by correlating the scores *U* and *T* in the following manner:

$$u_f = b_f t_f \tag{9}$$

where b_f is the regression coefficient for the *f* latent variable. The matrix *Y* can be calculated replacing the equation (5) in (4) as shown in equation (6).

$$Y = TBQ^T + F \tag{10}$$

For the analysis of unknown samples by PCR and PLS, the latent variables are employed to estimate the new scores $T_{unknown\ samples}$, which are substituted in equation (4), leading to equation (7).

$$Y_{unknown\ sample} = T_{unknown\ sample} BQ^T \tag{11}$$

In the literature, PCR and PLS were successfully employed to determine accurately the gadolinium concentration from geological samples, despite the presence of interferences [246]. Zhu et al. [247] developed a PLS model and REEs concentrations from CRM of soils were accurately predicted. Several determinations based on the application of both methods to spectroscopic data have been reported by several researchers [242,244,245,248–250].

Ridge Regression (RR) and Least Absolute Shrinkage and Selection Operator (Lasso), two multivariate calibration methods of regularization introduced by Hoerl and Kennard (1970) [251] and Tibshirani (1994) [252] can be applied to reduce the variance of the parameter estimators, especially in high dimensional spaces. The difference between these methods and reduction ones is that the latter obtain the coefficient estimates based on ordinary least squares, while RR and Lasso are subjected to regularization penalties on coefficients. In ridge regression, all coefficients are shrunk towards zero (but never exactly zero)

by a tuning parameter. However, RR model does not perform variable selection. This method attempts to minimize residual sum of squares (RSS) of predictors through the following function:

$$\hat{\beta}^{ridge} = \arg\min_{\beta} \left\{ \sum_{i=1}^{N} \left(y_i - \beta_0 - \sum_{j=1}^{P} x_{ij}\beta_j \right)^2 + \lambda \sum_{j=1}^{P} \beta_j^2 \right\} = RSS + \lambda \sum_{j=1}^{P} \beta_j^2 \qquad (12)$$

where $\lambda \sum_j \beta_j^2$ is the ℓ_2 penalty and λ is the tuning parameter. The ridge regression achieves their best prediction performance through a bias-variance trade-off [239]. A high value of λ will tend to shrink the regression parameters towards zero. If λ = 0, the penalty has no effect, and ordinary least squares will be carried out.

In Lasso regression, the estimated coefficient is obtained according to the following function:

$$\hat{\beta}^{lasso} = \arg\min_{\beta} \sum_{t=1}^{N} \left(y_i - \beta_0 - \sum_{j=1}^{P} x_{ij}\beta_j \right)^2 + \lambda \sum_{j=1}^{p} \left|\beta_j\right| = RSS + \lambda \sum_{j=1}^{p} \left|\beta_j\right| \qquad (13)$$

This function is similar to ridge regression, but the ℓ_1 penalty term is based on the absolute value of coefficient estimates and not on the squared values. In Lasso method the ℓ_1 penalty forces some non-relevant coefficients to become equal to zero for certain ranges of λ values, leading to the selection of a subset of variables and sparse solutions. These methods have been used and achieved great success in several fields of science, such as genetics studies [242], bioinformatics [253], environmental pollution [254], financial modeling [255], and medical diagnostic [256], to resolve a variety of issues. However, up to now, they were still not applied for REEs determination using ICP-MS.

Among the main advantages of these multivariate methods, it can be cited the accurate quantitative analysis, despite the presence of heavy spectroscopic interferences by other analytes, to avoid laborious separation procedures, the low cost, and fastness.

The predictive ability of the multivariate calibration models will be assessed through the root mean square errors of prediction (RMSEP) [66,257], and relative error of prediction (REP), using the following equations:

$$RMSE = \sqrt{\frac{1}{N}\sum_{j=1}^{N}(y_i - \hat{y}_i)^2} \quad (14)$$

$$REP\ (\%) = \sqrt{\frac{\sum_{i=1}^{N}(\hat{y}_i - y_i)^2}{\sum_{i=1}^{N}(y_i)^2}} x100 \quad (15)$$

where N is the number of samples, y_i the theoretical or prepared concentration and $\hat{y}_i$ the predicted concentration.

In this work, spectrometric data and multivariate calibration methods (PCR, PLS, RR, and Lasso) were used to construct multivariate models for interference correction in the REEs determination, and aspects, such as model optimization (or refinement) and model application, are described. The aim of this work is to apply these models to solve spectral overlapping and accurately to predict REEs concentrations in unknown samples mixtures (mixtures of REEs + Ba) and CRM.

9.2. Materials and methods

The reader is referred to the description in section 3.7, page 63.

9.3. Results and discussion

9.3.1. Univariate regression – Ordinary least regression (OLS)

For univariate regression, isotopes free or with minor interferences (^{139}La, ^{140}Ce, ^{141}Pr, ^{143}Nd, ^{147}Sm, ^{151}Eu, ^{157}Gd, ^{159}Tb, ^{163}Dy, ^{165}Ho, ^{166}Er, ^{169}Tm, ^{171}Yb, and ^{175}Lu) were selected. Using the standard analytical curve and ordinary least squares (OLS), the concentrations of the isotopes above mentioned were quantified in the validation set (n = 15) and in the three CRM. Despite using isotopes that suffer less spectral overlap, mean relative error values (RE %)

greater than 10 % were found for most REEs in validation set and for all REES in the CRM, respectively (Table 9.1). Table 9.1 also shows RMSEP and REP values. These results suggest that OLS is not suitable to efficiently determine the most REEs, except for La (RE = 8.6 %), Ce (RE = 9.2 %), Pr (RE = 8.0 %), and Nd (RE = 8.2 %), which presented RE < 10 % in validation set. The RE % values found for these four REEs may be attributed to the fact that these elements do not suffer significant interferences, as shown in Table S3. Therefore, La, Ce, Pr, and Nd may be determined by OLS, since isotopes free of interference or overlap are selected, while for the other REE (Sm, Eu, Gd, Tb, Dy, Ho, Er, Tm, Yb, and Lu), even selecting the isotopes with minor interference, other approaches are needed, such as separation techniques [232], mathematical correction [258], or chemometric methods [62] to cope with spectral overlap by oxides.

Table 9.1 Mean relative error for the validation set and for the three CRM quantified by univariate regression (OLS)

ID	**Relative Error (%)**													
	La	Ce	Pr	Nd	Sm	Eu	Gd	Tb	Dy	Ho	Er	Tm	Yb	Lu
1	14.1	10.5	1.9	5.5	10	19	18	10	7.0	8.5	12	15	24	7.0
2	9.8	14.7	9.4	6.0	8.6	24	20	-	7.0	4.6	11.5	17	31	15
3	7.3	6.5	8.0	5.7	9.6	40	46	12	4.5	-	18	14	25	4.3
4	8.6	9.5	6.6	10.5	8.4	-	17	7.9	16	6.2	12	12	21	5.2
5	7.2	11	12.5	5.6	-	16	14	4.0	4.0	6.0	27	26	-	3.3
6	5.5	13.9	5.8	14.2	8.0	29	64	8.8	-	4.8	-	11	-	3.8
7	7.6	-	7.6	5.7	6.1	12	18	16	7.5	6.3	-	13	15	4.9
8	7.6	8.5	5.9	13.3	7.2	-	78	7.2	11	7.0	13	-	22	-
9	8.7	-	9.6	5.8	12	12	-	4.4	5.0	25	15	18	22	3.8
10	10.9	-	7.3	11	9.6	13	76	4.4	6.0	5.0	18	24	25	11
11	7.5	6.2	6.5	5.4	9.5	17	13	3.8	5.0	12	16	19	22	3.7
12	10	8.5	5.6	11	-	14	17	8.0	8.8	6.3	14	10	14	2.5
13	6.5	7.5	9.6	5.7	7.1	12	15	4.2	12	-	18	21	16	1.5
14	11.7	6.7	-	7.1	11	22	16	11	3.0	5.8	19	10	23	10
15	6.8	7	6.1	7.6	8.4	15	53	12	-	9.0	26	20	25	7
Mean	8.6	9.2	8.0	8.2	16	22	33	12	12	13	17	16	19	11
RMSEP (µg L^{-1})	1.4	1.6	0.4	1.3	0.5	1.3	1.3	0.1	0.3	0.2	1.02	0.65	1.24	0.20
REP (%)	5.7	6.3	6.0	5.8	5.1	13.6	14.3	3.32	4.6	4.6	14.6	13.4	18.9	4.11
SRM1515	15	12	13	*	*	28	29	*	*	*	*	*	20	*
SRM1573	13	14	*	*	20	*	40	*	*	*	*	*	*	*
BCR670	11	14	11	12	14	24	26	19	20	14	16	15	15	19

* Not reported; - Not added

9.3.2.
Multivariate models

Since the quality of the multivariate calibration methods depends exclusively on the analytical solutions prepared, principal components analysis (PCA) was used to both detect absence/presence of outliers and to ensure the homogeneity between prediction and calibration datasets [259]. For this purpose, signal intensities of REEs in both, calibration and validation sets, were submitted to PCA independently, and the plot of the two first principal component scores (PC1 vs PC2) for the calibration and validation sets were plotted in the factor space. Figure 9.1 shows the score plot of the first principal component (PC1) against the second principal component (PC2) for both calibration and prediction analytical samples. As it is seen, none of the mixtures suffer deviation from factor space, discarding the presence of outliers. Also, it is clearly seen that prediction set is inside the factor space of the calibration set, which indicates homogeneity between them.

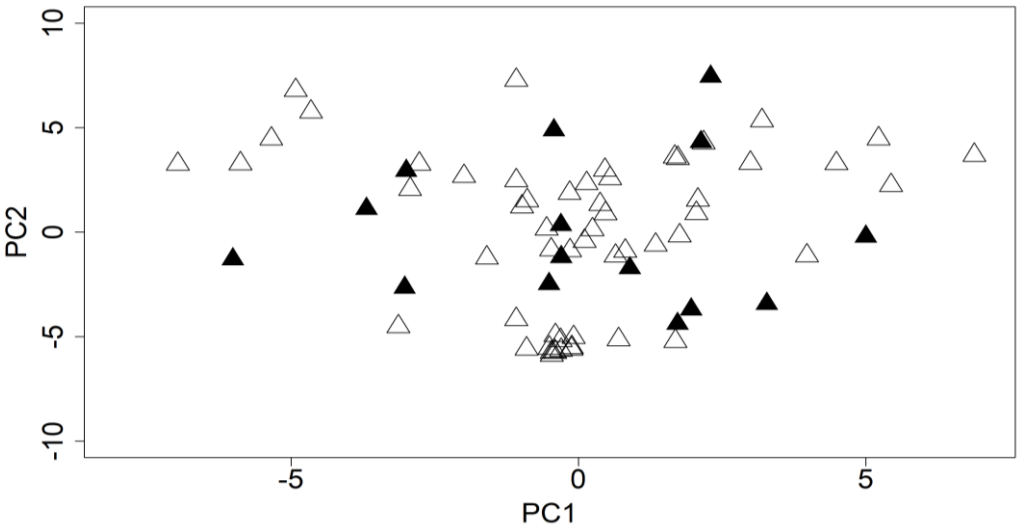

Figure 9.1 Score plots for the data matrices of the calibration (open markers) and prediction (filled markers) sets.

9.3.2.1.
PCR and PLS analysis

Firstly, the PCR and PLS regression were applied on the whole spectral

data for simultaneous determination of the elements. Here, the selection of an optimum number of factors for both reduction methods is a very important step before developing the models because if the number of factors selected was more than original data matrix, more noise will be added to the data, which may cause overfitting. In contrast, if the number of factors selected was too small meaningful data that could be necessary for the calibration set might be discarded.

To avoid over-fitting and to determine a model that fits well the data, ten-fold cross-validation procedure was used to select the optimum number of PCR-principal components (PCs) and PLS-latent variables (LVs) for each element. The number of factors that produced the minimum RMSEP value was selected as the optimum value.

Figure 9.2 presents a typical validation plot (ten-fold CV (train, black curve) and the bias-corrected CV estimate (adjCV, dashed red line)) of RMSE, for La, Ce, Pr, Nd, Sm, and Eu as function of the number of latent variables when PCR (left) and PLS (right) were applied. As observed, the RMSEP for cross-validation reaches a minimum value at a number of principal components equal to 15 for La, Ce, Pr, Sm and Eu and 13 for Nd, while the minimum values was attained with 10 latent variables for La, Ce, Sm, and Eu and 11 and 7 for Pr and Nd, respectively. In the same way, optimal numbers of factors were obtained for the other REEs (Figure H.1 – Supplementary material). As multivariate calibration is characterized by the factors number (PCs or LVs) selected for accurate data prediction. The optimum factors number selected should be equal to the original data matrix, within experimental error [260]. For PCR the most elements providing the same factors number that original matrix, indicating no overfitting data during the developing of the models. On the other hand, in PLS the numbers of factors were minors than PCR. Similar reports and results are sustained by other researchers [240,261,262].

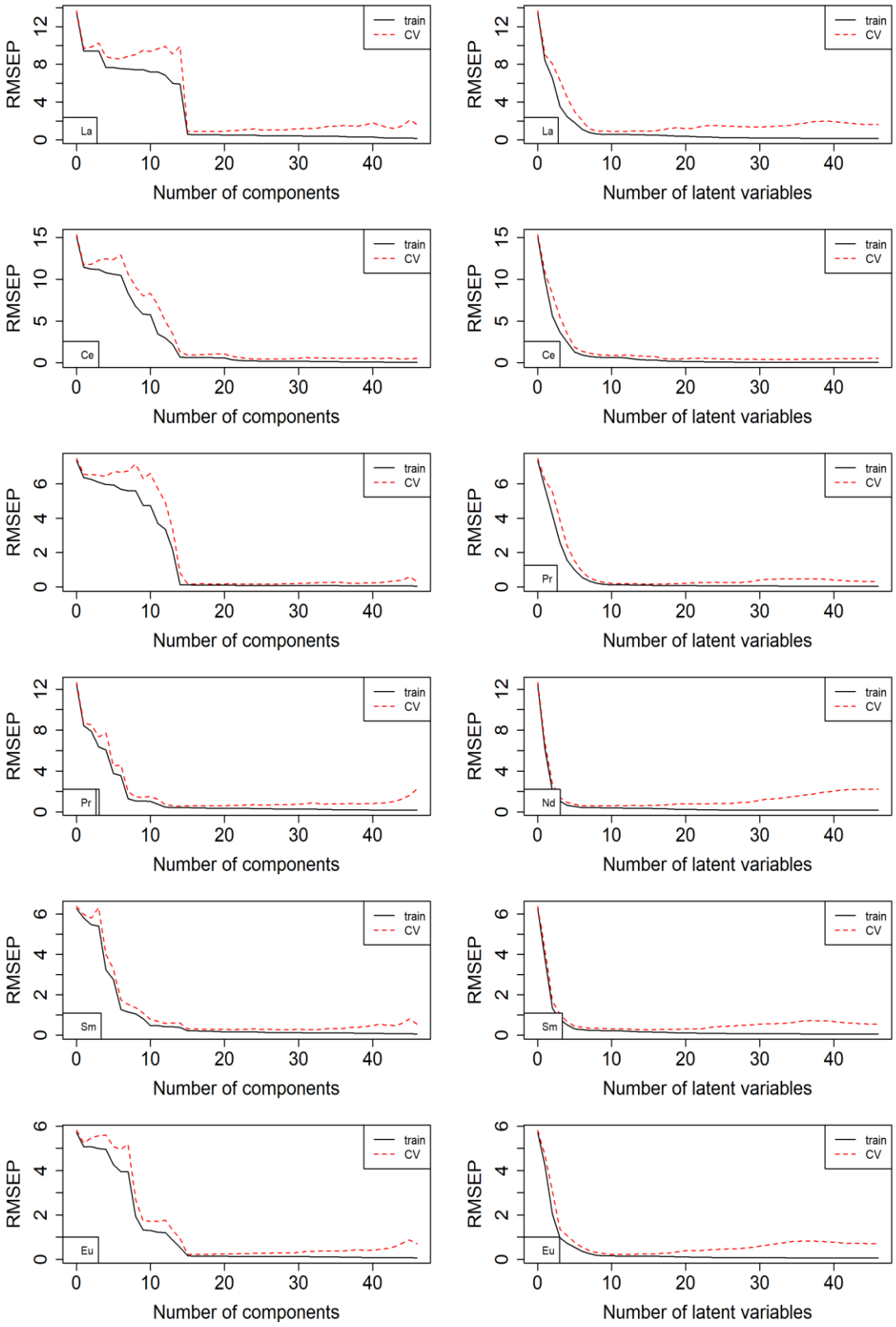

Figure 9.2 Cross-validated RMSEP curves for La, Ce, Pr, Nd, Sm, and Eu in function of the latent variables obtained by PLS (right) and PCR (left) multivariate calibration methods.

9.3.2.2. Ridge Regression and Lasso

In this study, a grid of λ ranging from 10^{-2} to 10^{10}, covering the full range of scenarios, was considered. Likewise, shrinkage methods were first applied to the whole spectral data, and then ten-fold cross-validation procedure was used to select the optimal λ value for each element. Prior to cross-validation, ridge regression and Lasso were set with α = 0 and α = 1, respectively in the free software R [66]. In terms of ℓ_2 and ℓ_1 regularization, this phenomenon is shown in Figure H.2 (Supplementary material), for both multivariate calibration, Lasso (lower) and RR (upper) only for Pr. As observed, if λ values increase, the estimated coefficients of Ridge and Lasso regressions will approach to zero, therefore, the variables also shrink towards zero. Other features are also noted when the value of log λ is -5, RR needs to use all variables (forty-six) for the construction of the model, while Lasso needs only twelve variables. This characteristic of Lasso to reduce the number of variables, choosing only a little subset of relevant features (variables, predictors), is known as variable selection.

Figure 9.3 displays the ten-fold cross-validation curves (red dotted line) for La, Ce, Pr, Nd, Sm, and Eu against mean square error (MSE), by RR (left) and Lasso (right) regressions, with upper and lower standard deviation curves along the λ sequence (error bars).[66] As can be seen, two vertical dot lines, λ.min (minimum error observed) and λ.1 (error within 1 standard error of minimum error), were selected, according to the glmnet package from R program.[65] In this case, λ.min represents the smallest cross-validation error, chosen as the tuning parameter. From Figure 9.3, it can be also observed that ridge regression reaches the λ.min adjusting λ values near to zero, but always considering all variables (forty-six variables), for the six elements (La, Ce, Pr, Nd, Sm, and Eu), while Lasso shrinks the most variables towards zero, considering only relevant variables. For instance, Lasso for La selected 6 relevant variables from a total of 46 variables (forty irrelevant variables were shrunk towards zero). Finally, the RR and Lasso models were re-fit using the λ.min selected by cross-validation, and by evaluating the coefficient estimates.

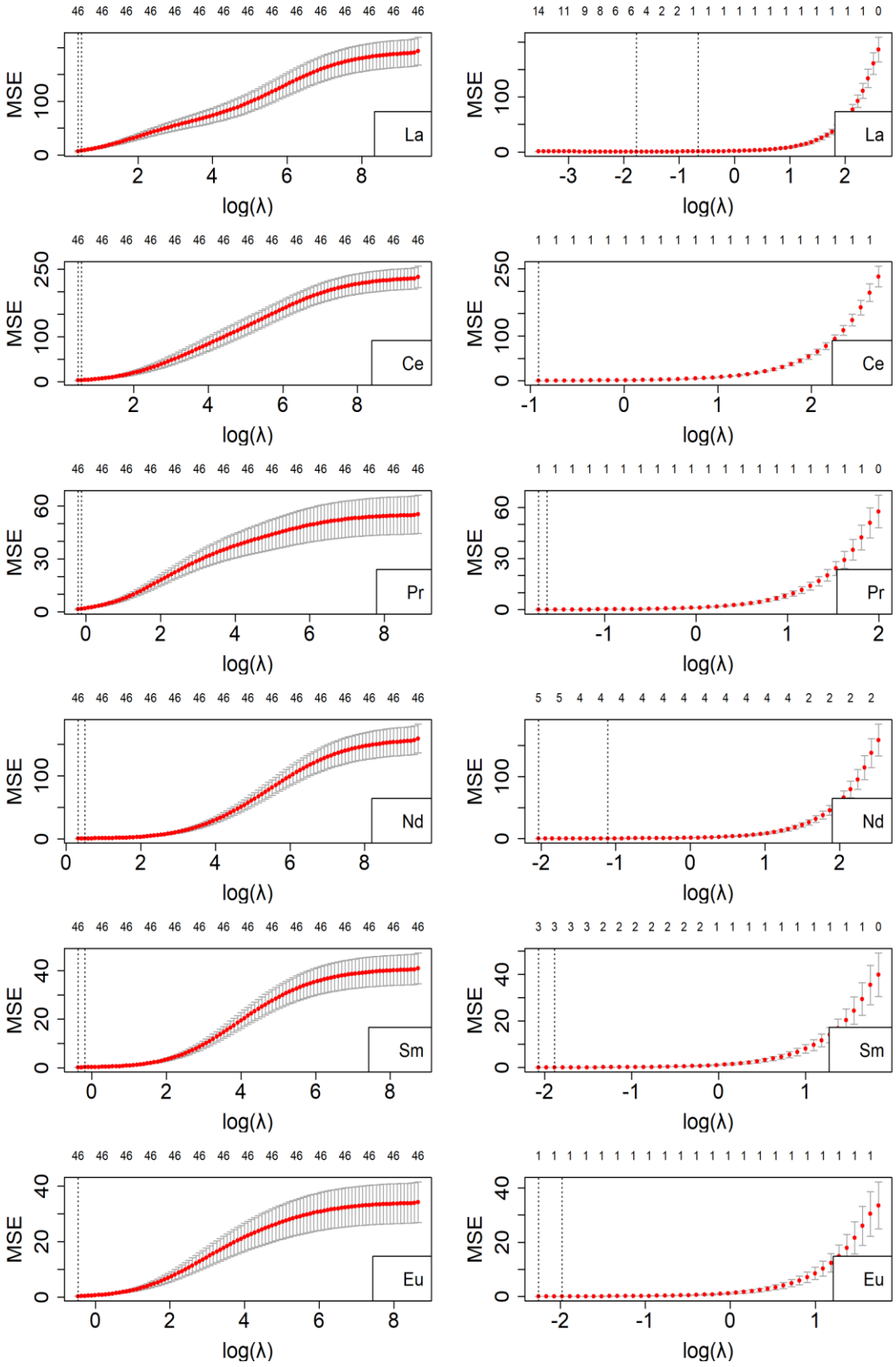

Figure 9.3 Plots of MSE of the cross-validation for La, Ce, Pr, Nd, Sm, and Eu as function of log (λ), by Lasso (right) and RR (left) multivariate calibration methods.

The ten-fold cross-validation curves of the other elements are displayed in Figure H.3 (Supplementary material). The benchmark results information on an optimum factors number and optimum λ values for each element and multivariate model as well as the statistical quantities for each multivariate calibration method are present in Table 9.2. As expected, all multivariate calibration methods showed better prediction performances, with lower RMSEP and REP values than OLS, for all REEs. Lower values of RMSEP indicate predictions with better precision and accuracy [263]. An inter-comparison among multivariate models based on the validation set shows that Lasso presented lower root mean square error of cross validation (RMSEC), RMSEP, and REP values than RR, PLS, and PCR, for all predicted REEs, indicating the best prediction and accuracy of Lasso among these models. For example, compared to the results of PCR and PLS, the RMSEP values of Lasso decreased remarkably (e.g., for Er, from 0.29 (PCR) and 0.25 (PLS) to 0.15 (Lasso), and for Gd, from 0.34 (PCR) and 0.25 (PLS) to 0.23 (Lasso)) for most REEs. Moreover, the Lasso method has the lowest RMSEP values than ridge regression for all REEs. On the other hand, RR compared to PLS shows lower RMSEP values for La, Ce, Nd, Sm, Gd, Dy, Er, and Yb, while PCR showed lower RMSEP values only for Eu, Tb, Ho, Tm, and Lu (Table 9.2). Therefore, according to RMSEP values obtained in this work, the multivariate calibration methods can be ordered in the following manner: Lasso > PLS ≈ RR > PCR. Better performance of Lasso can be attributed to the fact that this method offers both, continuous shrinkage regression and automatic variable selection, to produce a sparse model; while RR cannot provide a sparse model because it always includes all variables in the model (do not perform variable selection). Similarly, PLS and PCR produce variable selection, but they do not provide a sparse model. Among all models, it can be seen in Table 9.2 that PLS analysis needs a minor number of factors than PCR analysis for all RREs, as mentioned above, but they have no significant differences regarding predictive ability. Comparison between these two methods is mentioned elsewhere [243–245]. Lasso compared to ridge regression needs a reduced variables number, making much more easily interpretable the models developed by this method. Recently, shrinkage methods have received increasing attention due to their sparsity-inducing representations and high prediction accuracy in chemometrics [264]. For example, Sharif et al. (2017) [265] compared regression techniques to predict the

response of oilseed rape yield to climatic variations and concluded that Lasso model offered the most accurate yield predictions than OLS, PLS, and RR. Capellin et al. (2012) [266] used two datasets (named olive oil and grana cheese) and compared the performance of PLS and Lasso to predict the concentration of volatile organic compounds, and concluded that Lasso presented better prediction capabilities and interpretability than PLS. During oxide composition analysis in rocks by laser-induced breakdown spectroscopy, Lasso also showed lower RMSEP values and best-performance than PLS-1, PLS-2, and PCR [240].

Table 9.2 The benchmark results of different methods on the dataset (calibration set and validation set). nVAR: number of variables; nLV: number of latent variables or number of components; RMSEC: root-mean-squared error of calibration set; RMSEP: root-mean-square error of prediction; REP: relative error of prediction

Element	**Metrics**	**PCR**	**PLS**	**RR**	**Lasso**
La	nVAR	-	-	46	6
	nLV	15	10	-	-
	RMSEC (μg L^{-1})	0.784	0.792	1.150	0.716
	RMSEP (μg L^{-1})	0.836	0.901	0.545	0.415
	REP (%)	1.893	2.035	1.810	1.041
Ce	nVAR	-	-	46	1
	nLV	15	10	-	-
	RMSEC (μg L^{-1})	0.734	0.717	1.091	0.492
	RMSEP (μg L^{-1})	0.885	0.882	0.427	0.391
	REP (%)	1.502	1.521	1.910	0.995
Pr	nVAR			46	1
	nLV	15	11		
	RMSEC (μg L^{-1})	0.156	0.145	0.243	0.161
	RMSEP (μg L^{-1})	0.354	0.155	0.167	0.150
	REP (%)	1.622	1.371	2.677	1.064
Nd	nVAR			46	7
	nLV	13	7		
	RMSEC (μg L^{-1})	0.591	0.582	0.592	0.573
	RMSEP (μg L^{-1})	0.454	0.454	0.437	0.431
	REP (%)	1.484	1.224	1.930	1.320
Sm	nVAR			46	3
	nLV	15	10		
	RMSEC (μg L^{-1})	0.264	0.255	0.293	0.224
	RMSEP (μg L^{-1})	0.282	0.274	0.261	0.191
	REP (%)	1.454	1.523	2.651	1.343

Continuation Table 9.2

Element	Metrics	PCR	PLS	RR	Lasso
Eu	nVAR			46	5
	nLV	15	10		
	RMSEC (μg L^{-1})	0.238	0.226	0.307	0.215
	RMSEP (μg L^{-1})	0.249	0.239	0.284	0.243
	REP (%)	1.195	1.034	1.883	1.043
Gd	nVAR			46	16
	nLV	13	7		
	RMSEC (μg L^{-1})	0.404	0.371	0.382	0.384
	RMSEP (μg L^{-1})	0.336	0.254	0.251	0.232
	REP (%)	2.194	1.694	2.651	1.973
Tb	nVAR			46	1
	nLV	15	9		
	RMSEC (μg L^{-1})	0.082	0.073	0.235	0.092
	RMSEP (μg L^{-1})	0.075	0.083	0.151	0.069
	REP (%)	1.463	1.542	4.561	1.814
Dy	nVAR			46	4
	nLV	13	7		
	RMSEC (μg L^{-1})	0.226	0.212	0.201	0.242
	RMSEP (μg L^{-1})	0.283	0.275	0.264	0.181
	REP (%)	3.403	2.252	3.561	2.502
Ho	nVAR			46	1
	nLV	15	10		
	RMSEC (μg L^{-1})	0.114	0.121	0.131	0.112
	RMSEP (μg L^{-1})	0.075	0.074	0.120	0.076
	REP (%)	1.750	1.591	3.101	1.751
Er	nVAR			46	2
	nLV	13	7		
	RMSEC (μg L^{-1})	0.253	0.244	0.263	0.215
	RMSEP (μg L^{-1})	0.294	0.255	0.214	0.152
	REP (%)	2.532	2.111	1.545	1.832
Tm	nVAR			46	1
	nLV	15	9		
	RMSEC (μg L^{-1})	0.075	0.064	0.173	0.092
	RMSEP (μg L^{-1})	0.084	0.075	0.150	0.075
	REP (%)	1.742	1.621	3.140	1.462
Yb	nVAR			46	3
	nLV	13	7		
	RMSEC (μg L^{-1})	0.244	0.223	0.305	0.212
	RMSEP (μg L^{-1})	0.304	0.205	0.184	0.161
	REP (%)	3.433	2.451	2.732	2.392
Lu	nVAR			46	1
	nLV	15	11		
	RMSEC (μg L^{-1})	0.103	0.094	0.181	0.112
	RMSEP (μg L^{-1})	0.094	0.107	0.194	0.081
	REP (%)	1.972	2.054	3.143	1.703

Using the developed multivariate methods, the REEs concentrations measured in the validation set were predicted and the mean relative error (RE) for each element is presented in Table 9.3. The results obtained showed mean RE values < 10 for all elements, demonstrating clearly the superiority and ability of multivariate methods to predict accurately the concentrations, despite the presence of spectral interferences and overlapping. Moreover, Lasso showed the lowest range of RE (1.6 % - 4.6 %), followed by RR (2.3 % - 7.3 %), PLS (1.5 % - 7.7 %), and PCR (1.8 % - 8.2).

Table 9.3 Mean relative error (RE) of the concentrations measured in the validation set for all REEs, by applying the multivariate calibration methods.

Element	**RE (%)**			
	PCR	PLS	RR	Lasso
La	2.76	2.65	2.89	1.63
Ce	6.92	6.94	6.08	4.08
Pr	2.64	2.56	7.29	2.04
Nd	1.75	1.49	2.30	1.41
Sm	3.10	2.90	6.81	2.72
Eu	3.99	3.16	4.41	2.73
Gd	6.80	7.01	7.44	5.73
Tb	3.28	3.83	7.04	3.16
Dy	4.06	3.68	5.35	3.45
Ho	3.58	2.80	4.76	2.64
Er	5.47	5.61	6.76	4.00
Tm	4.77	4.05	3.60	2.62
Yb	8.15	7.69	7.04	4.59
Lu	3.49	3.69	4.81	2.89

To evaluate whether the predicted concentration of the validation set using multivariate calibration methods and OLS are statistically different, Wilcoxon signed-rank test was applied. Assuming nonparametric data (n < 30), the results were compared to each other by pairs for all REEs. The values obtained for Wilcoxon test are shown in Table H.4 in Supplementary material (only four REE:

Tm, Ho, Eu, and Er were showed). Values of Wilcoxon signed-rank test for multivariate models presented *p* values higher than 0.05, meaning that there are no significant differences among the studied methods. In addition, *p* values lower than 0.05 indicated significant differences between OLS and each multivariate method**.**

9.3.3. Certified Reference Material analysis

The proposed multivariate models were also applied to predict REEs concentrations in three CRM: BCR670 (*Aquatic Plant*, n=3), SRM 1515a (*Apple leaves*, n=3), and SRM 1573a (*Tomato leaves*, n=3). An inter-comparison among the multivariate models to predict the certified concentrations of the REEs in the three CRM based on the RE % and recoveries are present in Table 9.4 to Table 9.6. As it is observed, REEs concentrations predicted using the four multivariate models shown relative error < 10 %, indicating both precision and accuracy. However, Lasso shows the lowest mean RE for the three CRM (1.5 % for BCR 670, 1.8 % for SRM1515, and 1.9 % for SRM573), when compared to RR, PLS, and PCR. The concentration versus certified values predicted with Lasso model for the three CRMs is represented in Figure 9.4. The solid line denotes perfect equality between predicted concentrations and the values provided in the corresponding certificate. The proposed methods were satisfactory, simple, fast, sensitive and selective, and they can be used for routine determination of REEs in any kind of matrix.

Table 9.4 Relative errors (RE %) and recoveries (%) for the BRC 670 (Aquatic plant) using the multivariate calibration methods.

Isotope	**Recovery (%)**	**RE (%)**	**Recovery (%)**	**RE (%)**	**Recovery (%)**	**RE (%)**	**Recovery (%)**	**RE (%)**
	PCR	PCR	PLS	PLS	RR	RR	Lasso	Lasso
La	95.6	4.43	96.7	3.25	99.1	0.90	99.4	0.54
Ce	96.3	3.72	102.2	2.13	98.3	1.66	101.6	1.62
Pr	95.9	4.06	101.4	1.36	102	1.57	100.9	1.57
Nd	93.4	6.63	96.5	3.50	10.7	2.70	97.7	2.70
Sm	96.2	3.86	95.2	4.88	101.4	1.47	98.0	1.47
Eu	106.5	6.48	102.2	2.19	102.9	2.87	101.3	2.87
Gd	104.7	4.76	103.1	3.06	104	3.93	100.5	3.93
Tb	95.8	4.11	98.2	1.83	108	2.41	97.6	2.41
Dy	96.8	3.16	99.2	0.84	99.1	1.05	99.8	1.05
Ho	102.4	2.36	94.8	5.23	103.3	1.61	101.6	1.61
Er	96.2	3.80	97.8	2.22	97.9	3.29	98.2	3.29
Tm	92.7	7.25	96.4	3.63	94.2	5.77	96.1	5.77
Yb	96.3	3.73	97.1	2.90	100.3	0.27	100	0.27
Lu	105.5	5.52	101.7	1.05	103.3	3.23	97.9	3.23
Mean	98.2	4.6	98.7	2.7	101.1	2.8	99.3	1.5

Table 9.5 Relative errors (RE %) and recoveries (%) for the SRM 1515 (Apple leaves) using the multivariate calibration methods.

Isotope	Recovery (%)	RE (%)	Recovery (%)	RE (%)	Recovery (%)	RE (%)	Recovery (%)	RE (%)
	PCR	PCR	PLS	PLS	RR	RR	Lasso	Lasso
La	96.7	3.3	101.2	1.2	98.6	1.5	98.9	1.1
Ce	105.6	5.6	105.3	5.3	107.5	3.1	97.3	2.7
Nd	102.1	2.1	102.1	2.1	101.5	1.6	100.8	0.8
Sm	91.6	7.3	93.4	6.1	93.4	6.6	97.4	2.6
Eu	108.1	6.4	106.4	5.9	106.4	6.4	101.4	1.4
Gd	95.4	4.6	103.6	3.8	103.6	3.6	99.9	0.1
Tb	95.2	4.8	96.7	4.1	96.7	3.3	102.1	2.2
Yb	90.4	9.6	90.5	8.5	90.5	9.5	103.9	3.9
Mean	98.0	5.5	99.0	4.6	99.2	4.4	100.2	1.8

Table 9.6 Relative errors (RE %) and recoveries (%) for the SRM 1573 (Tomato leaves) using the multivariate calibration methods.

Isotope	Recovery (%)	RE (%)	Recovery (%)	RE (%)	Recovery (%)	RE (%)	Recovery (%)	RE (%)
	PCR	PCR	PLS	PLS	RR	RR	Lasso	Lasso
La	94.3	5.7	97.8	2.2	100.2	2.7	98.8	1.2
Ce	107.7	7.7	102.7	2.7	107.3	7.4	99.1	1.0
Sm	108.9	8.8	105.4	5.4	105.4	5.4	103.6	3.6
Gd	108.5	8.5	107.5	7.5	94.7	5.3	101.6	1.7
Mean	104.8	7.7	103.3	4.5	101.2	5.2	100.8	1.9

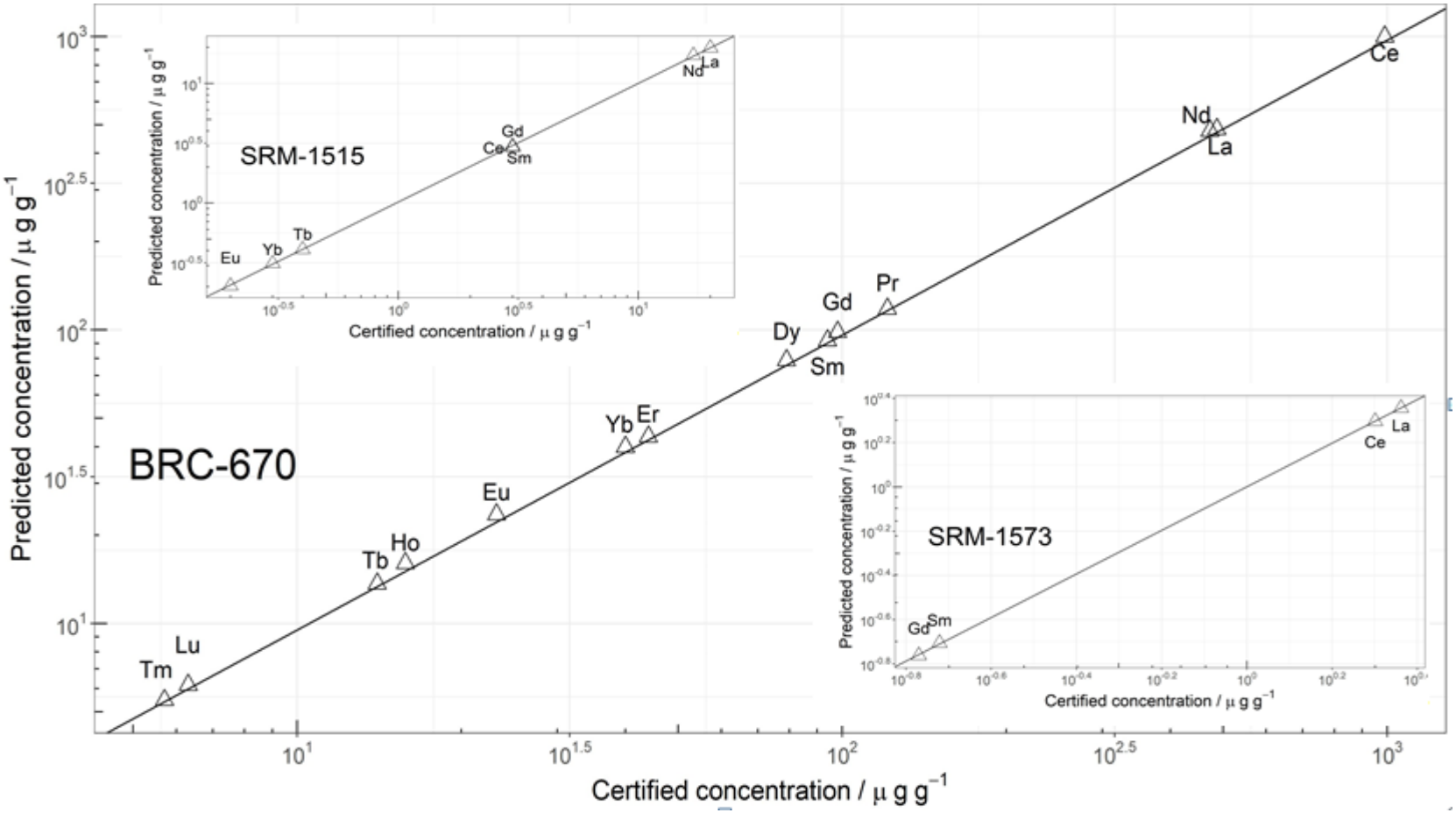

Figure 9.4 Accurate measurements of rare earth elements of the three Certified Reference Material using Lasso model.

9.4. Conclusions

In this paper, we proposed two shrinkage multivariate methods RR and Lasso, and their comparison to the two well-known reduction methods (PCR and PLS), for accurate determination of REEs by ICP-MS. Additionally, it was evaluated the classical regression technique called Ordinary Least Squares Method (OLS), which show relative error > 10 % for most measured REEs, due to its incapability to solve spectral overlapping. All multivariate models exhibit similar accuracy in predicting REEs concentrations for the validation set and the three certified reference material, concluding that the four multivariate models can overcome spectral interference in complex matrices. However, Lasso has demonstrated better performance in accuracy and simplicity. Moreover, Lasso shows lower RMSEP and REP values, as well as the lowest RE and better interpretability than RR, PLS, and PCR.

Acknowledgements

The authors are grateful to Coordenação de Aperfeiçoamento de Pessoal de Nível Superior (CAPES), and Fundação de Amparo e Pesquisa do Estado do Rio de Janeiro (FAPERJ) for financial support T. D. S. thanks to Conselho Nacional de Desenvolvimento Científico e Tecnológico (CNPq) for the scholarship.

10
Conclusions and future perspective

The results observed in the articles developed in the Laboratório de Espectrometria Atômica (LABSPECTRO) and Laboratório de Química Atmosférica (LQA) and presented in this thesis, allowed to infer that the use of living organisms as biomonitors of atmospheric deposition, as well as the determination of its chemical composition and use of chemometric techniques, are useful tools to diagnosing the air quality in any context (industrial, urban, peri-urban, and rural areas). With the information obtained it would be possible to adopt control or mitigation strategies for air pollution in the areas studied.

The different biomonitors employed in this work, demonstrated be reliable and efficient living organisms for accumulate pollutants and represent well the environment where they live. Likewise, both biomonitoring methods applied offering satisfactory results.

The use of chemometric tools helps to characterize the areas and identify the main sources of atmospheric pollution, especially when the techniques adopted are multivariate techniques such as principal component analysis (PCA) and hierarchical cluster analysis (HCA). The application of these tools in this work, allowed the identification of different sources of pollution for each studied area. Likewise, allowed grouping of regions with similar characteristics and pollution level.

However, it is necessary that environmental agencies and local/regional government make use of alternatives tools as the use of non-expensive biomonitors and application of chemometrics tools, besides monitoring only, to evaluate the sources contributing to the air pollution of each local/regional area of interest.

References

[1] S.k. Agarwal, Air Pollution, APH Publishing, Delhi, 2005. https://books.google.com.pe/books?id=dJlxyyLX0MoC&printsec=frontcover#v=onepage&q&f=false.

[2] J. Green, S. Sanchez, Air Quality in Latin America: An Overview, Washington, USA, 2012. http://www.cleanairinstitute.org/calidaddelaireamericalatina/cai-report-english.pdf.

[3] R.S. Sokhi, World Atlas of Atmospheric Pollution, UK, 2011.

[4] WHO, World Health Organization, 9 out 10 People Worldw. Breathe Polluted Air. (2018) 9 out of 10 people worldwide breathe polluted air,. http://www.who.int/news-room/headlines/02-05-2018-9-out-of-10-people-worldwide-breathe-polluted-air-but-more-countries-are-taking-action (accessed September 13, 2018).

[5] K. Szczepaniak, M. Biziuk, Aspects of the biomonitoring studies using mosses and lichens as indicators of metal pollution, Environ. Res. 93 (2003) 221–230. doi:10.1016/S0013-9351(03)00141-5.

[6] M. de la Guardia, The Quality of Air, 2016. https://books.google.com.br/books?id=ZQVKCgAAQBAJ&pg=PA117&lpg=PA117&dq=Chapter+6+–+Lichens+as+Biomonitors+of+Heavy-Metal+Pollution&source=bl&ots=bvQkAgolP5&sig=9FR6HQzr3QA59ogWTOGx0IDyVSM&hl=pt-BR&sa=X&ved=0ahUKEwjM6M-_tavTAhWJjZAKHfZ5CaYQ6AEINzAC#v=onep.

[7] M.E. Conti, G. Cecchetti, Biological monitoring: lichens as bioindicators of air pollution assessment--a review., Environ. Pollut. 114 (2001) 471–92. http://www.ncbi.nlm.nih.gov/pubmed/11584645.

[8] R.B. Vertika Shukla, D.K. Upreti, Lichens to Biomnitor the Environment, 2013. https://books.google.com.br/books?id=CRR_AAAAQBAJ&pg=PA98&lpg

=PA98&dq=sensitive+biomonitors&source=bl&ots=1II4j9TmVT&sig=su3gzGGdPyUVTf95lL0qkbo1Khc&hl=pt-BR&sa=X&ved=0ahUKEwjapL6Z6tfUAhWIlJAKHeEkA1EQ6AEIVTAG#v=onepage&q=sensitive biomonitors&f=false.

[9] H.T. Wolterbeek, J. Garty, M.A. Reis, M.C. Freitas, Biomonitors in use: lichens and metal air pollution, in: Bioindic. Biomonitors, 2003: pp. 377–419. doi:10.1016/S0927-5215(03)80141-8.

[10] J. Garty, Environment and elemental content of lichens, in: Trace Elem. Distrib. Eff. Environ., 2000.

[11] Z. Sengo, Air Plants: The Curious World of Tillandsias, California, USA, 2014. https://books.google.com.br/books?id=Vpc8BQAAQBAJ&dq=tillandsia&hl=pt-BR&source=gbs_navlinks_s.

[12] S.K. Agarwal, Heavy Metal Pollution, 2009.

[13] K.-H. Kim, E. Kabir, S. Kabir, A review on the human health impact of airborne particulate matter, Environ. Int. 74 (2015) 136–143. doi:10.1016/j.envint.2014.10.005.

[14] E. Liu, T. Yan, G. Birch, Y. Zhu, Pollution and health risk of potentially toxic metals in urban road dust in Nanjing, a mega-city of China, Sci. Total Environ. 476–477 (2014) 522–531. doi:10.1016/j.scitotenv.2014.01.055.

[15] M. Hoodaji, M. Ataabadi, P. Najafi, Biomonitoring of Airborne Heavy Metal Contamination, in: Air Pollut. - Monit. Model. Heal. Control, 2012: pp. 97–122. doi:10.5772/711.

[16] T. Damhus, R. Hartshorn, A. Hutton, Nomenclature of inorganic chemistry: IUPAC recommendations 2005, 2005. http://www.degruyter.com/view/j/ci.2005.27.issue-6/ci.2005.27.6.25/ci.2005.27.6.25.xml (accessed August 7, 2014).

[17] C. Hissler, P. Stille, C. Guignard, J.F. Iffly, L. Pfister, Rare Earth Elements as Hydrological Tracers of Anthropogenic and Critical Zone Contributions: A Case Study at the Alzette River Basin Scale., Procedia Earth Planet. Sci. 10 (2014) 349–352. doi:10.1016/j.proeps.2014.08.036.

[18] M.A. Alam, L. Zuga, M.G. Pecht, Economics of rare earth elements in ceramic capacitors, Ceram. Int. 38 (2012) 6091–6098. doi:10.1016/j.ceramint.2012.05.068.

[19] K. Redling, Rare earth elements in agriculture with emphasis on animal husbandry, (2006). http://edoc.ub.uni-muenchen.de/5936/ (accessed April 21, 2014).

[20] Y. Kanazawa, M. Kamitani, Rare earth minerals and resources in the world, J. Alloys Compd. 408–412 (2006) 1339–1343. doi:10.1016/j.jallcom.2005.04.033.

[21] M. Humphries, Rare earth elements: the global supply chain, 2010. http://books.google.com/books?hl=en&lr=&id=uzkYstWv_HYC&oi=fnd&pg=PA1&dq=Rare+Earth+Elements+:+The+Global+Supply+Chain&ots=w8qdWQwJk7&sig=mSN5cLQ0H421TYZHRbxF1yHM_sw (accessed September 26, 2014).

[22] D.A. Atwood, The Rare Earth Elements: Fundamentals and Applications, Lexington, USA, 2013. https://books.google.com.br/books?id=Mc-R90gp5B4C&dq=rare+earth+elements&hl=pt-BR&source=gbs_navlinks_s.

[23] Instituto Nacional de Estadística e Informática, Peru: Principales Indicadores Departamentales 2009-2016, Lima, 2017. https://www.inei.gob.pe/media/MenuRecursivo/publicaciones_digitales/Est/Lib1421/libro.pdf.

[24] A. Haller, A. Borsdorf, Huancayo Metropolitano, Cities. 31 (2013) 553–562. doi:10.1016/j.cities.2012.04.004.

[25] C. Huancayo, CLIMATE-DATA.ORG, (2017). https://en.climate-data.org/location/3326/.

[26] I. Brachet, E. Wrzoncki, Peru: Metallurgical Complex of La Oroya: When Investor Protection Threatens Human Rights, (2012). https://www.fidh.org/IMG/pdf/metallurgical_complex_of_la_oroya-2.pdf.

[27] I. Zasada, C. Fertner, A. Piorr, T.S. Nielsen, Peri-urbanisation and multifunctional adaptation of agriculture around Copenhagen, Geogr. Tidsskr. J. Geogr. 111 (2011) 59–72. doi:10.1080/00167223.2011.10669522.

[28] A. Haller, The “sowing of concrete”: Peri-urban smallholder perceptions of rural-urban land change in the Central Peruvian Andes, Land Use Policy. 38 (2014) 239–247. doi:10.1016/j.landusepol.2013.11.010.

[29] L.K. Boamponsem, J.I. Adam, S.B. Dampare, B.J.B. Nyarko, D.K.

Essumang, Assessment of atmospheric heavy metal deposition in the Tarkwa gold mining area of Ghana using epiphytic lichens, Nucl. Instruments Methods Phys. Res. Sect. B Beam Interact. with Mater. Atoms. 268 (2010) 1492–1501. doi:10.1016/j.nimb.2010.01.007.

[30] Y. Agnan, N. Séjalon-Delmas, A. Probst, Comparing early twentieth century and present-day atmospheric pollution in SW France: A story of lichens, Environ. Pollut. 172 (2013) 139–148. doi:10.1016/j.envpol.2012.09.008.

[31] R. Gerdol, R. Marchesini, P. Iacumin, L. Brancaleoni, Monitoring temporal trends of air pollution in an urban area using mosses and lichens as biomonitors, Chemosphere. 108 (2014) 388–395. doi:10.1016/j.chemosphere.2014.02.035.

[32] A.M.G. Figueiredo, C.A. Nogueira, M. Saiki, F.M. Milian, M. Domingos, Assessment of atmospheric metallic pollution in the metropolitan region of Sao Paulo, Brazil, employing Tillandsia usneoides L. as biomonitor, Environ. Pollut. 145 (2007) 279–292. doi:10.1016/j.envpol.2006.03.010.

[33] H.F. Kaiser, The application of electronic computers to factor analysis, XX (1960) 141–151. http://journals.sagepub.com/doi/pdf/10.1177/001316446002000116.

[34] R Team Core, A language and Environment for Statistical Computing. R Foundation for Statistical Computing, Vienna Austria, in: R Foundation for Statistical Computing, Vienna, Austria, 2015. https://www.r-project.org/.

[35] A. Kassambara, F. Mundt, Extract and visualize the results of multivariate data analyses, R Packag. Version. 1 (2016).

[36] M.H. Wickham, W. Chang, An Implementation of the Grammar of Graphics, (2016) 197.

[37] M. Chavent, V.K. Simonet, B. Liquet, V. Kuentz-simonet, ClustOfVar : An R Package for the Clustering of Variables, J. Stat. 50 (2012). https://hal.inria.fr/hal-00742795/document.

[38] M. Maechler, P. Rousseeuw, A. Struyf, M. Hubert, K. Hornik, M. Studer, P. Roudier, Finding Groups in Data: Cluster Analysis Extended Rousseeuw et al., (2015). doi:ISBN 0-387-95457-0.

[39] W. Revelle, Procedures for Psychological, Psychometric, and Personality Research, (2018) 443. https://personality-project.org/r/psych-manual.pdf.

[40] IBGE, Estimativas da populacao residente no brasil e unidades da federacao com data de referencia em 1 julho de 2016, (2016). ftp://ftp.ibge.gov.br/Estimativas_de_Populacao/Estimativas_2016/estimativa_2016_TCU.pdf (accessed July 2, 2018).

[41] A.L. Paraginski, A Natureza Das Inovações Em Agroindústrias De Arroz Do Rio Grande Do Sul, Rev. Adm. Innov. - RAI. 11 (2014) 55. doi:10.5773/rai.v11i1.1053.

[42] H. Bing, Y. Wu, J. Zhou, H. Sun, Biomonitoring trace metal contamination by seven sympatric alpine species in Eastern Tibetan Plateau, Chemosphere. 165 (2016) 388–398. doi:10.1016/j.chemosphere.2016.09.042.

[43] F. Ardini, F. Soggia, F. Rugi, R. Udisti, M. Grotti, Conversion of rare earth elements to molecular oxide ions in a dynamic reaction cell and consequences on their determination by inductively coupled plasma mass spectrometry, J. Anal. At. Spectrom. 25 (2010) 1588. doi:10.1039/b927108b.

[44] M. Kara, Y. Dumanoglu, H. Altiok, T. Elbir, M. Odabasi, A. Bayram, Seasonal and spatial variations of atmospheric trace elemental deposition in the Aliaga industrial region, Turkey, Atmos. Res. 149 (2014) 204–216. doi:10.1016/j.atmosres.2014.06.009.

[45] S. Taylor, R. McLennan, The continental crust, its composition and evolution: an examination of the geochemical record preserved in a sedimetary rocks, Oxford; Melbourne: Black Scientific Publications, 1985.

[46] S.M. Enamorado-Báez, J.M. Gómez-Guzmán, E. Chamizo, J.M. Abril, Levels of 25 trace elements in high-volume air filter samples from Seville (2001–2002): Sources, enrichment factors and temporal variations, Atmos. Res. 155 (2015) 118–129. doi:10.1016/j.atmosres.2014.12.005.

[47] Y.S. Wu, G.C. Fang, W.J. Lee, J.F. Lee, C.C. Chang, C.Z. Lee, A review of atmospheric fine particulate matter and its associated trace metal pollutants in Asian countries during the period 1995-2005, J. Hazard. Mater. 143 (2007) 511–515. doi:10.1016/j.jhazmat.2006.09.066.

[48] H. Wickham, R. Francois, L. Henry, K. Müller, A Grammar of Data Manipulation, Cran. (2017). https://cran.r-project.org/web/packages/dplyr/dplyr.pdf.

[49] E.D. Wannaz, M.L. Pignata, Calibration of four species of Tillandsia as air pollution biomonitors, J. Atmos. Chem. 53 (2006) 185–209. doi:10.1007/s10874-005-9006-6.

[50] L. Frati, G. Brunialti, S. Loppi, Problems related to lichen transplants to monitor trace element deposition in repeated surveys: A case study from central Italy, J. Atmos. Chem. 52 (2005) 221–230. doi:10.1007/s10874-005-3483-5.

[51] G.M.A. Bermudez, J.H. Rodriguez, M.L. Pignata, Comparison of the air pollution biomonitoring ability of three Tillandsia species and the lichen Ramalina celastri in Argentina, Environ. Res. 109 (2009) 6–14. doi:10.1016/j.envres.2008.08.014.

[52] L.M.B. Ventura, F. de O. Pinto, Inventário de emissões de fontes veiculares: região metropolitana do Rio de Janeiro, (2013) 350.

[53] DETRAN, Governo do Rio de Janeiro, Junho. (2018). http://www.detran.rj.gov.br/_estatisticas.veiculos/02.asp (accessed September 11, 2018).

[54] C. Su, R. Hampel, U. Franck, A. Wiedensohler, J. Cyrys, X. Pan, H.E. Wichmann, A. Peters, A. Schneider, S. Breitner, Assessing responses of cardiovascular mortality to particulate matter air pollution for pre-, during- and post-2008 Olympics periods, Environ. Res. 142 (2015) 112–122. doi:10.1016/j.envres.2015.06.025.

[55] T. Okuda, S. Matsuura, D. Yamaguchi, T. Umemura, E. Hanada, H. Orihara, S. Tanaka, K. He, Y. Ma, Y. Cheng, L. Liang, The impact of the pollution control measures for the 2008 Beijing Olympic Games on the chemical composition of aerosols, Atmos. Environ. 45 (2011) 2789–2794. doi:10.1016/j.atmosenv.2011.01.053.

[56] X. Wang, T. Wang, R.K. Pathak, M. Hallquist, X. Gao, W. Nie, L. Xue, J. Gao, R. Gao, Q. Zhang, W. Wang, S. Wang, F. Chai, Y. Chen, Size distributions of aerosol sulfates and nitrates in Beijing during the 2008 Olympic Games: Impacts of pollution control measures and regional transport, Adv. Atmos. Sci. 30 (2013) 341–353. doi:10.1007/s00376-012-2053-4.

[57] P. Kulkarni, S. Chellam, D.W. Mittlefehldt, Microwave-assisted extraction of rare earth elements from petroleum refining catalysts and ambient fine

aerosols prior to inductively coupled plasma-mass spectrometry., Anal. Chim. Acta. 581 (2007) 247–59. doi:10.1016/j.aca.2006.08.035.

[58] J. Riondato, F. Vanhaecke, L. Moens, R. Dams, Determination of rare earth elements in environmental matrices by sector-field inductively coupled plasma mass spectrometry., Fresenius. J. Anal. Chem. 370 (2001) 544–552. doi:10.1007/s002160100801.

[59] M. Costas, I. Lavilla, S. Gil, F. Pena, I. de la Calle, N. Cabaleiro, C. Bendicho, Evaluation of ultrasound-assisted extraction as sample pre-treatment for quantitative determination of rare earth elements in marine biological tissues by inductively coupled plasma-mass spectrometry, Anal. Chim. Acta. 679 (2010) 49–55. doi:10.1016/j.aca.2010.09.004.

[60] F. Ardini, F. Soggia, F. Rugi, R. Udisti, M. Grotti, Comparison of inductively coupled plasma spectrometry techniques for the direct determination of rare earth elements in digests from geological samples., Anal. Chim. Acta. 678 (2010) 18–25. doi:10.1016/j.aca.2010.07.036.

[61] E. Vigneau, M.F. Devaux, E.M. Qannari, P. Robert, Principal Component Regression, Ridge Regression and Ridge Principal Component Regression in Spectroscopy, J. Chemom. 11 (1997) 239–249. doi:10.1002/(SICI)1099-128X(199705)11:3<239::AID-CEM470>3.0.CO;2-A.

[62] M. Rupprecht, T. Probst, Development of a method for the systematic use of bilinear multivariate calibration methods for the correction of interferences in inductively coupled plasma-mass spectrometry, Anal. Chim. Acta. 358 (1998) 205–225. doi:10.1016/S0003-2670(97)00627-2.

[63] Y.-L. Xie, J.H. Kalivas, Evaluation of principal component selection methods to form a global prediction model by principal component regression, Anal. Chim. Acta. 348 (1997) 19–27. doi:10.1016/S0003-2670(97)00035-4.

[64] R. and K.H.L. Bjørn-Helge Mevik, Partial Least Squares and Principal Components Regression, (2015). http://mevik.net/work/software/pls.html.

[65] A.J. Friedman, T. Hastie, N. Simon, R. Tibshirani, M.T. Hastie, Lasso and Elastic-Net Regularized Generalized Linear Models, Available Online Https//cran.r-Project.org/web/packages/glmnet/glmnet.pdf. (Verified 29 July. 2015). (2015). http://www.jstatsoft.org/v33/i01/.

[66] T. Hastie, R. Tibshirani, J. Friedman, The Elements of Statistical Learning:

Data mining, Inference and Prediction, 2nd ed., Springer New York, New York, NY, 2009. doi:10.1007/978-0-387-84858-7.

[67] C.K. Bayne, R. Kramer, Chemometric Techniques for Quantitative Analysis, Technometrics. 41 (1999) 173. doi:10.2307/1270741.

[68] R. Janta, S. Chantara, Tree bark as bioindicator of metal accumulation from road traffic and air quality map: A case study of Chiang Mai, Thailand, Atmos. Pollut. Res. 8 (2017) 956–967. doi:10.1016/j.apr.2017.03.010.

[69] V.L. Mateus, I.L.G. Monteiro, R.C.C. Rocha, T.D. Saint'Pierre, A. Gioda, Study of the chemical composition of particulate matter from the Rio de Janeiro metropolitan region, Brazil, by inductively coupled plasma-mass spectrometry and optical emission spectrometry, Spectrochim. Acta - Part B At. Spectrosc. 86 (2013) 131–136. doi:10.1016/j.sab.2013.03.003.

[70] E.P.A. EPA, Determination of metals in ambient particulate matter using atomic absorption (AA) spectroscopy, 1999. https://www3.epa.gov/ttnamti1/files/ambient/inorganic/mthd-3-2.pdf.

[71] P. Giampaoli, E.D. Wannaz, A.R. Tavares, M. Domingos, Suitability of Tillandsia usneoides and Aechmea fasciata for biomonitoring toxic elements under tropical seasonal climate, Chemosphere. 149 (2016) 14–23. doi:10.1016/j.chemosphere.2016.01.080.

[72] L. Van der Wat, P.B.C. Forbes, Lichens as biomonitors for organic air pollutants, TrAC - Trends Anal. Chem. 64 (2015) 165–172. doi:10.1016/j.trac.2014.09.006.

[73] P. Malaspina, M. Casale, C. Malegori, M. Hooshyari, M. Di Carro, E. Magi, P. Giordani, Combining spectroscopic techniques and chemometrics for the interpretation of lichen biomonitoring of air pollution, Chemosphere. 198 (2018) 417–424. doi:10.1016/j.chemosphere.2018.01.136.

[74] S. Loppi, L. Frati, L. Paoli, V. Bigagli, C. Rossetti, C. Bruscoli, A. Corsini, Biodiversity of epiphytic lichens and heavy metal contents of Flavoparmelia caperata thalli as indicators of temporal variations of air pollution in the town of Montecatini Terme (central Italy), Sci. Total Environ. 326 (2004) 113–122. doi:10.1016/j.scitotenv.2003.12.003.

[75] O.W. Purvis, B. Pawlik-skowron, Lichens and Metals, in: 2008: pp. 175–200. https://ac.els-cdn.com/S0275028708800549/1-s2.0-

S0275028708800549-main.pdf?_tid=d55b1dfc-c880-11e7-992a-00000aab0f6c&acdnat=1510584312_c18ddc2e016bbb4464b275722abe2000.

[76] B. Koz, N. Celik, U. Cevik, Biomonitoring of heavy metals by epiphytic lichen species in Black Sea region of Turkey, Ecol. Indic. 10 (2010) 762–765. doi:10.1016/j.ecolind.2009.11.006.

[77] A. Fuga, M. Saiki, M.P. Marcelli, P.H.N. Saldiva, Atmospheric pollutants monitoring by analysis of epiphytic lichens, Environ. Pollut. 151 (2008) 334–340. doi:10.1016/j.envpol.2007.06.041.

[78] C. Boonpeng, W. Polyiam, C. Sriviboon, D. Sangiamdee, S. Watthana, P.L. Nimis, K. Boonpragob, Airborne trace elements near a petrochemical industrial complex in Thailand assessed by the lichen Parmotrema tinctorum (Despr. ex Nyl.) Hale, Environ. Sci. Pollut. Res. 24 (2017) 12393–12404. doi:10.1007/s11356-017-8893-9.

[79] P. Bedregal, P. Mendoza, M. Ubillús, B. Torres, J. Hurtado, R.E. Ily Maza, El uso de Usnea sp . y Tillandsia capillaris, como biomonitores de la contaminacion ambiental en la ciudad de Lima, Peru, Rev. Soc. Quim. Del Peru. 75 (2009) 479–487. http://www.scielo.org.pe/pdf/rsqp/v75n4/a10v75n4.pdf.

[80] A. Haller, Urbanites, smallholders, and the quest for empathy: Prospects for collaborative planning in the periurban Shullcas Valley, Peru, Landsc. Urban Plan. 165 (2017) 220–230. doi:10.1016/j.landurbplan.2016.04.015.

[81] I.T. Jolliffe, J. Cadima, J. Cadima, Principal component analysis : a review and recent developments, Philos. Trans. (2016).

[82] S.G. Bekir Onursal, Vehicular Air Pollution: Experiences from Seven Latin American Urban Centers, 1997. https://books.google.com.br/books?id=XSUS234DhEsC&dq=Leaded+gasoline+was+banned+in+Peru%3F&hl=pt-BR&source=gbs_navlinks_s.

[83] A. Sanchez-Chardi, Biomonitoring potential of five sympatric Tillandsia species for evaluating urban metal pollution (Cd, Hg and Pb), Atmos. Environ. 131 (2016) 352–359. doi:10.1016/j.atmosenv.2016.02.013.

[84] Z. Naderizadeh, H. Khademi, S. Ayoubi, Biomonitoring of atmospheric heavy metals pollution using dust deposited on date palm leaves in southwestern Iran, Atmosfera. 29 (2016) 141–155.

doi:10.20937/ATM.2016.29.02.04.

[85] F.G. Fujiwara, D.R. Gómez, L. Dawidowski, P. Perelman, A. Faggi, Metals associated with airborne particulate matter in road dust and tree bark collected in a megacity (Buenos Aires, Argentina), Ecol. Indic. 11 (2011) 240–247. doi:10.1016/j.ecolind.2010.04.007.

[86] X. Querol, a. Alastuey, T. Moreno, M.M. Viana, S. Castillo, J. Pey, S. Rodríguez, B. Artiñano, P. Salvador, M. Sánchez, S. Garcia Dos Santos, M.D. Herce Garraleta, R. Fernandez-Patier, S. Moreno-Grau, L. Negral, M.C. Minguillón, E. Monfort, M.J. Sanz, R. Palomo-Marín, E. Pinilla-Gil, E. Cuevas, J. de la Rosa, a. Sánchez de la Campa, Spatial and temporal variations in airborne particulate matter (PM10 and PM2.5) across Spain 1999-2005, Atmos. Environ. 42 (2008) 3964–3979. doi:10.1016/j.atmosenv.2006.10.071.

[87] M.L.D.P. Godoy, J.M. Godoy, L.A. Roldão, D.S. Soluri, R. a. Donagemma, Coarse and fine aerosol source apportionment in Rio de Janeiro, Brazil, Atmos. Environ. 43 (2009) 2366–2374. doi:10.1016/j.atmosenv.2008.12.046.

[88] F. Guéguen, P. Stille, V. Dietze, R. Gieré, Chemical and isotopic properties and origin of coarse airborne particles collected by passive samplers in industrial, urban, and rural environments, Atmos. Environ. 62 (2012) 631–645. doi:10.1016/j.atmosenv.2012.08.044.

[89] E. Rizzio, L. Bergamaschi, M.. Valcuvia, a Profumo, M. Gallorini, Trace elements determination in lichens and in the airborne particulate matter for the evaluation of the atmospheric pollution in a region of northern Italy, Environ. Int. 26 (2001) 543–549. doi:10.1016/S0160-4120(01)00037-X.

[90] N. Schleicher, S. Norra, Y. Chen, F. Chai, S. Wang, Efficiency of mitigation measures to reduce particulate air pollution-A case study during the Olympic Summer Games 2008 in Beijing, China, Sci. Total Environ. 427–428 (2012) 146–158. doi:10.1016/j.scitotenv.2012.04.004.

[91] A. Aslan, G. Budak, A. Karabulut, The amounts Fe, Ba, Sr, K, Ca and Ti in some lichens growing in Erzurum province (Turkey), J. Quant. Spectrosc. Radiat. Transf. 88 (2004) 423–431. doi:10.1016/j.jqsrt.2004.04.015.

[92] WHO, Cadmium, in: Air Qual. Guidel., Denmark, 2000: pp. 1–11. doi:10.1016/S0959-6380(00)80017-3.

[93] T.L. Roberts, Cadmium and Phosphorous Fertilizers : The Issues and the Science, Procedia Eng. 83 (2014) 52–59. doi:10.1016/j.proeng.2014.09.012.

[94] C. Hazotte, N. Leclerc, E. Meux, F. Lapicque, Direct recovery of cadmium and nickel from Ni-Cd spent batteries by electroassisted leaching and electrodeposition in a single-cell process, Hydrometallurgy. 162 (2016) 94–103. doi:10.1016/j.hydromet.2016.02.019.

[95] Y. Zhou, L. Niu, K. Liu, S. Yin, W. Liu, Arsenic in agricultural soils across China : Distribution pattern, accumulation trend, influencing factors, and risk assessment, Sci. Total Environ. 616–617 (2018) 156–163. doi:10.1016/j.scitotenv.2017.10.232.

[96] B. Gamboa-Loira, M.E. Cebrián, F. Franco-marina, L. López-carrillo, Arsenic metabolism and cancer risk : A meta-analysis, Environ. Res. 156 (2017) 551–558. doi:10.1016/j.envres.2017.04.016.

[97] E. Jablonska, K. Socha, E. Reszka, E. Wieczorek, J. Skokowski, L. Kalinowski, W. Fendler, B. Seroczynska, M. Wozniak, M.H. Borawska, W. Wasowicz, Cadmium, arsenic, selenium and iron – Implications for tumor progression in breast cancer, Environ. Toxicol. Pharmacol. 53 (2017) 151–157. doi:10.1016/j.etap.2017.05.014.

[98] WHO, Manganese, in: Air Qual. Guidel., 2001: pp. 1–13.

[99] R. Figueira, C. Sérgio, a. J. Sousa, Distribution of trace metals in moss biomonitors and assessment of contamination sources in Portugal, Environ. Pollut. 118 (2002) 153–163. doi:10.1016/S0269-7491(01)00203-2.

[100] E. Belon, M. Boisson, I.Z. Deportes, T.K. Eglin, I. Feix, A.O. Bispo, L. Galsomies, S. Leblond, C.R. Guellier, An inventory of trace elements inputs to French agricultural soils, Sci. Total Environ. 439 (2012) 87–95. doi:10.1016/j.scitotenv.2012.09.011.

[101] L. Luo, Y. Ma, S. Zhang, D. Wei, Y. Zhu, An inventory of trace element inputs to agricultural soils in China, J. Environ. Manage. 90 (2009) 2524–2530. doi:10.1016/j.jenvman.2009.01.011.

[102] Y. Montoro, R. Moreno, L. Gomero, M. Reyes, Características De Uso De Plaguicidas Químicos Y Riesgos Para La Salud En Agricultores De La Sierra Central Del Perú Characteristics of the Use of Chemical Pesticides and Health Risks in Farmers in the Central Highlands of Peru, Scielo. 4

(2009) 26–30. doi:10.17843/RPMESP.2009.264.1409.

[103] M. Mwinyihija, Main Pollutants and Environmental Impacts of the Tanning Industry, in: Ecotoxicological Diagnosis Tann. Ind., Springer Science, Aberdeen, 2010. doi:10.1007/978-1-4419-6266-9.

[104] N.C. Mondal, V.K. Saxena, V.S. Singh, Assessment of groundwater pollution due to tannery industries in and around Dindigul, Tamilnadu, India, Environ. Geol. 48 (2005) 149–157. doi:10.1007/s00254-005-1244-z.

[105] L. Sverre, M. Acosta, Chromium, in: Handb. Toxicol. Met., 3rd ed., Umea, 2007: p. 1024. http.//books.elsevier.com.

[106] M.I.C. Monteiro, I.C.S. Fraga, A. V Yallouz, N.M.M. de Oliveira, S.H. Ribeiro, Determination of total chromium traces in tannery effluents by electrothermal atomic absorption spectrometry, flame atomic absorption spectrometry and UV-visible spectrophotometric methods, Talanta. 58 (2002) 629–633.

[107] J. Liang, H.L. Fang, T.L. Zhang, X.X. Wang, Y.D. Liu, Heavy metal in leaves of twelve plant species from seven different areas in Shanghai, China, Urban For. Urban Green. 27 (2017) 390–398. doi:10.1016/j.ufug.2017.03.006.

[108] K. Tarricone, G. Wagner, R. Klein, Toward standardization of sample collection and preservation for the quality of results in biomonitoring with trees - A critical review, Ecol. Indic. 57 (2015) 341–359. doi:10.1016/j.ecolind.2015.05.012.

[109] R. Filipović-trajković, Z.S. Ilić, L. Šunić, S. Andjelković, The potential of different plant species for heavy metals accumulation and distribution, J. Food, Agric. Environ. (2012) 959–964.

[110] I. V. Deljanin, M.N. Tomašević, M.P.A. Urošević, D.Z. Antanasijević, A. a. Perić-Grujić, M. Ristić, Lead isotopic composition in tree leaves as tracers of lead in an urban environment, Ecol. Indic. 45 (2014) 640–647. doi:10.1016/j.ecolind.2014.05.027.

[111] T. Bhattacharya, S. Chakraborty, D. Tuteja, M. Patel, Zinc and Chromium Load in Road Dust, Suspended Particulate Matter and Foliar Dust Deposits of Anand City, Gujarat, Open J. Met. 3 (2013) 42–50. doi:10.4236/ojmetal.2013.32A1006.

[112] E. Simon, E. Baranyai, M. Braun, C. Cserháti, I. Fábián, B. Tóthmérész,

Elemental concentrations in deposited dust on leaves along an urbanization gradient, Sci. Total Environ. 490 (2014) 514–520. doi:10.1016/j.scitotenv.2014.05.028.

[113] G. Matin, N. Kargar, H.B. Buyukisik, Bio-monitoring of cadmium, lead, arsenic and mercury in industrial districts of Izmir, Turkey by using honey bees, propolis and pine tree leaves, Ecol. Eng. 90 (2016) 331–335. doi:10.1016/j.ecoleng.2016.01.035.

[114] J. Shi, G. Zhang, H. An, W. Yin, X. Xia, Quantifying the particulate matter accumulation on leaf surfaces of urban plants in Beijing, China, Atmos. Pollut. Res. 8 (2017) 836–842. doi:10.1016/j.apr.2017.01.011.

[115] D.E. Kimbrough, Y. Cohen, A.M. Winer, L. Creelman, C. Mabuni, A critical assessment of chromium in the environment, Crit. Rev. Environ. Sci. Technol. 29 (1999) 1–46. doi:10.1080/10643389991259164.

[116] World Health Organization, Chapter 6.4 Chromium, Air Qual. Guidel. - Second Ed. 3 (2000) 1–14. doi:10.1016/S0959-6380(00)80018-5.

[117] C.R. DE BASTOS, Agricultores familiares pluriativos na regiao do vale do Jaguari/RS: Um estudo em Nova Esperanca do Sul, Universidade Federal do Rio Grande do Sul, 2016. http://www.lume.ufrgs.br/handle/10183/149305.

[118] B.F. Giannetti, S.H. Bonilla, C.M.V.B. Almeida, Developing eco-technologies: A possibility to minimize environmental impact in Southern Brazil, J. Clean. Prod. 12 (2004) 361–368. doi:10.1016/S0959-6526(03)00033-7.

[119] K. Joseph, N. Nithya, Material flows in the life cycle of leather, J. Clean. Prod. 17 (2009) 676–682. doi:10.1016/j.jclepro.2008.11.018.

[120] K. Annan, R. Dickson, I. Nooni, I. Amponsah, The heavy metal contents of some selected medicinal plants sampled from different geographical locations, Pharmacognosy Res. 5 (2013) 103. doi:10.4103/0974-8490.110539.

[121] E. Simon, S. Harangi, E. Baranyai, I. Fábián, B. Tóthmérész, Influence of past industry and urbanization on elemental concentrations in deposited dust and tree leaf tissue, Urban For. Urban Green. 20 (2016) 12–19. doi:10.1016/j.ufug.2016.07.017.

[122] S. Srinivasa Gowd, M. Ramakrishna Reddy, P.K. Govil, Assessment of

heavy metal contamination in soils at Jajmau (Kanpur) and Unnao industrial areas of the Ganga Plain, Uttar Pradesh, India, J. Hazard. Mater. 174 (2010) 113–121. doi:10.1016/j.jhazmat.2009.09.024.

[123] S.A. Febriana, F. Jungbauer, H. Soebono, P.J. Coenraads, Inventory of the chemicals and the exposure of the workers' skin to these at two leather factories in Indonesia, Int. Arch. Occup. Environ. Health. 85 (2012) 517–526. doi:10.1007/s00420-011-0700-1.

[124] H.M. Júnior, J. da Silva, A. Arenzon, C.S. Portela, I.C.F. de S. Ferreira, J.A.P. Henriques, Evaluation of genotoxicity and toxicity of water and sediment samples from a Brazilian stream influenced by tannery industries, Chemosphere. 67 (2007) 1211–1217. doi:10.1016/j.chemosphere.2006.10.048.

[125] S.C. Wilson, P. V. Lockwood, P.M. Ashley, M. Tighe, The chemistry and behaviour of antimony in the soil environment with comparisons to arsenic: A critical review, Environ. Pollut. 158 (2010) 1169–1181. doi:10.1016/j.envpol.2009.10.045.

[126] S. Morais, F. Garcia, M. de L. Pereira, Heavy Metals and Human Health, in: Environ. Heal. - Emerg. Issues Pract., 2012: pp. 227–246. doi:10.5772/711.

[127] U.E. Bollmann, C. Tang, E. Eriksson, K. Jönsson, J. Vollertsen, K. Bester, Biocides in urban wastewater treatment plant influent at dry and wet weather: Concentrations, mass flows and possible sources, Water Res. 60 (2014) 64–74. doi:10.1016/j.watres.2014.04.014.

[128] S. Bolan, A. Kunhikrishnan, S. Chowdhury, B. Seshadri, R. Naidu, Y.S. Ok, Comparative analysis of speciation and bioaccessibility of arsenic in rice grains and complementary medicines, Chemosphere. 182 (2017) 433–440. doi:10.1016/j.chemosphere.2017.04.126.

[129] Z. Kertész, Z. Szoboszlai, A. Angyal, E. Dobos, I. Borbély-Kiss, Identification and characterization of fine and coarse particulate matter sources in a middle-European urban environment, Nucl. Instruments Methods Phys. Res. Sect. B Beam Interact. with Mater. Atoms. 268 (2010) 1924–1928. doi:10.1016/j.nimb.2010.02.103.

[130] K. Akiyama, Gas chromatographic analysis and aerosol mass spectrometer measurement of diesel exhaust particles composition, Talanta. 70 (2006)

178–181. doi:10.1016/j.talanta.2006.02.044.

[131] M. Matti Maricq, Chemical characterization of particulate emissions from diesel engines: A review, J. Aerosol Sci. 38 (2007) 1079–1118. doi:10.1016/j.jaerosci.2007.08.001.

[132] F. Amato, M. Pandolfi, M. Viana, X. Querol, A. Alastuey, T. Moreno, Spatial and chemical patterns of PM10 in road dust deposited in urban environment, Atmos. Environ. 43 (2009) 1650–1659. doi:10.1016/j.atmosenv.2008.12.009.

[133] F. Fujiwara, R.J. Rebagliati, J. Marrero, D. Gómez, P. Smichowski, Antimony as a traffic-related element in size-fractionated road dust samples collected in Buenos Aires, Microchem. J. 97 (2011) 62–67. doi:10.1016/j.microc.2010.05.006.

[134] D. Sanchez-Rodas, L. Alsioufi, A.M. Sanchez de la Campa, Y. Gonzalez-Castanedo, Antimony speciation as geochemical tracer for anthropogenic emissions of atmospheric particulate matter, J. Hazard. Mater. 324 (2017) 213–220. doi:10.1016/j.jhazmat.2016.10.051.

[135] X. Hu, M. He, S. Li, Antimony leaching release from brake pads: Effect of pH, temperature and organic acids, J. Environ. Sci. (China). 29 (2015) 11–17. doi:10.1016/j.jes.2014.08.020.

[136] R.G. Cooper, A.P. Harrison, The exposure to and health effects of antimony - review article, Indian J. Occup. Environ. Med. 13 (2009) 3–10. doi:10.4103/0019-5278.50716.

[137] A. Milan, R. Ho, Livelihood and migration patterns at different altitudes in the Central Highlands of Peru, Clim. Dev. 6 (2014) 69–76. doi:10.1080/17565529.2013.826127.

[138] E.D. Wannaz, H.A. Carreras, C.A. Pérez, M.L. Pignata, Assessment of heavy metal accumulation in two species of Tillandsia in relation to atmospheric emission sources in Argentina, Sci. Total Environ. 361 (2006) 267–278. doi:10.1016/j.scitotenv.2005.11.005.

[139] B.A. Markert, A.M. Breure, H.G. Zechmeister, Bioindicators & Biomonitors: Principles, concepts and applications, in: Trace Met. Other Contam. Environ., Oxford, 2003: p. 997. https://books.google.com.br/books?id=g8bXmuUBP2kC&hl=pt-BR&source=gbs_navlinks_s.

[140] E.D. Wannaz, G.A. Abril, J.H. Rodriguez, M.L. Pignata, Assessment of polycyclic aromatic hydrocarbons in industrial and urban areas using passive air samplers and leaves of Tillandsia capillaris, J. Environ. Chem. Eng. 1 (2013) 1028–1035. doi:10.1016/j.jece.2013.08.012.

[141] S. Goix, E. Resongles, D. Point, P. Oliva, J.L. Duprey, E. de la Galvez, L. Ugarte, C. Huayta, J. Prunier, C. Zouiten, J. Gardon, Transplantation of epiphytic bioaccumulators (Tillandsia capillaris) for high spatial resolution biomonitoring of trace elements and point sources deconvolution in a complex mining/smelting urban context, Atmos. Environ. 80 (2013) 330–341. doi:10.1016/j.atmosenv.2013.08.011.

[142] E. Schreck, G. Sarret, P. Oliva, A. Calas, S. Sobanska, S. Guédron, F. Barraza, D. Point, C. Huayta, R.M. Couture, J. Prunier, M. Henry, D. Tisserand, S. Goix, J. Chincheros, G. Uzu, Is Tillandsia capillaris an efficient bioindicator of atmospheric metal and metalloid deposition? Insights from five months of monitoring in an urban mining area, Ecol. Indic. 67 (2016) 227–237. doi:10.1016/j.ecolind.2016.02.027.

[143] M.L. Pignata, G.L. Gudio, E.D. Wannaz, R.R. Plá, C.M. González, H.A. Carreras, L. Orellana, Atmospheric quality and distribution of heavy metals in Argentina employing Tillandsia capillaris as a biomonitor, Environ. Pollut. 120 (2002) 59–68. doi:10.1016/S0269-7491(02)00128-8.

[144] G.A. Abril, E.D. Wannaz, A.C. Mateos, R. Invernizzi, R.R. Plá, M.L. Pignata, Characterization of atmospheric emission sources of heavy metals and trace elements through a local-scale monitoring network using T. capillaris, Ecol. Indic. 40 (2014) 153–161. doi:10.1016/j.ecolind.2014.01.008.

[145] J.H. Rodriguez, S.B. Weller, E.D. Wannaz, A. Klumpp, M.L. Pignata, Air quality biomonitoring in agricultural areas nearby to urban and industrial emission sources in Córdoba province, Argentina, employing the bioindicator Tillandsia capillaris, Ecol. Indic. 11 (2011) 1673–1680. doi:10.1016/j.ecolind.2011.04.015.

[146] A.C. Mateos, A.C. Amarillo, H.A. Carreras, C.M. González, Land use and air quality in urban environments: Human health risk assessment due to inhalation of airborne particles, Environ. Res. 161 (2018) 370–380. doi:10.1016/j.envres.2017.11.035.

[147] J.H. Rodriguez, M.L. Pignata, A. Fangmeier, A. Klumpp, Accumulation of polycyclic aromatic hydrocarbons and trace elements in the bioindicator plants Tillandsia capillaris and Lolium multiflorum exposed at PM10monitoring stations in Stuttgart (Germany), Chemosphere. 80 (2010) 208–215. doi:10.1016/j.chemosphere.2010.04.042.

[148] A.B. Ferreira, J.O. Santos, S.O. Souza, W.N.S. Júnior, J. do P.H. Alves, Use of passive biomonitoring to evaluate the environmental impact of emissions from cement industries in Sergipe State, northeast Brazil, Microchem. J. 103 (2012) 15–20. doi:10.1016/j.microc.2011.12.008.

[149] G. Abril, E.D. Wannaz, A.C. Mateos, M.L. Pignata, Biomonitoring of airborne particulate matter emitted from a cement plant and comparison with dispersion modelling results, Atmos. Environ. 82 (2014) 154–163. doi:10.1016/j.atmosenv.2013.10.020.

[150] M. Yaman, Comprehensive comparison of trace metal concentrations in inhaled air samples, World's Larg. Sci. Technol. Med. 13 (2006) 2513–2525. doi:10.2174/092986706778201620.

[151] E. Pellegrini, G. Lorenzini, S. Loppi, C. Nali, Evaluation of the suitability of Tillandsia usneoides (L.) L. as biomonitor of airborne elements in an urban area of Italy, Mediterranean basin, Atmos. Pollut. Res. 5 (2014) 226–235. doi:10.5094/APR.2014.028.

[152] D.-H. Koh, T.-W. Kim, S.H. Jang, H.-W. Ryu, Cancer Mortality and Incidence in Cement Industry Workers in Korea, Saf. Health Work. 2 (2011) 243–249. doi:10.5491/SHAW.2011.2.3.243.

[153] B. Krejcirikova, J. Kolarik, P. Wargocki, The effects of cement-based and cement-ash-based mortar slabs on indoor air quality, Build. Environ. 135 (2018) 213–223. doi:10.1016/j.buildenv.2018.03.011.

[154] J. Zuo, R. Rameezdeen, M. Hagger, Z. Zhou, Z. Ding, Dust pollution control on construction sites : Awareness and self-responsibility of managers, J. Clean. Prod. 166 (2017) 312–320. doi:10.1016/j.jclepro.2017.08.027.

[155] Q. Chen, Q. Zhang, C. Qi, A. Fourie, C. Xiao, Recycling phosphogypsum and construction demolition waste for cemented paste backfill and its environmental impact, J. Clean. Prod. 186 (2018) 418–429. doi:10.1016/j.jclepro.2018.03.131.

[156] W. Chen, J. Hong, C. Xu, Pollutants generated by cement production in China, their impacts, and the potential for environmental improvement, 103 (2015) 61–69. doi:10.1016/j.jclepro.2014.04.048.

[157] R. Lambert, C. Grant, S. Sauvé, Cadmium and zinc in soil solution extracts following the application of phosphate fertilizers, 378 (2007) 293–305. doi:10.1016/j.scitotenv.2007.02.008.

[158] A. Kabata-Pendias, Trace Elements in Soils and Plants, 4th ed., CRC Press, New York, 2010. doi:10.1201/b10158.

[159] S. Kratz, J. Schick, E. Schnug, Trace elements in rock phosphates and P containing mineral and organo-mineral fertilizers sold in Germany, Sci. Total Environ. 542 (2016) 1013–1019. doi:10.1016/j.scitotenv.2015.08.046.

[160] A.L. Wani, A. Ara, J.A. Usmani, Lead toxicity : a review, 8 (2015) 55–64. doi:10.1515/intox-2015-0009.

[161] M.T. De la Cruz, F. Laborda, M.S. Callén, J.M. López, A.M. Mastral, Study of Pb sources by Pb isotope ratios in the airborne PM(10) of Zaragoza, Spain., J. Environ. Monit. 11 (2009) 2052–7. doi:10.1039/b912274e.

[162] F.M. Gordon McGranahan, Air Pollution and Health in Rapidly Developing Countries, London, UK, 2012.

[163] J. de P. Ribeiro, A.C. Kalb, P.P. Campos, A.R.H.D. La Cruz, P.E. Martinez, A. Gioda, M.M. de Souza, C.R. Gioda, Toxicological effects of particulate matter (PM2.5) on rats: Bioaccumulation, antioxidant alterations, lipid damage, and ABC transporter activity, Chemosphere. 163 (2016) 569–577. doi:10.1016/j.chemosphere.2016.07.094.

[164] S. Giordano, P. Adamo, V. Spagnuolo, M. Tretiach, R. Bargagli, Accumulation of airborne trace elements in mosses, lichens and synthetic materials exposed at urban monitoring stations: Towards a harmonisation of the moss-bag technique, Chemosphere. 90 (2013) 292–299. doi:10.1016/j.chemosphere.2012.07.006.

[165] R. Zangrando, E. Barbaro, T. Kirchgeorg, M. Vecchiato, E. Scalabrin, M. Radaelli, D. ??or??evi??, C. Barbante, A. Gambaro, Five primary sources of organic aerosols in the urban atmosphere of Belgrade (Serbia), Sci. Total Environ. 571 (2016) 1441–1453. doi:10.1016/j.scitotenv.2016.06.188.

[166] A. Kfoury, F. Ledoux, C. Roche, G. Delmaire, G. Roussel, D. Courcot, ScienceDirect PM 2 . 5 source apportionment in a French urban coastal site under steelworks emission influences using constrained non-negative matrix factorization receptor model, JES. 40 (2016) 114–128. doi:10.1016/j.jes.2015.10.025.

[167] R. Bargagli, F.F. Monaci, F. Borghini, F.F. Bravi, C. Agnorelli, Mosses and lichens as biomonitors of trace metals. A comparison study on Hypnum cupressiforme and Parmelia caperata in a former mining district in Italy, Environ. Pollut. 116 (2002) 279–287. doi:10.1016/S0269-7491(01)00125-7.

[168] USEPA, Sampling of ambient air for total suspended particulate matter (SPM) and PM10 using high volume (HV) sampler, Environ. Prot. (1999).

[169] A.B. Rendle, The Classification of Flowering Plants, Volume 1, CUP Archive, Cambridge UK, 1971.

[170] K. Isaac-Olivé, C. Solís, M. a Martínez-Carrillo, E. Andrade, C. López, L.C. Longoria, C. a Lucho-Constantino, R.I. Beltrán-Hernández, Tillandsia usneoides L, a biomonitor in the determination of Ce, La and Sm by neutron activation analysis in an industrial corridor in Central Mexico., Appl. Radiat. Isot. 70 (2012) 589–94. doi:10.1016/j.apradiso.2012.01.007.

[171] G.J. Husk, J.F. Weishampel, W.H. Schlesinger, Mineral dynamics in Spanish moss, Tillandsia usneoides L. (Bromeliaceae), from Central Florida, USA, Sci. Total Environ. 321 (2004) 165–172. doi:10.1016/j.scitotenv.2003.09.001.

[172] K. Techato, A. Salaeh, N.C. van Beem, Use of Atmospheric Epiphyte Tillandsia usneoides (Bromeliaceae) as Biomonitor, APCBEE Procedia. 10 (2014) 49–53. doi:10.1016/j.apcbee.2014.10.014.

[173] E. Cortés, Investigation of air pollution in Chile using biomonitors, J. Radioanal. Nucl. Chem. 262 (2004) 269–276. doi:10.1023/B:JRNC.0000040885.09041.2e.

[174] A.G.. Castañeda Miranda, M.A.E.. Chaparro, M.A.E.. c Chaparro, H.N.. Böhnel, Magnetic properties of Tillandsia recurvata L. and its use for biomonitoring a Mexican metropolitan area, Ecol. Indic. 60 (2016) 125–136. doi:10.1016/j.ecolind.2015.06.025.

[175] N.A. Vianna, D. Gonçalves, F. Brandão, R.P. de Barros, G.M.A. Filho,

R.O. Meire, J.P.M. Torres, O. Malm, A.D.O. Júnior, L.R. Andrade, Assessment of heavy metals in the particulate matter of two Brazilian metropolitan areas by using Tillandsia usneoides as atmospheric biomonitor, Environ. Sci. Pollut. Res. 18 (2011) 416–427. doi:10.1007/s11356-010-0387-y.

[176] F. Guéguen, P. Stille, M. Lahd Geagea, R. Boutin, Atmospheric pollution in an urban environment by tree bark biomonitoring--part I: trace element analysis., Chemosphere. 86 (2012) 1013–9. doi:10.1016/j.chemosphere.2011.11.040.

[177] T. Moreno, C. Reche, I. Rivas, M. Cruz Minguillón, V. Martins, C. Vargas, G. Buonanno, J. Parga, M. Pandolfi, M. Brines, M. Ealo, A. Sofia Fonseca, F. Amato, G. Sosa, M. Capdevila, E. de Miguel, X. Querol, W. Gibbons, Urban air quality comparison for bus, tram, subway and pedestrian commutes in Barcelona, Environ. Res. 142 (2015) 495–510. doi:10.1016/j.envres.2015.07.022.

[178] G.J. Allan, P. Lecca, K. Swales, The impacts of temporary but anticipated tourism spending: An application to the Glasgow 2014 Commonwealth Games, Tour. Manag. 59 (2017) 325–337. doi:10.1016/j.tourman.2016.08.014.

[179] I. Pappalepore, M.B. Duignan, The London 2012 cultural programme: A consideration of Olympic impacts and legacies for small creative organisations in east London, Tour. Manag. 54 (2016) 344–355. doi:10.1016/j.tourman.2015.11.015.

[180] K. Swart, R. George, J. Cassar, C. Sneyd, The 2014 FIFA World Cup???: Tourists' satisfaction levels and likelihood of repeat visitation to Rio de Janeiro, J. Destin. Mark. Manag. (2016) 1–12. doi:10.1016/j.jdmm.2017.01.001.

[181] E. Kasimati, P. Dawson, Assessing the impact of the 2004 Olympic Games on the Greek economy: A small macroeconometric model, Econ. Model. 26 (2009) 139–146. doi:10.1016/j.econmod.2008.06.006.

[182] L. Huang, Research on effect of beijing post-olympic sports industry to China's economic development, Energy Procedia. 5 (2011) 2097–2102. doi:10.1016/j.egypro.2011.03.362.

[183] L.A. Lindau, G. Petzhold, V.B. Tavares, D. Facchini, Mega events and the

transformation of Rio de Janeiro into a mass-transit city, Res. Transp. Econ. 59 (2016) 196–203. doi:10.1016/j.retrec.2016.07.024.

[184] T.R. de Menezes, J.F. de Souza, Transportation and Urban Mobility in Mega-events: The Case of Recife, Procedia - Soc. Behav. Sci. 162 (2014) 218–227. doi:10.1016/j.sbspro.2014.12.202.

[185] M. Wang, H.X.H. Bao, Mega-event effects on the housing market: Evidence from the Beijing 2008 Olympic Games, Cities. (2017). doi:10.1016/j.cities.2017.07.014.

[186] W. Kim, H.M. Jun, M. Walker, D. Drane, Evaluating the perceived social impacts of hosting large-scale sport tourism events: SCALE development and validation, Tour. Manag. 48 (2015) 21–32. doi:10.1016/j.tourman.2014.10.015.

[187] G. Waitt, Social impacts of the Sydney Olympics, Ann. Tour. Res. 30 (2003) 194–215. doi:10.1016/S0160-7383(02)00050-6.

[188] C. Deccio, S. Baloglu, Nonhost Community Resident Reactions to the 2002 Winter Olympics: The Spillover Impacts, J. Travel Res. 41 (2002).

[189] H.J. Kim, D. Gursoy, S.B. Lee, The impact of the 2002 World Cup on South Korea: Comparisons of pre- and post-games, Tour. Manag. 27 (2006) 86–96. doi:10.1016/j.tourman.2004.07.010.

[190] D.G. Streets, J.S. Fu, C.J. Jang, J. Hao, K. He, X. Tang, Y. Zhang, Z. Wang, Z. Li, Q. Zhang, L. Wang, B. Wang, C. Yu, Air quality during the 2008 Beijing Olympic Games, Atmos. Environ. 41 (2007) 480–492. doi:10.1016/j.atmosenv.2006.08.046.

[191] J. Li, M. Hong, X. Yin, J. Liu, Effects of the accumulation of the rare earth elements on soil macrofauna community, J. Rare Earths. 28 (2010) 957–964. doi:10.1016/S1002-0721(09)60233-7.

[192] Y. Wang, J. Hao, M.B. McElroy, J.W. Munger, H. Ma, D. Chen, C.P. Nielsen, Ozone air quality during the 2008 Beijing Olympics – effectiveness of emission restrictions, Atmos. Chem. Phys. Discuss. 9 (2009) 9927–9959. doi:10.5194/acpd-9-9927-2009.

[193] S. Guo, M. Hu, Q. Guo, X. Zhang, J.J. Schauer, R. Zhang, Quantitative evaluation of emission controls on primary and secondary organic aerosol sources during Beijing 2008 Olympics, Atmos. Chem. Phys. 13 (2013) 8303–8314. doi:10.5194/acp-13-8303-2013.

[194] S. Wang, J. Gao, Y. Zhang, J. Zhang, F. Cha, T. Wang, C. Ren, W. Wang, Impact of emission control on regional air quality: An observational study of air pollutants before, during and after the Beijing Olympic Games, J. Environ. Sci. 26 (2014) 175–180. doi:10.1016/S1001-0742(13)60395-2.

[195] X. Li, L. Wang, Y. Wang, T. Wen, Y. Yang, Y. Zhao, Y. Wang, Chemical composition and size distribution of airborne particulate matters in Beijing during the 2008 Olympics, Atmos. Environ. 50 (2012) 278–286. doi:10.1016/j.atmosenv.2011.12.021.

[196] W. xing Wang, F. he Chai, K. Zhang, S. lan Wang, Y. zhen Chen, X. zhong Wang, Y. qin Yang, Study on ambient air quality in beijing for the summer 2008 olympic games, Air Qual. Atmos. Heal. 1 (2008) 31–36. doi:10.1007/s11869-008-0003-1.

[197] Y. Li, W. Wang, H. Kan, X. Xu, B. Chen, Air quality and outpatient visits for asthma in adults during the 2008 Summer Olympic Games in Beijing, Sci. Total Environ. 408 (2010) 1226–1227. doi:10.1016/j.scitotenv.2009.11.035.

[198] H. Lin, Y. Zhang, T. Liu, J. Xiao, Y. Xu, X. Xu, Z. Qian, S. Tong, Y. Luo, W. Zeng, W. Ma, Mortality reduction following the air pollution control measures during the 2010 asian games, Atmos. Environ. 91 (2014) 24–31. doi:10.1016/j.atmosenv.2014.03.051.

[199] G. He, M. Fan, M. Zhou, The effect of air pollution on mortality in China: Evidence from the 2008 Beijing Olympic Games, J. Environ. Econ. Manage. 79 (2016) 18–39. doi:10.1016/j.jeem.2016.04.004.

[200] M. of London, The emissions and air quality impacts of the 2012 Olympic Route Network and related traffic management arrangements, Transp. London. (2012) 29.

[201] M.L. Godoy, A. Almeida, G. Tonietto, J.M. Godoy, Fine and Coarse Aerosol at Rio de Janeiro prior to the Olympic Games: Chemical Composition and Source Apportionment, J. Braz. Chem. Soc. 41 (2017) 1–10. doi:10.21577/0103-5053.20170162.

[202] C.Y. dos S. Siqueira, M.V.P. Lemos, B.C. da C. Araujo, R. da R.P.E. de Oliveira, R.A. da S. San Gil, F.R. de Aquino Neto, Atmospheric distribution of organic compounds from urban areas near Olympic games sites in Rio de Janeiro, Brazil, Microchem. J. 133 (2017) 638–644.

doi:10.1016/j.microc.2017.04.027.

[203] A. York, M. Rouleau, Can traffic management strategies improve urban air quality? A review of the evidence, J. Transp. Heal. (2017) 0–1. doi:10.1016/j.jth.2017.08.001.

[204] T. Wang, S. Xie, Assessment of traffic-related air pollution in the urban streets before and during the 2008 Beijing Olympic Games traffic control period, Atmos. Environ. 43 (2009) 5682–5690. doi:10.1016/j.atmosenv.2009.07.034.

[205] CET-Rio, Gestão do tráfego nos Jogos Olímpicos RIO 2016, Rio de Janeiro, 2016. http://www.rio.rj.gov.br/dlstatic/10112/6594316/4177742/BoletimtecnicoOlimpiadaeParalimpiada.pdf.

[206] M. Zeri, J.F. Oliveira-Junior, G.B. Lyra, Spatiotemporal analysis of particulate matter, sulfur dioxide and carbon monoxide concentrations over the city of Rio de Janeiro, Brazil, Meteorol. Atmos. Phys. 113 (2011) 139–152. doi:10.1007/s00703-011-0153-9.

[207] C. Vassilakos, D. Saraga, T. Maggos, J. Michopoulos, S. Pateraki, C.G. Helmis, Temporal variations of PM2.5 in the ambient air of a suburban site in Athens, Greece, Sci. Total Environ. 349 (2005) 223–231. doi:10.1016/j.scitotenv.2005.01.012.

[208] C.M. da Silva, L.L. da Silva, S.M. Corrêa, G. Arbilla, A minimum set of ozone precursor volatile organic compounds in an urban environment, Atmos. Pollut. Res. 9 (2018) 369–378. doi:10.1016/j.apr.2017.11.002.

[209] C.G.P. Geraldino, E.M. Martins, C.M. da Silva, G. Arbilla, An Analytical Investigation of Ozone Episodes in Bangu, Rio de Janeiro, Bull. Environ. Contam. Toxicol. 98 (2017) 632–637. doi:10.1007/s00128-017-2041-6.

[210] E.M. Martins, A.C.L. Nunesa, S.M. Corrêa, Understanding ozone concentrations during weekdays and weekends in the urban area of the city of rio de janeiro, J. Braz. Chem. Soc. 26 (2015) 1967–1975. doi:10.5935/0103-5053.20150175.

[211] P.A. Kassomenos, S. Vardoulakis, A. Chaloulakou, A.K. Paschalidou, G. Grivas, R. Borge, J. Lumbreras, Study of PM10 and PM2.5 levels in three European cities: Analysis of intra and inter urban variations, Atmos. Environ. 87 (2014) 153–163. doi:10.1016/j.atmosenv.2014.01.004.

[212] F. Wang, D.S. Chen, S.Y. Cheng, J.B. Li, M.J. Li, Z.H. Ren, Identification of regional atmospheric PM10 transport pathways using HYSPLIT, MM5-CMAQ and synoptic pressure pattern analysis, Environ. Model. Softw. 25 (2010) 927–934. doi:10.1016/j.envsoft.2010.02.004.

[213] A. Gioda, R.C.G. Oliveira, C.L. Cunha, S.M. Corrêa, Understanding ozone formation at two islands of Rio de Janeiro, Brazil, Atmos. Pollut. Res. (2017) 0–1. doi:10.1016/j.apr.2017.10.003.

[214] A. Afzali, M. Rashid, B. Sabariah, M. Ramli, PM10 pollution: Its prediction and meteorological influence in PasirGudang, Johor, IOP Conf. Ser. Earth Environ. Sci. 18 (2014) 4–10. doi:10.1088/1755-1315/18/1/012100.

[215] B. Meryem, H. JI, Y. GAO, H. DING, C. LI, Distribution of rare earth elements in agricultural soil and human body (scalp hair and urine) near smelting and mining areas of Hezhang, China, J. Rare Earths. 34 (2016) 1156–1167. doi:10.1016/S1002-0721(16)60148-5.

[216] S. Massari, M. Ruberti, Rare earth elements as critical raw materials: Focus on international markets and future strategies, Resour. Policy. 38 (2013) 36–43. doi:10.1016/j.resourpol.2012.07.001.

[217] J.R. Riba, C. López-Torres, L. Romeral, A. Garcia, Rare-earth-free propulsion motors for electric vehicles: A technology review, Renew. Sustain. Energy Rev. 57 (2016) 367–379. doi:10.1016/j.rser.2015.12.121.

[218] G. Pagano, M. Guida, F. Tommasi, R. Oral, Health effects and toxicity mechanisms of rare earth elements — Knowledge gaps and research prospects, Ecotoxicol. Environ. Saf. 115 (2015) 40–48. doi:10.1016/j.ecoenv.2015.01.030.

[219] G. Pagano, F. Aliberti, M. Guida, R. Oral, A. Siciliano, M. Trifuoggi, F. Tommasi, Rare earth elements in human and animal health: State of art and research priorities, Environ. Res. 142 (2015) 215–220. doi:10.1016/j.envres.2015.06.039.

[220] C. Zhang, Q. Li, M. Zhang, N. Zhang, M. Li, Effects of rare earth elements on growth and metabolism of medicinal plants, Acta Pharm. Sin. B. 3 (2013) 20–24. doi:10.1016/j.apsb.2012.12.005.

[221] G. Pagano, M. Guida, A. Siciliano, R. Oral, F. Koçbas, A. Palumbo, I. Castellano, O. Migliaccio, P.J. Thomas, M. Trifuoggi, Comparative

toxicities of selected rare earth elements: Sea urchin embryogenesis and fertilization damage with redox and cytogenetic effects, Environ. Res. 147 (2016) 453–460. doi:10.1016/j.envres.2016.02.031.

[222] S.M. Nelms, Handbook of Inductively Coupled Plasma Mass Spectrometry, 1st ed., Blackwell Publishing Ltd., New York, 2009. doi:10.1002/9781444305463.

[223] E. Bulska, B. Danko, R.S. Dybczyński, A. Krata, K. Kulisa, Z. Samczyński, M. Wojciechowski, Inductively coupled plasma mass spectrometry in comparison with neutron activation and ion chromatography with UV/VIS detection for the determination of lanthanides in plant materials., Talanta. 97 (2012) 303–11. doi:10.1016/j.talanta.2012.04.035.

[224] Y. Suzuki, T. Suzuki, N. Furuta, Determination of rare earth elements (REES) in airborne particulate matter (APM) collected in Tokyo, Japan, and a positive anomaly of europium and terbium., Anal. Sci. 26 (2010) 929–35. http://www.ncbi.nlm.nih.gov/pubmed/20834122.

[225] B. Zawisza, K. Pytlakowska, B. Feist, M. Polowniak, A. Kita, R. Sitko, Determination of rare earth elements by spectroscopic techniques: a review, J. Anal. At. Spectrom. 26 (2011) 2373–2390. doi:10.1039/C1JA10140D.

[226] P. Dulski, Interferences of oxide, hydroxide and chloride analyte species in the determination of rare earth elements in geological samples by inductively coupled plasma-mass spectrometry, J. Anal. Chem. 350 (1994) 194–203. doi:10.1007/BF00322470.

[227] K.E. Jarvis, Determination of rare earth elements in geological samples by inductively coupled plasma mass spectrometry, J. Anal. At. Spectrom. 4 (1989) 563. doi:10.1039/ja9890400563.

[228] C.-H. Chung, I. Brenner, C.-F. You, Comparison of microconcentric and membrane-desolvation sample introduction systems for determination of low rare earth element concentrations in surface and subsurface waters using sector field inductively coupled plasma mass spectrometry, Spectrochim. Acta Part B At. Spectrosc. 64 (2009) 849–856. doi:10.1016/j.sab.2009.06.013.

[229] E.H. van Veen, M.T.C. de Loos-Vollebregt, Application of mathematical procedures to background correction and multivariate analysis in

inductively coupled plasma-optical emission spectrometry, Spectrochim. Acta, Part B At. Spectrosc. 53 (1998) 639–669. doi:10.1016/S0584-8547(98)00109-8.

[230] J. Riondato, F. Vanhaecke, L. Moens, R. Dams, Determination of rare earth elements in environmental matrices by sector-field inductively coupled plasma mass spectrometry., Fresenius. J. Anal. Chem. 370 (2001) 544–52. http://www.ncbi.nlm.nih.gov/pubmed/11496985.

[231] D. Dick, A. Wegner, P. Gabrielli, U. Ruth, C. Barbante, M. Kriews, Rare earth elements determined in Antarctic ice by inductively coupled plasma-Time of flight, quadrupole and sector field-mass spectrometry: An inter-comparison study, Anal. Chim. Acta. 621 (2008) 140–147. doi:10.1016/j.aca.2008.05.026.

[232] X. Cao, M. Yin, X. Wang, Elimination of the spectral interference from barium polyatomic ions on rare earth elements in inductively coupled plasma mass spectrometry by AG50W-x8 cation exchange chromatographic separation, Fenxi Huaxue. 29 (2001) 892–893.

[233] Y. Li, W. Guo, Z. Wu, L. Jin, Y. Ke, Q. Guo, S. Hu, Determination of ultra-trace rare earth elements in high-salt groundwater using aerosol dilution inductively coupled plasma-mass spectrometry (ICP-MS) after iron hydroxide co-precipitation, Microchem. J. 126 (2016) 194–199. doi:10.1016/j.microc.2015.12.006.

[234] A. Fisher, D. Kara, Determination of rare earth elements in natural water samples – A review of sample separation, preconcentration and direct methodologies, Anal. Chim. Acta. 935 (2016) 1–29. doi:10.1016/j.aca.2016.05.052.

[235] G. James, D. Witten, T. Hastie, R. Tibshirani, An Introduction to Statistical Learning, 5th ed., Springer New York, New York, NY, 2013. doi:10.1007/978-1-4614-7138-7.

[236] M. Melhem, B. Ananou, M. Ouladsine, J. Pinaton, Regression Methods for Predicting the Product's Quality in the Semiconductor Manufacturing Process, IFAC-PapersOnLine. 49 (2016) 83–88. doi:10.1016/j.ifacol.2016.07.554.

[237] P.K. Hopke, The evolution of chemometrics, Anal. Chim. Acta. 500 (2003) 365–377. doi:10.1016/S0003-2670(03)00944-9.

[238] R. Tibshirani, Regression shrinkage and selection via the lasso: A retrospective, J. R. Stat. Soc. Ser. B Stat. Methodol. 73 (2011) 273–282. doi:10.1111/j.1467-9868.2011.00771.x.

[239] H. Zou, T. Hastie, Regularization and variable selection via the elastic net (vol B 67, pg 301, 2005), J. R. Stat. Soc. Ser. B-Statistical Methodol. 67 (2005) 768. doi:DOI 10.1111/j.1467-9868.2005.00527.x.

[240] T.F. Boucher, M. V. Ozanne, M.L. Carmosino, M.D. Dyar, S. Mahadevan, E.A. Breves, K.H. Lepore, S.M. Clegg, A study of machine learning regression methods for major elemental analysis of rocks using laser-induced breakdown spectroscopy, Spectrochim. Acta - Part B At. Spectrosc. 107 (2015) 1–10. doi:10.1016/j.sab.2015.02.003.

[241] A. Niazi, Spectrophotometric simultaneous determination of uranium and thorium using partial least squares regression and orthogonal signal correction, J. Brazilian Chem. Soc. - JBCS. 17 (2006) 1020–1026.

[242] G.G. Dumancas, S. Ramasahayam, G. Bello, J. Hughes, R. Kramer, Chemometric regression techniques as emerging, powerful tools in genetic association studies, TrAC Trends Anal. Chem. 74 (2015) 79–88. doi:10.1016/j.trac.2015.05.007.

[243] Y.-W. Lin, B.-C. Deng, Q.-S. Xu, Y.-H. Yun, Y.-Z. Liang, The equivalence of partial least squares and principal component regression in the sufficient dimension reduction framework, Chemom. Intell. Lab. Syst. 150 (2016) 58–64. doi:10.1016/j.chemolab.2015.11.003.

[244] B. Hemmateenejad, M. Akhond, F. Samari, A comparative study between PCR and PLS in simultaneous spectrophotometric determination of diphenylamine, aniline, and phenol: Effect of wavelength selection, Spectrochim. Acta - Part A Mol. Biomol. Spectrosc. 67 (2007) 958–965. doi:10.1016/j.saa.2006.09.014.

[245] E. Dinç, D. Baleanu, G. Ioele, M. De Luca, G. Ragno, Multivariate analysis of paracetamol, propiphenazone, caffeine and thiamine in quaternary mixtures by PCR, PLS and ANN calibrations applied on wavelet transform data, J. Pharm. Biomed. Anal. 48 (2008) 1471–1475. doi:10.1016/j.jpba.2008.09.035.

[246] A. Behrens, Determination of gadolinium in geological samples by inductively coupled plasma mass spectrometry and multivariate calibration,

Spectrochim. Acta Part B At. Spectrosc. 50 (1995) 1521–1530. doi:10.1016/0584-8547(95)01362-8.

[247] W. Zhu, E.W.B. De Leer, M. Kennedy, P. Kelderman, G.J.F.R. Alaerts, Study of a Partial Least-squares Regression Model for Rare Earth Element Determination by Inductively Coupled Plasma Mass Spectrometry, J. Anal. At. Spectrom. 12 (1997) 661–665. doi:10.1039/a607621a.

[248] F.A. Jan, M. Ishaq, I. Ihsanullah, S.M. Asim, Multivariate statistical analysis of heavy metals pollution in industrial area and its comparison with relatively less polluted area: A case study from the City of Peshawar and district Dir Lower, J. Hazard. Mater. 176 (2010) 609–616. doi:10.1016/j.jhazmat.2009.11.073.

[249] E.H. Van Veen, S. Bosch, M.T.C. De Loos-Vollebregt, Spectral interpretation and interference correction in inductively coupled plasma mass spectrometry, Spectrochim. Acta Part B At. Spectrosc. 49 (1994) 1347–1361. doi:http://dx.doi.org/10.1016/0584-8547(94)80114-2.

[250] M.I. Kaniu, K.H. Angeyo, a. K. Mwala, M.J. Mangala, Direct rapid analysis of trace bioavailable soil macronutrients by chemometrics-assisted energy dispersive X-ray fluorescence and scattering spectrometry, Anal. Chim. Acta. 729 (2012) 21–25. doi:10.1016/j.aca.2012.04.007.

[251] A.E. Hoerl, R.W. Kennard, Ridge Regression: Biased Estimation for Nonorthogonal Problems, Technometrics. 12 (1970) 55–67. doi:10.1080/00401706.1970.10488634.

[252] R. Tibshirani, Regression Selection and Shrinkage via the Lasso, J. R. Stat. Soc. B. 58 (1994) 267–288. doi:10.2307/2346178.

[253] C. Cui, D. Wang, High dimensional data regression using Lasso model and neural networks with random weights, Inf. Sci. (Ny). 372 (2016) 505–517. doi:10.1016/j.ins.2016.08.060.

[254] S. Roberts, M. Martin, A critical assessment of shrinkage-based regression approaches for estimating the adverse health effects of multiple air pollutants, Atmos. Environ. 39 (2005) 6223–6230. doi:10.1016/j.atmosenv.2005.07.004.

[255] Y. Yang, L. Wu, Nonnegative adaptive lasso for ultra-high dimensional regression models and a two-stage method applied in financial modeling, J. Stat. Plan. Inference. 174 (2016) 52–67. doi:10.1016/j.jspi.2016.01.011.

[256] Z.Y. Algamal, M.H. Lee, Penalized logistic regression with the adaptive LASSO for gene selection in high-dimensional cancer classification, Expert Syst. Appl. 42 (2015) 9326–9332. doi:10.1016/j.eswa.2015.08.016.

[257] B.H. Mevik, H.R. Cederkvist, Mean squared error of prediction (MSEP) estimates for principal component regression (PCR) and partial least squares regression (PLSR), J. Chemom. 18 (2004) 422–429. doi:10.1002/cem.887.

[258] N.M. Raut, L.-S. Huang, K.-C. Lin, S.K. Aggarwal, Uncertainty propagation through correction methodology for the determination of rare earth elements by quadrupole based inductively coupled plasma mass spectrometry, Anal. Chim. Acta. 530 (2005) 91–103. doi:10.1016/j.aca.2004.08.067.

[259] P. Geladi, Chemometrics in spectroscopy. Part 1. Classical chemometrics, Spectrochim. Acta - Part B At. Spectrosc. 58 (2003) 767–782. doi:10.1016/S0584-8547(03)00037-5.

[260] M. Farouk, O.A. Elaziz, S.M. Tawakkol, A. Hemdan, M.A. Shehata, Comparative study between univariate spectrophotometry and multivariate calibration as analytical tools for quantitation of Benazepril alone and in combination with Amlodipine, Spectrochim. Acta - Part A Mol. Biomol. Spectrosc. 123 (2014) 473–481. doi:10.1016/j.saa.2013.12.094.

[261] R. Rendall, A.C. Pereira, M.S. Reis, Advanced predictive methods for wine age prediction: Part I – A comparison study of single-block regression approaches based on variable selection, penalized regression, latent variables and tree-based ensemble methods, Talanta. 171 (2017) 341–350. doi:10.1016/j.talanta.2016.10.062.

[262] Y.W. Lin, B.C. Deng, Q.S. Xu, Y.H. Yun, Y.Z. Liang, The equivalence of partial least squares and principal component regression in the sufficient dimension reduction framework, Chemom. Intell. Lab. Syst. 150 (2016) 58–64. doi:10.1016/j.chemolab.2015.11.003.

[263] M.D. Dyar, M.L. Carmosino, E.A. Breves, M. V. Ozanne, S.M. Clegg, R.C. Wiens, Comparison of partial least squares and lasso regression techniques as applied to laser-induced breakdown spectroscopy of geological samples, Spectrochim. Acta - Part B At. Spectrosc. 70 (2012) 51–67. doi:10.1016/j.sab.2012.04.011.

[264] Y.-W. Lin, N. Xiao, L.-L. Wang, C.-Q. Li, Q.-S. Xu, Ordered homogeneity pursuit lasso for group variable selection with applications to spectroscopic data, Chemom. Intell. Lab. Syst. (2017). doi:10.1016/j.chemolab.2017.07.004.

[265] B. Sharif, D. Makowski, F. Plauborg, J.E. Olesen, Comparison of regression techniques to predict response of oilseed rape yield to variation in climatic conditions in Denmark, Eur. J. Agron. 82 (2017) 11–20. doi:10.1016/j.eja.2016.09.015.

[266] L. Cappellin, E. Aprea, P. Granitto, R. Wehrens, C. Soukoulis, R. Viola, T.D. Märk, F. Gasperi, F. Biasioli, Linking GC-MS and PTR-TOF-MS fingerprints of food samples, Chemom. Intell. Lab. Syst. 118 (2012) 301–307. doi:10.1016/j.chemolab.2012.05.008.

[267] M.T. Pacheco, M.M.M. Parmigiani, M. de Fatima Andrade, L. Morawska, P. Kumar, A review of emissions and concentrations of particulate matter in the three major metropolitan areas of Brazil, J. Transp. Heal. 4 (2017) 53–72. doi:10.1016/j.jth.2017.01.008.

A
Published papers

Chemosphere 210 (2018) 849–858

Contents lists available at ScienceDirect

Chemosphere

journal homepage: www.elsevier.com/locate/chemosphere

Trace element biomonitoring in the Peruvian andes metropolitan region using *Flavoparmelia caperata* lichen

Alex Rubén Huamán De La Cruz [a, b], Jusber Kevin Huamán De La Cruz [c], Daniel Alvarez Tolentino [d], Adriana Gioda [a, *]

[a] Pontifical Catholic University of Rio de Janeiro (PUC-Rio), Department of Chemistry, Rio de Janeiro, Brazil
[b] National University of Centre of Peru (UNCP), Faculty of Chemical Engineering, Av. Mariscal Ramón Castilla Km. 5. No 3809, El Tambo, Huancayo, Peru
[c] National University of Centre of Peru (UNCP), Faculty of Nursing, Av. Mariscal Ramón Castilla Km. 5. No 3809, El Tambo, Huancayo, Peru
[d] Alas Peruanas University (UAP), Faculty of Environmental Engineering, Av. Coronel Parra s/n Paradero 5, Pilcomayo, Huancayo, Peru

Figure A.1: Published paper: Chapter 4.

http://dx.doi.org/10.21577/0103-5053.20180174

J. Braz. Chem. Soc., Vol. 00, No. 00, 1-9, 2018
Printed in Brazil - ©2018 Sociedade Brasileira de Química

Article

Biomonitoring of Toxic Elements in Plants Collected Near Leather Tanning Industry

Alex R. H. De La Cruz,[a] Lorreine D. S. C. Ferreira,[a] Vinicius P. Andrade[a] and Adriana Gioda[,a]*

[a]*Departamento de Química, Pontifícia Universidade Católica do Rio de Janeiro, Rua Marquês de São Vicente, 225, 22451-900 Gávea, Rio de Janeiro-RJ, Brazil*

The present work aimed the study of atmospheric deposition of toxic elements near to a tannery industry by collecting black material deposited on leaf surfaces of cinnamon trees (*Cinnamomum zeylanicum*). Elements such as As, Ba, Cr, Cu, Fe, Ni, Pb, Sb, V, and Zn were analyzed by inductively coupled plasma mass spectrometry (ICP-MS). For comparison purpose, black particles deposited on the leaf surface of lemon trees (*Citrus lemon*) collected away from the tannery industry were also analyzed. Results showed that the amount of toxic elements found in the black particles collected near tannery area was significantly higher than the amount of those measured in the comparison site. Enrichment factors (EF) of As and Cr were markedly impacted by anthropogenic emissions, whereas the other elements were moderately/slightly enriched. Cluster analysis (CA) identified the leather industry as the anthropogenic source, while As possibly comes from the wide use of pesticides and herbicides in agricultural practices. The results indicated that emissions from the leather industry and agricultural activities are the main source of pollution in this area.

Keywords: leather industry, ICP-MS, toxic elements, atmospheric particles

Figure A.2: Published paper: Chapter 5.

B
Submitted papers

Annals of the Brazilian Academy of Sciences - Manuscript ID AABC-2018-...

Daniel Sant'Anna <onbehalfof@manuscriptcentral.com>
Sáb 04/08/2018, 20:33
Para:agioda@hotmail.com <agioda@hotmail.com>
Cc:alebut2@hotmail.com <alebut2@hotmail.com>;ayuque@gmail.com <ayuque@gmail.com>;
delacruz_@gmail.com <delacruz_@gmail.com>;agioda@hotmail.com <agioda@hotmail.com>
04-Aug-2018

Dear Dr. Gioda:

Your manuscript entitled "Air quality biomonitoring of trace elements in the metropolitan area of Huancayo, Peru using transplanted Tillandsia capillaris as biomonitor" has been successfully submitted online and is presently being given full consideration for publication in the Annals of the Brazilian Academy of Sciences.

Your manuscript ID is AABC-2018-0813.

Please mention the above manuscript ID in all future correspondence or when calling the office for questions. If there are any changes in your street address or e-mail address, please log in to ScholarOne Manuscripts at https://mc04.manuscriptcentral.com/aabc-scielo and edit your user information as appropriate.

You can also view the status of your manuscript at any time by checking your Author Center after logging in to https://mc04.manuscriptcentral.com/aabc-scielo.

Thank you for submitting your manuscript to the Annals of the Brazilian Academy of Sciences.

Sincerely,
Annals of the Brazilian Academy of Sciences Editorial Office

Figure B.1: Submitted paper 1: Chapter 6.

Submission Confirmation for ATMENV-D-18-00209R1

Atmospheric Environment <eesserver@eesmail.elsevier.com>
Ter 31/07/2018, 17:04
Para:agioda@hotmail.com <agioda@hotmail.com>
*** Automated email sent by the system ***

Ms. Ref. No.: ATMENV-D-18-00209R1
Title: Evaluation of the impact of the Rio 2016 Olympic Games on air quality in the city of Rio de Janeiro, Brazil Research Paper
Atmospheric Environment

Dear Dr Gioda,

Thank you for submitting this revised manuscript to Evaluation of the impact of the Rio 2016 Olympic Games on air quality in the city of Rio de Janeiro, Brazil. The revised paper will be assessed by the Editor, and may be sent for re-review.

If the manuscript is sent for review we do try to respond within about eight weeks, however this is always dependent upon the availability and speed of our chosen referees.

You may check the status of your manuscript by logging onto the Elsevier Editorial System as an Author at https://ees.elsevier.com/atmenv/.

Your username is: agioda@hotmail.com

If you need to retrieve password details, please go to: http://ees.elsevier.com/atmenv/automail_query.asp

Kind regards,

Elsevier Editorial System
Atmospheric Environment

Figure B.2: Submitted paper 2: Chapter 8.

International Journal of Environmental Analytical Chemistry - Manuscript I...

International Journal of Environmental Analytical Chemistry <onbehalfof@manuscriptcentral.com>
Sáb 04/08/2018, 16:00
Para:agioda@hotmail.com <agioda@hotmail.com>
04-Aug-2018

Dear Dr Gioda:

Your manuscript entitled "Application of univariate and multivariate calibration methods for interferences correction in the determination of Rare Earth Elements by Inductively Coupled Plasma Mass Spectrometry" has been successfully submitted online and is presently being given full consideration for publication in International Journal of Environmental Analytical Chemistry.

Your manuscript ID is GEAC-2018-0302.

Please mention the above manuscript ID in all future correspondence or when calling the office for questions. If there are any changes in your street address or e-mail address, please log in to Manuscript Central at https://mc.manuscriptcentral.com/geac and edit your user information as appropriate.

You can also view the status of your manuscript at any time by checking your Author Centre after logging in to https://mc.manuscriptcentral.com/geac.

Thank you for submitting your manuscript to International Journal of Environmental Analytical Chemistry.

Sincerely,
International Journal of Environmental Analytical Chemistry Editorial Office

Figure B.3: Submitted paper 3: Chapter 9.

C
Papers published in related topics to the thesis

Chemosphere 163 (2016) 569–577

Contents lists available at ScienceDirect

Chemosphere

journal homepage: www.elsevier.com/locate/chemosphere

Toxicological effects of particulate matter ($PM_{2.5}$) on rats: Bioaccumulation, antioxidant alterations, lipid damage, and ABC transporter activity

Joaquim de Paula Ribeiro [a, b, 1], Ana Cristina Kalb [a, b, 1], Paula Peixoto Campos [c], Alex Rubén Huaman De La Cruz [d], Pablo Elias Martinez [a, b], Adriana Gioda [d], Marta Marques de Souza [a, b], Carolina Rosa Gioda [a, b, *]

[a] Instituto de Ciências Biológicas, Universidade Federal do Rio Grande, FURG, Rio Grande, RS, Brazil
[b] Programa de Pós Graduação em Ciências Fisiológicas, Instituto de Ciências Biológicas, FURG, Rio Grande, RS, Brazil
[c] Departamento de Farmacologia, Instituto de Ciências Biológicas, Universidade Federal de Minas Gerais, Belo Horizonte, MG, Brazil
[d] Pontifícia Universidade Católica do Rio de Janeiro (PUC-Rio), Departamento de Química, Rio de Janeiro, RJ, Brazil

Figure C.1: Paper in collaboration 1: Bioaccumulation and toxicological effects of particulate matter

D
Participation in congresses

Oral presentation

Alex R. H. de la Cruz, Atomic Espectrometry applied to environmental samples. In 2017, VII Workshop em Espectrometria Atomica/ Pre- symposium Course, Rio de Janeiro, Brazil-2017.

Conference papers and posters

Andrade, V. P.; **De La Cruz, A. R. H.**; Calderon, E. R. D.; Ayuque, R. F. O.; De La Cruz, J. K. H.; Gioda, A.; Air quality biomonitoring of trace elements in Huancayo city, Peru using transplanted Tillandsia capillaris as bioindicators. In 2018, 41a Annual meeting of the Brazilian Chemical Society, Foz do Iguacu, Parana, Brazil.

Alonso Freitas, G. A. F.; **Huaman De La Cruz, A. R.**; Padilla-Chavarria, H. I.; Gioda, A.; Dillenburg Saint'Pierre, T.; Kai, J.; Quantification and separation of rare earth elements from fluorescent lamp phosphors and synthesis of luminescent nanoparticles. In 2018, 41a Annual meeting of the Brazilian Chemical Society, Foz do Iguacu, Parana, Brazil.

Alex R. H. De La Cruz; Vinicius de Paiva Andrade; Carlos Zaki Antaki; Ellen Jéssica de Souza Macário dos Santos; Adriana Gioda; Biomonitoring of metals as an indicator of air quality in the city of Rio de Janeiro, using transplanted Tillandsias species. In 2017, XVI Regional Meeting of the Brazilian Chemical Society, Rio de Janeiro, Brazil.

Tatiane B. de Oliveira; Enrique R. D. Calderon; **Alex R. H. De la Cruz**; Paulo Artaxo; Adriana Gioda. Evaluation of the chemical composition of rainwater in

the Brazilian Amazon region. In 2017, XVI Regional Meeting of the Brazilian Chemical Society, Rio de Janeiro, Brazil.

Enrique R. D. Calderon; **Alex R. H. De la Cruz**; Vinicius de Paiva Andrade; Carlos Zaki Antaki;, Ellen Jéssica de Souza Macário dos Santos; Adriana Gioda. Exploratory study of air quality Internal based on the concentration of CO_2 in various environments of the university. In 2017, XVI Regional Meeting of the Brazilian Chemical Society, Rio de Janeiro, Brazil.

Vinicius de Paiva Andrade; **Alex R. H. De la Cruz**; Carlos Zaki Antaki;, Ellen Jéssica de Souza Macário dos Santos; Adriana Gioda. Biomonitoring of Fe, Zn and Pb using *Tillandsia usneoides*. In 2017, XVI Regional Meeting of the Brazilian Chemical Society, Rio de Janeiro, Brazil.

Alex Ruben Huaman De La Cruz; Enrique Roy Dionisio Calderon; Adriana Gioda; Lorreine dos Santos Cursino Ferreira. Biomonitoring of air pollution in urban areas of Rio de Janeiro, Brazil, using two tillandsia species. In 2017, The Brazilian Chemistry Society (SBQ) and the IUPAC – International Union of Pure and Applied Chemistry, Sao Paulo, Brazil.

Alex Ruben Huaman De La Cruz; Vinicius de Paiva Andrade; Carlos Zaki Antaki;, Ellen Jéssica de Souza Macário dos Santos; Adriana Gioda; Biomonitoring of heavy metals and air quality in Rio de Janeiro city, using transplanted *Tillandsia* species. In 2017, VI International Workshop on Pollutants in the Environment, Rio de Janeiro Brazil.

Alex De la Cruz, Jefferson Souza, Tatiana Saint'Pierre, Adriana Gioda. Application Of Elastic Net for spectral interferences correction in ICP-MS determination of REE in plant samples. In 2017, 14th Ryo Symposium on Atomic Spectrometry, Vitoria, Espiritu Santo, Brazil.

Jefferson Souza, **Alex De la Cruz**, Marcia Rocha, Tatiana Saint'Pierre. ARE DIETARY SUPPLEMENTS ACCOMPLISHING THE FOOD SAFETY REQUIREMENTS? HPLC-ICP-MS AS A POWERFUL TOOL FOR QUALITY

CONTROL. In 2017, 14th Rio Symposium on Atomic Spectrometry, Vitoria, Espiritu Santo, Brazil.

GIODA, A.; KHAN, S.; **CRUZ, A. R. H. L**.; CACERES, M. F.; CIFUENTES, J. M. C.; AUCELIO, R. Monitoring release of elemental mercury from compact fluorescent lamps in a control room at different points using three multipath-path atomic absorption spectrophotometers. In 2016: 14th International Conference of Indoor Quality and Climate, Ghent, Belgium.

Alex Ruben Huaman De La Cruz; Adriana Gioda; Comparison of ridge and Lasso regression techniques for determination of Gadolinium by Inductively Coupled Plasma Mass Spectrometry. In 2016, 18th National Meeting of Analytical Chemistry (ENQA). Florianopolis, Santa Catarina, Brazil.

Cruz, A. R. H.; Ferreira, L. S. C.; Gioda. Assessment of the environmental impact caused by metals from leather industry using plants as biomonitors. In 2016, 39th Meeting of the Brazilian Society of Chemistry (SBQ), Goiania, Brazil

E
Supplementary material - 1

Figure E.1 The city of Huancayo surrounded by mountains

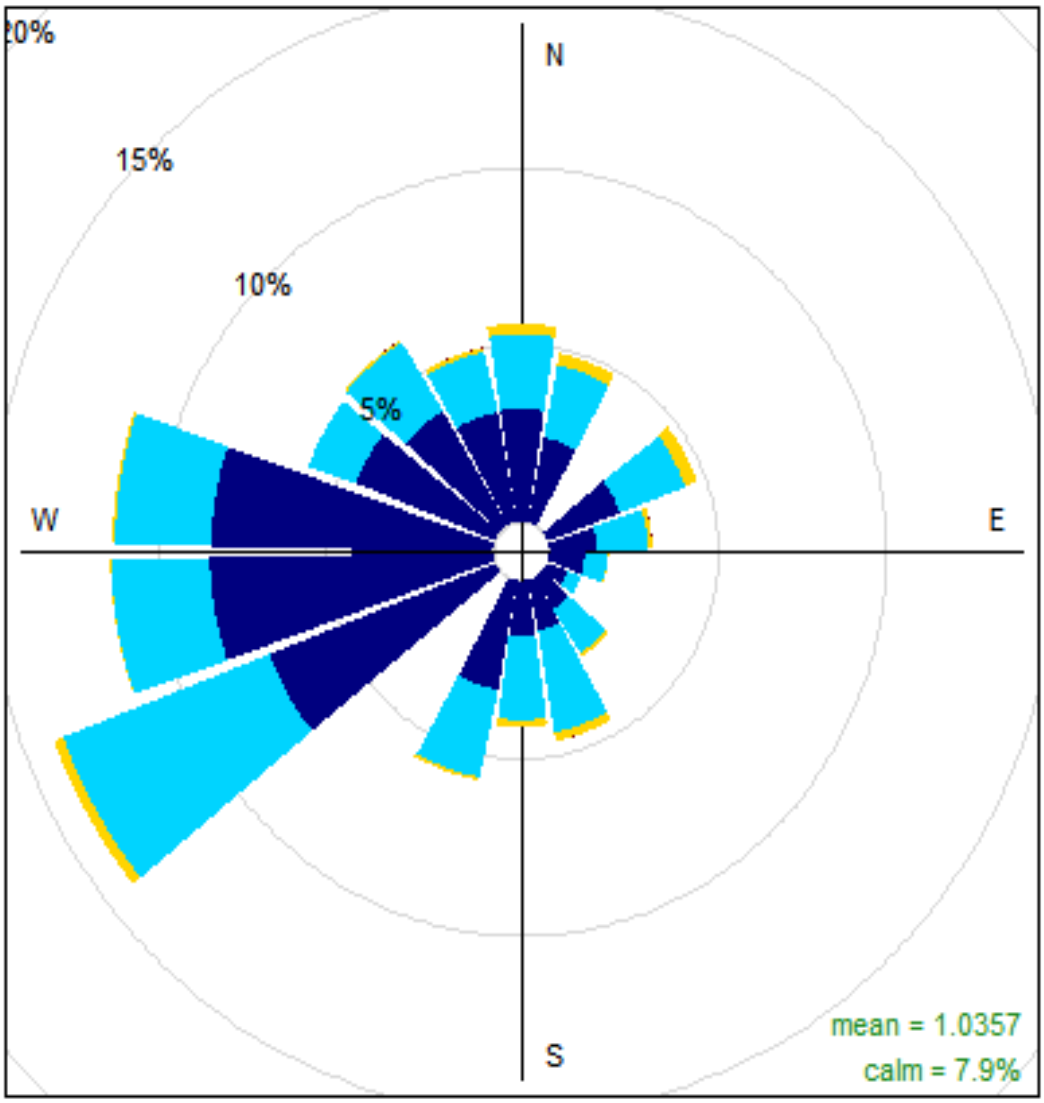

Figure E.2 Wind roses created from February to March 2017 based on measurements performed at the center of Huancayo (12, 06°S; 75, 21°W)

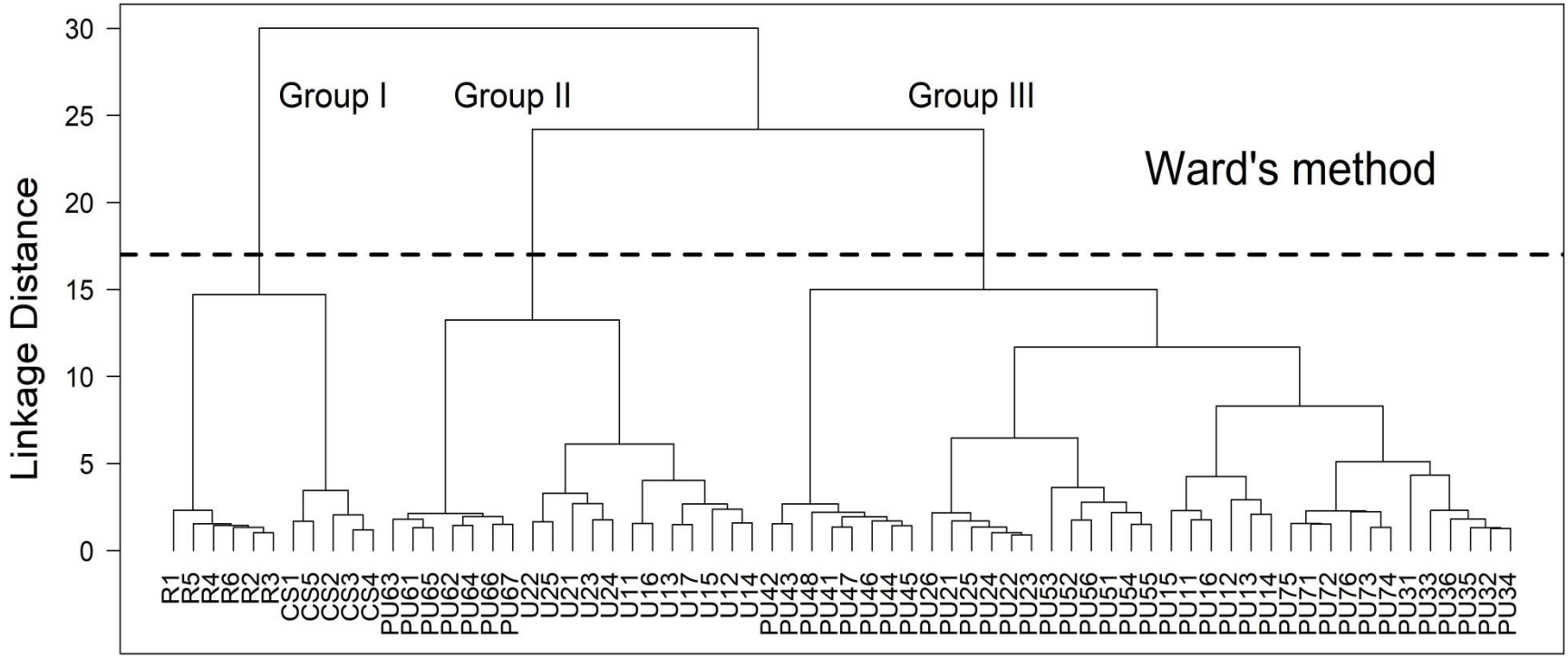

Figure E.3 Dendrogram of the concentration of trace elements in *F. caperata* lichens sampled from each site

Table E.1 Instrumental conditions for ICP-MS measurements

ICP-MS conditions	**Values**
RF power	1150 W
Frequency	27.2 MHz
Plasma gas flow rate	11.5 L min^{-1}
Auxiliary gas flow rate	0.55 L min^{-1}
Nebulizer gas flow rate	0.97 L min^{-1}
Sample uptake rate	0.6 mL min^{-1}
Measurement mode	Dual (PC/analog)
Acquisition time	1 s
Dwell time	200 ms
Replicates	6

Table E.2 Quality control results (µg g^{-1} dry weight or DW) obtained from ICP-MS analysis of SRM-1515 “Apple leaves”.

SRM 1515 *Apple Leaves*				
Elements	Certified Material Mean ± S.D.	Experimental results Mean ± S.D.	Recovery (%)	RSD (%)
Al	289 ± 9	290 ± 17	102	5.99
As	0.040 ± 0.007	0.041 ± 0.006	108	6.42
Ba	49 ± 2	42 ± 1	88	2.61
Ca	15260 ± 150	11882 ± 320	78	5.45
Cd	0.010 ± 0.002	0.011 ± 0.002	113	3.46
Co	0.090 ± nd	0.091 ± 0.003	109	3.70
Cr	0.30 ± nd	0.30 ± 0.02	108	4.72
Cu	5.64 ± 0.24	5.56 ± 0.17	99	3.04
Fe	83 ± 5	93 ± 2	112	2.35
Hg	0.044 ± 0.004	0.051 ± 0.004	116	2.83
K	16100 ± 200	13229 ± 255	82	2.69
Mg	2710 ± 80	2447 ± 57	90	2.33
Mn	54 ± 3	48 ± 2	90	4.12
Ni	0.91 ± 0.12	1.05 ± 0.05	111	4.45
P	1590 ± 110	1403 ± 84	88	5.93
Pb	0.47 ± 0.024	0.44 ± 0.02	94	5.43
Rb	10.20 ± 1.5	9.73 ± 0.43	95	4.39
Sb	0.01 ± nd	0.012 ± 0.003	115	5.56
Sr	25 ± 2	24 ± 2	98	6.45
V	0.26 ± 0.03	0.25 ± 0.01	99	4.55

Zn	12.5 ± 0.31	12.7 ± 0.69	102	5.40

S.D.: Standard Deviation, nd: no data, RSD: Relative Standard Deviation

Table E.3 Quality control results (μg g^{-1} dry weight or DW) obtained from ICP-MS analysis of SRM-1573 "Tomato leaves".

SRM 1573 *Tomato Leaves*				
Elements	Certified Material Mean ± S.D.	Experimental results Mean ± S.D.	Recovery (%)	RSD (%)
Al	598 ± 12	551 ± 32	92	5.91
As	0.11 ± 0.01	0.13 ± 0.01	113	5.27
Ba	63 ± nd	49 ± 2.4	79	4.87
Ca	50500 ± 900	34390 ± 1200	68	5.24
Cd	1.52 ± 0.04	1.35 ± 0.01	89	0.07
Co	0.57 ± 0.02	0.49 ± 0.03	86	5.69
Cr	1.99 ± nd	1.77 ± 0.06	89	3.19
Cu	4.70 ± 0.14	4.20 ± 0.18	89	4.34
Fe	368 ± 7	389 ± 16	106	4.86
Hg	0.034 ± 0.004	0.040 ± 0.003	114	5.38
K	27000 ± 500	22206 ± 600	82	3.97
Mg	12000 ± nd	9072 ± 352	76	3.88
Mn	246 ± 8	197 ± 4	80	2.04
Ni	1.59 ± 0.07	1.61 ± 0.03	101	0.76
P	2160 ± 40	2049 ± 62	95	3.18
Rb	14.89 ± 0.27	12.56 ± 0.56	84	4.54
Sb	0.060 ± 0.006	0.050 ± 0.002	79	6.15
Sr	85 ± nd	70 ± 3	83	3.90
V	0.84 ± 0.01	0.64 ± 0.03	76	4.98
Zn	30.9 ± 0.71	30.6 ± 1.51	99	4.92

S.D.: Standard Deviation, nd: no data, RSD: Relative Standard Deviation

Table E.4 Quality control results (µg g^{-1} dry weight or DW) obtained from ICP-MS analysis of BCR - 670 “Aquatic plant”.

BCR 670 *Aquatic plant*				
Elements	Certified Material Mean ± S.D.	Experimental results Mean ± S.D.	Recovery (%)	RSD (%)
As	1.98 ± 0.19	1.50 ± 0.07	76	2.75
Cd	0.080 ± 0.003	0.070 ± 0.001	86	6.92
Cr	2.05 ± 0.10	1.82 ± 0.07	89	1.68
Cu	1.82 ± 0.30	1.37 ± 0.21	75	1.66
Fe	975 ± 10	961 ± 12	99	3.63
Ni	2.35 ± nd	2.56 ± 0.11	109	4.23
Pb	2.06 ± 0.12	1.52 ± 0.03	74	2.01
Sb	0.224 ± nd	0.161 ± 0.002	71	0.32
Zn	24 ± 2	24 ± 1	101	5.27

S.D.: Standard Deviation, nd: no data, RSD: Relative Standard Deviation

F
Supplementary material – 2

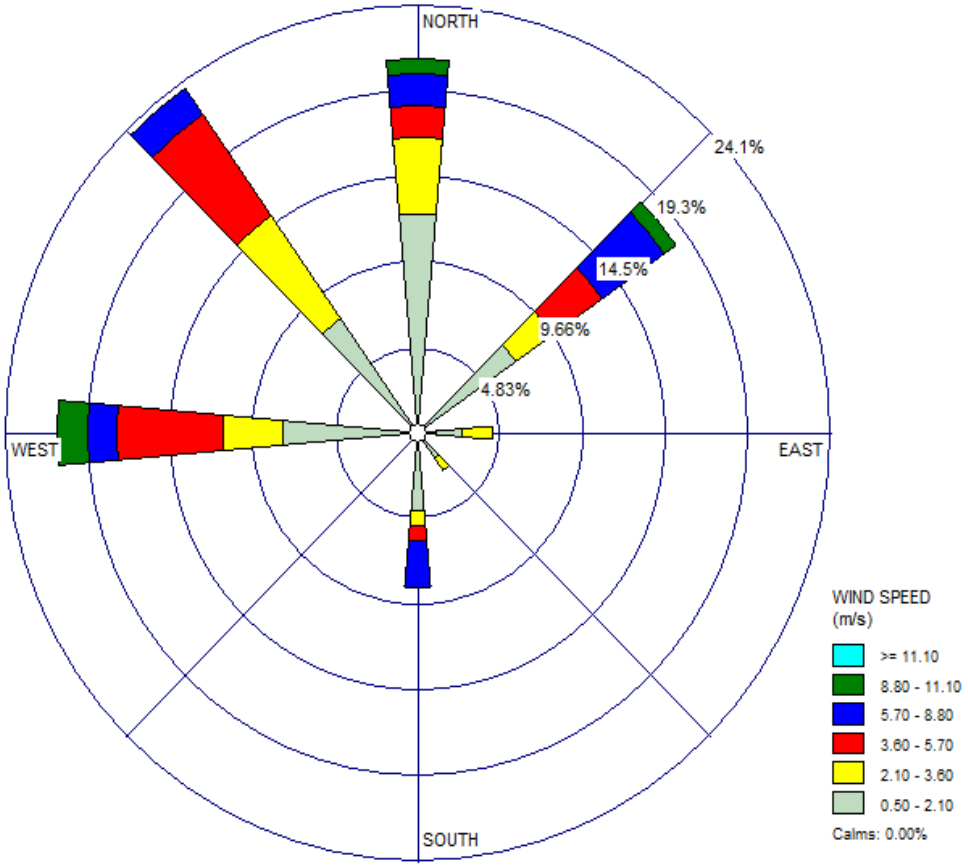

Figure F.1 Wind roses from September to December 2017, obtained from geophysical institute of Peru, Chupaca (12° 2’ 18’’ S; 75° 20’ 17’’ W).

Table F.1 Characteristics of each transplanting point carried out in the Metropolitan area of Huancayo.

Sites ID	City	Population [A]	Site features	Emission sources	Latitude	Longitude
1	SC	11,378	Urban/ rural	Soil dust/traffic/agricultural activities	12° 1’ 5.23’’ S	75° 14’ 33.75’’ W
2	SC				12° 0’ 44.01’’ S	75° 14’ 42.68’’ W
3	SC				12° 0’ 33.06’’ S	75° 14’ 50.72’’ W
4	SC				12° 0’ 52.33’’ S	75° 14’ 37.74’’ W
5	SC				12° 0’ 24.48’’ S	75° 14’ 54.93’’ W
6	SC				12° 0’ 0.91’’ S	75° 15’ 8.33’’ W
7	SC				11° 59’ 55.36’’ S	75° 15’ 10.76’’ W
8	Ch	22,099	Urban/ rural	Traffic/agricultural activities	12° 3’ 17.46’’ S	75° 16’ 48.75’’ W
9	Ch				12° 3’ 23.43’’ S	75° 17’ 3.27’’ W
10	Ch				12° 3’ 27.88’’ S	75° 17’ 17.02’’ W
11	Ch				12° 3’ 42.58’’ S	75° 17’ 15.75’’ W
12	Ch				12° 3’ 48.58’’ S	75° 17’ 4.74’’ W
13	Ch				12° 3’ 46.58’’ S	75° 17’ 18.91’’ W
14	Ch				12° 3’ 42.05’’ S	75° 17’ 31.32’’ W
15	T	160,685	Urban	Traffic	12° 3’ 15.30’’ S	75° 13’ 8.67’’ W
16	T				12° 3’ 6.80’’ S	75° 13’ 14.00’’ W
17	T				12° 2’ 39.95’’ S	75° 13’ 33.74’’ W
18	T				12° 2’ 58.98’’ S	75° 13’ 19.89’’ W
19	T				12° 1’ 45.93’’ S	75° 14’ 6.92’’ W
20	T				12° 3’ 25.86’’ S	75° 12’ 57.87’’ W
21	H	117,559	Urban	Traffic	12° 4’ 15.55’’ S	75° 12’ 29.74’’ W
22	H				12° 4’ 18.12’’ S	75° 12’ 18.85’’ W
23	H				12° 4’ 1.04’’ S	75° 12’ 18.54’’ W
24	H				12° 3’ 58.62’’ S	75° 12’ 42.52’’ W
25	H				12° 3’ 41.78’’ S	75° 12’ 31.98’’ W
26	H				12° 4’ 28.53’’ S	75° 12’ 7.40’’ W

G
Supplementary material - 3

Table G.1 Monitoring stations, measured pollutants and meteorology data from Rio de Janeiro measured during Olympic Games 2016.

Sampling Sites	**Pollutants**						**Meteorology**						
	SO_2	CO	O_3	NO_x	PM_{10}	CH_4	WD	SR	WS	T	P	RH	Prec
Copacabana	X	x	x		X		X	X	X	X	x	X	x
Centro		x	x				x	x	x	x			x
São Cristóvão	x	x	x		x		x	x	x	x	x	x	x
Tijuca	x	x	x	x	x		x	x	x	x	x	x	x
Irajá	x	x	x	x	x	x	x	x	x		x	x	x
Bangu	x	x	x	x	x		x		x	x	x		x
Mobile Station	x				x	x					x	x	

WD: wind direction, WS: wind speed, T: temperature, SR: solar radiation, P: pressure, Prec: precipitation, RH: relative humidity, white space: Not measured.

Table G.2 Equipment and methods used to measure the pollutants

Pollutant	**Method**	**Equipment**
SO2 (μg m^{-3})	Ultraviolet fluorescent radiation	EC 9850; Serinus 50 series
NO-NO_2 (μg m^{-3})	Chemiluminescence detection	ML 9841; Serinus 40 series
CO (ppm)	Non-dispersive infrared spectrophotometry (NDIR) technology	EC 9830; Serinus 30 series
O3 (μg m^{-3})	Non-dispersive ultraviolet (UV) absorption technology	EC 9810; Serinus 10 series
PM_{10} (μg m^{-3})	β-ray attenuation	Met One BAM 1020

Table G.3 Description of air pollutants and meteorological variables from 2016 Olympic Games at each monitoring station in the three periods: before, during and after and whole period.

	Whole period (Jul 01-Oct 31, 122 days)	**Before (Jul 01-Aug 04, 35 days)**	**During (Aug 05-Sep 18, 44 days)**	**After Sep 19-Oct 31, 43 days**
Centro	**Mean ± SD**	**Mean ± SD**	**Mean ± SD**	**Mean ± SD**
Pollutants				
PM_{10} (µg/m³)	NM	NM	NM	NM
SO_2 (µg/m³)	NM	NM	NM	NM
O_3 (µg/m³)	21.55 ± 17.56	18.274 ±	22.82 ±	22.86 ±
CO (ppm)	0.40 ± 0.28	18.01a	19.13b	14.97b 0.33 ±
NO (µg/m³)	NM	0.47 ± 0.37a	0.43 ± 0.26b	0.15c
NO_2 (µg/m³)	NM	NM	NM	NM
		NM	NM	NM
Meteorology				
Air temperature (°C)	NM	NM	NM	NM
Relative humidity (%)	NM	NM	NM	NM
Copacabana	**Mean ± SD**	**Mean ± SD**	**Mean ± SD**	**Mean ± SD**
Pollutants				
PM_{10} (µg/m³)	64.08 ± 20.01	61.78 ± 23.19a	66.88 ±	62.90 ±
SO_2 (µg/m³)	2.86 ± 4.07	4.17 ± 5.13a	19.13b	17.85a 2.23 ±
O_3 (µg/m³)	21.99 ± 13.93	18.60 ± 13.44a	2.97 ± 4.09b	2.97b
CO (ppm)	0.08 ± 0.12	0.11 ± 0.16a	22.18 ±	24.49 ±
NO (µg/m³)	NM	NM	14.87b	12.73c
NO_2 (µg/m³)	NM	NM	0.08 ± 0.12b	0.05 ± 0.06c
			NM	NM
			NM	NM
Meteorology				
Air temperature (°C)	23.52 ± 3.43	22.48 ± 2.89a	23.75 ± 3.40b	24.11 ± 3.66b
Relative humidity (%)	71.59 ± 14.28	69.97 ± 14.05a	70.95 ± 14.87a	73.57 ± 13.65b
Sao Cristovao	**Mean ± SD**	**Mean ± SD**	**Mean ± SD**	**Mean ± SD**
Pollutants				
PM_{10} (µg/m³)	29.14 ± 19.33	43.74 ± 25.02a	32.58 ±	22.24 ±
SO_2 (µg/m³)	8.96 ± 11.11	12.34 ± 12.96a	19.99b	13.57c 5.88 ±
O_3 (µg/m³)	21.46 ± 21.70	19.06 ± 19.95a	8.76 ± 11.28b	7.41c
CO (ppm)	0.26 ± 0.41	0.40 ± 0.59a	20.05 ±	25.69 ±
NO (µg/m³)	NM	NM	20.61a	24.04b 0.09 ±
NO_2 (µg/m³)	NM	NM	0.32 ± 0.34b	0.09c
			NM	NM
			NM	NM
Meteorology				
Air temperature (°C)	23.94 ± 3.99	22.92 ± 3.66a	24.37 ± 4.10b	24.35 ± 3.99b
Relative humidity (%)	66.34 ± 15.28	65.18 ± 14.96a	63.36 ± 15.67a	70.51 ± 14.20b
Tijuca	**Mean ± SD**	**Mean ± SD**	**Mean ± SD**	**Mean ± SD**

Pollutants				
PM_{10} (µg/m³)	38.05 ± 20.07	42.74 ± 26.85a	38.71 ± 17.19b	33.52 ± 14.77c
SO_2 (µg/m³)	3.02 ± 4.61	3.26 ± 3.93a	3.55 ± 6.01a	2.23 ± 2.97b
O_3 (µg/m³)	27.92 ± 20.77	20.83 ± 17.77a	30.87 ± 22.27b	30.92 ± 19.93b
CO (ppm)	0.42 ± 0.25	0.48 ± 0.31a	0.43 ± 0.24b	0.37 ± 0.19c
NO (µg/m³)	16.25 ± 21.1	23.74 ± 30.70a	14.30 ± 16.76b	12.17 ± 12.04c
NO_2 (µg/m³)	63.89 ± 24.41	74.14 ± 28.55a	66.29 ± 22.87b	52.99 ± 16.83c
Meteorology				
Air temperature (°C)	22.06 ± 5.05	20.84 ± 4.37a	22.44 ± 5.09b	22.65 ± 5.35b
Relative humidity (%)	61.24 ± 17.25	59.74 ± 15.35a	59.27 ± 18.27a	64.49 ± 17.18b
Bangu	**Mean ± SD**	**Mean ± SD**	**Mean ± SD**	**Mean ± SD**
Pollutants				
PM_{10} (µg/m³)	41.25 ± 27.89	56.11 ± 39.97a	39.52 ± 24.08b	30.26 ± 17.19c
SO_2 (µg/m³)	3.15 ± 6.03	5.36 ± 8.61a	1.61 ± 4.34b	2.91 ± 3.94c
O_3 (µg/m³)	55.44 ± 33.56	46.65 ± 33.5a	57.34 ± 34.37b	60.77 ± 31.22b
CO (ppm)	0.39 ± 0.27	0.48 ± 0.35a	4.48 ± 7.83b	0.28 ± 0.14c
NO (µg/m³)	4.73 ± 8.97	7.70 ± 13a	30.36 ± 18.65b	2.34 ± 2.83c
NO_2 (µg/m³)	25.46 ± 17.08	28.35 ± 18.62a		17.94 ± 10.12c
Meteorology				
Air temperature (°C)	NM	NM	NM	NM
Relative humidity (%)	67.99 ± 61.26	62.32 ± 15.45a	61.39 ± 16.39a	79.76 ± 103b
Iraja	**Mean ± SD**	**Mean ± SD**	**Mean ± SD**	**Mean ± SD**
Pollutants				
PM_{10} (µg/m³)	46.19 ± 27.55	64.11 ± 34.06a	45.28 ± 22.54b	31.74 ± 14.27c
SO_2 (µg/m³)	3.02 ± 4.61	4.92 ± 9.79a	5.24 ± 7.54a	5.15 ± 9.32a
O_3 (µg/m³)	37.30 ± 31.18	29.01 ± 29.84a	39.42 ± 33.95b	41.75 ± 27.75c
CO (ppm)	0.42 ± 0.32	0.47 ± 0.41a	0.43 ± 0.24b	0.32 ± 0.17b
NO (µg/m³)	16.67 ± 34.87	32.40 ± 53.55a	13.98 ± 26.59b	6.62 ± 9.16c
NO_2 (µg/m³)	35.28 ± 18.47	46.99 ± 21.64a	34.18 ± 16.13b	26.87 ± 11.72c
Meteorology				
Air temperature (°C)	25.62 ± 4.58	24.56 ± 4.29	26.06 ± 4.63a	26.02 ± 4.62b
Relative humidity (%)	63.41 ± 16.14	61.99 ± 15.91	61.44 ± 17a	66.64 ± 14.86b

NM: Not measured, Means with the same letter (a, b, and c) code are not significantly different (Tukey multiple comparisons of means, $p < 0.05$).

H
Supplementary material - 4

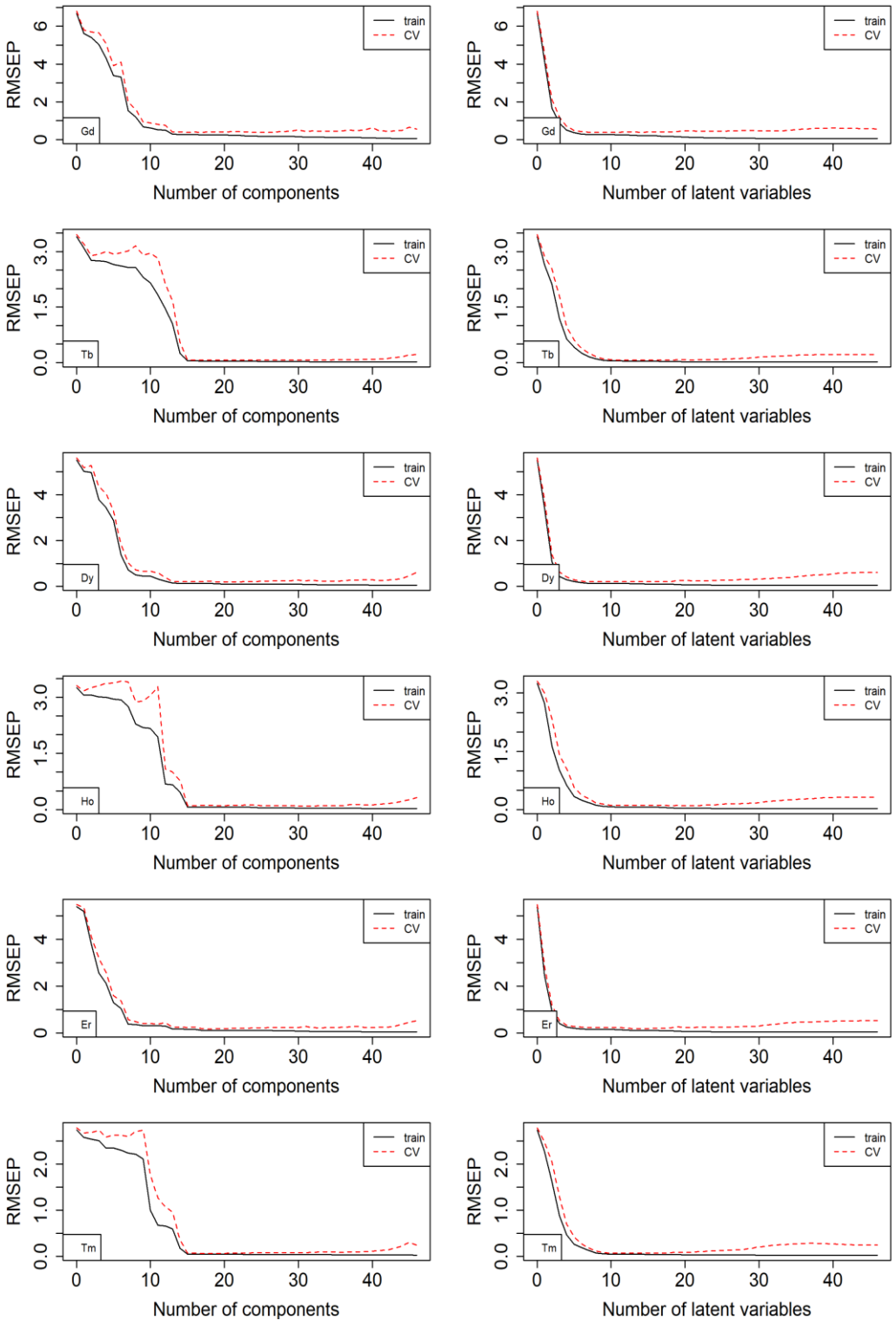

Figure H.1 Cross-validated RMSECV curves for Gd, Tb, Dy, Ho, Er, and Tm in function of the latent variables obtained by PLS (right) and PCR (left) multivariate calibration methods.

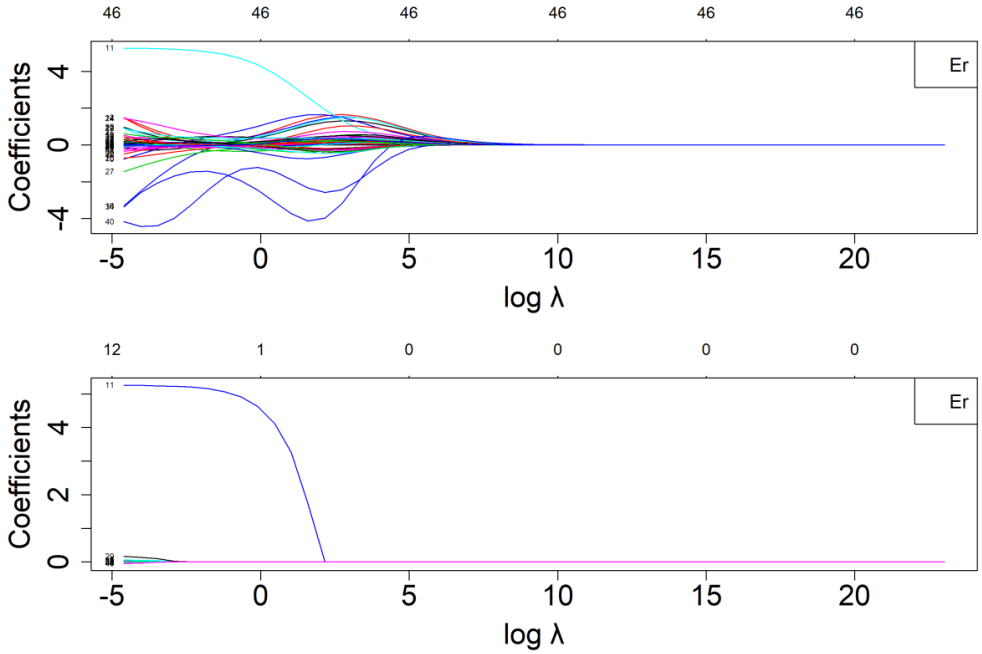

Figure H.2 Plots of regression coefficients estimates as function of log (λ), by Lasso (lower) and RR (upper) methods.

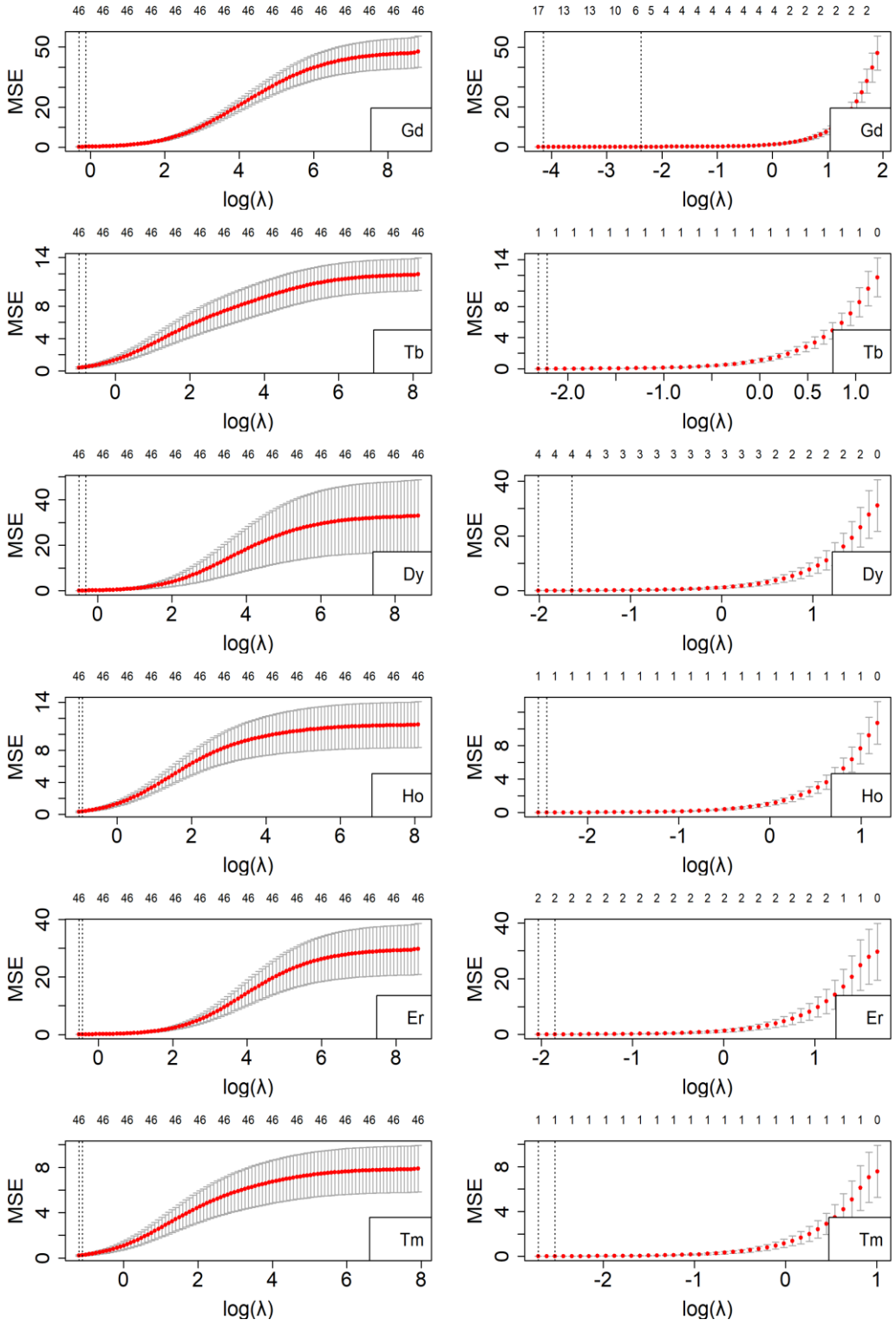

Figure H.3 Plots of MSE of the cross-validation for Gd, Tb, Dy, Ho, Er, and Tm as function of log (λ), by Lasso (right) and RR (left) multivariate calibration methods.

Table H.1 Certified and informed concentration values (μg kg^{-1}) in BRC-670 *AquaticPlant,* SRM 1515a-*Apple leaves*, and SRM 1573a-*Tomato leaves*

Element	SRM 1515a[nc]	SRM 1573a[nc]	BCR670[c]
La	20	2.3	0.487 ± 0.02[a]
Ce	3	2	0.99 ± 0.04[a]
Pr	*	*	0.121 ± 0.006[a]
Nd	17	*	0.473 ± 0.015[a]
Sm	3	0.19	94 ± 7[b]
Eu	0.2	*	23.2 ± 1.5[b]
Gd	3	0.17	98 ± 8[b]
Tb	0.4	*	14 ± 1.1[b]
Dy	*	*	79 ± 7[b]
Ho	*	*	15.8 ± 1.8[b]
Er	*	*	44 ± 2.8[b]
Tm	*	*	5.7 ± 0.7[b]
Yb	0.3	*	40 ± 4[b]
Lu	*	*	6.3 ± 0.5[b]

* Not reported; nc = Not certified; c = Certified values, in μg g^{-1} [(a)] and in [b]μg kg^{-1} [(b)]

Table H.2 Instrumental conditions for the ICP-MS measurements.

ICP-MS conditions	Values
RF power	1150 W
Frequency	27.2 MHz
Plasma gas flow rate	11.5 L min^{-1}
Auxiliary gas flow rate	0.55 L min^{-1}
Nebulizer gas flow rate	0.97 L min^{-1}
Sample uptake rate	0.6 mL min^{-1}
Measurement mode	Dual (PC/analog)
Acquisition time	1 s
Dwell time	200 ms
Replicates	6

Table H.3 Spectral interferences on the REE isotopes

Isotope	Abundance (%)	Interference
^{138}La	0.090	^{138}Ce, ^{138}Ba
^{139}La	99.910	-
^{136}Ce	0.185	^{136}Ba
^{138}Ce	0.251	^{138}Ba
^{140}Ce	88.450	-
^{142}Ce	11.114	^{142}Nd
^{141}Pr	100	-
^{142}Nd	27.2	^{142}Ce
^{143}Nd	12.2	-
^{144}Nd	23.8	^{144}Sm
^{145}Nd	8.3	-
^{146}Nd	17.2	^{130}BaO
^{148}Nd	5.7	^{148}Sm, ^{132}BaO
^{150}Nd	5.6	^{150}Sm, ^{134}BaO
^{144}Sm	3.07	^{144}Nd
^{147}Sm	14.99	^{130}BaOH
^{148}Sm	11.24	^{148}Nd, ^{132}BaO
^{149}Sm	13.82	^{132}BaOH
^{150}Sm	7.38	^{150}Nd, ^{136}CeO, ^{136}BaO
^{152}Sm	26.75	^{152}Gd, ^{136}CeO, ^{136}BaO
^{151}Eu	47.81	^{135}BaO, ^{134}BaOH
^{153}Eu	52.19	^{137}BaO, ^{136}BaOH
^{152}Gd	0.20	^{152}Sm, ^{136}CeO, ^{136}BaO, ^{135}BaOH
^{154}Gd	2.18	^{154}Sm, ^{138}BaO, ^{137}BaOH, ^{142}NdO
^{155}Gd	14.80	^{138}BaOH, ^{139}LaO
^{156}Gd	20.47	^{156}Dy, ^{140}CeO
^{157}Gd	15.65	^{141}PrO
^{158}Gd	24.84	^{156}Dy, ^{142}CeO, ^{142}NdO
^{160}Gd	21.86	^{160}Dy, ^{144}SmO, ^{144}NdO
^{159}Tb	100	^{143}NdO
^{156}Dy	0.06	^{156}Gd, ^{140}CeO
^{158}Dy	0.10	^{158}Gd, ^{142}CeO, ^{142}NdO
^{160}Dy	2.34	^{160}Gd, ^{144}NdO, ^{144}SmO
^{161}Dy	18.91	^{145}NdO
^{162}Dy	25.51	^{162}Er, ^{146}NdO
^{163}Dy	24.90	^{147}SmO
^{164}Dy	28.18	1^{64}Er, ^{148}SmO, ^{148}NdO
^{165}Ho	100	^{149}SmO
^{162}Er	0.14	^{162}Dy, ^{146}NdO
^{164}Er	1.61	^{164}Dy, ^{148}SmO, ^{148}NdO
^{166}Er	33.61	^{150}SmO, ^{150}NdO
^{167}Er	22.93	^{151}EuO
^{168}Er	26.78	^{168}Yb, ^{152}SmO, ^{152}GdO
^{170}Er	14.93	^{170}Yb, ^{154}GdO, ^{154}SmO
^{167}Tm	100	^{153}EuO
^{168}Yb	0.13	^{168}Er, ^{152}GdO, ^{152}SmO
^{170}Yb	3.04	^{170}Er, ^{154}GdO, ^{154}SmO

Continuation of Table H.3

Isotope	Abundance (%)	Interference
^{171}Yb	14.28	^{155}GdO
^{172}Yb	21.83	^{156}DyO, ^{156}GdO
^{173}Yb	16.13	^{157}GdO
^{174}Yb	31.83	^{174}Hf, ^{158}DyO, ^{158}GdO
^{176}Yb	12.76	^{176}Lu, ^{176}Hf, ^{160}GdO, ^{160}DyO
^{175}Lu	97.41	^{159}TbO
^{176}Lu	2.59	^{176}Yb, ^{176}Hf, ^{160}GdO, ^{160}DyO

Table H.4 Wilcoxon prediction set results for Tm, Ho, Eu and Er, using the multivariate calibration methods, OLS and prepared concentration.

Tm	**Exp**	**OLS**	**PCR**	**PLS**	**RR**	**Lasso**	**Ho**	**Exp**	**OLS**	**PCR**	**PLS**	**RR**	**Lasso**
Exp		0.001	0.327	0.675	0.490	0.807	Exp		0.278	0.824	0.666	0.294	0.726
OLS	0.001		0.001	0.001	0.006	0.001	OLS	0.278		0.255	0.432	0.014	0.142
PCR	0.327	0.001		0.077	0.379	0.894	PCR	0.824	*0.255*		0.281	0.367	0.967
PLS	0.675	0.001	0.077		0.315	0.485	PLS	0.666	*0.432*	0.281		0.184	0.784
RR	0.490	0.006	0.379	0.315		0.085	RR	0.294	0.014	0.367	0.184		0.173
Lasso	0.807	0.001	0.894	0.485	0.085		Lasso	0.726	*0.142*	0.967	0.784	0.173	
Eu	Exp	OLS	PCR	PLS	RR	Lasso	Er	Exp	OLS	PCR	PLS	RR	Lasso
Exp		0.01185	0.778	0.900	0.346	0.660	Exp		0.009	0.900	0.660	0.683	0.330
OLS	0.012		0.010	0.012	0.007	0.008	OLS	0.009		0.008	0.012	0.014	0.008
PCR	0.778	0.010		0.510	0.363	0.533	PCR	0.900	0.008		0.851	0.610	0.975
PLS	0.900	0.012	0.510		0.364	0.285	PLS	0.660	0.012	0.851		0.925	0.950
RR	0.346	0.007	0.363	0.364		0.432	RR	0.683	0.014	0.610	0.925		0.972
Lasso	0.660	0.008	0.533	0.285	0.432		Lasso	0.330	0.008	0.975	0.950	0.972	

The values in bold are those with a $p \leq 0.05$, indicating a statistically significant value.